

CRANFIELD UNIVERSITY

JOHN LOIZOU

**AN ASSESSMENT OF THE AUTONOMOUS INTEGRITY
MONITORING PERFORMANCE OF A COMBINED GPS/GALILEO
SATELLITE NAVIGATION SYSTEM, AND ITS IMPACT ON THE CASE
FOR THE DEVELOPMENT OF GALILEO**

SCHOOL OF ENGINEERING

PhD THESIS

CRANFIELD UNIVERSITY

SCHOOL OF ENGINEERING

PhD THESIS

Academic Year 2003 – 2004

JOHN LOIZOU

**An Assessment of the Autonomous Integrity Monitoring
Performance of a Combined GPS/Galileo Satellite Navigation
System, and its Impact on the Case for the Development of Galileo**

Supervisor: T Bowling

March 2004

This thesis is submitted in fulfilment of the requirements for the degree of
Doctor of Philosophy

© Cranfield University 2004. All rights reserved. No part of this publication may be reproduced
without the written permission of the copyright owner.

Abstract

In 1999 Europe, through the European Commission and the European Space Agency, began detailed definition of a second generation Global Navigation Satellite System (GNSS). This GNSS development programme, known as “Galileo”, was intended to both complement and compete against the existing US Global Positioning System (GPS).

Unlike GPS, Galileo is intended to be privately financed, following the initial development investment from the EC and ESA, which implies that Galileo should provide some revenue-earning services. From its earliest inception, the basis of these services has been assumed to be through the provision of Signal Integrity through an Integrity Flag broadcast through the Galileo system— a service which GPS cannot provide without some external system augmentation. This thesis undertakes a critical evaluation of the value of this integrity system in Galileo.

This thesis has two parts. The first demonstrates that the conditions required to attract adequate private finance to the Galileo programme are incompatible with the system architecture derived from the early Galileo system studies and taken forward into the system early deployment phase, which includes an Integrity system within Galileo.

The second part of this thesis aims to demonstrate that receivers which can combine the signals from GPS and Galileo may offer a free Integrity service which meet the needs of the majority of users, possibly up to the standards required for aviation precision approach. A novel Receiver Autonomous Integrity Monitoring (RAIM) technique is described, using an Errors in Variables/Total Least Squares approach to the detection of inconsistencies in an over-determined set of GNSS signal measurements. The mathematical basis for this technique is presented, along with results which compare the simulated performance of receivers using this algorithm against the expected performance of Galileo’s internal integrity determination system.

Acknowledgements

Although many people have contributed directly or indirectly to the production of this thesis, I would like to give particular thanks to the following:

- Matthew Powe, for his thorough critique of the EIV method;
- Richard Lowe, Alec Bastin, James Rickards and Chris Johnson, who all contributed greatly to the development of the tools used in this analysis;
- The British National Space Centre for funding the original RAIM study which provided the basis for this thesis;
- The Galileo System Test Bed project officers of the European Space Agency, for supporting the Standalone Test Case which refined the EIV algorithm and produced the results presented herein;
- The Engineering and Physical Sciences Research Council, for providing funding for the Total Technology PhD registration;
- My supervisor, Tom Bowling of Cranfield University;
- And my wife Janice, for her patience and understanding.

TABLE OF CONTENTS

1. INTRODUCTION	1
1.1 Purpose and Scope	1
1.2 Background	2
1.3 Thesis Objectives and Problem Statement.....	6
1.4 Approach.....	7
1.5 An Introduction to RAIM.....	8
1.6 Structure.....	9
1.7 Originality of Work.....	10
2. BACKGROUND TO THE INTEGRITY JUSTIFICATION STUDY	12
2.1 Introduction	12
2.2 The PwC “Inception” Study.....	12
2.3 Galileo Structural Analysis Survey (GALSAS).....	13
2.4 ESA GalileoSat Phase B and Galileo Phase B2.....	14
2.5 Other Studies – GALA and GEMINUS.....	15
3. METHODS AND LITERATURE (INTEGRITY JUSTIFICATION STUDY).....	17
3.1 Introduction	17
3.2 The GALSAS Study	17
3.2.1 Primary Research Interview Guidelines	18
3.2.2 Consolidated Research	20
3.3 Inception Study	22
3.4 Other Studies – GALA and GEMINUS.....	23
3.4.1 GALA WP 1 Market Research Methods and Overall Results	23
3.4.2 GALA WP 2 Overall Requirements and System Trade-Offs.....	25
3.4.3 GALA WP 9 Programmatics and Business Issues.....	26
3.4.4 GEMINUS.....	27
3.5 UKISC Galileo Working Group Survey	29
4. RESULTS FOR THE INTEGRITY JUSTIFICATION STUDY	32
4.1 Results from the GALSAS Survey – Primary Research	32
4.2 Results from the GALSAS Survey – Consolidated Results.....	34
4.2.1 Current Size and Structure of the European Market	34
4.2.2 Mid-Term Trends In The European Market.....	35
4.3 Results from the Inception Study.....	37
4.3.1 Reaction to the Report.....	37
4.3.2 Baseline Case	39
4.3.3 Effect of Loss of Safety of Life and Commercial Service Revenues	43
4.3.4 Exclude the Cost of Integrity.....	46
4.4 Integrity Justification Study Conclusions	48
5. BACKGROUND TO THE RAIM STUDY	52
5.1 Introduction	52
5.2 Purpose and Scope of the RAIM Study	52
5.3 Objectives of the RAIM Study	54
5.4 Performance Metrics.....	54
5.4.1 Accuracy.....	55
5.4.2 Integrity.....	56
5.4.3 Availability.....	56
5.4.4 Continuity.....	56
5.5 Required Navigation Performance for Precision Approach	57
5.6 Galileo IDS System Specifications.....	57
5.6.1 Galileo SAS Service Specifications.....	60
5.6.2 The Challenge of “Time to Alarm”	60

5.7	IDS System Costs.....	61
5.8	Existing Literature on Combined RAIM Systems Performance	62
5.8.1	The Integrity Requirement in Satellite Navigation: System Design Trade-Offs	62
5.8.2	Integrity Performance Models for a Combined Galileo/GPS Navigation System	63
5.8.3	Potential Performance Levels of a Combined Galileo/GPS Navigation System.....	64
5.8.4	New Integrity Concept at User Level for a Future Galileo and GPS Environment.....	64
5.9	Existing Literature on Advanced Integrity Monitoring Algorithms	65
5.10	Current Galileo Integrity Concept.....	66
5.10.1	SISA/IF Concept.....	66
5.10.2	Receiver Autonomous Integrity Monitoring (RAIM).....	66
5.10.3	RAIM and SISA/IF Integration	67
6.	SIMULATION TOOLS AND TECHNIQUES.....	71
6.1	Set of Tools.....	71
6.2	“RAIM Availability” spreadsheet.....	72
6.2.1	Input.....	72
6.2.2	Cartesian	72
6.2.3	User_Position	72
6.2.4	LOS (“Line of Sight”).....	72
6.2.5	Table.....	73
6.2.6	G_Sheet	73
6.2.7	Availability.....	73
6.2.8	Display.....	74
6.2.9	SVD	74
6.3	“Bias Modelling” spreadsheet	75
6.4	Service Volume Simulator (SVS)	75
6.5	Navigation Engine (NavEng).....	80
6.6	Matlab Flight Trials Simulator	85
7.	ASSUMPTIONS, PARAMETERS AND VARIABLES	88
7.1	UERE vs Elevation Characteristics.....	88
7.1.1	GPS IIF UERE Characteristics.....	88
7.1.2	Galileo UERE Characteristics	89
7.1.3	Orbit Determination & Time Synchronisation Errors	90
7.2	Constellation Configurations.....	91
7.2.1	Galileo Constellation Parameters.....	91
7.2.2	GPS Constellation Parameters	92
7.2.3	Galileo/GPS Plane Offset.....	93
7.2.4	Galileo/GPS Time Offset	95
7.3	Masking Angle.....	96
7.4	Service Volume Simulation Resolution	96
7.5	Translation of RNP Specifications to RAIM Requirements.....	98
7.5.1	Vertical Alert Limit (VAL)	98
7.5.2	Probability of False Alarm (P_{FA}).....	98
7.5.3	Probability of Missed Detection (P_{MD}).....	99
7.5.3.1	WAAS MOPS Approach	99
7.5.3.2	Signal in Space Integrity Failure Occurrence Probability	99
7.5.3.3	Local Effects Integrity Failure Occurrence Probability.....	100
7.5.3.4	Conditional P_{MD}	100
7.5.3.5	P_{MD} Conclusion.....	101
7.5.4	Satellite Availability Rates and Outage Occurrence Probabilities	101
8.	DETAILED PROCESSING MODEL.....	103
8.1	Basic Functions.....	103
8.2	Calculation of Satellite to User Geometry.....	103
8.2.1	Satellite position in ECI Cartesian Coordinates	103
8.2.2	Calculate True User Cartesian Coordinates.....	106

8.2.3	Generation of the Observation Matrix	110
8.3	Simulation of Pseudorange Errors	110
8.4	Calculation of Navigation Solution and Position Errors	111
8.5	Application of RAIM Algorithms	112
8.6	Calculation of Availability, Including Satellite Outage Probability	113
9.	LEAST SQUARES RESIDUALS (LSR) RAIM METHOD.....	115
9.1	Weighted Position Solution and Vertical Accuracy	115
9.2	Weighted RAIM Test Statistic	115
9.3	Protection Levels	118
9.4	Underlying Assumptions	120
10.	“ERRORS IN VARIABLES” (EIV) RAIM METHOD	123
10.1	Introduction to EIV	123
10.2	Total Least Squares Positioning Solution	123
10.3	Setting the Weighting Matrices	126
10.3.1	Setting the C matrix	127
10.3.2	Setting the D matrix	129
10.4	EIV RAIM Test Statistics	133
10.4.1	Unweighted EIV Fault Detection Plane	133
	USSE' Test Statistic	133
10.4.3	H/e Test Statistic	135
10.5	Combining Two Test Statistics.....	139
10.5.1	Overall Concept.....	139
10.5.2	H/e Test Statistic Standard Deviation.....	144
10.5.3	Backstop Threshold.....	146
10.5.4	Threshold Balancing.....	147
10.6	Calculate the Vertical Protection Limit	149
10.7	EIV Method - Processing Logic Pseudocode	151
10.7.1	Initialise the algorithm.....	151
10.7.2	Calculate the Test Statistics	152
10.7.3	Calculate the Detection Thresholds	152
10.7.4	Calculate the VPL.....	155
10.7.5	Calculate Fault Detection State.....	155
11.	NUMERICAL EXAMPLES FOR LSR AND EIV METHODS.....	156
11.1	Calculate LSR VPL	156
11.2	Calculate LSR Test Statistic	159
11.3	EIV Method	161
11.3.1	Define Weighting Matrices	161
11.3.2	Calculate the EIV Test Statistics	161
11.3.3	Calculate the H/e Standard Deviation	163
11.3.4	Calculate the Detection Thresholds	165
11.3.5	Calculate the EIV VPL.....	166
12.	RAIM EXPERIMENTATION RESULTS	168
12.1	Service Volume Simulation Results	168
12.1.1	Galileo Only, LSR RAIM, 10° Masking	171
12.1.2	Galileo Only, EIV RAIM, 10° Masking	172
12.1.3	Galileo + GPS, LSR RAIM, 10° Masking.....	173
12.1.4	Galileo + GPS, EIV RAIM, 10° Masking.....	174
12.1.5	Galileo Only, LSR RAIM, 5° Masking	176
12.1.6	Galileo Only, EIV RAIM, 5° Masking	176
12.1.7	Galileo + GPS, LSR RAIM, 5° Masking.....	177
12.1.8	Galileo + GPS, EIV RAIM, 5° Masking.....	178
12.1.9	Galileo SISA/IF (WAAS Equation, 3 Critical Satellites), 10° Masking.....	179

12.2	Navigation Engine Simulation Results	181
12.2.1	Galileo Only, RAIM Results	183
12.2.1.1	Unbiased Case	183
12.2.1.2	Biased Case	185
12.2.2	Galileo + GPS, RAIM Results.....	188
12.2.2.1	Unbiased case.....	188
12.2.2.2	Biased Case	190
12.3	Flight Trials Simulation Results.....	193
12.3.1	LSR RAIM, Step Bias	195
12.3.2	EIV RAIM, Step Bias, Snapshot User Clock	196
12.3.3	EIV RAIM, Step Bias, Filtered User Clock.....	198
12.3.4	LSR RAIM, Ramp Bias	199
12.3.5	EIV RAIM, Ramp Bias, Snapshot User Clock	200
12.3.6	EIV RAIM, Ramp Bias, Filtered User Clock	201
12.3.7	EIV RAIM, Ramp Bias, System-Switchable User Clock.....	202
12.3.8	EIV RAIM, Ramp Bias, Ideal Clock	205
12.3.9	EIV RAIM, Step Bias, with FDE.....	206
12.3.10	EIV RAIM, Ramp Bias, with FDE	207
13.	DISCUSSION.....	208
13.1	Service Volume Performance	208
13.2	Navigation Engine Performance	210
13.3	Flight Trials Simulation Performance.....	211
13.4	Comments on the Physical Implementation of the EIV Method	214
13.5	RAIM in the Context a of Global Integrity Service	216
13.5.1	Context of Galileo Integrity Service	217
13.5.2	Time To Alarm – A Problem for Galileo.....	218
13.5.3	RAIM as a Solution to the Integrity Problem	219
13.5.4	Further Development of EIV	220
13.5.5	The Future for the Galileo IDS	220
14.	CONCLUSIONS AND RECOMMENDATIONS.....	221
14.1	Conclusions.....	221
14.2	Recommendations for Further Research.....	222
15.	REFERENCES	224
16.	BIBLIOGRAPHY	229
APPENDIX A	SAMPLE RESULTS FROM GALSAS STUDY	231
A.1	UK Civil Aviation Authority - Safety Requirements Group	231
A.2	BT Cellnet	235
A.3	CMT TechServ	239
APPENDIX B	RESULTS FROM UKISC WORKING GROUP SURVEY	244
B.1	Galileo “Prime Contractors” view	244
B.2	“Non-Primes” view.....	247
APPENDIX C	PERFORMANCE OF MDE ALGORITHM	252
APPENDIX D	INTRODUCTION TO SINGULAR VALUE DECOMPOSITION.....	257
D.1	The SVD Process	260
D.2	SVD of a 2-Dimensional Matrix.....	261
D.3	SVD Solution of the Least-Squares (LS) Problem.....	264
D.4	SVD Solution of the Total Least-Squares (EIV) Problem	265

TABLE OF FIGURES

Figure 3-1: GALA Classification of User Classes by Accuracy and Integrity Requirements [5] .24	.24
Figure 3-2: GEMINUS and GALA Galileo Services [2]	28
Figure 4-1: The European GNSS market by market segments – 1999: 935 MEURO.....	35
Figure 4-2: The European GNSS market by market segments – 2005: 8,383 MEURO.....	36
Figure 4-3: Inception Study Costs and Revenues.....	40
Figure 4-4: Inception Study Base Case Cash Flow (public funding = €2.1 Bn)	41
Figure 4-5: Base Case, with Finance rate of 4.6% (public funding = €2.1 Bn)	42
Figure 4-6: Base Case, with Finance rate of 12% (public funding = €3.2 Bn)	42
Figure 4-7: Inception Estimate of GOC Market Revenues (€K 2001 prices) [4]	44
Figure 4-8: Cash Flow without Service Revenues (public funding = €2.1 Bn).....	45
Figure 4-9: Cash Flow without Service Revenues (public funding = €3.2 Bn).....	46
Figure 4-10: Costs and Revenues, excluding IDS development and operations	47
Figure 4-11: Cash Flow for System with no IDS (public funding = €2.1 Bn).....	47
Figure 4-12: Cash Flow for System with no IDS (public funding = €2.93 Bn).....	48
Figure 5-1: “GALA” Study Integrity decision tree showing two “Integrity Barriers” - RAIM and ground-based monitoring (using Boolean Logic “AND” & “OR” gates)	70
Figure 6-1: SVS Snapshot Case Window	76
Figure 6-2: Example output from Service Volume Simulator	79
Figure 6-3: Navigation Engine Input Window.....	82
Figure 7-1: Comparison of Published GPS Block IIF UERE Characteristics.....	89
Figure 7-2: Comparison of Published Galileo L1/E5b UERE Characteristics.....	90
Figure 7-3 : vertical alert limit = 15m, Plane Separation = 0 degrees	95
Figure 7-4 : vertical alert limit = 15m, Plane Separation = 30 degrees.....	95
Figure 9-1 : Typical distribution of vertical errors and RAIM test statistic for normal operations (Gaussian noise, no bias).....	117
Figure 9-2 : LSR RAIM Test Statistic Characteristic	118
Figure 9-3 : Typical distribution of vertical errors and RAIM test statistic with critical bias on failed satellite (Gaussian noise on all satellites).....	119

Figure 9-4: Improvement in VPL with Satellites Disabled	121
Figure 10-1 : Comparison of $\sqrt{\text{USSE}}$ with $\sqrt{\text{WSSE}}$	134
Figure 10-2 : $\sqrt{\text{USSE}}$ Test Statistic Characteristic.....	135
Figure 10-3 Geometry change with vertical displacement	137
Figure 10-4 : H/e Test Statistic Distribution vs Horizontal Error.....	138
Figure 10-5: H/e Test Statistic Distribution vs Vertical Error.....	138
Figure 10-6 : Ideal H/e Test Statistic Probability Density	139
Figure 10-7 : Vertical Error (z-axis) vs $\sqrt{\text{USSE}}$ Test Statistic (x-axis).....	141
Figure 10-8 : Vertical Error (z-axis) vs H/e Test Statistic (y-axis).....	141
Figure 10-9: $\sqrt{\text{USSE}}$ Statistic (x-axis) vs H/e Test Statistic (y-axis).....	142
Figure 10-10 : Vertical Error vs $\sqrt{\text{USSE}}$ Statistic, showing EIV VPL.....	143
Figure 10-11 : EIV Test Statistic Distribution in 3 dimensions	144
Figure 10-12 : H/e Test Statistic Characteristic.....	145
Figure 10-13 : Root USSE' Characteristic (Special Case).....	148
Figure 10-14 : H/e Characteristic (Special Case).....	148
Figure 10-15 : Calculation of EIV Worst case Bias	150
Figure 11-1: H/e Test Statistic for Worked Example	165
Figure 11-2 : Curve of VPL against Bias for a Fixed P_{MD}	167
Figure 12-1 : Baseline GPS and Galileo UERE curves for RAIM analysis	169
Figure 12-2 : Key (RAIM Availability Percentage) for SVS Output Graphs.....	169
Figure 12-3 : Galileo only, LSR RAIM Availability, 10° Mask, 20m VAL	171
Figure 12-4: Galileo only, EIV RAIM Availability, 10° Mask, 20m VAL	172
Figure 12-5 : Galileo+GPS LSR RAIM Availability, 10° Mask, 20m VAL.....	173
Figure 12-6: Galileo+GPS LSR RAIM Availability, 10° Mask, 15m VAL.....	174
Figure 12-7: Galileo+GPS EIV RAIM Availability, 10° Mask, 15m VAL	175
Figure 12-8 : Galileo+GPS EIV RAIM Availability, 10° Mask, 12m VAL	175
Figure 12-9 : Galileo only, LSR RAIM Availability, 5° Mask, 20m VAL.....	176
Figure 12-10 : Galileo only, EIV RAIM Availability, 5° Mask, 15m VAL	177

Figure 12-11 : Galileo+GPS LSR RAIM Availability, 5° Mask, 15m VAL	178
Figure 12-12 : Galileo+GPS EIV RAIM Availability, 5° Mask, 12m VAL	179
Figure 12-13 : Galileo only SISA/IF Availability, 10° Mask at 15m VAL	180
Figure 12-14 : Galileo only SISA/IF Availability, 10° Mask at 12m VAL	181
Figure 12-15 : NavEng Run for Galileo Only, LSR RAIM, no Bias	183
Figure 12-16 : NavEng Run for Galileo Only, EIV RAIM, no Bias	184
Figure 12-17 : NavEng Run for Galileo Only, LSR RAIM, with Bias	185
Figure 12-18 : NavEng Run for Galileo Only, EIV RAIM, with LSR worst case Bias	186
Figure 12-19: NavEng Run for Galileo Only, EIV RAIM, with EIV worst case Bias	187
Figure 12-20 : NavEng Run for Galileo + GPS, LSR RAIM, no Bias	188
Figure 12-21 : NavEng Run for Galileo + GPS, EIV RAIM, no Bias	189
Figure 12-22 : NavEng Run for Galileo + GPS, LSR RAIM, with Bias	190
Figure 12-23 : NavEng Run, LSR RAIM, with Bias and satellites disabled	191
Figure 12-24 : NavEng Run for Galileo + GPS, EIV RAIM, with Bias	192
Figure 12-25 : LSR RAIM Response to Step Bias	195
Figure 12-26 : EIV RAIM Response to Step Bias	197
Figure 12-27 : EIV RAIM response to Step Bias, with Filtered Clock	199
Figure 12-28 : LSR RAIM Response to Ramp Bias	200
Figure 12-29 : EIV RAIM Response to Ramp Bias	201
Figure 12-30 : EIV RAIM Response to Ramp Bias (Filtered Clock)	202
Figure 12-31 : EIV RAIM Response to Ramp Bias (Switchable Clock)	203
Figure 12-32 : Selection of Executive Clock	204
Figure 12-33 : EIV RAIM Response to Ramp Bias (Ideal Clock)	205
Figure 12-34 : EIV RAIM response to Step Bias, with FDE Active	206
Figure 12-35 : EIV RAIM response to Ramp Bias, with FDE Active	207
Figure C- 1: Comparison of VPL calculated using LSR and MDE approaches, for GPS+Galileo	254
Figure C- 3: Comparison of VPL calculated using LSR and MDE approaches, for GPS-only	255

Figure D - 1: Graphical Representation of the SVD Process	257
Figure D - 2: Graphical Representation of the Thin SVD Process	258
Figure D - 3: Action of Matrix A on Unit Circle	262
Figure D - 5: Action of U (“Hang”) Matrix on Unit Circle	263
Figure D - 7 : Action of Σ (“Stretch”) Matrix on Unit Circle	263
Figure D - 8: Action of V (“Align”) Matrix on Stretched Circle	264

NOTATION AND GLOSSARY

The following acronyms and abbreviations have been used in this thesis.

APV	Approach with Vertical Guidance
BNSC	British National Space Centre
C	EIV weighting matrix
CAA	Civil Aviation Authority
CAS	Commercial Access Service
CBA	Cost Benefit Analysis
CSS	Comparative System Study
D	EIV tuning matrix
DCM	Direction Cosine Matrix
DG TREN	Directorate General of Transport and Energy
DLL	Dynamic Link Library
DOP	Dilution of Precision
d_5	Fifth diagonal term on D matrix
EC	European Commission
ECAC	European Civil Aviation Conference
ECEF	Earth Centred, Earth Fixed
ECI	Earth Centred, Inertial
EIV1	see USSE'
EGNOS	European Geostationary Navigation Overlay Service
EIDS	European Integrity Determination System
EIV	Errors in Variables
ESA	European Space Agency
EU	European Union
	European Organization for Civil Aviation Equipment
EUROCAE	Manufacturers
FAA	Federal Aviation Authority
FDE	Fault Detection and Exclusion
FOC	Full Operational Capability
FTE	Flight Technical Error
G	Observation matrix
GIC	Ground Integrity Channel
GLONASS	Global Navigation Satellite System (Russian system)
GNSS	Global Navigation Satellite Systems

GOC	Galileo Operating Company
GPS	Global Positioning System
GSTB	Galileo System Test Bed
GVC	Galileo Vehicle Company
H	EIV Perturbations matrix
H/e	Ratio of mismatches from EIV method (EIV test statistic 2)
HLD	High Level Definition
HRMS	Horizontal Root Mean Square
ICAO	International Civil Aviation Organisation
IDS	Integrity Determination System
IF	Integrity Flag
IOV	In-Orbit Validation
IR	Integrity Risk
IRR	Internal Rate of Return
JAA	Joint Aviation Authority
k	number of standard deviations
LOS	Line of Sight
LSR	Least Squares Residual
MDE	Marginally Detectable Error
MEO	Medium Earth Orbit
MOPS	Minimum Operational Performance Standards
MSAS	Multi-Transport Satellite Augmentation System
MTBF	Mean Time Between Failures
MTTR	Mean Time To Repair
N	Number of satellites in view
NATS	National Air Traffic Services Ltd
NavEng	Navigation Engine simulator
NSE	Navigation System Error
OAS	Open Access Service
OD&TS	Orbit Determination & Time Synchronisation
OSPF	Orbitography and Synchronisation Processing Facility
PDF	Probability Density Function
PDOP	Position Dilution of Precision
P_{FA}	Probability of False Alarm
P_{MD}	Probability of Missed Detection
PPP	Public Private Partnership
PRS	Public Regulated Service

PVT	Position, Velocity and Timing
RAAN	Right Ascension of Ascending Node
RAIM	Receiver Autonomous Integrity Monitoring
RMS	Root Mean Square
RNP	Required Navigation Performance
RTCA	Radio Technical Commission for Aeronautics
RTK	Real-Time Kinematic
S/A	Selective Availability
SARPS	Standards and Recommended Practices
SAS	Safety of Life Service, Safety Access Service
satnav	satellite navigation
SBAS	Space-Based Augmentation Systems
SISA	Signal in Space Accuracy
SISE	Signal in Space Error
SoL	Safety of Life
SPS	Standard Positioning Service
SRD	System Requirements Document
STK	Satellite Tool Kit
SVD	Singular Value Decomposition
SVS	Service Volume Simulator
$T(N, P_{FA})$	Chi-squared test statistic
TLS	Total Least Squares
TSE	Total System Error
TTA	Time To Alarm
TFFF	Time To First Fix
USERE	User Equivalent Range Error
UKISC	United Kingdom Industrial Space Committee
USSE'	Unweighted Modified Sum of Squared Errors (EIV test statistic 1)
V_{55}	Fifth diagonal term on output V matrix from SVD process
VAL	Vertical Alert Limit
VPL	Vertical Protection Limit
$V_{slope(max)}$	Maximum ratio of vertical error to LSR RAIM test statistic
W	Weighting matrix
WAAS	Wide Area Augmentation System
WLS	Wireless Location Services
WP	Work Package

WSSE	Weighted Sum of Squared Errors
\mathbf{y}	Vector of pseudorange residuals
ZTD	Zenith Tropospheric Delay
i	Inclination (of orbital plane)
λ	Chi-squared distribution non-centrality parameter
σ_5	Smallest singular value from SVD process
σ_v	Standard vertical error (one standard deviation)
X^2	Chi-squared distribution
ω	True Anomaly
Ω	Right Ascension of Ascending Node (RAAN)

1. INTRODUCTION

1.1 Purpose and Scope

This thesis has been produced as a result of the author's involvement in a number of aspects of the European "Galileo" satellite navigation programme, since the early definition phase of the system. The Galileo programme is, at the time of writing, arguably the most significant space engineering programme currently being undertaken within Europe. Apart from the technical challenges associated with developing a highly accurate global navigation and timing system, the development of the Galileo programme also has a number of political, economic and managerial hurdles to overcome before the system can be deployed.

When the Council of European Transport Ministers declared an intention to proceed with the initial definition of a civil-owned and operated satellite navigation system in June 1999 it seemed that Galileo would provide an example of European industrial co-operation breaking a virtual US monopoly, in a similar way to Airbus and Ariane in the airliner and space launcher fields, respectively. Although the European Commission and European Space Agency had put in enormous effort into pushing the programme forward, a number of key technical, political and financial issues remained unresolved.

Foremost amongst these was the issue of funding. From its inception, Galileo has been presented as a project to be funded as some form of Public/Private Partnership (PPP), in which commerce and industry would subscribe to the programme in return for revenues to be earned from commercial exploitation of the Galileo signals. This thesis will demonstrate that the existence of the American Global Positioning System (GPS), with its free-to-air signals, and plans for significant performance upgrades over the next decade or so, make the case for a PPP for Galileo, as currently defined, unsustainable. Specifically, this thesis will demonstrate that the Integrity Determination System, a key element and design driver in the Galileo architecture, adds significant cost to the system which can never be recouped through sale of any integrity-dependent services.

As a research project under the Engineering and Physical Sciences Research Council's (EPSRC) "Total Technology PhD" programme, this thesis has two components:

- A "management" element, which presents the results of an analysis of the business case used to justify the inclusion of a discrete Integrity Determination System in the Galileo architecture. This includes the results arising from two surveys with which the author was involved into the aspirations held by the European (or,

specifically, UK) satellite navigation industry for Galileo, and a separate review of a business case for Galileo developed by PriceWaterhouseCoopers;

- A “technical” element, which presents the results of an analysis of the predicted performance of a combined future GPS/Galileo constellation when used to undertake receiver autonomous integrity monitoring.

The technical element, which is by far the larger component, considers the use of techniques known as Receiver Autonomous Integrity Monitoring (RAIM) as a low cost alternative to the inclusion of a dedicated integrity function within Galileo. Specifically, a novel RAIM algorithm, based on a mathematical technique known as “Errors in Variables” or Total Least Squares through Singular Value Decomposition is developed. This technique is shown, under certain conditions, to offer integrity performance significantly better than traditional Least Squares Residuals RAIM techniques, and a patent has been applied for, to protect the commercial applicability of this process.

The implication of these results, especially when considered along with the results of the management element, is that the Galileo baseline architecture is over-designed; the Integrity Determination System is an unnecessary expense, the costs of which are unlikely to be recouped from commercial operations, and therefore should be removed from the baseline Galileo system architecture.

1.2 Background

Since the US-owned and operated Global Positioning System first started transmitting signals that could be used by civilians for accurate position, velocity and timing (PVT) applications in the mid-1980s, a huge satellite navigation (satnav) industry has developed. Although the industrial segment dedicated to hardware (i.e. GPS chipsets and their associated receivers) is largely American, European industry plays a leading role in the development of applications and services which use GPS signals.

GPS does not have a monopoly on satellite navigation (the Russian GLONASS system is still operational, China launched its first military navigation satellite in late 2000 and a number of small commercial satnav systems have been launched in the last twenty years), but its signal is recognised as the *de facto* standard. Originally conceived and deployed as a US military system, GPS is still funded mainly by the Pentagon, although latterly the US Department of Transportation has also contributed to the system, in recognition of its importance as an asset to civil commerce and industry. More significantly, GPS remains under US military control and will remain so for the foreseeable future, although statutes have been passed committing the United States to the

continued free provision of a civil GPS signal, within the constraints of its primary, military mission.

The importance of GPS to commerce and industry is not confined to the United States; European users in industries as diverse as oil prospecting, agriculture and road haulage have become increasingly reliant on signals from the GPS constellation of satellites. Not wishing to remain reliant on the United States for access to what is increasingly regarded as a critical resource, the European Union (EU) has embarked on a satellite navigation programme of its own. This programme began in 1996 with the go-ahead for development of EGNOS, the European Geostationary Navigation Overlay System. As its name suggests, EGNOS is not a global satnav system in itself; it is an extension to the GPS and GLONASS systems, comprising a network of ground stations which monitor the accuracy of the satnav signals being transmitted over Europe. Dedicated EGNOS payloads are piggy-backed on various Geostationary communication satellites to enable signal correction and integrity warning signals to be broadcast to GPS and GLONASS users. EGNOS is Europe's contribution to the Global Navigation Satellite System Phase 1 (GNSS-1). As well as GPS, GLONASS and EGNOS, the GNSS-1 architecture is currently planned to comprise the Wide Area Augmentation System (WAAS), and the Multi-Transport Satellite Augmentation System (MSAS) which, when fully operational, will provide EGNOS-type overlay services to North America and Japan/Far East respectively.

The system performance specifications for EGNOS and the other overlay systems (generically referred to as space-based augmentation systems or SBAS) are, in general, driven by the requirements of civil aviation. More specifically, the defining specifications for SBAS are those that would allow the systems at Full Operational Capability (FOC) to be certified for use for Category 1 (Cat I) precision approaches, in accordance with the International Civil Aviation Organisation (ICAO) standards. Thus, in the US WAAS is funded primarily by the Federal Aviation Authority (FAA), and in Europe EGNOS is partially funded by organisations such as NATS (UK National Air Traffic Services) – and hence, indirectly, by the airlines themselves, as the prospective beneficiaries of the service.

Being reliant on Geostationary satellites for the transmission of correction and integrity signals (and hence suffering from “blocking” of the signal in built-up areas), WAAS and EGNOS cannot be regarded as truly ‘multi-modal’ – they may eventually be suitable for Cat I approaches to airports but they offer little benefit to rail and road users in urban areas, for example. The European approach to GNSS Phase 2 is to develop and deploy its own global constellation of navigation satellites, under a programme given the title Galileo.

In 1998 the European Space Agency (ESA) commissioned the Comparative System Study (CSS) to consider various possible architectures for a European-owned GNSS-2 constellation. In parallel, the European Commission, working under the auspices of the Directorate General of Transport and Energy (DG TREN) of the European Union, began a series of studies to determine the case for a European satnav system independent from GPS, and to consider issues such as how such a system should be funded.

By June 1999 the Council of European Transport Ministers made a declaration on its intention to proceed with the initial definition of the Galileo system. ESA was to take the lead for definition of the space and associated ground segments, under its GalileoSat programme, while the EU itself would manage a series of associated studies to run in parallel with ESA's system engineering activities. These EU studies included:

- GALA – Galileo overall architecture study
- GEMINUS – Galileo system and service definition study
- GALSAS – The Structural Analysis Study of the European Satellite Navigation Applications Segment.

In order to provide a justification for the development of the Galileo system over and above the desire for European independence from GPS for satellite navigation services, a set of high-level requirements which would distinguish Galileo from GPS were agreed between ESA and the EU, and presented as a “High Level Definition” (HLD) document. From these requirements a set of system specifications were developed and formally issued as ESA's “System Requirements Document” (SRD) which, through a number of revisions over GalileoSat Phase B and subsequent studies, form the basis of the system specification for Galileo. The high-level requirements behind the SRD highlighted the perceived shortcomings of GPS, and hence were intended to provide the justification for the development of Galileo. These shortcomings may be considered to be:

- GPS does not transmit an integrity signal. Although a “satellite health flag” in the navigation message broadcast by each satellite provides a limited form of integrity, the nominal update rate for this flag is too infrequent to allow it to be used for safety critical applications (such as aviation);
- The Coarse Acquisition (C/A) signal which GPS provides for civilian use may be degraded or even turned off at the discretion of the United States military command;
- The C/A signal transmitted by the current generation of GPS satellites is broadcast on a single frequency, whereas in order to make accurate corrections to compensate for ionospheric signal delays coherent transmission on two frequencies is required;

- Being a system controlled by the US military, national and international aviation authorities are unable to certify GPS as a primary navigation aid, even though it provides navigation accuracy some orders of magnitude better than any available terrestrial systems;
- The GPS constellation has been sized to provide acceptable accuracy and availability in military operational environments. Typically these have largely unobstructed views from horizon to horizon. As a result the availability of GPS (i.e. the fraction of time when at least 4 satellites are visible) is restricted in urban environments;
- The GPS service is provided at risk to the user, with no guarantee of accuracy or availability, and with no liability for the performance of the system.

The baseline system architecture for Galileo arising from the ESA Comparative System Study and fed into the GalileoSat SRD was developed to create a system which addresses these shortcomings.

A key element of the GalileoSat baseline definition is that the system should meet its specifications stand-alone, i.e. it must be able to operate entirely independently of GPS. However, because GPS is recognised as being the *de facto* standard for satellite navigation and, with the enhancements planned for GPS in the next two decades and the projected market for accurate positioning services, Galileo also has a driving requirement that its signal must be compatible and interoperable with that of GPS. That is to say Galileo should not present undue interference to the GPS signals, and it should be relatively easy to manufacture receivers that can combine signals from the two constellations such that within the derived navigation equation it is transparent whether any or all of the satellites being used are Galileo or GPS satellites.

A separate element of the Galileo programme that is crucial to this thesis is the political requirement that a significant proportion of private funding should be used to develop, deploy and operate the system. Since GPS has led to the development of a vast civil industry (mainly in the US), both in the manufacture of equipment and in the development of applications and services, it is reasonable to assume that the deployment of Galileo would stimulate similar industrial benefits in Europe. Private industry stands to gain significant rewards from the development and deployment of this system, and current dogma dictates that the system should be at least partly funded from private investment, through some form of Public-Private Partnership (PPP).

GalileoSat Phase B was followed by ESA's Galileo Phase B2 (Design and Development Phase), and Phase C0 (Detailed Development) activities. In turn, European Union funds were committed to the Galilei

studies – successors to GEMINUS and GALA, and intended to develop further the full system and service definition, along with a better understanding of the business case for Galileo.

1.3 Thesis Objectives and Problem Statement

The apparently unrelated requirements on the Galileo programme mentioned above (specifically, the desire for stand-alone performance at least as good as GPS; the inclusion of a near real time integrity signal; interoperability with GPS; and funding from a Public-Private Partnership) can be combined to formulate the problem statement for this thesis as follows:

The conditions required to attract adequate private finance to the Galileo programme are incompatible with the system architecture derived from the results of the ESA Comparative System Study, GalileoSat and GALA system definition activities. Receivers which can combine the free-to-air signals from future GPS and the Galileo Open Access Service will offer performance (in terms of position, velocity and timing accuracy, availability, integrity and continuity of service) which meet the needs of the vast majority of users. Specifically, Receiver Autonomous Integrity Monitoring (RAIM) techniques applied to a combined Galileo/GPS constellation will offer adequate system integrity for the majority of users. In order to attract private investment into the Galileo programme the system specifications need to be re-evaluated to meet the requirements of the mass market, and the system architecture needs to be simplified accordingly.

The ultimate objective of this thesis is to test this problem statement and, one hopes, to demonstrate that the Galileo programme is more likely to be successful financially and technically by moving some of the requirements for meeting integrity performance specifications away from the system infrastructure, and into the user receivers. The enabling objectives to test this hypothesis include:

- Demonstration that the business case for inclusion of an Integrity Determination System within the Galileo infrastructure is unsound, as currently specified.
- Demonstration that by combining the free-to-air signals from GPS with the free-to-air signals from Galileo, currently implemented standard RAIM algorithms can provide overall performance that exceeds the current specifications for the Galileo Commercial Access Service ;
- Development and evaluation of a novel RAIM technique, which offers accuracy and integrity performance that is comparable to the

requirements for civil aviation Category I (Cat I) precision approaches, and hence exceeds the current specifications for the Galileo Safety of Life Service;

- Demonstration that this novel RAIM technique can be shown, by simulation, to meet the specified requirements for false alarm and missed detection probabilities for aviation precision approach applications.

As will be shown, the Galileo programme faces a number of technical, managerial and financial challenges. The research performed for the production of this thesis was undertaken under a number of activities intended to revisit some of the systems engineering decisions leading to the Galileo system and mission requirements specifications. It is hoped that the results herein may lead to a design simplification, and hence cost reduction, for Galileo.

1.4 Approach

This thesis has two distinct but closely related components:

- **The Integrity Justification Study:** A financial analysis, based on an appraisal of underlying assumptions made in an EC-sponsored study into the business case for Galileo. These results are put into context with an analysis of two surveys into the views of key members of the UK satellite navigation industry. From these surveys, subjective statements from representatives of various industrial, commercial and administrative organisations, regarding the justification for Galileo as a whole, and its various proposed services are distilled into an argument regarding the justification for the IDS;
- **The RAIM Study:** The development and analysis of a novel RAIM algorithm that can be applied to a combined Galileo/GPS constellation to meet the needs of aviation users, which demonstrates that the Integrity Dissemination System currently included in the design of the Galileo ground segment is an unnecessary cost that would not be attractive to private investors and hence ought to be removed, or at least substantially de-scoped in its required stand-alone performance.

In general terms, the non-technical element of this thesis attempts to undertake an investment analysis from the perspective of a potential private investor considering funding the Galileo programme.

Although in the recent development of Galileo a number of studies have been performed which purport to be cost-benefit analyses (CBA) of one form or another, these invariably have been performed from the point of view of the EC or other Governmental agencies, and have attempted to provide a justification for Galileo based upon the macro-economic

benefits the system is expected to provide as a return on the public investment. Instead, the Integrity Justification Study presents a critical assessment of the projected market for satellite navigation applications in Europe, and derives conclusions about likely revenue streams for Galileo commercial services.

The technical component of this thesis, the “RAIM Study”, considers how Galileo is likely to perform in an environment in which GPS is offering dual-frequency free-to-air signals. Taking the often observed phenomenon that if there is a way to get a useful service for free, somebody will find a way to get it, this thesis concentrates on the use of RAIM techniques to provide an alternative to Galileo’s controlled-access integrity signal. This study compares the likely performance of an advanced RAIM algorithm developed by the author with the specified performance for Galileo’s commercial and safety-of-life services.

The conclusions of these two studies together strongly support the problem statement presented in the previous section. It is therefore recommended that potential investors in the system and other agencies involved in funding and specifying the Galileo system should call for a removal of signal integrity dissemination from within the Galileo specifications.

1.5 An Introduction to RAIM

Given the central role that the concept of Receiver Autonomous Integrity Monitoring has to this thesis, it is worth presenting a brief introduction to RAIM at this point, although it is discussed more fully within the RAIM Study.

As mentioned previously, the provision of signal integrity from within the Galileo system itself is seen as a key differentiator between Galileo and GPS. In this context “Integrity” is defined as:

“...the trust which can be placed in the correctness of the information supplied by the total system. Integrity includes the ability of a system to provide timely and valid warnings to the user when the system must not be used for the intended operation”.

Section 5.4.2 provides a fuller explanation of the meaning of this definition. In simple terms, Integrity is the property that someone using the system for a safety-critical purpose, such as landing an aircraft in poor weather, needs to have confidence that if something goes wrong and their estimate of position (i.e. altitude) is incorrect, they will be given correct and timely warning.

It is possible to provide integrity through some kind of external augmentation system (for example, the WAAS and EGNOS systems

referred to previously) or, as is currently defined for Galileo, by building it into the system specifications from the outset. The problem is that any such system is inevitably expensive, with its need for multiple redundancy in all critical systems including wide area communications networks, software developed to the most exhaustive level of test and validation and, most critically, with extremely demanding specifications on time to alarm (TTA). The Integrity Justification Study within this thesis demonstrates this point.

An alternative method of providing signal integrity information is through Receiver Autonomous Integrity Monitoring techniques. These algorithms rely on users being able to access more satellites than the minimum number required for a navigation solution, in order to estimate the integrity of the signal from these redundant measurements. Currently, with a GPS constellation of 24 satellites providing only a single frequency in its Standard Positioning Service (SPS), RAIM cannot meet Category I requirements for aviation precision approach, although RAIM-enabled receivers can be used as a navigation aid for less demanding phases of flight. However, by using both Galileo and upgraded GPS systems together the quality of the integrity information available from RAIM algorithms will increase dramatically, due to both the increased size of the useable constellation and the improved accuracy of the signals compared with current GPS.

The idea that the relatively simple methods that underpin most RAIM algorithms could be used as an alternative to the complex, monolithic integrity determination systems mentioned above is quite divisive within the GNSS world. On the one hand, there is an argument that the best place to evaluate the quality of a user's position solution is at the receiver itself, enabling both local effects and system-level faults to be detected, which implies the use of some form of RAIM. On the other hand, the argument is made that with a wide network of ground receivers a dedicated integrity determination system should always be able to detect a potentially hazardous error on a broadcast signal before an individual user's RAIM algorithm.

This thesis attempts to evaluate the likely performance of RAIM algorithms in a future GNSS environment in which users have access to signals from more than one system simultaneously. This over-determination of the navigation position solution from the large number of received ranging measurements potentially allows users to apply RAIM to a level appropriate for aviation precision approach.

1.6 Structure

The structure of this thesis is intended to allow the two discrete studies discussed previously to be read and understood in isolation, if required.

- Chapters 2 and 3 provides the background to the “Integrity Justification Study”, along with a literature review and description of the methods used. This effectively identifies the state of the art for the cost benefit analyses for Galileo at the time this research was undertaken.
- Chapter 4 provides the results and conclusions for this study, including some simple financial analyses. Additional results from surveys undertaken for this study are provided in Appendix A.
- Chapter 5 provides the background to the RAIM study including literature search, whilst Chapters 6 and 7 describe the various tools used and assumptions taken.
- Chapter 8 presents a detailed processing model of the core functionality utilised in the various simulation tools and techniques used in the RAIM study.
- Chapters 9, 10 and 11 define, in some detail, the two RAIM methods (one well established, one novel) evaluated in this thesis, along with a numerical example for each. Chapter 12 presents the results obtained from various forms of simulation used to evaluate the performance of these algorithms.
- Chapters 13 and 14 discuss these results, and bring their conclusions together with the findings from the Integrity Justification Study. These lead to some recommendations, including identification of scope for further work.

1.7 Originality of Work

Throughout this thesis extensive references are made to other people’s work, and to work produced by the author when working as part of a team. As a result, it is not always immediately apparent what elements of the subsequent text, and associated figures and tables, are original work produced by the author in the context of this thesis. To provide clarity this section lists those elements of this thesis which the author does not claim as original work.

The following figures and tables have been taken from the GALSAS study [1], for which the author was co-credited, but which are not claimed as original results for this thesis:

- Figure 4-2
- Table 3-1, Table 4-1.

In addition, text appearing in Sections 2.3, 3.2, and 4.2 is largely taken from the GALSAS study report, for which the author can only claim partial credit.

The following figures and tables have been taken from GEMINUS [2] GALA [3], and Inception study [4] documents or ICAO requirements documents:

- Figure 3-1, Figure 3-2, Figure 4-3, Figure 4-4, Figure 4-7.
- Table 4-2, Table 5-1, Table 5-2.

Within the RAIM Study, the following figure is taken directly from the GALA study describing the Galileo baseline Integrity system:

- Figure 5-1

Also within the RAIM Study, when describing the Least Squares Residuals, Marginally Detectable Errors and Errors in Variables RAIM methods, a number of equations and some explanatory text has been taken directly from the source documents referred to in the corresponding sections. Sections within this thesis which use equations and text in this way are:

- Sections 9.1, 9.2, 9.3, 10.1 and 10.2.

Any other direct quotations from source documents are clearly marked and attributed in the text.

The software and simulation tools used in the RAIM study have been developed either by the author, or under the direction of the author. Specifically, all prototype tools developed in Excel or Matlab were produced by the author, whereas the further development of these tools as C++ or Matlab applications were produced by the author's colleagues at VEGA, as previously acknowledged. The underlying specifications for all of these tools were defined by the author, and are as given in the detailed processing model and RAIM method definition sections of this thesis. The author acknowledges that these tools were coded with an elegance and efficiency for which he has boundless admiration.

These software and simulation tools are held by VEGA Group plc (www.vega-group.com) and could be made available under licence to any interested parties, on request.

2. BACKGROUND TO THE INTEGRITY JUSTIFICATION STUDY

2.1 Introduction

When the European Council of Transport Ministers failed to endorse the European Commission's proposals for the full-scale development of Galileo at their meeting on 20th December 2000 the most critical open question regarded the plans for a PPP. Specifically, the Council demanded evidence that the programme would be sufficiently attractive to private investors that public funding for the project could be capped. The EC position paper presented at this meeting presented a cost and funding profile for the programme that showed a total cost of 3.25 Billion Euro up until 2008, of which 1.5 Billion Euro were expected to come from the private sector. In addition, annual running costs of 225 Million Euro were presented as an additional cost that the private "Galileo Vehicle Company" (GVC) would be expected to cover.

2.2 The PwC "Inception" Study

Similarly, when the Council of Transport Ministers again failed to agree on plans for the next phase of the Galileo programme in December 2001, the major cause was the then recently published "Inception" study [4], performed by a team led by PricewaterhouseCoopers (PwC), which concluded:

"...our analysis shows that the economics of Galileo do not support investment by the private sector on purely financial criteria, but that the benefit to the European economy should be significant. The reason is a market imperfection. Many of the benefits, such as improved efficiency in the use of airline fleets, are likely to accrue to consumers rather than be captured by the industries that use Galileo services, because competition will ensure that the value cannot be realised in higher prices. Industrial users of the service will not therefore be able to increase margins to make a payment to the Galileo operator. There should however be a case for the public sector to promote Galileo if it can do so at a cost which represents value for money for the economy as a whole taking account of the wider economic and strategic benefits."

As will be discussed subsequently, the Inception study goes on to propose a PPP based on a "Concession Company Model", in which an annual "Level of Availability Payment" (basically, a service charge) is made from public funds to the GVC (or "Concession Owner"). The amount of this payment is related to the amount of public funding provided for the development and deployment phases (e.g. with 0.8

Billion Euro public funding of deployment costs, the Level of Availability Payment would be about 390 Million Euro per year. With 1.4 Billion Euro public funding of deployment costs, the Level of Availability Payment would be about 270 Million Euro per year).

In January 2002, and in preparation for the eventually decisive meeting of the Council of European Transport Ministers in March 2002, the European Commission issued an "Information Note" on the Galileo programme. Although not explicit in the amount of private funding the EC envisages the project requiring, and whilst proposing a funding mechanism at odds with the conclusions of the Inception study (the EC preferring a "Joint Undertaking", for which Galileo required the first such company structure to be set up under Article 171 of the Treaty under which the EC operates), the overall costs to deploy and operate Galileo broadly agreed with PwC's estimates.

This thesis will demonstrate that such a high level of annual public payments or private investment is both implausible and unnecessary; the design of Galileo arising from the CSS and GalileoSat studies contains elements which add significant cost to the system but, in practice, will offer little direct benefit to users. Specifically, the proposed Integrity Determination System (IDS¹), which in many ways is currently driving the whole system architecture, offers no functionality that cannot be more easily achieved at user-segment level by combining free-to-air signals from Galileo with those from GPS. As a result, in its incarnation at the time of writing, Galileo will not gain sufficient private investment to be viable.

2.3 Galileo Structural Analysis Survey (GALSAS)

The technical component of this thesis is put into context by combining its results with the satellite navigation market analysis study performed as the non-technical component. The Galileo Structural Analysis Survey (GALSAS) provides information on current and forecast markets for various satnav applications, and these results are used to estimate revenues for the different architectural cases analysed in the technical component.

The European Commission contracted the study "Structural Analysis of the European Satellite Navigation Application Segment" [1] to obtain an improved understanding of the European satellite navigation market and

¹ In a major revision to the Galileo architecture in December 2001, the IDS as a discrete element was removed from the baseline. However, the functionality remains, with the earlier "Integrity Control Centre" and "Navigation Control Facility" now combined into a "Mission Control Facility". Although the term IDS is now not used in the Galileo programme, it is kept in this thesis because it covers the functionality whose value is questioned, rather than physical elements of the system.

the driving forces for future market development. The major objectives of the study were to provide:

- Market segmentation and structural characteristics of the downstream value chain of the service supply segment
- An outline of future development scenarios regarding the European satellite navigation industry over the next 10 – 15 years putting particular emphasis on the intended GALILEO programme
- Recommendations concerning improving and sustaining Europe's competitiveness in the area of satellite navigation as a conclusion of the analysis.

The study, which was executed by TECHNOMAR and its partners VEGA and METAMARKET during 2000, is based on extensive field research; nearly 100 face-to-face and telephone interviews with suppliers of satellite navigation based products and services, authorities and additional experts were conducted. During these interviews the market figures collected from various studies were completed and checked for plausibility. Additionally, an Executive Seminar to deepen the study findings was held with representatives from industry.

This study provides an objective and independent market-oriented picture of the position of the European satellite navigation industry and its perspectives at the time of the early definition of the Galileo system.

From May – October 2000 the author was on the team responsible for the GALSAS study, and the results of this industrial and market survey provide a key input to this thesis, as discussed subsequently. Some elements of the description of methods and consolidated results have been taken directly from the published study report [1].

2.4 ESA GalileoSat Phase B and Galileo Phase B2

In November 1999 ESA issued the contract for the GalileoSat Phase B (System Definition) study (the Comparative System Study having effectively been the Phase A activity). This 20M Euro contract was not let competitively; instead, Alenia Spazio of Italy was encouraged by ESA to form a consortium comprising nearly 50 different countries from all over Europe, and work-packages were issued to these countries in order to meet the ESA principle of *juste retour* for financial contributions from member states. Within the GalileoSat Phase B study the author, representing VEGA Group PLC of the UK, led a team of technical staff from which produced a number of documents which together comprise the Operations and Integrated Logistics Support (ILS) Analysis for GalileoSat Phase B.

In August 2001 the next phase of ESA's programme began. Since this phase was not yet a full development/deployment phase (Phase C/D in ESA terminology), and since the terms "Galileo" and "GalileoSat" had caused confusion in the earlier studies (GalileoSat being specifically the ESA programme), the new contract was entitled "Galileo Phase B2". Once again awarded to Alenia Spazio, although now acting in a joint venture with Alcatel Space Industries of France, Astrium GmbH of Germany and Astrium Ltd of the UK, known collectively as "Galileo Industries" (GalIn). Again, the author led a multi-national technical team, this time on the development of the "Operations Support Requirements Document" (OSRD) for Galileo.

These activities provided the design information and performance specifications that are used in development of the arguments in the conclusion of the Integrity Justification Study.

2.5 Other Studies – GALA and GEMINUS

Although a number of studies purporting to be market assessments, cost benefit analyses and service definition for Galileo have taken place since the June 1999 Declaration to proceed with Galileo's definition, the most prominent (along with "Inception") are GALA (Galileo Overall Architecture Study) and GEMINUS (Galileo system and service definition).

As stated in [2], the objectives of GEMINUS were

"to provide:

- *A review of existing and new user requirements investigations;*
- *A comprehensive list of institutional requirements;*
- *A comprehensive list of economic and financial requirements and recommendations required for the implementation of the ad-hoc financial mechanisms;*
- *Timely inputs to the Galileo Program Management Board for coordination with the PPP approach."*

The GALA study was decomposed into a number of work packages. The most significant for this Integrity Justification Study are:

- WP 1 Market Research Methods and Overall Results;
- WP 2 Overall Requirements and System Trade-Offs;
- WP 9 Programmatics and Business Issues.

The intention was that GALA and GEMINUS combined would produce a set of Galileo service specifications, along with system-level requirements and a high-level system architecture, closely aligned with the needs and market prospects of satellite navigation system users.

These two studies were undertaken in parallel, with activities within both GALA and GEMINUS intended to ensure the consistency of the results. The extent to which this was achieved is debatable. There is much overlap in the scope of the outputs from both studies, and the terminology used, for example to define services, is inconsistent across the studies. Nevertheless, these studies were used to produce Galileo Mission Requirements and System Requirements documents on which the subsequent Galileo Phase B and Phase B2 activities have been based. A critical conclusion derived from these studies is that Galileo needs an Integrity Determination System included within its architecture [3].

The Integrity Justification Study described in the following sections provides a critique of the methods used to form this conclusion.

3. METHODS AND LITERATURE (INTEGRITY JUSTIFICATION STUDY)

3.1 Introduction

This section of the thesis brings together various assessments of the market for satellite navigation applications in order to derive conclusions relevant to the problem statement for this thesis. Two surveys undertaken by the author (for the GALSAS Study and the UK Industrial Space Committee's "Galileo Working Group") provide the primary research for this section. In addition, results from the Inception study have been analysed, and the business case reproduced using an architecture without an Integrity Determination System. Other relevant reports and working notes arising from the GALA and GEMINUS studies have also been analysed, with key results presented subsequently.

Inevitably, the process of selectively extracting quotations, figures and opinions from a limited number of study reports and interviews in order to support a problem statement cannot be presented as objective and definitive evidence. However, it is hoped that the methods used in this section demonstrate a logical argument regarding the way the Galileo architecture has developed, and how this architecture is inconsistent with the other demands on the programme.

Section 4 presents the results arising from the primary research and literature survey conducted in this part of the thesis, concluding with a consolidation of these results into a logical argument that links this Integrity Justification Study with the subsequent RAIM Study.

3.2 The GALSAS Study

The results from the GALSAS study presented in Section 4 have been derived using two distinct methods:

1. "Primary Research", i.e. the results from face-to-face and telephone interviews conducted by the author, some of which are presented in summary form at Appendix A;
2. "Consolidated Research", i.e. results presented in the Structural Analysis Survey final report, which brought together the primary results from a number of researchers and derived a number of estimates regarding the likely market for GNSS applications over the next two decades.

3.2.1 Primary Research Interview Guidelines

The primary research interviews were conducted following simple interview guidelines with the following headings:

- Profile of the company
 - GNSS related product or service programme
 - Brief description of the programme content
 - The company's position within the satnav value-adding chain
 - Geographical area of related business activity
 - When were these activities started?
 - Motivation of the company to enter the GNSS market
 - Intended further extension of activities (what, when, why)
 - Core business activity of the company and strategic links to GNSS activities
- Company data
 - Total employment
 - Total turnover
 - Independent company or subsidiary/part of a group of companies
- Competitive Environment
 - What or who are the major competitors of the company in the relevant market segment?
 - What is the market position of the company and of the major competitors (market share or ranking; are there any companies dominating the market? Which ones?)
 - What does the company expect as the development of the competitive environment? Will there be new suppliers and for what reasons, e.g. motivation for entering the GNSS market, core business and links to GNSS, strategic orientation?

- How does the company expect the future role of the European satnav industry in the relevant market to develop? Differentiate between receiver, system, and service suppliers.
- Market Data
 - Company's market estimates (by country, European, global): market potential, current market volume, mid-term trend.
- Technology
 - How far do the current GNSS systems (GPS, GLONASS) or any other relevant navigation sources such as Loran, or GSM extensions NOT meet the requirements in the market segments covered by the company? What are the major deficiencies to be improved?
 - What are the expected mid- to long-term technological trends influencing market development in the market segments/applications covered by the company, e.g.
 - Reduction of currently existing technical market barriers
 - New product solutions
 - Extension or alteration of existing applications due to new or improved product solutions
 - New/additional applications
 - New service concepts expected due to new or improved products and technological trends
- Market trends and factors
 - Introduction or modification of regulations, legal measures, etc. requiring or stimulating a new application of the GNSS signal (navigation, positioning, timing etc.), particularly in the transport sector, e.g. road pricing, Free Flight, etc.
 - Emergence of new product or service markets using GNSS as a component
 - Development and introduction of new applications by the users themselves, e.g. telematic systems, mobile communication services

- Mid-term trends related to costs/prices of the relevant products and services
- What are the factors hindering market development?
 - Technological factors (on GNSS side, on user side), e.g. accuracy, availability, etc.
 - Economic factors, e.g. product price, service fees, etc.
 - Regulatory factors (standards, regulations, etc.)
- What should be done to reduce these barriers?
- What are the basic requirements (e.g. completed certification, agreement of frequencies, etc.), and what time would be required to launch a new Galileo based product / service on the market?
- Market reaction to the introduction of Galileo
- Conclusions

Results from this survey are presented in Section 4.1

3.2.2 Consolidated Research

The following description is taken *verbatim* from the final report of the Structural Analysis Survey [1].

“The data collection phase of this study was performed as follows:

- **Desk research**
 - *Evaluation of relevant literature, market studies provided by DG TREN or previously produced by members of the study team;*
 - *Database research to collect additional market information, suppliers of satnav products and services, and to identify those market players to be interviewed during field research*
- **Field research**
 - *Face-to-face interviews and telephone interviews with:*
 - *Suppliers of GNSS-based products and services*
 - *Major users of GNSS-based products and services*
 - *Industrial associations*
 - *Research institutes*
 - *Regulatory bodies and supervisory authorities*

- *Governmental institutions and agencies*
- *The interviews have been conducted by the members of the project team with industry managers or officers in charge of the company's or authority's GNSS related activities, i.e. usually the marketing or business development manager in the case of suppliers.*
- *In accordance with the objectives of this study, i.e. a qualitative analysis of the satnav downstream value chain, an informal approach has been adopted rather than data collection based on a standardised questionnaire. Each interview had to be adapted to the specific market involvement of the respondent*
- *Within each market segment face-to-face and telephone interviews were conducted with major players, including the market leaders with the European industry, and some less important players to achieve a representative sample. The structure of the interviews related to market activities and location of the interviewees is summarised in the table below. Additional telephone interviews not included in the list have been conducted with users and distributors of related products to identify market players and to check market or technical details.”*

Aviation	10	Germany	34
Maritime	5	France	19
Rail	4	United Kingdom	17
Car nav + telematic services	19	Spain	11
Fleet management	14	Italy	9
Surveying, augmentation	12	USA	3
Agriculture, timing	4	Belgium	2
Mobile communication	10	Sweden	1
Leisure	4	Denmark	1
Chipsets, receivers	2	Switzerland	1
Authorities, R&D, associations	10		98
Others (GNSS-Systems, etc.)	4		
	98		

Table 3-1: Distribution of surveys, by market segment and nationality

N.B. Of the interview reports identified above, the seventeen attributed to UK organisations (i.e. 17.3% of the total field research activities in the GALSAS study) were performed by the author of this thesis. The remainder were undertaken by other GALSAS study partners. The results from this consolidated research are presented in Section 4.2 of this thesis.

3.3 Inception Study

The PriceWaterhouseCoopers (PwC) Inception Study [4] has two main sections: “Business Plan” and “Structure, Procurement and Finance “. Although both sections are of some interest for this thesis, only the business plan has been analysed in detail.

The Inception study presents independent estimates of the costs of the various phases of the Galileo programme, and revenues from a list of potential markets and applications. From these estimates, a business plan is developed, concluding with recommendations regarding the amount of public subscription likely to be required in order for Galileo to have a credible business case to attract private investment.

Although the results of the Inception study have already had a profound effect on the Galileo programme, the study did not adequately address the question at the heart of this thesis, i.e. is there sufficient justification for including an integrity signal in the Galileo architecture, from a business perspective. The study does include a brief discussion of alternative means of providing global integrity information (the implication being that the case for a European-only integrity determination system is taken for granted), but concludes with the statement:

“... there is insufficient basis for determining whether or not the lack of a global integrity service will affect the take-up of Galileo at all, still less for estimating the extent of such an impact.”

Section 4.3 of this thesis attempts to undertake such an analysis. A simple Excel spreadsheet was produced which was intended to reproduce the Inception results, and which could then be used to model alternative assumptions. This spreadsheet has three distinct components:

- A section in which the assumed costs are stated year by year from 2002 to 2027, for the Development, Deployment and Replenishment Phases, plus recurring Operations costs. These are summed by year to produce the total pre-finance cost figures per annum;
- A section in which the assumed public funding is stated, per year from 2002 to 2006 or beyond (depending upon the case being analysed). These are then combined with the Costs figures to determine the annual public funding shortfall;
- A section in which assumed rates for the cost of finance and the mean rate of tax on profits are stated, along with the assumed annual revenues. These are combined to generate a cash flow forecast.

The final step is to use Excel's "IRR" function to estimate the Internal Rate of Return corresponding to the cash flow forecast. The results from the preceding steps are plotted as the various figures presented in Section 4.3.

Note that this is a far simpler model than is actually used by the Inception study. Specifically, the handling of tax and finance costs have been simplified, and the assumed rates (12% for finance, 20% for tax) are intended to be indicative, and have no supporting justification. This analysis is intended to present a *relative* quantitative analysis, rather than a definitive statement on the amount of public funding required to support the architectures analysed in Section 4.3 (i.e. the baseline case presented in Inception, and a "No Integrity" case in which the capital and operating costs associated with the IDS have been removed, as have the service revenues the Inception study associates with the Safety of Life and Commercial Access services).

Internal Rate of Return is a well known method for comparing the effective interest rate on a set of cash flow figures. IRR is the metric used in the Inception study to compare different assumptions regarding the financial structure of Galileo, and is therefore also used in this thesis to consider the effect of alternative assumptions.

3.4 Other Studies – GALA and GEMINUS

3.4.1 GALA WP 1 Market Research Methods and Overall Results

Figure 3-1, taken from [5], presents an analysis of the number of user applications with a given accuracy/integrity requirement – the bigger the circle, the larger the number of applications. Note this refers solely to the number of applications, not the value of the market or number of users.

In GALA, four basic classes of user were defined from the studies of the user needs, as shown in Figure 3-1:

- Position, Velocity and Time (PVT) – This basic class covers mass market applications. The associated service is intended to be delivered free of service charges (following the assumption that GPS continues as a free service)
- Accuracy and Integrity (AI) – This class is defined to provide high accuracy and availability for less demanding safety of life users and professional markets. The service is intended for subscribed users only.
- Ranging and Timing (RT) – This class is for users with very precise ranging, positioning and timing requirements, i.e. for the

knowledgeable professional. Again this service is intended for subscribed users only.

- High Integrity service (HI) – This class of users require the highest integrity, availability, continuity and resistance to signal interference. The associated service is suitable for demanding safety of life markets. Access to this service would be restricted to trusted subscribers.

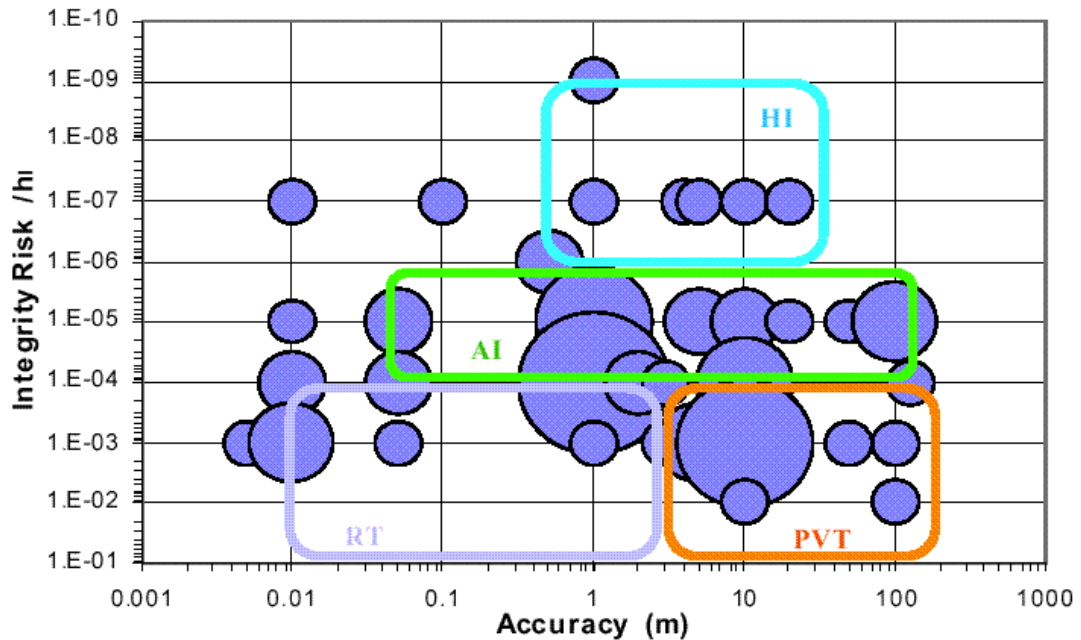


Figure 3-1: GALA Classification of User Classes by Accuracy and Integrity Requirements [5]

Inevitably, this method of grouping requirements into service classes is rather coarse. Specifically, this approach does not take into account user's Continuity requirements, which in some applications (such as aviation precision approach, as discussed subsequently) drive the overall system performance as much as accuracy and integrity risk.

The GALA "Market Research Methods and Overall Results" document² [6] presents a detailed discussion of the number of applications, and associated revenues, expected within each service type. A "bottom-up" approach was taken, in which one hundred discrete applications for satellite navigation services were identified, the associated performance requirements (accuracy, integrity, availability, etc.) were derived, and

² also referred to as the WP1 Report, because it presents the results from GALA Work Package #1

likely market revenues estimated. By consolidating the results for each application, the likely market for these four basic user classes were presented.

This GALA document also includes a brief analysis of the potential threat on Galileo revenues from competition from combined Galileo and GPS free-to-air services. Although the WP 1 document does recognise that this is a significant threat to the potential business case for Galileo, it doesn't give this issue the emphasis it may deserve.

3.4.2 GALA WP 2 Overall Requirements and System Trade-Offs

Within the GALA Work Package 2 activities, the key document relevant to this thesis is a report entitled "Integrity" [3]. This document, produced by Alcatel Space Industries, presents an analysis of the options available for the provision of integrity to users of Galileo, and is the cornerstone of the justification used to include the IDS in the system baseline.

The key conclusion stated in this report is:

"For some applications simple RAIM techniques may be sufficient to achieve the require [sic] performance, but to reach higher requirements an external monitoring of the Galileo satellites integrity will be necessary."

This conclusion is derived from the analysis of a risk model in which the ground-based integrity system and the RAIM algorithm are treated as separate "integrity barriers" which, when combined, yield a lower value for the total user integrity risk than a model using either of the "integrity barriers" alone.

However, there is an unstated assumption, which is prerequisite for the conclusion to be valid: in order for a system with both "integrity barriers" to be better than one with RAIM alone, the ground integrity channel must:

- a) be able to detect integrity failures that the RAIM system would not; and
- b) provide this increased integrity without significantly increasing the false alarm probability.

The only evidence presented in this document to support the argument for an IDS is the statement:

"...the response of user integrity monitoring techniques (like RAIM) to the failure of more than one satellite is often unpredictable; which confirms the need to monitor from Ground Mission Segment each SIS individually."

Although it is true that for traditional RAIM algorithms it is theoretically possible for multiple failures to combine in such a way that a protection limit is exceeded without an alarm being generated, this situation is very unlikely [7]. This statement therefore adds little weight to the case for an IDS.

Annex 4 to GALA WP2 [3] is, perhaps, the most directly relevant report to this thesis arising from all the preceding Galileo development activities. This report, “Galileo System Definition – GPS integrity monitoring assessment” [8] by Dr Washington Ochieng and his team at Imperial College, London, was produced for Alcatel Space Industries under GALA WP 2.2.2.4.

Dr Ochieng’s report undertakes an analysis very similar in scope and approach to the RAIM study component of this thesis. Unfortunately, both this report and the WP 2 “Integrity” document to which it is appended have not been placed in the public domain, making it inappropriate to use as the key reference document for this work that it deserves to be. However, a number of papers derived from this work have been published, and these are discussed in Section 5.8.3, within the RAIM Study component of this thesis.

3.4.3 GALA WP 9 Programmatics and Business Issues

Under GALA WP 9, Astrium UK produced a document entitled “Galileo Cost-Benefit Analysis” [9] which makes an interesting comment on the potential market for integrity-based services:

“There have been several comments made that Galileo is being design too much as a GPS look-alike and so competing on equal terms with a free service. This leaves the main differentiators as integrity and service guarantees which are attractive only to a small fraction of the market. In addition local services provide some level of integrity for many user groups.

If Galileo could adopt a signal design that was more attractive to the larger market sectors then there may be some scope for charging or at least being able to charge a reasonable royalty. The most promising markets are probably the in-mobile market and the in-vehicle market. A signal, for example, that was useable inside a jacket pocket or a handbag would be have [sic] advantages over GPS. In addition TTFF [Time to First Fix] and reacquisition time are key parameters where improvements could be offered.”

This comment demonstrates a key point: those involved in defining the Galileo architecture have, to some extent, specified services to

differentiate Galileo from GPS, only because they will differentiate the systems, and not because there is any clear evidence that the market needs these services.

3.4.4 GEMINUS

The GEMINUS Study produced a number of detailed reports covering a broad spectrum of issues under the study's remit. The key deliverable items relevant to this thesis, and hence analysed in detail, are:

- Deliverable D4 "Service Definition" – Annex D to the Final Report
- Deliverable D6 "Business Model" – Annex E to the Final Report
- Ad-Hoc Working Paper Assessing the Commercial Opportunities for the Galileo Operator – Annex F to the Final Report
- Deliverable D1.1.2 "GALA User Requirements Review"
- Deliverable D2.2 "Operator's Requirements"
- Deliverable D8.2 "GEMINUS Final Summary Report" [2]

Unlike GALA, GEMINUS took into consideration what performance specifications are feasible for a satellite navigation system when defining its proposed set of services and concluded that Galileo should provide:

- OAS-1: A global Open Access Service, which meets public requirement for basic free of charge service – single frequency, similar to current GPS. Matches or improves on GPSIII and/or GPSIIF;
- OAS-2: A global Open Access Service, which meets public requirement for a fuller free of charge service – multiple frequency. Matches or improves on GPSIII and/or GPSIIF;
- RSS: Regional Safety Service, a commercial safety service, unencrypted and charged for through institutional means rather than direct user charge. Meets needs of aviation over Europe as a minimum.

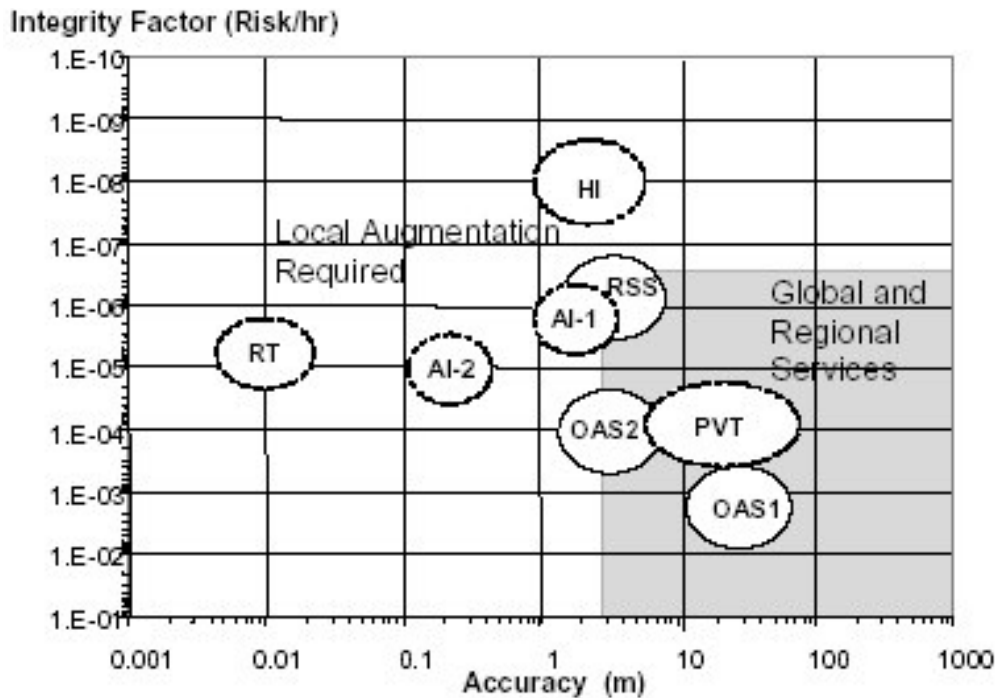


Figure 3-2: GEMINUS and GALA Galileo Services [2]

Figure 3-2, extracted from the GEMINUS final report [2] shows:

“...a comparison of the GEMINUS proposed service with GALA WP1 service requirements...The Integrity and Accuracy figures from the GALA WP1 study (broken bubbles) are the figures required by the market whereas the figures from the GEMINUS study (solid bubbles) are the figures that approach the user requirements - but which are also technically feasible, without any local augmentation or RAIM integrity protection.”

The GEMINUS services are defined in more detail in Deliverable D4 “Service Definition” – Annex D to the Final Report, in which the requirements for the Regional Safety Service (the service most relevant to this thesis) are specified as:

- Vertical Alert Limit: 10 – 15m;
- Horizontal Alert Limit: 7.5 – 12.5m;
- Integrity Risk: 1×10^{-6} per hour;
- Continuity Risk: 2×10^{-3} per hour;
- Availability: 99.75%

As will be discussed subsequently in the RAIM Study section, these requirements are broadly in line with the specifications for aviation precision approach (with the exception of the Continuity requirement, which is considerably less stringent than is required for aviation). The Final Report [2] also states:

“It was agreed that limiting the scope of regional Galileo services to meeting Cat I requirements was reasonable, as CAT2/3 will be achieved by local augmentation.”

The GEMINUS Study is therefore explicit in associating the most demanding requirements on Galileo with Category I precision approach.

3.5 UKISC Galileo Working Group Survey

In October 2001, the author took an action at a meeting of the “UK Industrial Space Committee, Galileo Working Group” (UKISC Gal WG) to produce a list of “challenging questions” regarding the justification for the Galileo system. By attempting to form a consensus on the answers to these questions, the UKISC Gal WG hoped to be in a position to provide a robust justification for the development of the Galileo system in the event of wavering support from within UK Government. Unlike the majority of activities associated with the Galileo project, this exercise had no acronym associated with it, labouring instead under the cumbersome title “Galileo – Key Questions For Which We Ought To Have Good Answers”.

The author produced a set of questions which was distributed to the members of the Working Group. These questions were:

- 1. Why do we need Galileo? In what way is GPS augmented by EGNOS inadequate? What will Galileo offer above GPS + EGNOS?*
- 2. What services are planned for Galileo? What performance does Galileo promise, and how does this compare with plans for GPS upgrades, and the position location functions of 3G telecomms systems?*
- 3. Will Galileo offer a free-to-air dual-frequency service, of similar performance to that expected from GPS Block IIF?*
- 4. How does the timescale for Galileo deployment compare with plans for competing satellite and terrestrial positioning systems?*
- 5. How much will Galileo cost European taxpayers? How much will Galileo cost UK taxpayers? What are the expected development, deployment and recurring costs? What are the current estimates of the required annual charge to taxpayers for Galileo as a ‘public service’?*

6. *What mechanisms will allow private investors to get revenue back from Galileo? What evidence is there that the Galileo system will attract private investment?*
7. *If the US accelerate their “GPS Modernization Program”, and/or increase the size of their constellation, would there still be a revenue stream for investors in the Galileo system?*
8. *Given that combined Galileo/GPS free signal receivers will inevitably be produced, and that the projected positioning accuracy of such receivers exceeds the projected specifications for any of Galileo’s satellite-only services, what user groups are expected to be willing to pay for Galileo’s commercial services? How big is this projected market?*
9. *Who is the customer for the Galileo system (as opposed to its services)? Who is ensuring that the service specifications meet real-world requirements, and that development costs are minimised? Who will ensure that it’s not another Channel Tunnel or Concorde – technically brilliant but unable ever to cover its development costs from commercial operations in a competitive market?*
10. *What plans are there for Galileo to be used by European military forces as an alternative to GPS? Will it offer some form of “protected” signal for authorised users? If Galileo is to be operated as a commercial venture, what controls will there be on access to this protected signal by forces other than those of the Western European Union? Will US forces be given access to such signals? Russians?*
11. *The US retains the right to turn SA back on to prevent GPS being used against US interests. On what services will Galileo have the same facility? How is this reconciled with Galileo’s “guaranteed availability” which is meant to differentiate Galileo from GPS?*
12. *Much store is made of the claim that Galileo will provide some ‘liability cover’ for users. What are the technical, legal and financial implications of this requirement? What evidence is there that such cover adds value to the system?*
13. *What test will be made of the commitment for private investment to Galileo? When is this test likely to be undertaken? How much public money will be spent on the programme before this test? If the outcome of the test is that there is not enough private investment forthcoming to take the system to full deployment and operations, what options are available to the EU? Are the strategic arguments in favour of an independent European satellite navigation system so strong that deployment of the system would continue even if private investment was not forthcoming?*

14. *From the point of view of the various consortia apparently considering investing in Galileo, the best strategy might be to support and direct the development of the programme without making any major financial commitment to its future, until it has passed the point of no return at which time they can choose not to invest, knowing that the system will be deployed entirely from public money. What plans are in place to defend the programme against such a strategy?*
15. *Given that the case for Galileo is basically 'strategic' (in a political, rather than a military sense), what are the arguments for and against Galileo as an entirely public-funded programme from the outset?*
16. *Which end-user groups are actively involved in defining the requirements for Galileo? How much demand has the European transport market shown for an alternative to GPS?*
17. *Given that GPS and WAAS/EGNOS is expected to become a standard fit on civil aircraft over the next few years, how does the civil aviation community, in Europe and globally, view Galileo?*

Since respondents to this set of questions were supplying opinions to the Working Group, it is not appropriate to present their responses as attributable quotations within this thesis. However, the responses fall broadly into two camps

- Those representing potential Prime Contractors for spacecraft, ground system and receiver development activities (the "Primes" view);
- Those representing smaller companies, or organisation closer to the service delivery aspects of the programme, rather than hardware manufacture (the "Non-Primes" view).

A summary of the responses for these two positions is presented at Appendix B. These results also influence the logical argument presented as a conclusion to the Integrity Justification Study, in Section 4.4.

4. RESULTS FOR THE INTEGRITY JUSTIFICATION STUDY

4.1 Results from the GALSAS Survey – Primary Research

In Appendix A, a summary of the interview reports produced by the author as part of the GALSAS study [1] are presented. Although not the complete set of survey results, this representative sample is sufficient to demonstrate the conclusions from this survey of organisations involved (or potentially involved in the future) with UK satellite navigation applications summarised below:

1. Applications developers expect a fairly rapid surge in the number of installed GPS receivers (mobile phones, vehicles, etc.), and that the next stage in the market's development will be based around applications sold without a bundled receiver. This requires some kind of interface standard to be developed;
2. Galileo must be sufficiently compatible with GPS that any applications developed and intended to use a standard "GPS interface" could also be connected to the output from a Galileo receiver;
3. Galileo is too far away to have an impact on most application developer's strategic thinking. From their current understanding of the system, the market for the Controlled Access Services will be very limited;
4. In order to succeed, Galileo receivers need to be cheaper than GPS, or the OAS needs to offer better accuracy and availability than GPS;
5. A key opportunity for improvement would be in-building performance. The in-building performance of GPS is a weakness; if Galileo can offer better performance in buildings and in built-up areas, this would be a significant advantage;
6. The drivers for change in the GNSS market are integrated GNSS/comms receivers, and the increase in uptake of in-car GPS;
7. There is a huge potential market for location-based services, which require integrated comms and navigation receivers;
8. Now that SA has been turned off, and with the introduction of WAAS, EGNOS, etc., GPS offers some advantages over cellular-based location systems, and this will be exploited in the next few years;
9. Within the US, the availability of the GPS signal has been accepted as a "given" – it is unthinkable that it will ever be turned off or

significantly degraded. As a result, for non-safety critical applications, the mass market will only choose Galileo receivers ahead of GPS if they are cheaper, more accurate, smaller or require less power; the higher availability, integrity and guaranteed service features of Galileo do not in themselves offer a marketing advantage;

10. In order to penetrate markets established by GPS, Galileo receivers must be compatible with GPS. This will offer enormous benefits to users, but will make it difficult for Galileo to market chargeable services, since the accuracy and availability possible from GPS/Galileo OAS combined will meet the needs of the vast majority of mass-market location service applications.
11. With SA off, GPS offers the accuracy required by most mass-market applications – the next few years will see a major expansion in the number of GPS receivers installed;
12. Applications developed to provide services based on derived positioning information will require a standard interface, so that the application is independent of whether the positioning data comes from satnav, communications station triangulation or any other source. Any positioning system that does not comply with such a standard will not succeed;
13. The satnav market is expected to begin to accelerate once the integration of the receivers into the host (mobile phone, vehicle, watch, etc.) becomes transparent to the user (i.e. in terms of physical size, power usage/battery requirements, additional cost and user interface).
14. Operators of cellular telephone networks in the UK see a large market for Wireless Location Services, which require some position technology to be either built into the network, or into the handset itself;
15. Wireless Location Services now being introduced are based on network infrastructure (i.e. do not use satnav). With SA off, GPS offers a significant improvement in the accuracy available;
16. Mobile phone network operators see 10m accuracy as the limit for their requirements;
17. The major growth period for this market is expected to be well before the likely start of Galileo operations;
18. Although the better urban performance of Galileo compared with GPS is a marketable feature, it is unlikely that the Controlled Access

Service would be implemented as the Wireless Location Services technology by cellular network operators.

19. The UK Civil Aviation Authority (CAA) regard the Galileo programme as “not sufficiently user driven”, and this is a source of frustration. Based on their current understanding of the system, Galileo in itself does not offer any significant advantages over GPS with EGNOS and other augmentation systems;
20. However, Galileo in conjunction with GPS/EGNOS would provide a redundant, independent GNSS, which does offer the opportunity for greater reliance on GNSS (and, potentially, a scaling down in terrestrial navigation aids);
21. There is a significant concern about the use of “controlled access signals” on Galileo. Encryption of navigation signals, possibly with a “pay-to-use” mechanism for the decryption key, adds a number of failure modes and other complications to a safety-critical service which the aviation community is unlikely to support – especially given that the GPS/EGNOS signal will be free-to-air;
22. There is a strong probability that GPS and augmented-GPS based navigation systems will become *de facto* international standards, through the way European civil aviation standards and regulations set by the Joint Aviation Authority (JAA) and EUROCAE tend to follow behind equivalent American bodies. This could present a significant delay to the acceptance of Galileo by the aviation community, and in order to mitigate this risk European delegates to the International Civil Aviation Organisation (ICAO) should ensure that as regulations are developed for the use of GPS, these should be extended to include Galileo at the same time.

4.2 Results from the GALSAS Survey – Consolidated Results

The following results are presented *verbatim* from the Structural Analysis Survey final report [1].

4.2.1 Current Size and Structure of the European Market

*Market data compiled during the study indicate that the value of the current European satellite navigation market is in the order of **935 MEURO**; nearly 30 % of the world market in 1999. The market size is defined as sales revenue from product units or service packages, which make use of satellite navigation, e.g. car navigation systems, surveying systems, etc. About 85 % of the European market is product sales and the remaining 15 % is revenue created by GNSS related services.*

By far the largest market segment in Europe (and on the world market) is car navigation: about 680 MEURO, of which 88 % are hardware sales. Among the remaining market segments personal navigation, surveying, aviation, fleet management, and augmentation services show some market importance with about 40 – 50 MEURO each:

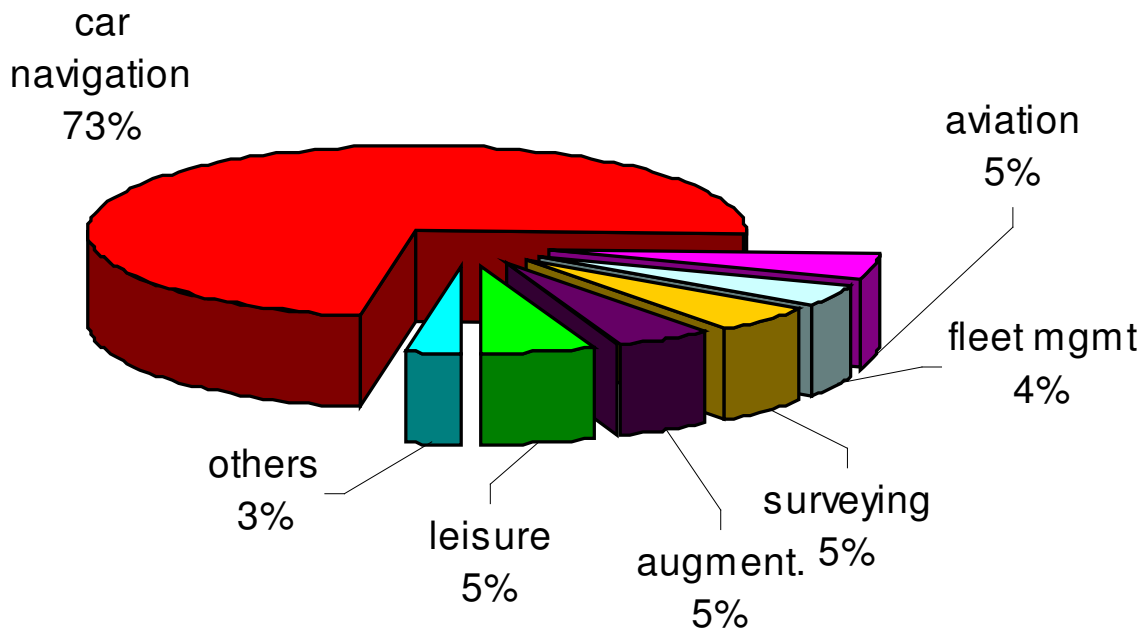


Figure 4-1: The European GNSS market by market segments – 1999: 935 MEURO

4.2.2 Mid-Term Trends In The European Market

The majority of GNSS applications and market segments are still in an early growth phase, thus considerable growth rates are expected in the mid-term, e.g. in agriculture, aviation, fleet management. However, saturation effects will start to reduce growth rates in a few years time in several major applications such as car navigation.

Both the size and the structure of the market may change dramatically in about 2 years from now depending on the further development of GNSS application in mobile communications. The introduction of location-based services by mobile communication service providers and the intended mandatory localisation of emergency calls in Europe (E-112) will boost the satellite navigation market, provided that GNSS is the localisation source of choice. Depending on the still to be defined technical requirements for localisation in mobile communication applications the total European satellite navigation market in 2005 could be in the order of:

- 2,800 MEURO (without GNSS localisation in mobile communication),
- 8,300 MEURO (partial GNSS localisation in mobile communication),
or
- 22,000 MEURO (mandatory GNSS localisation in mobile communication).

According to the assumptions and market expectations gathered during interviews the European satellite navigation market in 2005 will probably show a completely different picture to the current market: mobile communication will be the most important market segment with 72 % of the total market, followed by car navigation with 23 %:

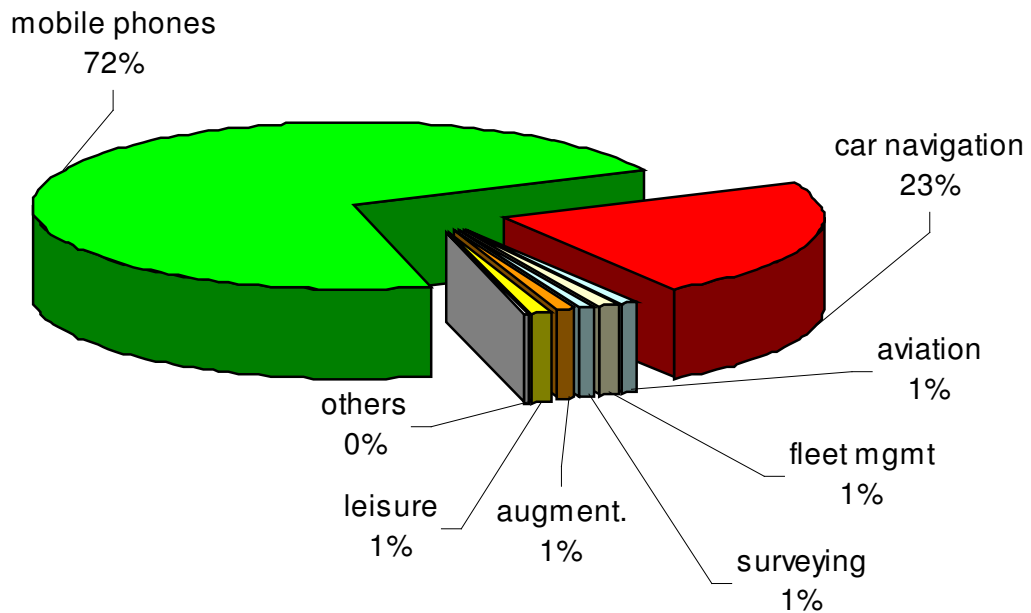


Figure 4-2: The European GNSS market by market segments – 2005: 8,383 MEURO

Market segment	European market: 1999 MEURO	European market: 2005 MEURO
<i>Aviation – products & services</i>	44	65
<i>Commercial maritime</i>	4	6
<i>Car navigation – products & services</i>	680	1 920
<i>Fleet management – products & services</i>	40	90
<i>Rail</i>	1	24
<i>Surveying & mapping, off-shore</i>	49	86
<i>Agriculture</i>	5	12
<i>Augmentation services</i>	45	60
<i>Mobile communication (excl. services)</i>	0	6 000
<i>Timing</i>	6	10
<i>Personal navigation</i>	50	90
Total European market	935	8 383

Table 4-1: Estimates of the current market and its mid-term development

4.3 Results from the Inception Study

4.3.1 Reaction to the Report

The Inception Study [4] has been, arguably, the most influential analysis regarding the market and business case for Galileo, probably because it was led by a well-respected, independent consultancy firm (PriceWaterhouseCoopers). Most previous Galileo activities had been undertaken by organisations with a vested interest in the continuation of the programme.

The final report from the Inception study provides an excellent example of how a set of results can be interpreted in diametrically opposing ways. The immediate public reaction to the study came from the European Council of Finance Ministers (“ECOFIN”), in which a group of ministers (including, notably the UK Chancellor of the Exchequer and the German Finance Minister) responded to the Inception study with a public statement that Galileo requires more public funding than they had previously been led to believe by the European Commission [10]. Given that the Inception report includes statements such as:

“...our analysis shows that the economics of Galileo do not support investment by the private sector on purely financial criteria...”

“...We estimate the cost of the system to be Euro 3.6 billion. The EC and ESA have budgeted Euro 1.25 billion for the Development phase and application development. This leaves a balance of Euro 2.35 billion to be spent on deploying the system. This will need to be met by a combination of public sector support and private sector funding...”

“...The level of private funding which is needed depends on the amount of support which the public sector is willing to make available for Deployment costs up to 2008. If support for Deployment is low then the project will only be viable with a high availability payment during the concession. If support for the Deployment costs is high then there will be less need for private capital and the availability payment during the concession can be lower...”

It is quite understandable that Finance Ministers might be concerned that proceeding with Galileo might commit them to up to three times as much public funding as they had previously been expecting, depending upon the degree of reticence from the private sector to finance the programme.

However, the European Commission, in their January 2002 Information Note [11], have interpreted the Inception Study as unqualified support for the programme, with statements such as:

“Except for the development phase funded by the European Space Agency, national budgets will not bear any of the public funding costs for the various phases of the GALILEO programme”

and

“...There are no financial, economic or technical arguments which can justify postponing the start of the development phase of the GALILEO programme”

Clearly, the report lends itself to selective interpretation. The following sub-sections reassess some of the analyses in the Inception report, as they apply to this thesis. This is all original work, and has not been previously published in any form.

4.3.2 Baseline Case

The Inception Study produced an independent assessment of costs for the Galileo system, as follows:

- Development Phase – € 1367M
- Deployment Phase – € 2029M
- Replenishment – € 1781M
- Operations (pa) – € 135M

Table 4-2 also presents the base case estimated revenues made by PwC and used in the Inception Study analyses. Given reasonable assumptions regarding the time distribution of these costs and revenues, they can be combined to produce Figure 4-3. Note that this figure is derived from Inception Study data, with operating costs and capital expenditure combined, unlike corresponding figures presented in the PwC report.

Application	Service	2010	2015	2020
Personal communications and location	OS	47.7	275.8	288.1
Cars (route guidance etc)	OS	10.2	17.2	17.7
LCVs (route guidance)	OS	3.1	5.3	5.5
Trains & Buses (route guidance etc)	OS	0.4	0.8	0.8
Road Tolling	OS	0.0	0.2	0.3
Police & Fire (vehicle resource)	PRS	0.3	2.6	5.6
P&F (pedestrian resource)	PRS	0.8	10.5	19.0
P&F (vehicle tracking)	PRS	0.0	0.1	0.2
Oil & Gas (marine seismic exp)	CS	0.2	1.3	2.0
O&G (high resolution seis site survey)	CS	0.2	1.0	1.5
O&G (land and trans zone seis)	CS	1.7	9.3	13.7
O&G (FPSO positioning)	CS	0.1	1.1	2.8
O&G (rig positioning)	CS	1.0	7.6	16.0
O&G (VSP)	CS	1.6	8.7	12.7
Commercial Aviation	SOL	0.0	21.0	98.1
General Aviation	SOL	0.0	3.3	14.9
Marine Engineering & Navigation	CS	0.2	2.2	6.4
Personal Outdoor recreation	OS	0.1	0.2	0.5
Mining 3D Positioning	CS	0.0	0.8	3.8
Mining surveying	CS	0.1	2.5	5.4
Mining autonomous vehicles	CS	-	0.2	0.4
Mining truck dispatch	CS	0.0	0.2	0.7
Total		67.7	371.8	516.1

Table 4-2: Inception Study Base Case Estimated Revenues (€M 2001 prices) [4]

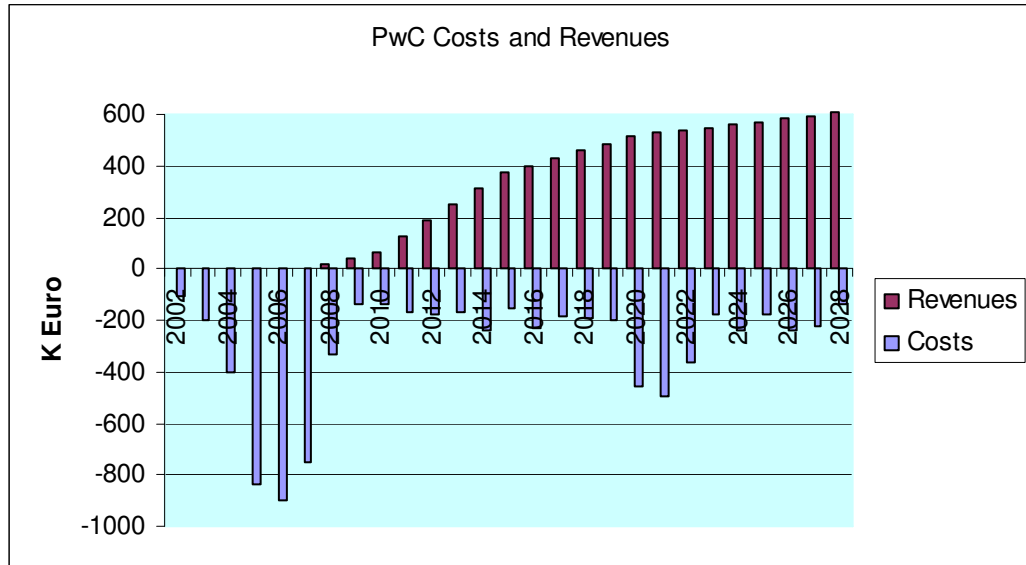


Figure 4-3: Inception Study Costs and Revenues

The costs presented in this chart are net of any financing requirements. The Inception report goes on to combine the “Net Operating Cash Flow with tax obligations in the [Galileo Operating Company], capital expenditure for the Development and Deployment, and asset replenishment programme” to produce a pre-finance cash flow forecast.

The report then concludes:

“...the Project IRR [Internal Rate of Return] in our base case is just 4.1% real. This is less than the cost of private capital and means that public sector support will be needed for capital expenditure on Deployment or in the operating phase if any private sector finance is to be obtained.”

However, closer analysis suggests that even this figure of 4.1% IRR is optimistic. Firstly, as mentioned above, this uses a pre-finance costs cash flow. Secondly, it assumes a far higher public sector contribution than is currently budgeted for Galileo. In fact, some 48 pages after the base case analysis is presented in the Inception report, the following statement is made:

“In the case of Galileo, we understand that a budget of Euro 1.25 bn has been made available by the EC and ESA to fund the Development phase of the project, including some applications development.

Our base case funding assumptions suggest that up to Euro 1.4bn of public sector grant will be needed in the

Development phase, and a further Euro 700m in the deployment phase.”

Applying these values (i.e. an initial public commitment of €2.1 Bn) to the Base Case cost and revenue model presented above, with no finance cost and an assumed mean rate of tax of 20% on operating profit does indeed produce an Internal Rate of Return of 4.1% for the period 2005 to 2027, as shown in Figure 4-4. This chart shows that positive cash flow would be expected to begin around 2012, which agrees with PwC’s analysis.

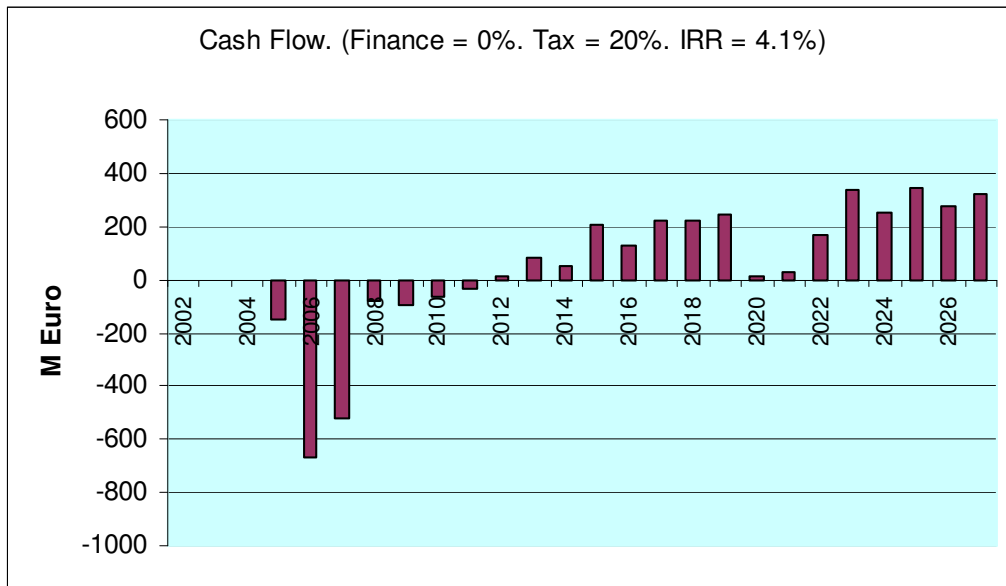


Figure 4-4: Inception Study Base Case Cash Flow (public funding = €2.1 Bn)

Clearly, with such a low IRR using pre-finance cash flow, adding in the cost of money will make the case much worse. Figure 4-5 demonstrates that with a cost of debt servicing of only 4.6%, the IRR diminishes to zero, and positive cash flow will not occur until 2015.

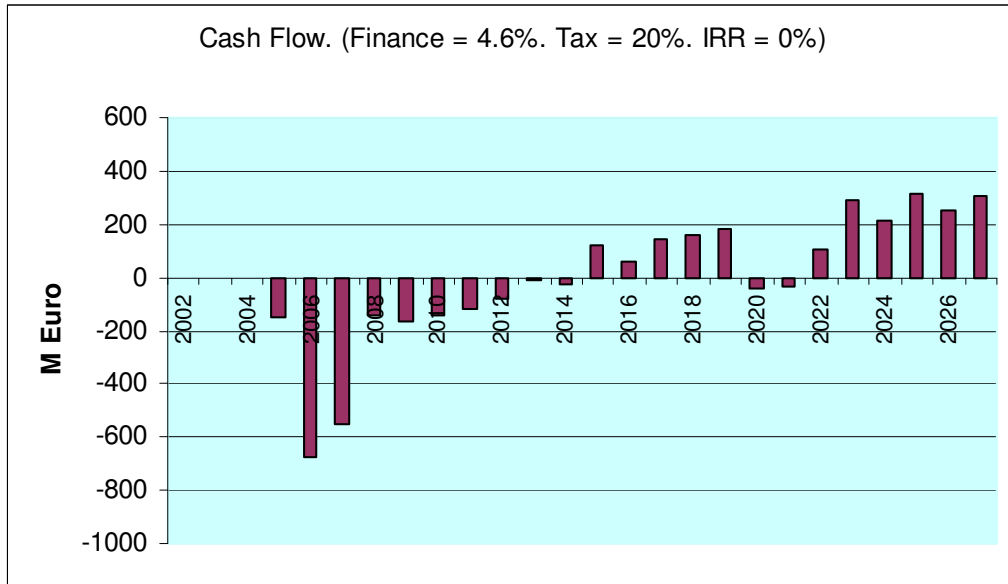


Figure 4-5: Base Case, with Finance rate of 4.6% (public funding = €2.1 Bn)

Note that this analysis uses a significantly simplified financial model, whereas the Inception Study goes in to great detail regarding potential funding models for Galileo (which is beyond the scope of this thesis). Nevertheless, this does demonstrate the basic point that Galileo will need much more than even the €2.1 Bn of public money for development and deployment assumed by PwC before any credible business case for investment can be made.

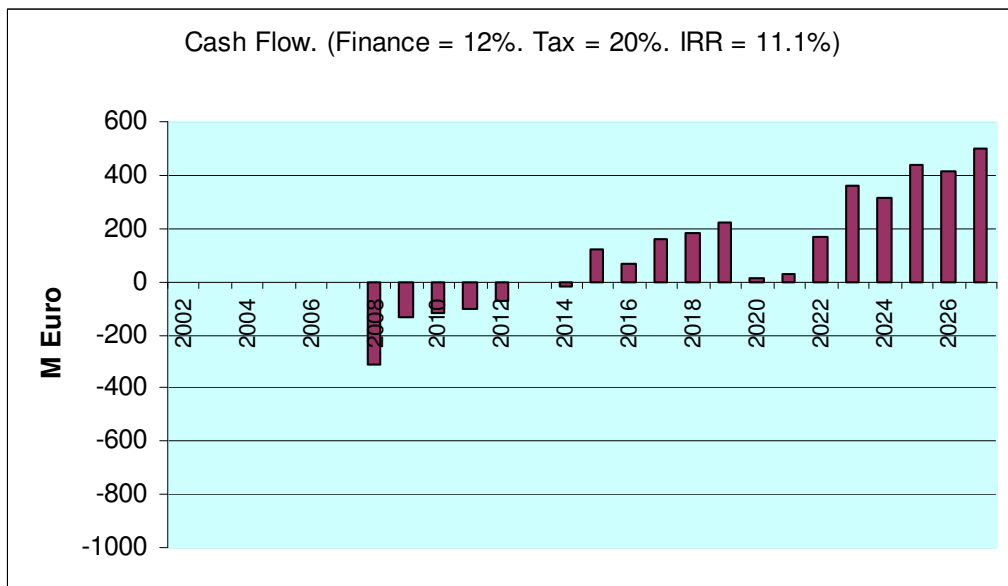


Figure 4-6: Base Case, with Finance rate of 12% (public funding = €3.2 Bn)

Figure 4-6 presents a more realistic case, in which the cost of finance has been taken as 12% pa. In this case it has been assumed that there is full public funding for the entire Development and Deployment phase (i.e. public funding of all Galileo activities before 2008). Total public funding of € 3.2 Bn is required which, when applied to the model used previously results in an Internal Rate of Return of 11.1%, which is similar to the cost of finance assumed in this model and hence may be assumed to provide a reasonably attractive business case for private investors.

These assumptions are clearly at odds with the EC's position that private funding will be forthcoming in the deployment phase of 2006 to 2007. However, this model suggests that the additional public funding requirement is an inevitable consequence of the long time before positive cash flow can be expected (2015, in this case).

4.3.3 Effect of Loss of Safety of Life and Commercial Service Revenues

A key assumption in the Inception report's Business Plan is that the Galileo Operating Company will be able to collect both "Purchase Revenues" (i.e. a 5% royalty on the chipset sales for Galileo receivers) and "Service Revenues" (i.e. revenues that service providers will pay the GOC for making the signal in space available to their customers). Figure 4-7 (taken directly from the Inception report) shows the estimated split between these revenue streams.

A large part of the Service Revenue contribution has been assumed to come from the aviation sector. Indeed, the report states their estimated revenues:

"...assume that a percentage of the costs saved by the aviation industry from the elimination of the need for terrestrial infrastructure will be captured by the GOC. In the base case, it is estimated that GPC will receive 50% of the value of the cost of these savings."

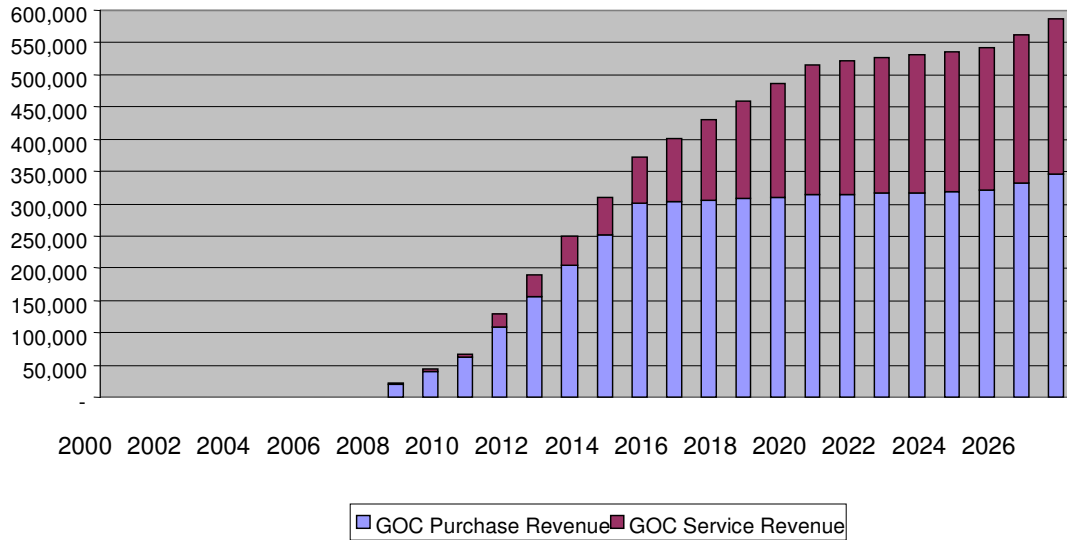


Figure 4-7: Inception Estimate of GOC Market Revenues (€K 2001 prices) [4]

This is obviously a very contentious assumption. Indeed the UK's National Air Traffic Services (NATS) has produced a robust rebuttal of the aviation revenues claimed by Inception [12]. Given the investment that that aviation industry in Europe and the US have made to EGNOS and WAAS respectively, they are understandably very resistant to any attempt to build a business case for Galileo based on revenues from aviation.

So what would be the impact on Inception's business plan if service revenues arising from licensing access to Galileo's integrity signal were not forthcoming? Table 4-2 includes a column indicating for each application whether it is associated with the Open Access Service (shown as OS), Public Regulated Services (PRS), Commercial Access Service (CS) or Safety of Life Service (shown as SOL). It is possible using this table to remodel the cash flow forecast, to consider the case in which no service revenues associated with CS or SOL are forthcoming (i.e. only the PRS provides service revenues). The cash flow in this case is shown in Figure 4-8.

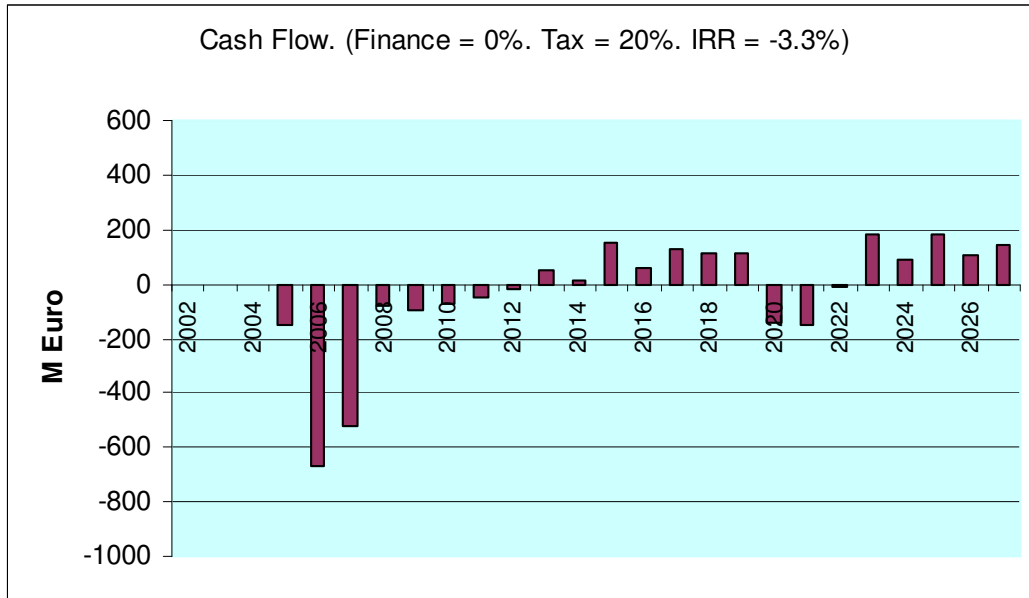


Figure 4-8: Cash Flow without Service Revenues (public funding = €2.1 Bn)

Note that the IRR demonstrated by this cash flow is negative (-3.3%), i.e. without service revenues, even at 0% finance this programme still would not make money in the period before 2027.

Using the higher public subscription of €3.2 Bn discussed previously, the business case becomes a little more attractive, as long as the cost of money is still 0%. However, as shown in Figure 4-9, even this case would not be regarded as a particularly good investment, with an IRR of 5.3%.

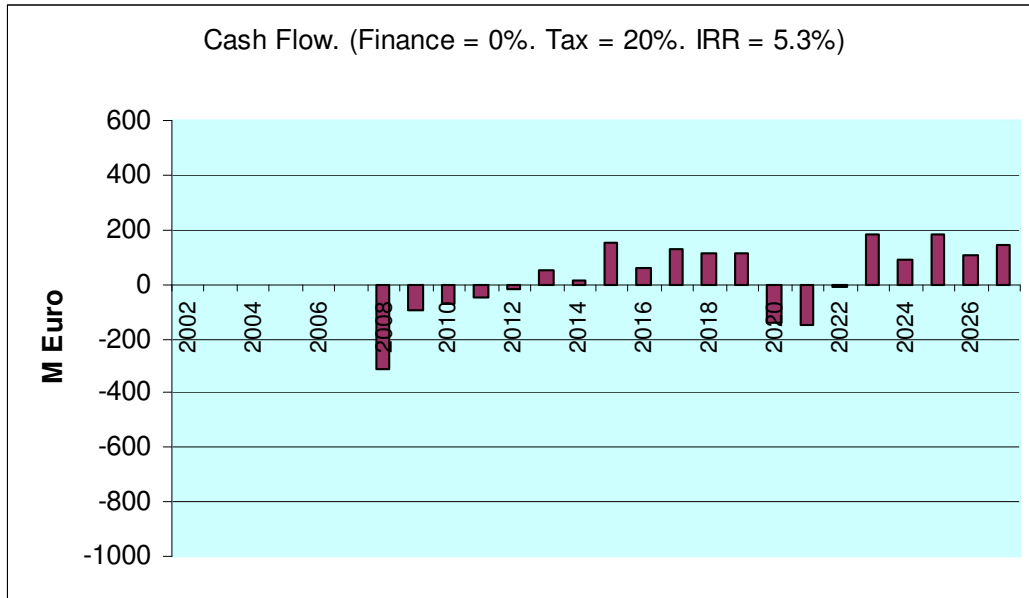


Figure 4-9: Cash Flow without Service Revenues (public funding = €3.2 Bn)

4.3.4 Exclude the Cost of Integrity

Taking the results from the previous section further, if there is serious doubt about the ability to raise revenues based on the sale of the Integrity service, why include this service at all? What would be the effect on the business case if the Integrity Determination System were removed?

Section 5.7 of this thesis, within the RAIM study, presents the costs for the European Integrity Determination System taken from the GalileoSat Phase B Baseline Design Review report [13]. These figures are given at 1998 economic conditions. Escalating these figures at 3% pa for 3 years to bring them approximately to the same 2001 conditions as used with the Inception study yields:

- IDS Development and Deployment Phase Costs - €448M
- IDS Recurring Costs (pa) - € 19M

Figure 4-10 presents the costs and revenues associated with these revised assumptions, whilst Figure 4-11 shows the associated cash flow.

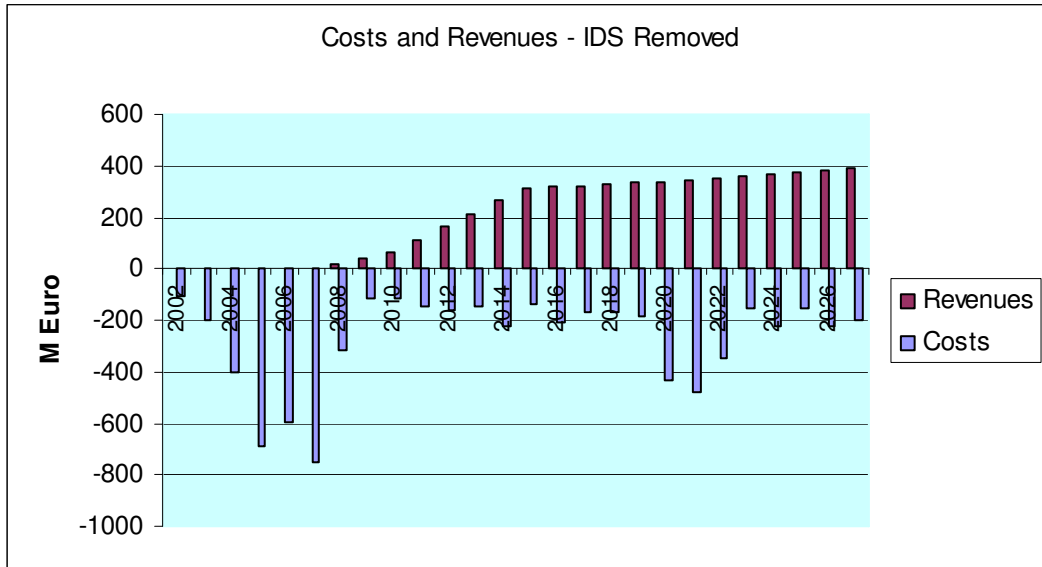


Figure 4-10: Costs and Revenues, excluding IDS development and operations

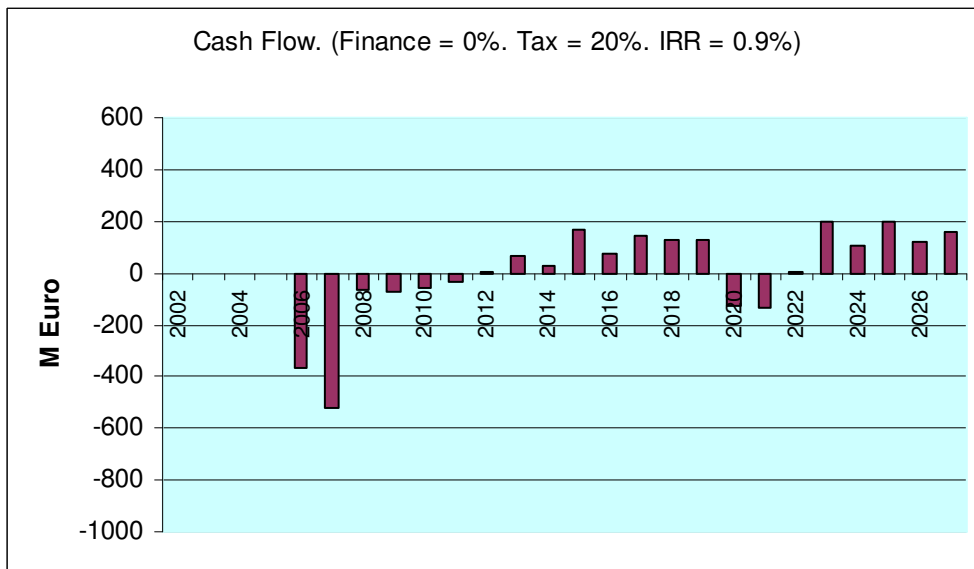


Figure 4-11: Cash Flow for System with no IDS (public funding = €2.1 Bn)

Although this demonstrates a positive internal rate of return, it is clearly not sufficient to be an attractive investment. This highlights the fundamental flaw in the assumption that the Integrity system has a justifiable business case: Depending upon the amount of public contribution to the programme, private funding (much of which would be spent on development and deployment of the IDS) will be required to start in 2005 or 2006, whilst significant returns (if any) are unlikely to start coming in from high-integrity users until around 2015 [4]. It is

extremely difficult to build a viable business case for the IDS with around 10 years between the start of the investment and the start of the revenue stream.

Given the evidence previously presented which suggests that there is a significant risk associated with relying on revenues from the aviation sector, it appears to make financial sense to remove the IDS from the baseline. With such a slimmed-down architecture, the amount of public funding required to make a PPP feasible should reduce. So how much public money is required to make this a workable proposition?

In Section 4.3.2 it was shown that for the Inception Study baseline case, assuming both purchase and service revenues, an initial public subscription of €3.2 Bn would allow private investors to earn an IRR of 11.1%, assuming a cost of finance of 12% pa. In order to generate the same IRR in this revised case, with no service revenues and no Integrity Determination System costs, total public subscription is reduced to around €2.9 Bn, a saving of over a quarter of a billion Euro, with a business case that is not reliant on service revenues. This is demonstrated in Figure 4-12.

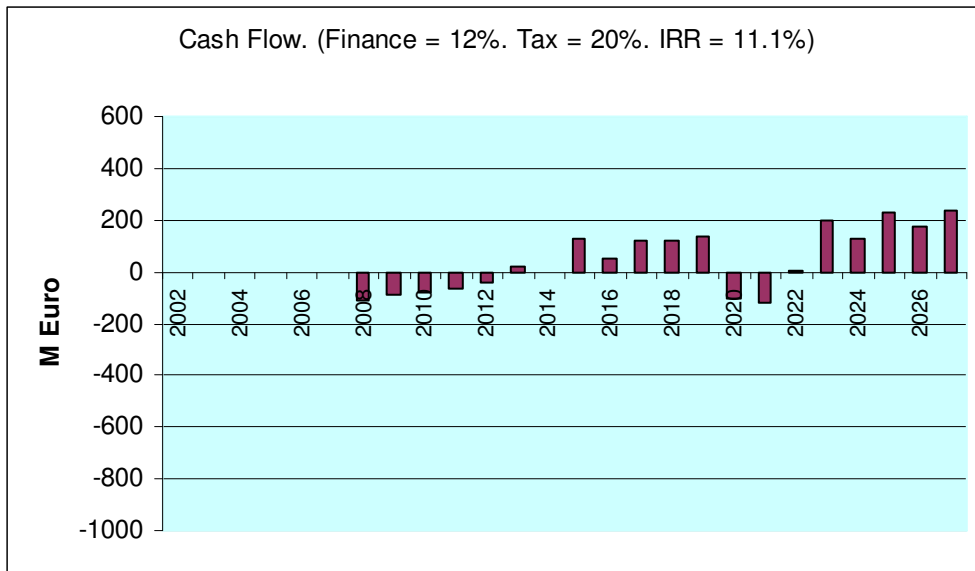


Figure 4-12: Cash Flow for System with no IDS (public funding = €2.93 Bn)

4.4 Integrity Justification Study Conclusions

The results of the preceding analyses, including the survey results summarised in Annexes A and B, have been brought together into the following set of points which develops the central argument arising from the Integrity Justification Study, and leads naturally into the RAIM Study:

1. The overriding argument in favour of deployment of Galileo is one of sovereignty for Europe, in a technical field dominated by the United States.
2. A huge industry has built up around GPS, and is growing. Galileo could also reasonably be expected to generate business for European industry in this area.
3. Since private industry is expected to generate profits from the existence of a Galileo Signal in Space (SIS), the view of the European Commission is that private investment should be available to partly fund the development of the system.
4. In order to provide a supporting justification for the development of Galileo (other than that of sovereignty), a number of features were proposed to differentiate Galileo from GPS. These include the provision of ground-based signal integrity; a guaranteed level of signal availability; better accuracy than GPS from the stand-alone system; and a legal liability cover for fee-paying users of the signal.
5. These distinguishing features generated the key specifications which define the system architecture produced in the Galileo Phase B2 study, such as the existence of an Integrity Dissemination System (IDS).
6. The currently planned constellation, with 27 MEO satellites (plus 3 spares) providing accurate SIS as well as ground-generated integrity and Signal in Space Accuracy (SISA) signals has been driven almost entirely by the intention to design a system which on its own (i.e. without GPS, EGNOS or any other current or planned system) will meet the requirements of ICAO for civil aviation precision approach or approach with vertical guidance.
7. In parallel with the system engineering activities performed under GalileoSat, the studies on service definition and business case analysis have presented conclusions which suggest that these distinguishing features would not in fact offer a significant marketing advantage to anyone trying to sell a pay-for-use Galileo service.
8. For the aviation community the existence of WAAS in the US, and the current development of EGNOS and MSAS in Europe and Japan respectively, cannot be ignored or wished away. The general perception is that GPS satellite navigation augmented by integrity signals delivered from Geostationary satellites is accepted for use by ICAO, and that the world's airlines will be using these systems for the next twenty-five years at least.
9. A number of studies have projected a massive growth in the demand for satellite navigation services in the next decade, and that this growth will occur with or without the existence of Galileo. The vast majority of this market is expected to come from land vehicle

applications (car navigation, vehicle telematics, rail) and wireless location services (WLS) for mobile communications.

10. These users do not need high levels of integrity, guaranteed availability or liability cover, and would not be prepared to pay any significant premium for a service which could, by-and-large, be provided free by GPS.
11. However, much of the expected growth in the satnav market discussed in the previous point will come from urban areas. In such an environment GPS availability is sometimes limited.
12. In order to provide a better service (in terms of overall availability, continuity of service and time-to-first-fix (TTFF)) to urban users the obvious solution is to offer dual-mode receivers, in which ranging measurements from any combination of visible Galileo or GPS satellites could be combined to give a navigation solution.
13. There are a number of viable models by which some revenue could be generated for the Galileo system operator in such a scenario – most typically this would come from some form of royalty payment on the Galileo portion of dual-system receiver electronics.
14. However, taken to its logical conclusion this suggests that the vast majority of any possible commercial revenue streams for private investors in Galileo could be generated by a system which is to all intents and purposes a facsimile of GPS.
15. Any potential investor in Galileo is likely to ask: “What is the commercial advantage in providing a high-quality integrity system, redundant control centres, liability cover, etc, from a constellation with 30 satellites and dozens of discrete terrestrial components. Why not have fewer MEO satellites and ground stations, and a single control centre, just like GPS, and let EGNOS provide the ground-based integrity signal, augmented by RAIM as required. How much additional revenue would all these additional bells and whistles offer me, and is it worth the investment?”
16. There is therefore likely to be a conflict between the desire of private investors for a system which has minimum development risk and the best projected rate of return on investment, and the European Commission which has very publicly promoted Galileo as a system with significant distinguishing features from GPS.
17. The Integrity Determination System has been included within the Galileo baseline architecture with no real evidence that it adds value to the programme.
18. The amount of public money required to make Galileo attractive as a public/private partnership is far in excess of the € 1.25Bn currently presented as the planned public contribution.

19. Within industry there are widely divergent views as to whether or not a PPP is workable.
20. If it can be demonstrated that a combined Galileo and GPS system will offer integrity performance suitable for aviation precision approach, there will be a powerful argument for the removal of the IDS from the Galileo system baseline.

The technical component of this thesis presented in the following sections attempts to provide this demonstration.

5. BACKGROUND TO THE RAIM STUDY

5.1 Introduction

The main analytical sections of this thesis are based on two projects undertaken by the author, as an employee of VEGA Group PLC:

- The “Combined GPS/Galileo Receiver Autonomous Integrity Monitoring (RAIM) Performance Evaluation Study” for the British National Space Centre (BNSC) under the BNSC SATCOM 2001 programme;
- The “User Integrity Algorithms Stand-Alone Test Case” for the European Space Agency (ESA) under the Galileo System Test Bed (GSTB) programme from 2002 to 2004.

The first study provided the initial development of the novel RAIM algorithm discussed subsequently. The second study, for ESA, produced a far more detailed analysis of this algorithm and of the potential performance of RAIM algorithms for Galileo-only and Galileo + GPS receivers.

5.2 Purpose and Scope of the RAIM Study

The Integrity Justification Study presented previously argues that there is little commercial merit in the investment required for Galileo’s Integrity Determination System (IDS). The Galileo System Requirements Document (SRD) specifies a 20m Vertical Alert Limit (VAL) for the Safety Access Service when using a satellite-only receiver, and an overall availability of 99.5%. Such a specification does not enable the system to be used for Cat I precision approach, which has a more demanding requirement on VAL.

The SRD specification for Galileo’s Safety Access Service (SAS), may therefore offer aviation users an alternative to the GPS-based Wide Area Augmentation System (WAAS) and European Geostationary Navigation Overlay Service (EGNOS) systems for non-precision phases of flight, but in itself it does not offer any more functionality to meet more demanding specifications. Indeed, both WAAS and EGNOS have 20m VAL as an interim target capability, with Cat I performance as a long term objective [14].

An alternative method of providing signal integrity information is through Receiver Autonomous Integrity Monitoring techniques. These algorithms rely on users being able to access more satellites than the minimum number required for a navigation solution, in order to estimate the integrity of the signal from these redundant measurements. Currently,

with a GPS constellation of 24 satellites providing only a single frequency in its Standard Positioning Service (SPS), RAIM cannot meet Cat I requirements, although RAIM-enabled receivers can be used as a navigation aid for less demanding phases of flight. However, by using both Galileo and upgraded GPS systems together the quality of the integrity information available from RAIM algorithms will increase dramatically, due to both the increased size of the useable constellation and the improved accuracy of the signals compared with current GPS.

The first aim of this RAIM Study is to present an analysis of the projected integrity performance for receivers combining the free-to-air Galileo Open Access Service signals and dual-frequency signals from GPS Block IIF satellites. The availability of integrity using standard RAIM techniques is compared with the current specifications for the Galileo IDS.

The second aim of the analysis is to introduce a novel RAIM technique developed by the author which improves on the performance of traditional RAIM algorithms when applied to very large constellations. Integrity performance exceeding that specified for Galileo's Safety Access Service (SAS), and approaching that required for Cat I, is demonstrated, using only the free-to-air signals from Galileo and GPS.

The impact that these results have on the justification for an integrity dissemination system within the Galileo architecture is presented and discussed.

The integrity performance (in terms of availability and protection limit) provided by RAIM receivers is a complex function of:

- The size of the effective available constellation (i.e. the number of satellites that can be accessed at any time), and the relative geometry of the satellites in view;
- The probability density function (PDF) of the error distribution in the received pseudorange signals from each satellite;
- The availability of each broadcast signal (i.e. the percentage of time that each satellite broadcasts a ranging signal).

RAIM performance for receivers using the current GPS constellation has been thoroughly analysed and the conclusions have been enshrined in RTCA Minimum Operational Performance Standards (MOPS) [15]. Also, some work has been performed which shows how RAIM performance varies with changes in the three parameters listed above (notably by US navigation equipment manufacturers such as Litton) [16]. However, this work has concentrated on the limited improvements that might be expected from upgrades to the GPS constellation.

Although some analyses have been undertaken to demonstrate the RAIM performance that might be expected from a combined GPS/Galileo Open Access Service (OAS) receiver under the EU GALA and ESA GalileoSat programmes, these reports have made a number of simplifying assumptions that do not fairly reflect the potential performance of a combined system. Specifically, work undertaken by Imperial College, London on behalf of Alcatel used only a relatively dated RAIM technique, and its conclusions were ambiguous regarding the value of a discrete Integrity Determination System [17]. There was, therefore, a need for an independent study, looking at the performance of state-of-the-art RAIM algorithms, to assess the benefits that a fee-charging IDS might offer. This analysis was the basis of the study undertaken for the BNSC.

The initial study led to the development, and application for patent [18], for the novel RAIM algorithm discussed subsequently. Furthermore, ESA awarded a contract for additional research and development of this algorithm as part of the experimentation plan for Galileo algorithm development. These two studies together provide the technical core of this thesis.

5.3 Objectives of the RAIM Study

The objectives of this study are to demonstrate or disprove the following statements:

- That by combining the free-to-air signals from a 24-satellite GPS constellation broadcasting freely available signals on two frequencies, with the free-to-air signals from a 27-satellite Galileo constellation broadcasting OAS signals on two frequencies, currently implemented standard RAIM algorithms can provide overall performance that exceeds the current specifications for the Galileo Commercial Access Service (CAS);
- That the same combined constellation, using a novel RAIM technique, offers accuracy and integrity performance that is comparable to the requirements for civil aviation Category I (Cat I) precision approaches, and hence exceeds the current specifications for the Galileo Safety of Life Service;
- That this novel RAIM technique can be shown, by simulation, to meet the specified requirements for false alarm and missed detection probabilities.

5.4 Performance Metrics

The elements of navigation system performance are:

- Accuracy (e.g. of position and time);

- Integrity (e.g. integrity risk and time to alarm);
- Continuity (e.g. of position accuracy, or of integrity)
- Availability (e.g. of position and time, or of integrity);

Each of these terms needs to be precisely defined to ensure that the various cases are compared consistently. A number of different definitions of these figures of merit are used in the literature. Those used throughout this thesis are those used by ICAO in its definition of “total system parameters” for Required Navigation Performance (RNP) [19].

Each phase of flight or type of flight operation has a set of RNPs which are used in its definition. For example, in the approach and landing phase a number of standards are defined to be appropriate for all types of aircraft landing at all types of airfield. Terms such as “Approach with Vertical Guidance II” or “Category I” define precision approach navigation services with various demands on their RNP. These terms and distinctions are discussed in a little more detail below.

5.4.1 Accuracy

“The degree of conformance between the estimated, measured, or desired position and/or the velocity of a platform at a given time and its true position or velocity”.

There are many ways to express accuracy (e.g. 1σ RMS error, Spherical Error Probable, etc.). It is necessary to decide which definition of accuracy is most appropriate for each case in which accuracy is specified. RNP Total System Error (TSE) accuracy specifications for approach and landing standards state accuracy limits at the 95th and 100th percentile, laterally and vertically, e.g.:

Decision Height	Lateral (95%)	Lateral (100%)	Vertical (95%)	Vertical (100%)
60 m	40m	121 m	12 m	37 m

Table 5-1 : RNP Cat I TSE accuracy to minimum decision height (DH)

In the subsequent analysis, where User Equivalent Range Error (UERE) is specified, this refers to 1σ RMS error. Where vertical or horizontal error performance requirements are specified, these are generally 95% confidence limit errors. In general this is stated, to avoid confusion. Where no qualifying statement is given the accuracy referred to is a 1σ RMS error.

In addition, the difference between Total System Error and Navigation System Error (NSE) needs to be explained. NSE is, unsurprisingly, the

error (typically at 95% confidence) allowable for the end-to-end navigation system measurement, processing and display chain. TSE is (typically but not definitively) the root sum square of NSE and the pilot or autopilot Flight Technical Error (FTE) specification.

5.4.2 Integrity

“...the trust which can be placed in the correctness of the information supplied by the total system. Integrity includes the ability of a system to provide timely and valid warnings to the user when the system must not be used for the intended operation”.

Integrity specifications are presented as two parameters: Integrity Risk (IR) and Time To Alarm (TTA). For example, TSE values for Cat I approach are $IR = 3.3 \times 10^{-7}$, $TTA = 6$ seconds [20]. This means that the probability that the error in position measurement exceeds the accuracy stated above at any instant during a Cat I approach and is not warned to the user within 6 seconds must be less than 3.3×10^{-7} . Cat I integrity requirements are presented in Table 5-2.

5.4.3 Availability

“...the percentage of time that the services of the system are within required performance limits. Availability is an indication of the ability of the system to provide useable service within the specified coverage area” - i.e. probability that specified service is available.

Note this will vary depending on the specifications of the application being analysed. For example, for an application that requires only 3-dimensional positioning information with a given accuracy, the availability figure would relate to the fraction of time in a given environment (i.e. given minimum elevation blocking angles) for which at least 4 satellites can be simultaneously observed with suitable geometry to provide a sufficiently accurate navigation solution.

For an application which includes, for example, RAIM, and for which inaccurate signals are to be identified and removed from the navigation solution (i.e. Fault Detection and Exclusion, or FDE), at least 6 satellites need to be in view. In this case the figure for availability would be very different from the previous example, even if exactly the same constellation were being analysed.

5.4.4 Continuity

“...the capability of the total system...to perform its function without non-scheduled interruptions during the intended operation. The continuity risk is the probability that the system will be unintentionally interrupted and not provide guidance information for the intended operation”.

Continuity requirements are therefore specified as a probability and a time period. For example, for Cat I approaches, the Total System Error Continuity requirement is “8.0 x 10⁻⁶, 15 secs”. This means that in any continuous 15 second period during a Cat I approach, the probability that the system fails to deliver a valid navigation solution is less than one in 125,000. Cat I NSE continuity requirements are presented in Table 5-2.

5.5 Required Navigation Performance for Precision Approach

The required performance specifications for Global Navigation Satellite Systems (GNSS) used in aviation applications are defined in ICAO Standards and Recommended Practices (SARPS) [20]. At present signal-in-space performance requirements for approach with vertical guidance (APV) and precision approach have been specified for APV-I, APV-II and Category I. Category II and Category III GNSS performance requirements are under review and should appear in SARPS at some point in the future. Table 5-2 below presents the defined specifications for APV-I, APV-II and Cat I, along with the provisional specifications assumed for Cat II. These values are used in the subsequent analyses in this study to estimate the availability of RAIM to meet these performance specifications.

Operation	Accuracy (H, 95%)	Accuracy (V, 95%)	Horiz Alert Limit	Vertical Alert Limit	Integrity	Time to Alert	Continuity	Availability
APV-I	220 m	20 m	556 m	50 m	1-2 x 10 ⁻⁷	10 s	1- 8 x 10 ⁻⁶	.99 to .99999
APV-II	16 m	8.0 m	40 m	20 m	1-2 x 10 ⁻⁷	6 s	1- 8 x 10 ⁻⁶	.99 to .99999
Cat I	16 m	6.0 m to 4.0 m	40 m	15 m to 10.0 m	1-2 x 10 ⁻⁷	6 s	1- 8 x 10 ⁻⁶	.99 to .99999
Cat II (provis.)	TBD	TBD	21 m	10 m to 5.0 m	1- 0.5 x 10 ⁻⁹	1 s	1- 4 x 10 ⁻⁶	.99 to .99999

Table 5-2: Required Navigation Performance Specifications

Note that the “Integrity” risk is specified per approach (which is commonly taken as a period of 150 seconds), whilst the “Continuity” risk is per 15 second interval.

5.6 Galileo IDS System Specifications

The following extract is taken from the Galileo Master High Level Definition (HLD) document, Issue 2 dated 3 April 2001 [21]:

“The performance of the Safety-of-Life service...is compatible with the requirements of the Approach with Vertical Guidance (APV-II) as defined by ICAO SARPs.

Performance would be equivalent to CAT-I precision approach requirements except for the vertical accuracy and integrity performance for which some design margins have been taken. As the studies and the experimentation on GALILEO progress, it may be possible to reduce those design margins and therefore to state better performance with the goal of achieving CAT-I performances.

Through the Definition Phase, it has been verified that the performance needs of other modes of transport (land, rail, maritime) are covered adequately through those requirements. The service availability above 99.9% would make it usable for primary means only. Combination of this GALILEO service either with the current GPS as augmented by EGNOS corrections, or the future improved GPS and EGNOS integrity-only, would support CAT-I performance and offer the prospect of sole means availability. Other applications covered would be ship docking, train control, advance vehicle control, robotics (satellite signals combined with local components when required).

The coverage area of the GALILEO integrity service is global, and to this extent, the system architecture is being optimised for this requirement.

		Safety-Of-Life Service
Type of Receiver	Carriers	Dual Frequency (single frequency under evaluation)
	Computes Integrity	Yes
	Ionospheric correction	Based on dual-frequency measurements
Coverage		Global
Accuracy (95%)		H: 4 m V: 8 m
Integrity	Alarm Limit	HAL: 12 m VAL: 20 m
	Time-To-Alarm	6 seconds
	Integrity risk	$2 \times 10^{-7} / 150 \text{ s}$
Continuity Risk		$8 \times 10^{-6} / 15 \text{ s}$
Timing Accuracy wrt UTC/TAI		50 nsec
Certification/Liability		Yes
Availability		99 % - 99.9 %

Service Performance for Safety of Life Service with the Satellite Navigation Signals only and without any other augmentations/elements”

Issue 2 draft 3 of the ESA Galileo System Requirements Document (SRD) [22] also states that:

“A Galileo Safety-of-Life Service Satellite-Only Receiver,

- located at any point within the Full Earth Coverage Area...,*
- receiving the Safety-of-life Service Navigation Message,*
- under the General Environment,*

shall be able to generate an Alert whenever the calculated horizontal position error exceeds 12 metres or the vertical position error exceeds 20 metres.

...with an Integrity Risk of 3.5×10^{-7} over 150 secs...with Continuity of $1 - 10^{-5}$ per 15 seconds...”

I.e. the current Galileo integrity signal specifications are for a performance level broadly aligned with APV-II TSE requirements. Furthermore, Issue 1 of the IDS Requirements Specification, produced by Alcatel [23], makes the following statement:

*“The main function of the Integrity Processing Facility (IPF) is to provide the integrity flags (IF) for the GalileoSat satellites. The IF support the integrity level of GalileoSat system which at the maximum is defined by the provision of CAT I precision approach requirements. **Note that providing just only integrity level comprising three parameters – Integrity Risk, Alert Limit, System Time-to-Alert – might be insufficient to meet the Required Navigation Performance (RNP), which, apart from the integrity parameters, introduces accuracy, availability and continuity requirements.** Therefore, the IPF has to satisfy also these main requirements particularly the continuity level expressed as the probability of false alarms.”*

Taking these three statements together, it is clear that as currently defined the Galileo **IDS alone will not meet Cat I precision approach specifications**. An article by ESA project team members in the Summer 2001 issue of “Galileo’s World” magazine [24] also makes the following statement regarding integrity performance drivers:

“For Galileo, as for satellite navigation in general, the aviation community has formulated the most detailed requirements. However, this is not expected to be the largest sector of Galileo users.

Moreover, the aviation requirement has been formulated for the demanding case of landing at an airport in poor visibility, which...may best be served by global or regional integrity facilities enhanced by local services.

A less demanding requirement, either on alert limit or on alert time, could have a major impact on the configuration of the integrity system, including an impact on the trade-off between multiple regional systems and unified global systems.”

This statement is consistent with the sentiment of the previous extracts, i.e. that the IDS should provide a vertical alert limit of only 20m, and that aviation users intending to use Galileo for Cat I precision approach will need to augment the system, either using some local augmentation system or by combining the signals with those from GPS and/or EGNOS/WAAS.

5.6.1 Galileo SAS Service Specifications

The Galileo requirement for safety of life service is detailed in the following table. It has been extracted from the Galileo System Requirements document (SRD) [22] .

Performance parameter	Requirement
Horizontal Alarm Limit	12 m
Vertical Alarm Limit	20 m
Time to Alert	6 s
Integrity risk	3.5×10^{-7} /150s
Continuity risk	10^{-5} / 15 s
Availability	99.5 %

Table 5-3: Galileo Safety Of Life Performance requirement

Although not stated explicitly here, in the course of Galileo System Test Bed experimentation the Availability requirement has been taken to mean the availability at the worst user location [45], rather than a global average of availability. This is a significant constraint, as will be demonstrated and discussed later.

5.6.2 The Challenge of “Time to Alarm”

The term “TTA” defined as either “Time to Alert” or “Time to Alarm” has occurred at a number of points in the preceding discussion, and warrants some amplification., as it is an integral part of defining integrity service performance specifications. TTA is the amount of time for which a user

may be given hazardously misleading information without an alert being provided by an integrity system. For example, considering the specifications in Table 5-3, a user of this service may at some instant have a navigation position solution whose vertical component differs from truth by more than 20m. The probability that in any 150 second period such a transgression can occur for more than 6 seconds without the user receiving an integrity alert must be less than 3.5×10^{-7} , as discussed previously.

Meeting this particular requirement presents a significant challenge to designers of the Galileo IDS. Indeed this one requirement determines the number of uplink stations that Galileo requires, the quality of service required from the various global data networks used by the ground segment, the level of redundancy required in control systems and the amount of testing required to certify the safety of life service. It is no surprise that the extracts quoted above both cast doubt over the systems ability to meet this demanding TTA requirement.

Note that a 6 second TTA requirement is demanding for a ground-based integrity system, but is almost insignificant for a RAIM-based system. We can assume, with some justification, that a system determining its integrity from signals received on-board should be able to process these signals and deliver a valid output to the user well within 6 seconds.

5.7 IDS System Costs

The following cost estimates, provided by Alenia Spazio, have been extracted from the ESA Galileo Definition Study Final Presentation, dated 22 March 2001 [13]:

- The overall cost of the Galileo Development, IOV phase and Deployment (i.e. all activities from 2001 – 2007) is estimated at €3.1 Billion, at 1998 economic conditions.
- Within this total, the European Integrity Determination System (EIDS) has an estimated cost of € 410M.
- Replenishment costs attributed to the EIDS are estimated at € 17M per year, for 20 years (from a total recurring cost of € 270 M per year for the whole system).
 - Therefore, total costs from 2001 to 2027 attributable solely to the European component of the IDS are around € 750M at 1998 economic conditions.
- Considering the option to have a Global IDS:

- The additional cost of the Development, IOV phase and Deployment (i.e. all activities from 2001 – 2007) is estimated at 8% of € 3.1 Billion, i.e. **€ 248 M** at 1998 economic conditions (assuming that the “Global Centralised Integrity” option discussed in the Final Review is taken as the Global IDS system architecture).
- Additional recurring costs, based on the same assumptions, are 2.8% of € 270M, i.e. **€ 7.6M per year**.
 - Therefore, additional costs from 2001 to 2027 attributable to the non-European components of the IDS are around €400M at 1998 economic conditions.
 - **Hence the estimated cost of a complete (European plus Global) IDS, deployed and operating for 20 years is around € 1.15 Billion at 1998 economic conditions.**

Note these estimates exclude the cost of development or deployment of any local augmentation systems. Therefore, on current assumptions and issued specifications this is the cost of a system that would not meet the specifications for Cat I, and would not improve upon the specifications for WAAS and EGNOS, other than providing global coverage.

5.8 Existing Literature on Combined RAIM Systems Performance

The following sub-sections present a brief review of recent papers covering combined Galileo/GPS RAIM systems performance. In each case, an assessment of the methodology employed is presented, along with a synopsis of the main results.

5.8.1 The Integrity Requirement in Satellite Navigation: System Design Trade-Offs

The first two listed authors of this paper [25] are from Tor Vergata University of Rome. The two others are from Alenia Aerospazio, Rome. The main conclusion of this paper is that in order to support Cat I requirements through RAIM a combined dual-frequency GNSS constellation would require a minimum of 18 satellites in view above 5° masking angle. Although the paper does not state the corollary explicitly, it is clear that 27 Galileo satellites with 24 GPS satellites could not consistently provide the required degree of coverage

However, the methodology employed in this paper is seriously flawed. Specifically, constellation geometries as seen by the user are generated randomly, with a large number of iterations used to estimate the availability of RAIM integrity for a given number of satellites in view. The

problem with this, as opposed to using real constellation geometries propagated over time, is that random geometries will occasionally (indeed, often) cluster satellites into a small patch of sky, effectively producing a poorer position solution and protection limit than would be expected in practice. Given that availability requirements for Cat I are of the order of 99.99%, even one or two unnecessarily poor geometries out of 10,000 iterations will lead to a false conclusion that RAIM cannot meet the availability requirements.

Two RAIM approaches are used in this paper – a “classical” RAIM algorithm, and a “modified” or weighted RAIM algorithm. Both approaches use standard Least Squares Residuals techniques, the “modified” approach being identical to the “Weighted RAIM for Precision Approach” presented in [26].

5.8.2 Integrity Performance Models for a Combined Galileo/GPS Navigation System

This paper [17] was based on work produced under the EC GALA programme, discussed previously. The first three listed authors are from Imperial College, London. The fourth author is from University College London and the other authors are from Alcatel Space. This paper does not focus on specific navigation performance standards and so it is not possible to compare the estimated RAIM performance with Cat I requirements directly. However, results are presented for a Vertical Alert Limit of 18m, which suggest that RAIM availability using combined Galileo and GPS will be greater than 99% globally, and approaching 100% over all of the ECAC region except in the extreme North, for a missed detection probability of $(1-0.999)$ and a false alarm probability of $(1-0.9998)$. The RAIM method used in the analysis by Imperial College is based on the “Marginally Detectable Error” (MDE) algorithm formalised in [27].

In order to assess the merit of this work, the author of this thesis modelled the MDE algorithm and compared the results with a weighted least squares residuals approach. The results were relatively close for small constellation sizes (representative of GPS or Galileo alone), but when the constellations are combined the MDE method was found to give significantly lower values for VPL (and hence higher expected availability values) than are found from the LSR approach. The reasons for this discrepancy are discussed in Appendix C; at this point it suffices to say that the MDE approach appears to underestimate the false alarm probability when the number of redundant measurements becomes large.

5.8.3 Potential Performance Levels of a Combined Galileo/GPS Navigation System

This paper [28] was based on work produced under the EC GALA programme discussed in Section 3.4.2. The first three listed authors are from Imperial College, London. The fourth and fifth authors are from University College London and the other authors are from Alcatel Space. The content of this paper is very similar to that discussed in the previous section. However, this paper makes the explicit statement that in order to meet an 18m VAL a combined GPS/Galileo RAIM system would “require additional augmentation or system enhancement” such as the ground integrity channel (GIC) to be provided by the IDS or EGNOS. Alternatively, the paper suggests that without a separate augmentation or integrity channel, the potential system capability would be a VAL of 25 to 30 m.

There is no evidence to support this statement. Indeed, the original GALA document quite clearly shows that over almost all of the world, RAIM availability approaching 100% can be expected with a VAL of 18m. Unfortunately the GALA document has not been placed in the public domain.

This paper has therefore been used within the Galileo programme as evidence of the need for the Galileo IDS, because RAIM would be inadequate. However, as discussed previously (and subsequently in Appendix C), the underlying methodology, and many of the supporting assumptions, do not stand up to close scrutiny.

It should be noted that this work was supported by Alcatel Space who, within the Galileo Industries consortium, are positioning themselves to be the prime contractor for the IDS and hence have a vested interest in concluding that a GIC is still required.

5.8.4 New Integrity Concept at User Level for a Future Galileo and GPS Environment

All authors are from GMV of Spain. This paper [29] appears to be the first public acknowledgement that with new RAIM algorithms, combined Galileo/GPS RAIM receivers can be expected to give better than 20m Vertical Protection Limit, and therefore the value of the IDS is questionable. This paper also introduces a new RAIM algorithm used for fault detection and exclusion (FDE) being developed by GMV. An interesting additional conclusion from this paper is that a Galileo constellation optimised for RAIM performance as part of a combined GNSS will not be a symmetrical Walker as is the current baseline for Galileo.

Although the precise analysis method used by GMV is not presented in this paper, two points stand out which question the relevance of the results. Firstly, the analysis was performed with a Galileo constellation of 30 operational satellites, not 27. This will inevitably produce an over optimistic estimate of combined systems RAIM performance. Secondly, the analysis appears to use Position Dilution of Precision (PDOP) as a figure of merit for constellation geometry, which implies that a weighted RAIM solution is not being used. As is clearly demonstrated in [25] discussed above, using a classical, unweighted RAIM approach will produce a pessimistic estimate of combined systems RAIM performance.

5.9 Existing Literature on Advanced Integrity Monitoring Algorithms

A number of papers discussing advanced or novel approaches to integrity monitoring have been reviewed. The most significant papers are discussed below.

1. Weighted RAIM for Precision Approach

The authors are from Stanford University. This paper [26] presents an excellent description of the standard weighted least squares residuals RAIM technique, modelled and discussed subsequently in this report.

The emphasis of this paper is on the expected RAIM performance for users of GPS with measurement error corrections provided by geostationary space-based augmentation systems such as WAAS, for which a vertical protection limit of 26m is estimated using RAIM, with 99.8% availability.

2. On GPS Positioning and Integrity Monitoring

The author is from National Cheng Kung University, Taiwan. This paper [30] is discussed in some detail in Section 10 of this thesis, since it provides the basis for the “Errors in Variables” technique modelled subsequently.

3. Advantages of Autonomous Integrity Monitored Extrapolation Technology for Precision Approach

The authors are with Litton Aero Products and Litton Guidance & Control Systems, respectively. This paper [16] presents a proprietary approach to autonomous integrity called Autonomous Integrity Monitored Extrapolation (AIME™). This technique involves integrating RAIM-type algorithms with inertial navigation systems to provide the ability to “coast” for several minutes when some or all satellite signals are absent, hence increasing RAIM continuity and availability. This paper concludes that

AIME combined with SBAS corrections can potentially be used for Cat II precision approach.

5.10 Current Galileo Integrity Concept

5.10.1 SISA/IF Concept

The proposed integrity service to be provided by the Galileo system is based on the so-called Signal In Space Accuracy/Integrity Flag concept (SISA/IF) [31]. An estimate of satellite range accuracy is generated at the Galileo Orbitography and Synchronisation Processing Facility (OSPF), this basically indicates the quality of the ephemeris and clock data. A bound is then placed on this error to represent the predicted range error at a certain confidence level for the worst user location within a given region – this SISA value is then uplinked and broadcast by Galileo satellites. An independent network of monitoring stations then performs a statistical analysis on the measured pseudorange residuals (for a given satellite and service region) to determine the probability that the broadcast SISA value actually bounds the residuals. An integrity flag is generated and broadcast if the probability parameter fails to meet a defined threshold.

5.10.2 Receiver Autonomous Integrity Monitoring (RAIM)

Receiver Autonomous Integrity Monitoring (RAIM) methods check the consistency of the measurements to infer the quality of the position estimate. For RAIM to be available, the user receiver requires redundant measurements and suitable satellite geometry. RAIM availability can be examined by checking the number of redundant measurements and the relative geometry of the observed satellites from the user to ensure that the undetected measurement errors cannot make the position error exceed a pre-defined alarm limit. RAIM availability and/or protection limits can be improved by increasing the number of satellites and the precision of the measurements.

A number of different RAIM algorithms have been developed over the years. Some are primarily design tools that predict whether or not RAIM will be available for a given position at a given time, whilst others are implemented within receivers to perform the fault detection procedure.

Some techniques use a filtering or averaging technique such as the position comparison method [32]. However, the majority of RAIM techniques use a “snapshot” approach in which only measurement data from a single epoch is used to check the consistency of the solution. Such techniques include the range comparison method [33], the residual analysis method [34], and the parity method [35]. It has been shown [36] that with decision boundaries set to yield the same false alarm rate, these methods provide the same level of integrity, i.e. fundamentally

these methods are identical, although conceptually they appear quite different. Within this thesis they are represented by a single Least Squares Residuals (LSR) method.

Some RAIM techniques have also been designed to use data collected and filtered over multiple epochs. This generates predicted measurements (receiver-satellite ranges) with which to compare each new measurement. Although such techniques promise very high performance, especially when combined with additional sensors such as inertial navigation system [16], they are difficult to model and analyse in the general case, and evaluation of their predicted performance is excluded from the scope of this thesis.

5.10.3 RAIM and SISA/IF Integration

The Integrity Determination System within the Galileo architecture is intended to provide timely information regarding the integrity of the signals being broadcast by the Galileo satellites (and, potentially, also from the GPS and GLONASS constellations). This information is vital for high-integrity, safety-of-life applications, the most demanding of which is likely to be aviation precision approach.

In practice, users of an integrity service will generally include Receiver Autonomous Integrity Monitoring algorithms in their receivers [15]. RAIM allows the receiver to detect local integrity failures, caused for example by multipath effects, meteorological conditions, local interference or even deliberate jamming, which could not be protected by the IDS, therefore the use of RAIM is likely to be mandated for all high-integrity applications.

The problem then is to find a way in which information provided by the IDS can be combined with a RAIM algorithm to maximize the level of integrity or, more precisely, to minimize the horizontal and vertical protection limits for a given False Alarm and Missed Detection probability (P_{FA} and P_{MD} respectively).

Consider an aviation user of a combined RAIM/IDS system processing signals from all Galileo and GPS IIF satellites in view. With no faults on any satellites the IDS system will normally declare all satellites as “OK” and, independently the RAIM algorithm should conclude that all measurements are consistent therefore it is safe to continue with the approach. However, with any error distribution on the ranging signals, there will occasionally be cases where even with no faults one satellite’s ranging signals will be an “outlier” – sufficiently inconsistent with other measurements as to cause doubt as to the quality of the calculated navigation solution. The RAIM algorithm would be expected to generate an alarm in this event, and the frequency with which such events can be

tolerated is set by P_{FA} (which is in turn set by the Continuity specifications for the corresponding phase of flight).

If IF/SISA information provided by the Galileo system is to be included in the receiver's integrity determination process, the RAIM algorithms should adapt their fault detection thresholds dynamically, to prevent the false alarm rate from increasing and becoming a problem. If the detection threshold doesn't adapt dynamically, and the receiver is set to indicate a fault detected by either the IDS or the RAIM then there is a real chance of the required false alarm or missed detection probability being exceeded.

Treating the RAIM and IDS-processing elements of the receiver separately, there are four distinct cases:

1. RAIM and IDS both show no fault, therefore it is safe to continue the approach;
2. RAIM and IDS both show a fault, therefore the approach must be aborted;
3. RAIM shows a fault, but IDS shows no fault, in which case the assumption must be that there is some local effect on the received signals, therefore the approach must be aborted;
4. IDS-processing shows a fault, but RAIM shows no fault, in which case it is not clear what should happen.

At first glance one might assume that a conservative approach should be taken, so that if either independent system declares a fault, the approach should be aborted. However, this is in itself a risky manoeuvre, which is why the continuity requirements for landing aids are so demanding. Where RAIM and IDS-processing are used together it is imperative that the overall false alarm probability does not exceed the Continuity specifications in RNP standards.

This raises the question "What failure or combination of failures can the IDS detect and generate an appropriate alert, but which might not be detected by RAIM".

This is not a trivial problem: In its current inception the IDS has the task of calculating and uplinking SISA for every satellite, at a rate of the order of every 100 minutes [31]. This SISA should bound the approximately Gaussian distribution of normal end-to-end system noise. When a

“feared event³” such as an evil waveform⁴ or a clock error is detected, the IDS must ensure that Integrity Flags are set to warn users that the satellite in question has errors exceeding the broadcast SISA.

So how should the receiver respond to a set Integrity Flag? Consider a case where a user is in a phase of flight that requires 15m vertical alert limit, and the calculated RAIM VPL is 14.8m with all satellites operating normally. If an IF is then detected instructing the receiver to exclude a satellite, which would raise the VPL to 15.1 m, but the RAIM algorithm shows no significant inconsistency, should the approach be aborted? The answer will depend upon the value of SISA and the relative geometry of the failed satellite and the user.

Within the GALA study report on Integrity [3] previously discussed, a decision tree is presented in order to demonstrate how RAIM and SISA monitoring information can be combined to provide an improved overall Total User Integrity Risk. This figure is reproduced at Figure 5-1.

This figure displays two fallacious assumptions:

1. That RAIM does not provide an integrity barrier for multiple SIS errors (which is not true; LSR RAIM may, in some circumstances, not detect certain combinations of multiple failure, but in the majority of cases RAIM will detect multiple failures [26]);
2. It does not take into account the inevitable overlap between ground detections and RAIM detections. The overall performance can only be improved if the ground detection system can detect errors the RAIM system would miss. No evidence has been provided that this is the case. Other studies looking at the robustness of GPS against intentional and unintentional interference effects [37] are unambiguous in stating that RAIM can detect failures that ground based systems would inevitably miss, *but that there is no evidence of a reciprocal case.*

This, therefore, provides the context and starting point for the analytical part of this thesis: To demonstrate that RAIM algorithms using Galileo and GPS together can provide Integrity performance that exceeds that specified for the Galileo IDS.

³“Feared Event” or “FE” is a term used in satellite navigation meaning a possible cause of noise or bias on one or more measurements, for which system designers need to develop appropriate mitigation techniques and/or limit the applicability of the services accordingly.

⁴ An “Evil Waveform” is a specific example of a Feared Event. Experience from GPS has shown that under certain circumstances particular combinations of signal structure and receiver design can lead to a particularly insidious form of ranging error, which affects only users of particular types of receiver, at particular times. Evil Waveforms are very rare events, but they are regarded as the classic kind of FE which define the ~~need~~ ^{need} for sophisticated integrity determination systems.

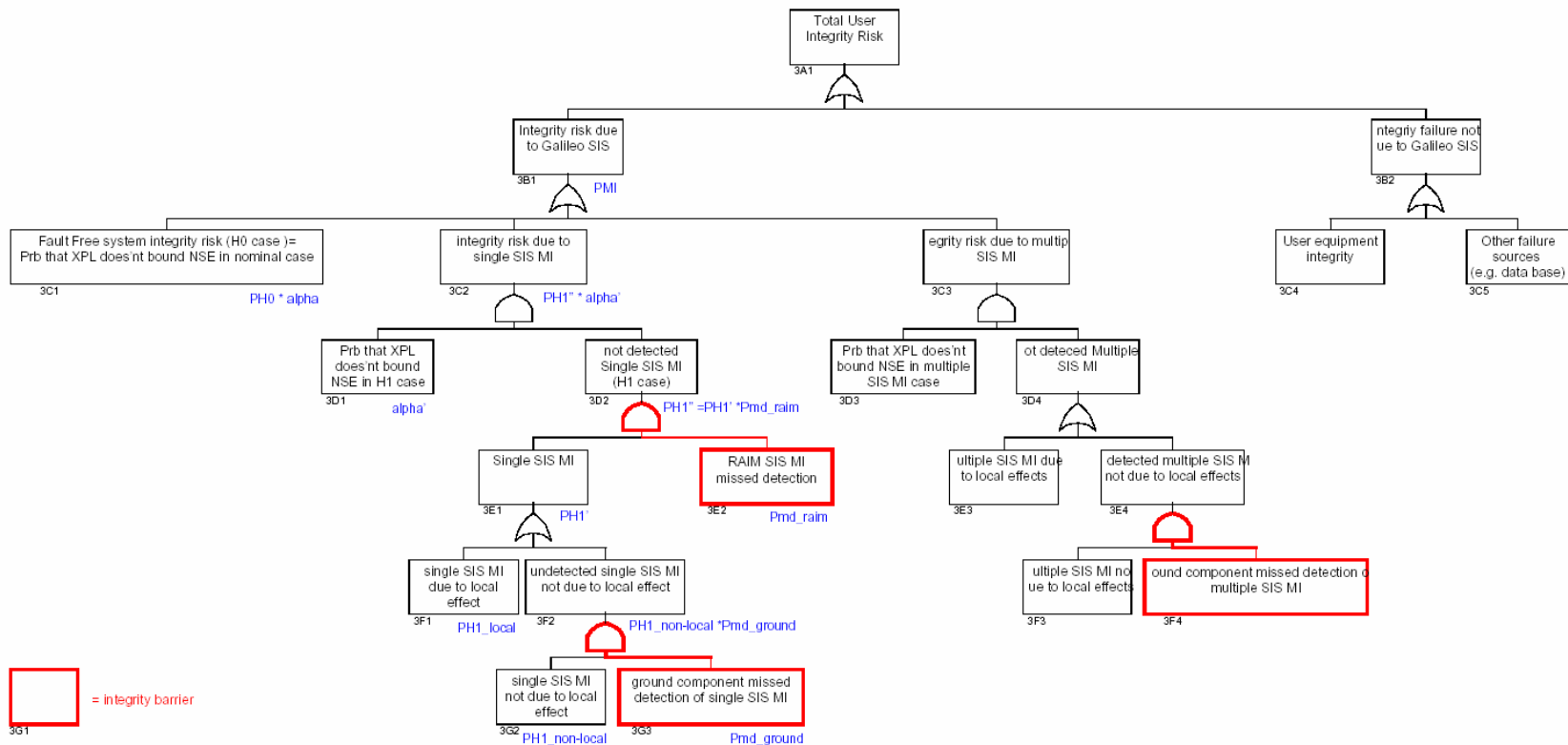


Figure 5-1: “GALA” Study Integrity decision tree showing two “Integrity Barriers” - RAIM and ground-based monitoring (using Boolean Logic “AND” & “OR” gates)

6. SIMULATION TOOLS AND TECHNIQUES

6.1 Set of Tools

In order to meet the objectives of this study as stated in Section 5.3, the following set of simple simulation tools have been developed.

- “RAIM Availability” spreadsheet – Excel/Visual Basic application that calculates RAIM availability for a particular user visibility geometry using the “Least Squares Residual” (LSR) weighted RAIM approach discussed in Section 9 and the novel “Errors in Variables” (EIV) RAIM techniques presented in Section 10.
- “Bias Modelling” spreadsheet – Excel/Visual Basic application that develops the techniques for Monte Carlo analysis of RAIM performance, by simulating the application of Gaussian noise and biases to pseudorange measurements.
- “Service Volume Simulator” (SVS) – An application written in C++ which produces the same outputs as the “RAIM Availability” spreadsheets, but which runs three orders of magnitude faster, and hence produces high temporal and spatial resolution graphical outputs of RAIM availability. This tool also produces a simple output data file which is post-processed using Excel.
- “Navigation Engine” (NavEng) – An application written in C++ which produces similar outputs to the “Bias Modelling” spreadsheet, but which enables large numbers of samples to be used in Monte Carlo simulations to determine the false alarm and missed detection performance of RAIM algorithms under evaluation. This tool also produces a simple output data file which is post-processed using Excel.
- “Flight Trials Simulator” – An application running under Matlab which uses accurate aircraft position information from a series of flight trials and simulates the reception of navigation signals from Galileo and GPS constellations. These signals are processed by LSR and EIV RAIM algorithms, and the ability to detect Feared Events (i.e. unexpected biases on a pseudorange measurement) with various characteristics is evaluated.

These tools are briefly discussed in the following subsections.

6.2 “RAIM Availability” spreadsheet

The RAIM Availability spreadsheet provides the basic analytical tool from which all subsequent tools have been developed. The complete tool comprises the worksheets discussed below.

6.2.1 Input

This is the worksheet on which the scenario is defined. The Galileo and GPS satellite parameters and UERE curves are set on this worksheet, along with the plane difference between constellations and the minimum masking angle. Against each satellite’s parameters, a flag can be set to “F” which will exclude that satellite from the subsequent analysis.

This worksheet also calculates the orbital rate, sine and cosine of inclination and right ascension for each satellite, in preparation for the next stage of the calculation.

6.2.2 Cartesian

This worksheet extracts the time (epoch) at which the required snapshot calculation is to be performed and calculates the position of each satellite in x, y, z co-ordinates. The transformation from Keplerian elements to Earth-centred, inertial (ECI) cartesian co-ordinates is performed using a standard “3-1-3” transformation [38]. This transformation is simplified, since the eccentricity of each satellite’s orbit is assumed to be zero. In this case there is no “argument of perigee” component in the Keplerian elements. The transformation of any satellite’s position to ECI Cartesian coordinates is described under the Detailed Processing Model in Section 8.2.

6.2.3 User_Position

This worksheet extracts the user latitude and longitude for which the required snapshot calculation is to be performed and calculates the position of the user, at the epoch, in the same ECI x, y, z co-ordinate frame as was used for the satellites. The process is described in Section 8.2.

6.2.4 LOS (“Line of Sight”)

For each satellite, this worksheet evaluates the distance between the user and the satellite (“Range”), the elevation angle (by application of the cosine rule) and hence whether or not each satellite is visible above the defined masking angle. This worksheet also presents figures for the degree of coverage (DoC, i.e. the number of satellites in view) for each constellation individually and for the two combined. It is also possible to

extend this worksheet to present these DoC figures as a function of time for the specified user location.

6.2.5 Table

The primary function of this worksheet is to evaluate the components D_x , D_y and D_z of the unit vector from the user to each visible satellite. These are then transformed to North, East and Up components of a unit vector by performing a 3-2-3 [38] coordinate transformation from the ECI coordinate system to local user cartesian coordinates.

A secondary function translates these components into a coarse statement of direction (i.e. a quadrant) to each satellite. Although not used directly, this information is extremely useful in understanding the relative influence of each satellite when considering specific cases.

6.2.6 G_Sheet

The majority of the data processing activities are performed on this worksheet. The satellites in view are first presented in descending order of elevation angle. The UERE for each satellite is then evaluated, from the lookup tables on the "Input" sheet. The Observation matrix or **G** matrix is also produced, along with the Weighting or **W** matrix.

With N satellites in view, the **G** matrix is simply an $N \times 4$ matrix in which the first three columns contain the North, East and Up components of the unit vector previously derived, and the fourth column contains "1", which represents the existence of a clock offset.

By using a series of Visual Basic macros in Excel to cater for the variable size of the matrices (which are set by the number of satellites in view), the various steps of the LSR RAIM method discussed subsequently in Section 7 are performed, culminating in the calculation of the Vertical Protection Limit available for the specified user position, epoch, constellation types and continuity/integrity risk probabilities.

6.2.7 Availability

This worksheet provides an interface in which the user location is specified, along with start time, end time, time step size and required minimum vertical alert limit. Using this data, a macro runs through the preceding steps of the analysis and calculates the vertical protection limit at each time step. When complete, a figure for the percentage availability of RAIM to the specified alert limit is presented.

6.2.8 Display

Taking the previous worksheet a stage further, this sheet provides an interface in which North, South, East and West spatial limits and step sizes are specified, along with start time, end time, time step size and required minimum vertical alert limit. A macro then evaluates whether or not RAIM is available for each combination of time and user position.

	-10	-5	0	5	10	15	20	25	30	35	40	45	50	55	60	65	70	75	80
80	78.7%	79.3%	79.3%	79.3%	78.0%	79.3%	78.7%	77.3%	78.7%	79.3%	78.7%	78.7%	78.0%	80.0%	81.3%	84.7%	88.7%	83.3%	84.7%
75	71.3%	73.3%	77.3%	74.7%	74.7%	74.0%	71.3%	74.7%	74.7%	72.0%	72.0%	72.7%	72.0%	73.3%	76.0%	76.0%	76.7%	73.3%	75.3%
70	77.3%	76.0%	76.7%	76.0%	78.0%	78.0%	78.7%	76.0%	75.3%	74.7%	74.0%	76.0%	75.3%	76.7%	78.0%	81.3%	82.0%	81.3%	79.3%
65	89.3%	86.0%	88.0%	88.0%	84.0%	86.0%	84.7%	85.3%	84.7%	83.3%	84.0%	85.3%	84.7%	86.7%	88.0%	89.3%	90.0%	92.0%	94.7%
60	96.7%	96.7%	95.3%	98.0%	96.0%	94.7%	93.3%	92.7%	91.3%	91.3%	90.7%	92.0%	94.7%	96.7%	96.7%	96.7%	98.7%	99.3%	100.0%
55	100.0%	100.0%	99.3%	98.0%	98.7%	98.7%	96.7%	97.3%	97.3%	95.3%	96.7%	98.0%	98.7%	98.7%	99.3%	100.0%	100.0%	100.0%	100.0%
50	100.0%	100.0%	100.0%	100.0%	99.3%	98.7%	98.7%	97.3%	98.0%	98.0%	98.0%	100.0%	100.0%	99.3%	100.0%	99.3%	100.0%	100.0%	100.0%
45	100.0%	100.0%	100.0%	100.0%	99.3%	99.3%	98.0%	100.0%	96.7%	96.0%	98.0%	98.7%	99.3%	98.7%	98.7%	98.7%	98.0%	100.0%	100.0%
40	100.0%	100.0%	100.0%	100.0%	100.0%	100.0%	100.0%	98.7%	98.7%	97.3%	98.0%	98.7%	99.3%	100.0%	98.0%	98.0%	98.7%	100.0%	100.0%
35	100.0%	100.0%	100.0%	100.0%	99.3%	100.0%	100.0%	99.3%	99.3%	99.3%	98.7%	99.3%	100.0%	98.7%	98.0%	98.0%	100.0%	100.0%	100.0%
30	100.0%	100.0%	100.0%	100.0%	100.0%	99.3%	99.3%	100.0%	99.3%	100.0%	100.0%	99.3%	100.0%	100.0%	99.3%	100.0%	100.0%	100.0%	100.0%
25	97.3%	100.0%	98.7%	99.3%	99.3%	99.3%	98.7%	98.0%	96.7%	96.0%	95.3%	95.3%	97.3%	97.3%	97.3%	96.7%	100.0%	98.7%	96.7%
20	92.7%	93.3%	93.3%	94.7%	94.7%	95.3%	94.7%	90.7%	92.0%	91.3%	92.7%	92.7%	94.0%	95.3%	91.3%	92.7%	94.0%	93.3%	92.7%
15	87.3%	88.0%	90.0%	91.3%	92.0%	91.3%	92.0%	87.3%	87.3%	91.3%	92.0%	88.7%	90.0%	89.3%	88.7%	90.7%	90.7%	88.7%	90.0%
10	88.0%	91.3%	91.3%	93.3%	90.7%	92.7%	93.3%	88.7%	90.0%	92.0%	89.3%	95.3%	89.3%	92.0%	90.0%	91.3%	90.7%	92.7%	92.7%
5	92.0%	89.3%	88.0%	87.3%	84.7%	86.7%	84.7%	84.0%	83.3%	82.0%	81.3%	83.3%	86.7%	86.7%	88.0%	86.7%	89.3%	94.0%	95.3%
0	88.7%	84.7%	86.7%	82.7%	80.7%	81.3%	78.7%	77.3%	77.3%	79.3%	78.0%	77.3%	80.0%	84.0%	82.0%	87.3%	86.7%	88.7%	94.0%

Table 6-1: Example output from “Display” function

Table 6-1 presents a sample output from this function.

6.2.9 SVD

The EIV process is performed on a worksheet called “SVD”, which includes a number of macros to perform the necessary matrix manipulations with matrix dimensions that are a function of the number of satellites in view. Within this worksheet the EIV RAIM process described in Section 10 has been modelled.

Unlike the previous methods described, Excel does not include all of the functions necessary to perform the EIV/Total Least Squares analysis. Specifically, the Singular Value Decomposition (SVD) linear algebra function at the heart of this method has been included using an Excel add-in called “PopTools”. This is freely available on the internet [39] and uses validated mathematical methods, along with routines for iterating spreadsheets and performing Monte Carlo simulations. PopTools was

developed by Greg Hood at the Pest Animal Control Co-operative Research Centre, based at Wildlife and Ecology, CSIRO, Canberra, Australia. It depends heavily on a numerical library developed by Dr Jean DeBord, which is available at his TPMath web site.

6.3 “Bias Modelling” spreadsheet

This tool uses the same worksheets as the “LSR RAIM” spreadsheet, with the addition of macros and a user interface to include a random noise error on any or all satellite’s signals, along with a discrete bias if required. To model Gaussian noise, a random number between 0 and 1 is generated for each satellite, which is then used in Excel’s “Normsinv” function to produce the number of standard deviations (and sign) associated with this probability level. When this is then multiplied by the UERE value associated with the satellite’s elevation angle a random error (in metres) is generated. By adding this value (which may be positive or negative) to the “true” modelled distance between the receiver and the satellite, a pseudorange is generated.

A routine has been added to the “G_Sheet” worksheet which calculates the weighted least squares position solution (as described in Section 9.1) and generates a flag if the vertical position error exceeds the LSR RAIM-calculated vertical protection limit.

6.4 Service Volume Simulator (SVS)

Although Excel is an extremely useful application for simple and rapid development and visualisation of the techniques discussed in this thesis, it is relatively slow computationally – when calculating protection limits using both LSR and EIV RAIM methods simultaneously, each geometrical case takes of the order of two seconds to process on a 1.47 MHz AMD Athlon PC. Clearly, it is impractical to attempt to calculate RAIM availability statistics with reasonable temporal and spatial resolution using Excel – the number of cases, and hence the processing time required, rapidly becomes prohibitive. As a result the LSR and EIV RAIM VPL protection algorithms and RAIM availability calculations were coded in C++ to produce a tool running approximately three orders of magnitude faster. Figure 6-1 shows the window for snapshot (i.e. single geometry) analysis. A separate window enables the user to run multiple analyses, with relatively high spatial and temporal resolution.

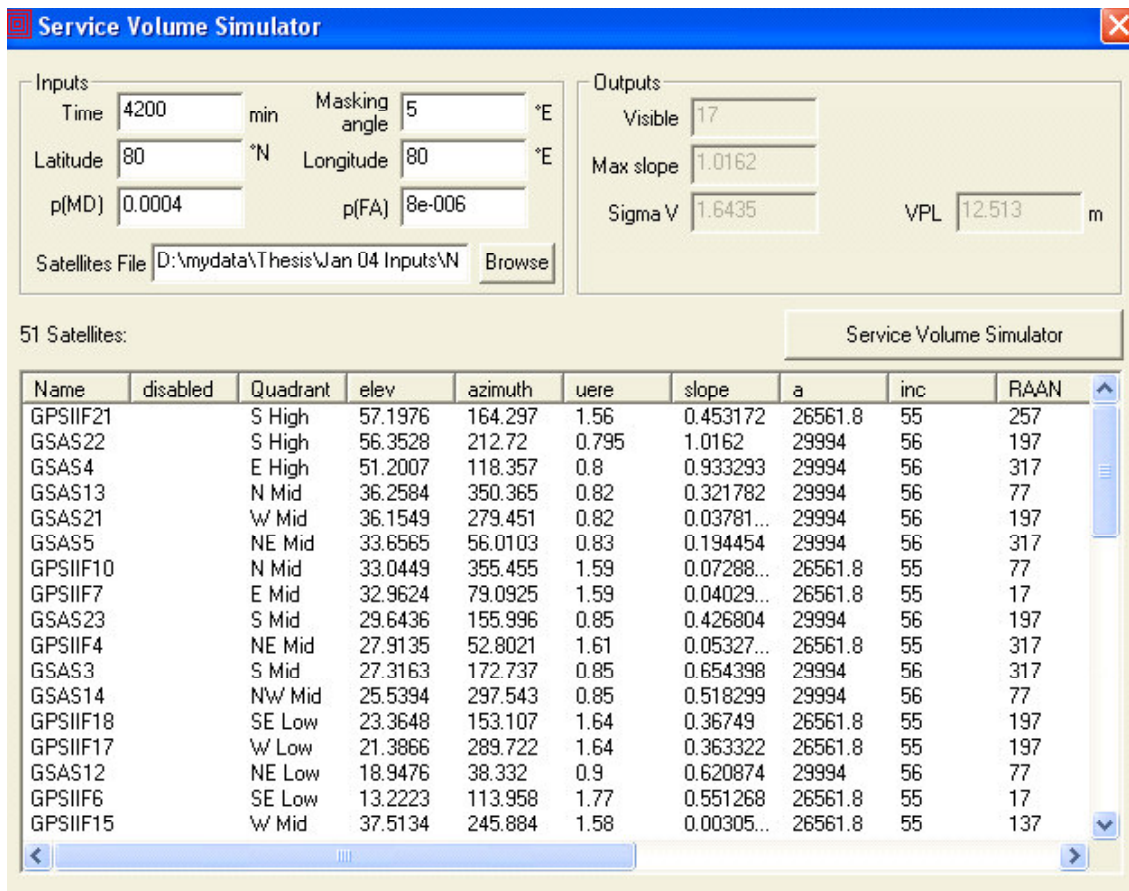


Figure 6-1: SVS Snapshot Case Window

Validation of the software implementation was performed simply by comparing the results produced by this tool with those produced by Excel, for a large number of cases. As can be seen in Figure 6-1, this window displays all of the individual parameters produced by the Excel spreadsheet.

In order to model the EIV method in this tool, it is obviously necessary to include the Singular Value Decomposition function which is the key element of the Total Least Squares solution. This can be taken from an appropriate text providing numerical recipes for C++ programs or, as in this case, a dedicated linear algebra toolset can be used. The tool used here is called “gMatVec C++ Matrix/Vector Library”, which is freeware downloadable from a number of internet sites [40], although any commercial linear algebra package including the SVD function, such as the widely available LAPACK, could be used. Alternatively, MATLAB could also be used.

One point to note is that different implementations of the SVD function have different conventions which need to be borne in mind. Specifically, the SVD function in “Poptools” for Excel always ranks the singular values

extracted from the matrix in descending order of size. Some C++ SVD functions may not sort the singular values automatically. Therefore this ordering process must be manually coded in order for the EIV process described subsequently to work correctly.

Both the LSR and EIV methods discussed subsequently require some statistical functions to be employed. For LSR, normal distribution and central χ^2 distribution functions are required. For EIV, non- central χ^2 distribution functions are also required, as will be demonstrated. In order to evaluate these techniques, statistical function libraries have been incorporated into these tools [41]. These libraries use statistical functions defined in [42].

The Service Volume Simulation was developed with the following requirements:

- Allow the user to specify a “snapshot” analysis case, which is a combination of epoch, receiver latitude and longitude, minimum masking angle, false alarm probability (P_{FA}) and missed detection probability (P_{MD});
- Allow the user to specify a “service volume” analysis case, which is a combination of:
 - start and end epoch;
 - time step/number of time steps;
 - receiver latitude and longitude;
 - latitude/longitude step size or number of steps within the range;
 - minimum masking angle;
 - false alarm probability;
 - missed detection probability.
- Accept constellation definition files which specify the orbital elements for the satellites to be used in a service volume analysis, and tables which specify the relationship between UERE and elevation angle. This table may be different for different satellite types (i.e. a different table may be specified for Galileo SAS, Galileo OAS and/or GPS IIF satellites);
- Include Dynamic Link Libraries (DLL) in which RAIM algorithms to be evaluated are defined;

- Allow the user to exclude any satellites from the analysis at run-time;
- Present the Vertical Protection Limit calculated using any included algorithms, for a snapshot geometry (i.e. combination of epoch and user latitude/longitude);
- Present maps of the specified service area, overlaid with colour-coded (grey-scale) plots showing percentage of time for which RAIM is available to the specified Vertical Alert Limit (VAL);
- Allow the user to change the specified VAL;
- Allow the user to specify the availability percentages associated with each grey scale element;
- Allow the user to copy maps to documents for reporting purposes;
- Allow service volume simulations to be performed on a PC with a resolution at least as demanding as:
 - Time span – three days (i.e. the repeat period of a combined Galileo/GPS constellation);
 - Time step – 1 minute
 - Global coverage (180 degrees to –180 degree longitude, 90 degrees to –90 degrees latitude)
 - Spatial resolution down to 1 degree for global coverage. Finer for analysis over small service areas (e.g. 0.5 degree in lat and long over ECAC region)
 - Up to one hundred million iterations in a service volume analysis.

Given the large number of samples required to produce high-definition service volume analyses, the SVS is optimised for speed rather than for high-fidelity. Specifically, a spherical earth approximation is used, and orbits propagated using a Keplerian model, assuming zero orbital eccentricity.

The SVS also provides as an additional output a single figure representing the overall availability of integrity (as a percentage) for the specified service volume and conditions. This figure use a weighting function to ensure that each geographical location (i.e. a given latitude and longitude) is weighted according to the surface area associated with the latitude of the location (i.e. points close to the equator are weighted more highly than points close to the poles).

The SVS does not provide a direct assessment of integrity availability taking into account assumed satellite outage probabilities. However, by running each test case a number of times, with 0, 1 or 2 satellites out at any time, and by combining the overall integrity availability figures with a weighting corresponding to the probability of each degraded constellation state, a figure for the overall availability of integrity taking into account satellite outages can be evaluated.

Output from the Service Volume Simulator takes the form of a map, overlaid with a grid, the shade of which represents the percentage availability of RAIM with the specified P_{MD} , P_{FA} requirements and vertical alert limit.

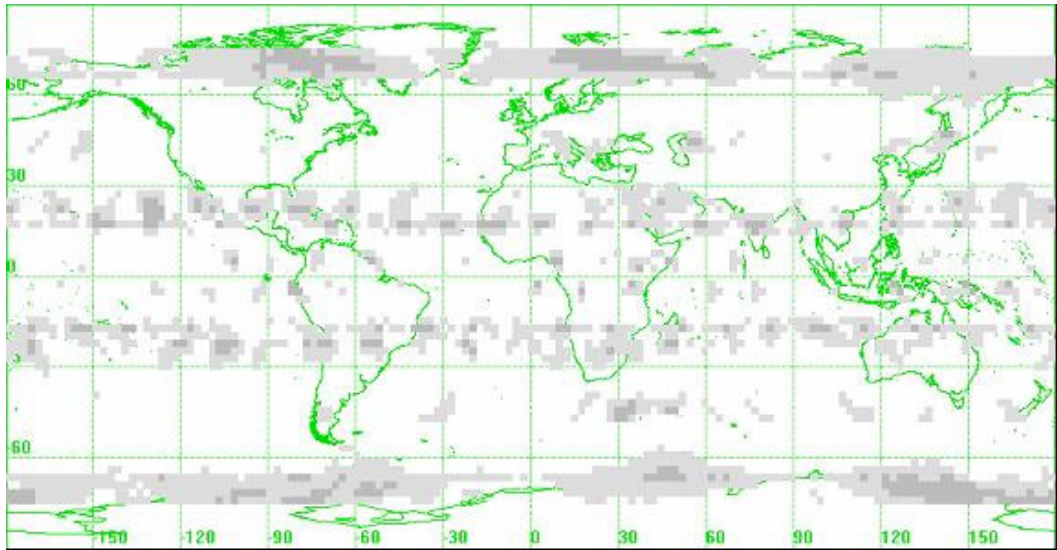


Figure 6-2: Example output from Service Volume Simulator

A text file representation of this availability plot is also available as an output. This allows runs to be repeated with 0, 1, 2 or 3 satellites disabled, and the availability figures combined based on these state probabilities. This combination of data is performed in Matlab or Excel.

In addition, the SVS outputs the following data:

- Average RAIM availability, weighted to take into account the surface area associated with each latitude/longitude step;
- RAIM availability at the worst user location;
- Latitude and Longitude of worst user location.

6.5 Navigation Engine (NavEng)

As previously discussed, the required navigation performance requirements of continuity and integrity for aviation precision approach and the associated Galileo Safety of Life service are very demanding. In order to demonstrate that a RAIM algorithm can meet these requirements, simulations are required to be performed using a very large number of samples. To this end the Navigation Engine Monte Carlo Simulation (“NavEng”) was developed, to enable the performance of RAIM algorithms to be evaluated in terms of false alarm probability and probability of missed detection.

The NavEng tool was developed with the following requirements:

- Allow the user to specify a “snapshot” analysis case, which is a combination of:
 - Epoch;
 - receiver latitude and longitude;
 - receiver altitude;
 - minimum masking angle;
 - false alarm probability (P_{FA});
 - missed detection probability (P_{FD});
 - Number of pseudo-random samples to be used.
- Accept the same constellation definition files as used by the SVS;
- Include Dynamic Link Libraries (DLL) in which full RAIM algorithms to be evaluated are defined. These algorithms will include the calculation of VPL and of test statistics, based on simulated pseudorange measurements;
- Allow the user to exclude any satellites from the analysis at run-time;
- Allow the user to apply a fixed bias to one or more satellites in view at run-time;
- Present the Vertical Protection Limit calculated using any included algorithms, for a snapshot geometry (i.e. combination of epoch and user latitude/longitude);
- Output a text file containing:

- Vertical error arising from Least Squares navigation solution using simulated pseudorange measurements, for each sample;
 - Horizontal error arising from Least Squares navigation solution using simulated pseudorange measurements, for each sample;
 - RAIM test statistic, for each sample, for each algorithm included in the analysis.
- Output a second text file containing:
 - The variation of vertical error with increasing bias on each satellite in view, in a noise free system;
 - The variation of horizontal error with increasing bias on each satellite in view, in a noise free system;
 - The variation of test statistic for the Least Squares RAIM algorithm with increasing bias on each satellite in view, in a noise free system;
 - The variation of test statistic for the RAIM algorithm under test, with increasing bias on each satellite in view, in a noise free system

A NavEng Post-processor (in the form of an Excel spreadsheet) application is then used to:

- Plot the relationship between true vertical error and test statistic for each analysed RAIM algorithm;
- Plot the probability density of test statistic values, and compare this with standard distributions such as the Chi-squared distribution, to provide a comparison of the strength of the tails of the distributions produced by the algorithms under analysis;
- Plot the relationship between true horizontal error and test statistic for each analysed RAIM algorithm.

A separate post-processor is used to produce RAIM Algorithm Characteristic curves, presenting plots of the relationship between error (vertical or horizontal) with test statistic, for the RAIM algorithm under test.

The Navigation Engine Monte Carlo Simulations are based on the same input data set as discussed for the Service Volume Simulations. Figure 6-3 presents a screenshot of the NavEng user interface.

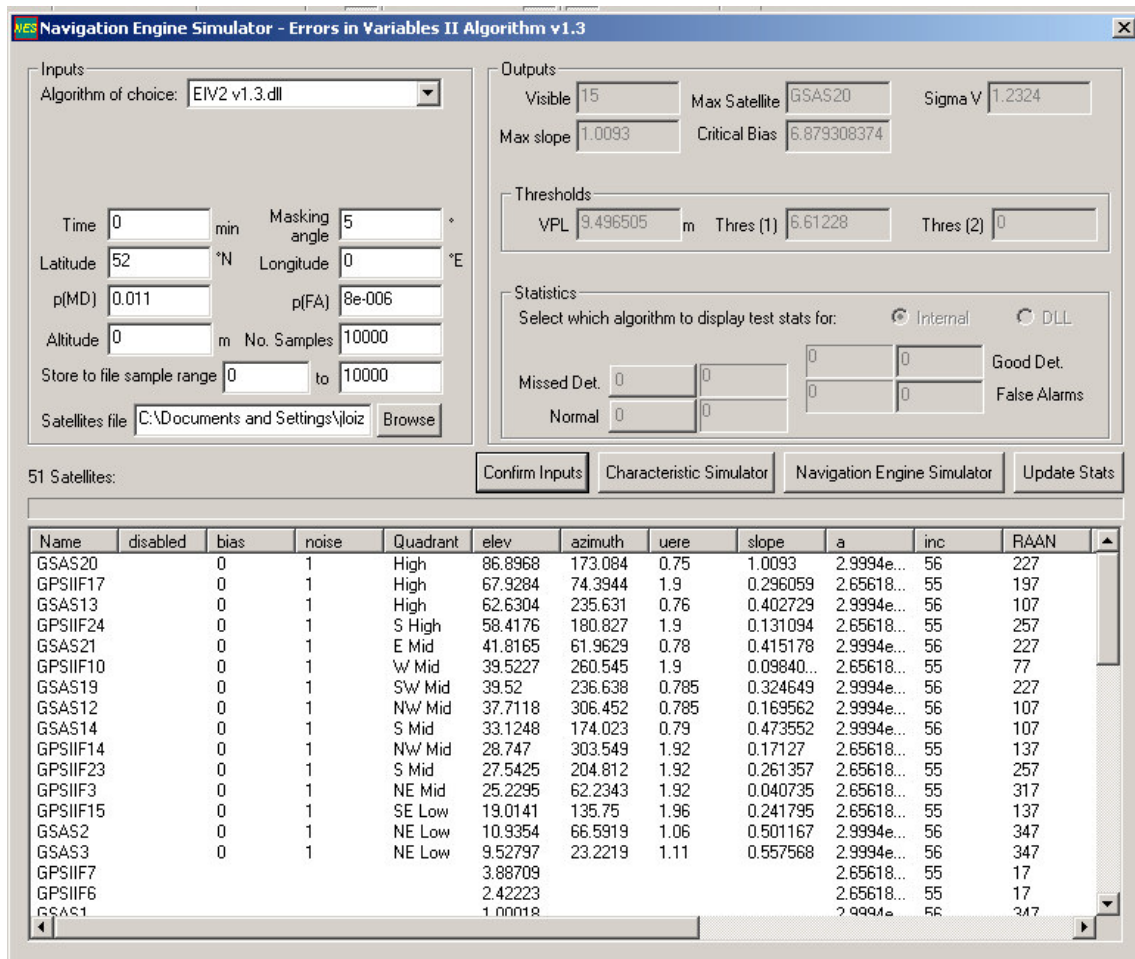


Figure 6-3: Navigation Engine Input Window

Unlike the SVS, NavEng runs are performed for a single, snapshot combination of user location and epoch. However, random noise is applied, therefore the user selects the number of samples to be performed in each Monte Carlo simulation. In addition, the user may disable any satellite in view, apply a bias to the ranging signal from any satellite, or increase the noise by multiplying the UERE for a satellite by any desired amount.

The NavEng tool provides three distinct types of data:

1. Output displayed on the MMI:

After confirmation of the inputs (satellite file, user location and epoch, disabled satellites, biases and noise) the MMI displays information such as:

- the number of useable satellites in view;
- the VPL, calculated using the weighted least squares residuals algorithm;
- the Critical Satellite, i.e. the satellite with the steepest slope of vertical error against LSR test statistic;
- the Critical Bias, i.e. the bias which, in the absence of any other noise, would just generate the LSR test statistic when applied to the Critical Satellite.

After running the Navigation Engine Simulator the MMI also displays two sets of four figures, representing the number of samples falling into each of four categories:

- Normal operations – vertical error is below VPL and test statistic is below test threshold;
- Alarm – vertical error is above VPL and test statistic is above test threshold;
- False Alarm – vertical error is below VPL and test statistic is above test threshold;
- Missed detection – vertical error is above VPL and test statistic is below test threshold.

The two sets of numbers cater for RAIM algorithms such as EIV which generate two independent test statistics. With eight figures displayed it is possible for the user to determine the number of samples in which either or both test statistics are exceeded, and whether or not the VPL is also exceeded.

The user can then change the values displayed for VPL and Test Threshold(s), which offers a coarse check that the number of false alarms (with no bias applied) or missed detections (with a critical bias applied) approximates the values determined by P_{FA} and P_{MD} .

2. File Output from Navigation Engine Simulator:

On completion of a run the NavEng tool writes a text file to the hard disk, with the date and time of the run included in the file name for ease of reference. The content of this text file is in three parts:

- Header data – presenting the input case specified by the user on the MMI (satellite file, receiver latitude, longitude, altitude, epoch, etc.);

- Columns of data representing, for each sample:
 - Vertical Error;
 - Horizontal Error;
 - LSR RAIM Test Statistic;
 - Test statistic(s) from the RAIM algorithm implemented in the attached DLL.
- The probability density associated with each test statistic. The maximum and minimum value occurring for each test statistic is evaluated, and the range between the two extremes divided into 50 “bins”. The number of samples with a test statistic falling into the value of each bin is reported.

These data are post processed to produce appropriate graphical output

3. File Output from Characteristics Simulator:

A key concept in the development of new RAIM algorithms is the idea of a RAIM test statistics “characteristic”. This characteristic represents the relationship between the test statistic and the vertical error, for the case of increasing bias applied to each satellite in view in turn, in the absence of any other noise or bias. Typically, each satellite will have a different gradient of this characteristic, and the maximum value occurring (referred to as “ $V_{\text{Slope(max)}}$ ”) identifies the most critical satellite, and drives the value of VPL in the LSR RAIM algorithm.

The output from the NavEng Characteristics Simulator is a set of tables presenting:

- The variation of vertical error with bias applied to each satellite;
- The variation of horizontal error with bias applied to each satellite;
- The variation of LSR Test Statistic with bias applied to each satellite;
- The variation of RAIM Test Statistic(s), for the DLL-installed RAIM algorithm, with bias applied to each satellite.

These data are post processed to produce appropriate graphical output.

6.6 Matlab Flight Trials Simulator

Although the NavEng tool demonstrates the ability of a RAIM algorithm to detect a bias on a pseudorange measurement, it does not allow the nature of the bias to be specified. In effect, NavEng can only demonstrate the ability to detect step biases. In practice, a Feared Event (FE) acting on a pseudorange measurement is likely to have some ramping function, and the ability to detect such FE's needs to be demonstrated.

To this end the Flight Trials Simulator was developed using Mathworks' "Matlab v6.5" mathematical modelling tool. The basic Matlab tool was augmented with the Matlab Statistics library in order to provide the functions required by the LSR and EIV RAIM algorithms. It is referred to as a "Flight Trials" Simulator, because it uses a trajectory file provided by National Air Traffic Services Ltd (NATS) which gives very accurate 1 Hz position data for a set of flight trials performed by a BAC 1-11 aircraft into Boscombe Down airfield in September 2001. This data set acts as "truth" in the flight trials simulator.

This tool simulates broadcast almanacs and pseudorange measurements from the Galileo and GPS constellations as discussed subsequently and used elsewhere in this thesis. A standard, unfiltered Least Squares navigation position solution is generated to produce user position and clock estimates corresponding to the "truth" data. In addition, RAIM algorithms produce test statistics using the same almanacs and pseudorange measurements. By injecting a bias which has a specified rate of increase and duration of application, Feared Events with various characteristics are simulated and the ability of the RAIM algorithms to detect these FEs is evaluated.

The process used in this tool is as follows:

1. Define a "Broadcast Almanac" for the Galileo constellation. This is effectively the set of parameters defined in Table 7-3 which define the nominal Galileo constellation;
2. Define a "True Almanac" for the Galileo constellation. This is very similar to the broadcast almanac, except for small changes that are made to each satellite's semi-major axis, inclination, right ascension of ascending node and mean anomaly. Also, for each satellite, a small "satellite clock synchronisation error" is incorporated, to represent the difference between Galileo System Time and the local estimate of system time at the satellite. These position and time biases together constitute the "Orbit Determination & Time Synchronisation" (OD&TS) Error for each satellite. Each value has been randomly selected from a distribution such that the overall

OD&TS error has a normal distribution with a standard deviation as specified for the Galileo constellation.

3. Repeat steps 1 and 2 for the GPS constellation defined in Table 7-4. Note that in addition to the randomly selected satellite time synchronisation error between each GPS satellite and GPS system time, an offset is also included to simulate the synchronisation error between the GPS and Galileo system times. [48] states that although it is planned to disseminate information regarding the synchronisation of the two system times, the residual error (i.e. the error after taking this disseminated correction into account) may be up to 5 ns, therefore this figure has been used as a fixed offset between the system times.
4. Define UERE vs Elevation characteristics for each constellation, to be used by the user in setting the weighting matrix used in the weighted least squares solution.
5. Define an initial true user receiver clock error.
6. Define a randomly selected value for the tropospheric zenith delay (ZTD).
7. Initialise the user receiver's estimate of position and user clock error.
8. At runtime, the user defines an epoch at which a bias begins to be applied, the rate at which this bias increases, the duration for which the bias increases and duration for which the bias is held at its maximum value, before dropping off as a step function to zero.
9. For each simulated 1 second interval:
 - a. Get the "true" user position;
 - b. Propagate the Galileo and GPS constellations using the "true" almanacs;
 - c. Calculate the "true" distance from the user to each satellite;
 - d. Determine the "Critical Satellite", i.e. that satellite for which an applied unit bias generates the largest vertical positioning error;
 - e. Generate the measured pseudorange, by adding to this "true" distance:
 - i. An elevation dependant component of tropospheric residual error, as a function of elevation angle from the user to each satellite, using the ZTD parameter fixed

- during initialisation. NB This component is correlated across all observations;
- ii. An elevation dependant component of ionospheric residual error, randomly selected and uncorrelated across observations;
 - iii. Elevation dependant components of noise representing multipath jitter;
 - iv. Non-elevation dependant components representing additive white Gaussian receiver noise;
 - v. A component representing the pseudorange error due to “true” satellite and user clock synchronisation errors;
 - vi. If appropriate, add an additional Feared Event Bias component to the pseudorange of the critical satellite.
- f. Calculate the expected range to each satellite, based upon the broadcast almanac and the user’s estimate of position and user clock error;
 - g. Generate the Observation Matrix;
 - h. Generate the elevation dependent Weighting matrix using the appropriate UERE vs Elevation curves;
 - i. Generate the vector of pseudorange residuals, i.e. the difference between the expected range and the measured pseudorange to each satellite;
 - j. Calculate the navigation position solution (Latitude, Longitude, Height and clock error) using a standard weighted least squares position solution (as defined in Section 9.1), and update the user estimate accordingly;
 - k. Pass the Observation matrix, Weighting matrix and range residuals vector to LSR and EIV RAIM algorithms, and calculate the vertical protection limits, detection thresholds and test statistics;
10. Evaluate for each epoch the vertical error, and the detection state from each RAIM algorithm, i.e. were there any instances in which an alarm was triggered when the vertical protection limited was not exceeded (false alarms) or cases where the VPL was exceeded without an alarm (missed detections).

7. ASSUMPTIONS, PARAMETERS AND VARIABLES

The tools discussed in the previous section require a set of validated input data in order to produce meaningful results. This section presents the key assumptions, parameters and variables which have been set in the subsequent analysis, and discusses the validity of these assumptions.

[43] presents a “Reference Set Of Parameters For RAIM Availability Simulations”. This document, produced for the European Organisation of Civil Aviation Equipment Manufacturers (EUROCAE) working group on Galileo, attempts to produce a harmonised set of assumptions for use in RAIM availability simulations of the type presented in this thesis. To the greatest extent possible the assumptions presented by EUROCAE are used in the subsequent analysis. However, as will be discussed below, there are a number of points on which the reference set of data used in this thesis diverge from that presented in [43].

7.1 UERE vs Elevation Characteristics

As demonstrated in [43] the parameter which has the greatest impact on the predicted RAIM performance is the UERE vs Elevation characteristic assumed for the satellites in view. This section discusses the selection of the UERE curves used in the subsequent analysis, from those available in published literature.

7.1.1 GPS IIF UERE Characteristics

There is considerable disagreement regarding the likely performance of the freely available signals provided by the future GPS Block IIF satellites. Figure 7-1 compares the characteristics for a dual frequency (L1/L5) open access service extracted from three different sources:

- The EUROCAE reference set of RAIM parameters [43];
- Estimates presented in the public domain by the US Department of Defense (DoD) [44];
- Assumptions taken by Alcatel Space Industries on behalf of the Galileo System Test Bed programme and published in a “Context Assumptions” document [45].

Clearly the Galileo programme has made a more conservative estimate of future GPS performance than the US DoD. In the absence of any better information, it has been decided to use the EUROCAE estimate (effectively the compromise solution) of future GPS performance in the subsequent analysis. This characteristic is presented in Table 7-1.

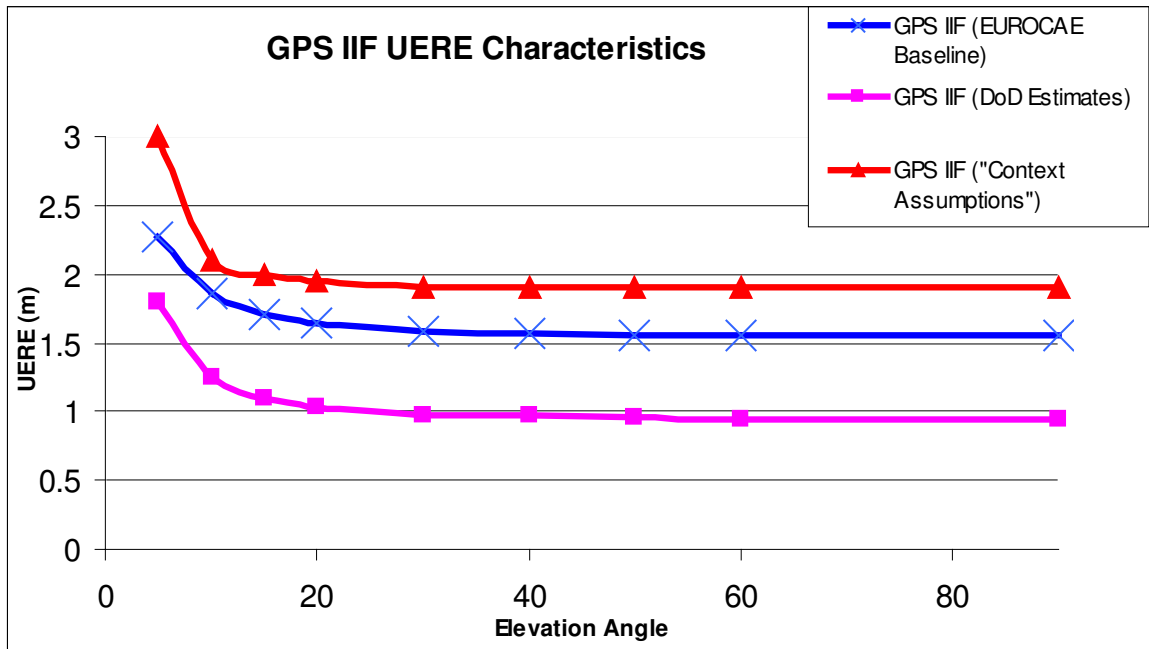


Figure 7-1: Comparison of Published GPS Block IIF UERE Characteristics

ELEVATION (°)		5	10	15	20	30	40	50	60	90
Total Error	cm	227	186	171	164	159	157	156	156	156

Table 7-1 : Baseline GPS IIF L1/L5 UERE budget (from EUROCAE Reference Set)

7.1.2 Galileo UERE Characteristics

Figure 7-2 presents a comparison of published estimates for Galileo UERE vs Elevation performance, for freely available (i.e. unencrypted) signals using the L1 and 5b signals together to provide a dual frequency service. Note that these estimates are much closer than the equivalent estimates for GPS IIF performance.

As before, the median estimate has been taken for use in the subsequent analysis. This is the UERE characteristic taken as the baseline for a free-to-air aviation service from the Galileo System Test Bed programme's UERE budget document [46], and is presented in Table 7-2. The OD&TS contribution is 65 cm across all elevations.

Note that this curve is slightly more optimistic regarding the performance of Galileo than the EUROCAE reference set of RAIM parameters assumptions.

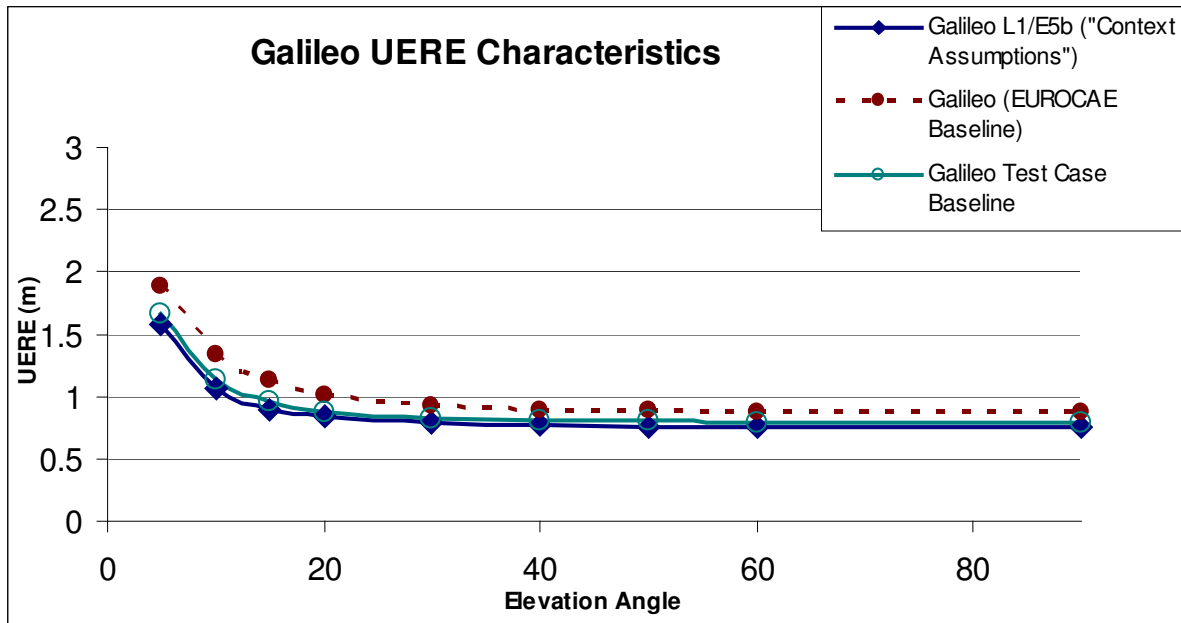


Figure 7-2: Comparison of Published Galileo L1/E5b UERE Characteristics

ELEVATION (°)		5	10	15	20	30	40	50	60	90
Total Error	cm	166	114	96	88	83	81	80	79	79

Table 7-2 : Baseline Galileo L1/E5b UERE budget (from GSTB Test Case Experimentation Plan)

The Galileo and GPS characteristics are presented again in comparison to one another in Figure 12-1 when introducing the results from the Service Volume Simulation analyses.

7.1.3 Orbit Determination & Time Synchronisation Errors

In the Flight Trials Simulations tool described previously it was stated that the Orbit Determination & Time Synchronisation (OD&TS) component of the UERE for each satellite has to be separated from the overall UERE, in order for the Signal in Space Error to be distinguished from the error due to local effects. This allows for OD&TS errors to be modelled for each satellite, as components of its clock offset, semi-major axis, inclination, right ascension of ascending node and mean anomaly.

[43] estimates the OD&TS error for GPS Block IIF to be 1.5m. It has been assumed in this thesis that this total comprises the following random vector components:

- 0.8m GPS time synchronisation error;

- 1.25m orbit determination error.

For Galileo [46] estimates the OD&TS error as, 0.72m, comprising:

- 0.6m Galileo time synchronisation error;
- 0.4m orbit determination error.

NB These components are added vectorially (i.e. the total is the square root of the sum of the squares) to yield the overall OD&TS error.

7.2 Constellation Configurations

7.2.1 Galileo Constellation Parameters

Table 7-3 shows the nominal Galileo constellation parameters used for all analyses in this thesis. It includes only the 27 satellites of the Walker constellation 27/3/1 and does not consider the 3 operational spares.

The semi-major axis for this constellation leads to an orbital period of about 14.4 hours, so that there are exactly five orbits in three days. This results in a repeating ground track such that every three days the geometry of the constellation relative to a user on the ground is repeated. Furthermore, because the satellites in each plane are regularly spaced, every 24 hours the effective geometry of the nominal constellation from a fixed user location is repeated, albeit with different satellites in view.

Note that the epoch for which these parameters apply is set by the epoch used for the GPS Constellation in the next section.

SV ID	Semi-major Axis (km)	Eccentricity	Inclination (deg.)	RAAN (deg.)	Arg. of Perigee (deg.)	Mean Anomaly (deg.)
1	29993.707	0.00	56.0	317 ⁵	0.00	0.00
2	29993.707	0.00	56.0	317	0.00	40.00
3	29993.707	0.00	56.0	317	0.00	80.00
4	29993.707	0.00	56.0	317	0.00	120.00
5	29993.707	0.00	56.0	317	0.00	160.00
6	29993.707	0.00	56.0	317	0.00	200.00
7	29993.707	0.00	56.0	317	0.00	240.00
8	29993.707	0.00	56.0	317	0.00	280.00
9	29993.707	0.00	56.0	317	0.00	320.00
10	29993.707	0.00	56.0	77	0.00	13.33
11	29993.707	0.00	56.0	77	0.00	53.33
12	29993.707	0.00	56.0	77	0.00	93.33
13	29993.707	0.00	56.0	77	0.00	133.33
14	29993.707	0.00	56.0	77	0.00	173.33
15	29993.707	0.00	56.0	77	0.00	213.33
16	29993.707	0.00	56.0	77	0.00	253.33
17	29993.707	0.00	56.0	77	0.00	293.33
18	29993.707	0.00	56.0	77	0.00	333.33
19	29993.707	0.00	56.0	197	0.00	26.66
20	29993.707	0.00	56.0	197	0.00	66.66
21	29993.707	0.00	56.0	197	0.00	106.66
22	29993.707	0.00	56.0	197	0.00	146.66
23	29993.707	0.00	56.0	197	0.00	186.66
24	29993.707	0.00	56.0	197	0.00	226.66
25	29993.707	0.00	56.0	197	0.00	266.66
26	29993.707	0.00	56.0	197	0.00	306.66
27	29993.707	0.00	56.0	197	0.00	346.66

Table 7-3 : Galileo Constellation Parameters

7.2.2 GPS Constellation Parameters

Table 7-4 shows the GPS constellation parameters for the constellation used in this thesis [47]. These parameters are with respect to an epoch of 1 July 1990 00:00:00.

The satellites in this constellation complete two orbits per day, giving them a repeating ground track every day. Note that unlike the Galileo constellation, the GPS nominal constellation is not symmetrical.

⁵ The Right Ascension of Ascending Node (RAAN) assumed for all Galileo satellites has been set as a function of the RAAN of the GPS satellites. In the baseline case (presented in this table) the three planes of the Galileo constellation have been placed at a worst case with GPS, i.e. there is a 0° offset between the RAAN of the first Galileo plane and the first GPS plane. The effect of variations in this assumption are discussed in Section 7.2.3.

SV ID	Semi-major Axis (km)	Eccentricity	Inclination (deg.)	RAAN (deg.)	Arg. of Perigee (deg.)	Mean Anomaly (deg.)
1	26559.7	0.00	55	317	0.00	280.7
2	26559.7	0.00	55	317	0.00	310.3
3	26559.7	0.00	55	317	0.00	60
4	26559.7	0.00	55	317	0.00	173.4
5	26559.7	0.00	55	17	0.00	339.7
6	26559.7	0.00	55	17	0.00	81.9
7	26559.7	0.00	55	17	0.00	115
8	26559.7	0.00	55	17	0.00	213.9
9	26559.7	0.00	55	77	0.00	16
10	26559.7	0.00	55	77	0.00	138.7
11	26559.7	0.00	55	77	0.00	244.9
12	26559.7	0.00	55	77	0.00	273.5
13	26559.7	0.00	55	137	0.00	42.1
14	26559.7	0.00	55	137	0.00	70.7
15	26559.7	0.00	55	137	0.00	176.8
16	26559.7	0.00	55	137	0.00	299.6
17	26559.7	0.00	55	197	0.00	101.7
18	26559.7	0.00	55	197	0.00	200.5
19	26559.7	0.00	55	197	0.00	233.7
20	26559.7	0.00	55	197	0.00	335.9
21	26559.7	0.00	55	257	0.00	142.2
22	26559.7	0.00	55	257	0.00	255.6
23	26559.7	0.00	55	257	0.00	5.3
24	26559.7	0.00	55	257	0.00	34.5

Table 7-4: GPS orbital parameters

7.2.3 Galileo/GPS Plane Offset

As mentioned above, the baseline combined Galileo/GPS constellation has been defined as one in which the three Galileo planes are coplanar with three of the six GPS planes. In practice, because of the difference in the orbital altitudes of the two constellations, there is a relative movement of the planes over time. The perturbation of the Line of Nodes for an earth-orbiting satellite is affected mainly by the J2 harmonic term of the earth’s magnetic field. Using the orbital altitude and inclination values specified for Galileo and GPS above, it can be shown that there is a relative plane movement of about 5.2° per year between the systems. Given that there is 60° between each of the GPS planes, that implies that there is a repeat period of about 11.5 years between occurrences of this “worst”⁶ relative geometry, and the geometry will go from “worst” to “best” case in just over 5 years. Put another way, for a Galileo design life

⁶ Note that this is a simplification, disregarding the asymmetry of the GPS constellation. In practice there will be a very specific “worst case” geometry between Galileo and GPS, taking into account the relative position of the satellites within the planes. This has been disregarded in this analysis.

of 20 years, the “best” and “worst” case relative geometries are both likely to occur twice. As a result, all analysis for combined constellations have been performed using the “worst” case 0° relative plane offset assumption described above.

For completeness, the relative effect on a service volume simulation for the “best” and “worst” case relative geometries is presented below.

Algorithm:, LSR Baseline Algorithm

- No of satellites = 51
- Masking Angle, 5°
- $P_{FA} = 8 \times 10^{-6}$
- $P_{MD} = 0.012$

Plane Separation (degrees)	30	0
Vertical Alert Limit (metres)	10	
Lowest availability	64.35%	65.09%
@ Longitude	-75	-73
@ Latitude	73	-1
Total availability	87.71%	87.04%
Vertical Alert Limit (metres)	12	
Lowest availability	86.11%	85.14%
@ Longitude	143	-71
@ Latitude	69	-131
Total availability	98.29%	97.91%
Vertical Alert Limit (metres)	15	
Lowest availability	98.52%	98.61%
@ Longitude	-155	-17
@ Latitude	-17	103
Total availability	99.99%	99.99%

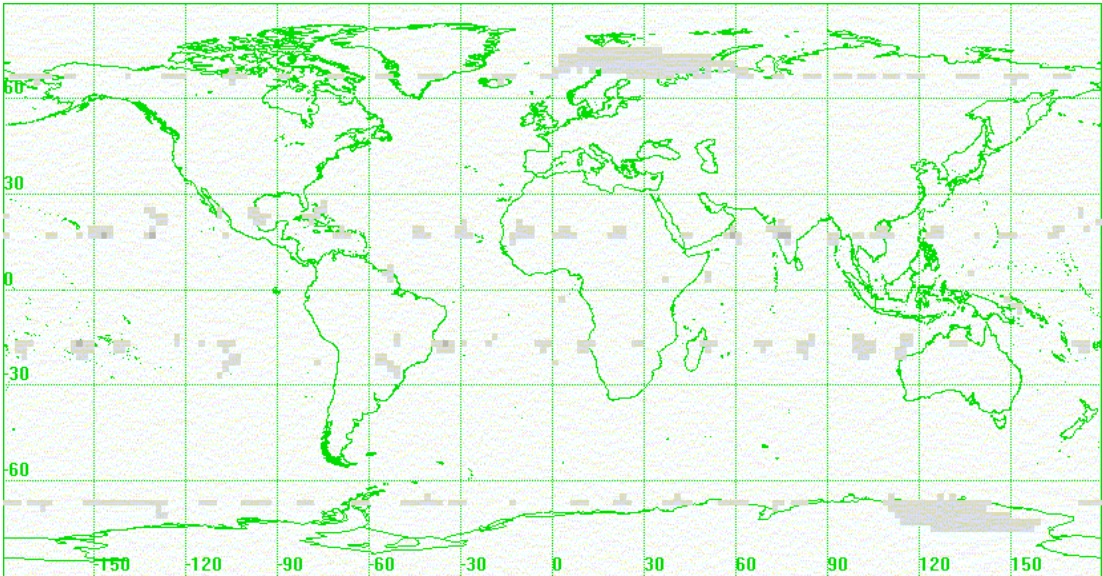


Figure 7-3 : vertical alert limit = 15m, Plane Separation = 0 degrees

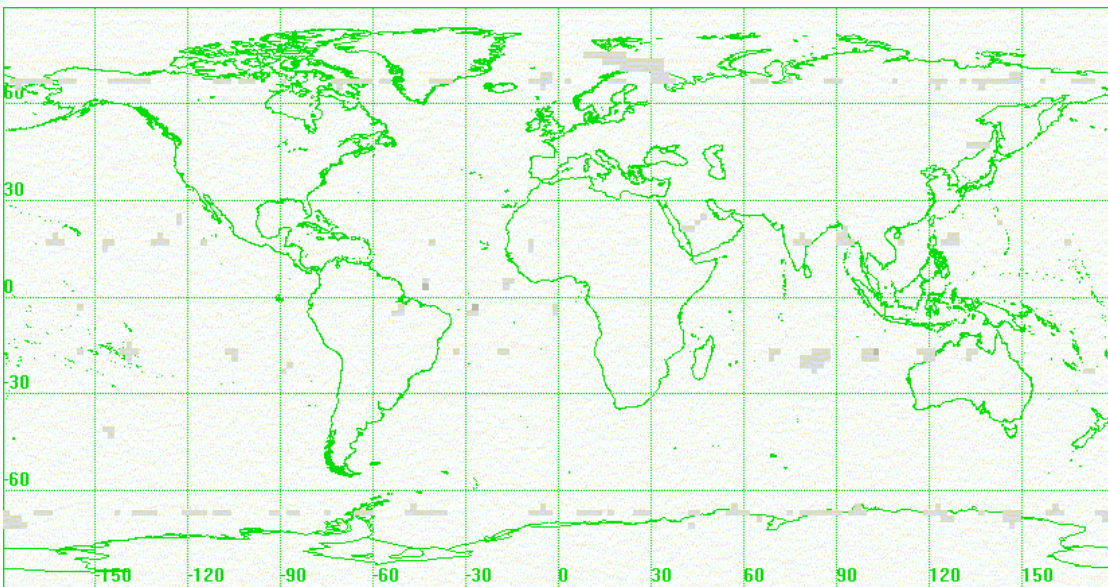


Figure 7-4 : vertical alert limit = 15m, Plane Separation = 30 degrees

7.2.4 Galileo/GPS Time Offset

In Section 6.6 the functional description of the Matlab-based Flight Trials Simulator discusses the offset between Galileo and GPS time. EUROCAE [43] recommends that this parameter be treated as a “Fifth Unknown” in solving the navigation problem for a combined Galileo/GPS constellation. However [48] states that it can be assumed that the synchronisation between GPS and Galileo system time will be disseminated by either or both systems, with a relative error of at most 5 ns. Furthermore, [49] shows that for a combined Galileo/GPS

constellation, the positional error induced by errors up to 5ns in relative synchronisation have a negligible effect on positional accuracy.

In accordance with the conclusions of [48] these simulations therefore assume that a residual time synchronisation offset of 5 ns exists between the GPS and Galileo system times after consideration of any broadcast parameter of the synchronisation between these systems.

7.3 Masking Angle

The EUROCAE paper [43] demonstrates that the parameter which has the largest impact on RAIM availability results after UERE characteristics is masking angle, i.e. the limiting angle above the horizon below which satellites are assumed to be either not seen or excluded from the navigation solution processing algorithms. In line with common practice for aviation use of GNSS, EUROCAE recommends 5° masking angle as the baseline for RAIM availability calculations.

However, the Galileo programme has defined a “Use Case” for Galileo Safety of Life service users with a minimum masking angle of 10°, and the performance specifications for the Galileo SAS service is defined with respect to this masking angle.

The baseline assumption taken within this thesis is a 5° masking angle, to be consistent with EUROCAE. However, where a result is required for comparison with Galileo SAS specifications the analysis is repeated using a 10° mask. In all cases it is assumed that the user receiver can adequately process all satellites in view above the masking angle, i.e. the receiver is not restrict to, for example, 12 satellites in view.

7.4 Service Volume Simulation Resolution

The EUROCAE paper [43] states that the consistency of service volume simulation results is relatively unaffected by the temporal resolution of the analysis. That is to say, a run of the SVS using 15 minute time steps will yield overall RAIM availability figures very similar to those from an equivalent run using a 5 minute time step. It therefore concludes that a 15 minute time step is adequate for RAIM availability simulations.

However, [45] provides far more stringent requirements for SVS temporal resolution, and also places requirements on spatial resolution (i.e. the number of degrees in latitude and longitude between each point on the ground in the simulation service volume).

As previously stated the SVS developed for this thesis was optimised for speed in order to undertake very high resolution service volume simulations. The highest resolution that can be accommodated is in fact

limited by the memory available in the PC running the simulation, rather than the time taken to perform the analysis.

In order to demonstrate that the time step and spatial resolution of 2 minutes by 2° latitude by 2° longitude is sufficient the following results have been reproduced (Table 7-5), using a baseline simulation period of 4320 minutes (3 days).

- Number of satellites = 27 (i.e. Galileo only)
- Masking Angle = 5°
- $P_{FA} = 8 \times 10^{-6}$
- $P_{MD} = 0.012$

Time step (minutes)	2	1	3
Time steps	2160	4320	1441
Latitude step (degrees)	2	2	1
Latitude steps	90	90	180
Longitude step (degrees)	2	2	1
Longitude steps	180	180	360
Vertical Alert Limit (metres)			
	10		
Lowest availability	47.36%	47.71%	47.74%
Total availability	67.65%	67.65%	67.65%
Vertical Alert Limit (metres)			
	12		
Lowest availability	76.85%	77.15%	76.96%
Total availability	89.45%	89.45%	89.52%
Vertical Alert Limit (metres)			
	15		
Lowest availability	93.75%	93.87%	93.47%
Total availability	98.60%	98.60%	98.64%

Table 7-5 : Comparison of SVS results for different spatial and temporal resolutions

7.5 Translation of RNP Specifications to RAIM Requirements

In order to evaluate the performance of RAIM algorithms against RNP specifications, these specifications need to be expressed in terms of the mathematical parameters used by the RAIM algorithms. Specifically, the acceptable Integrity Risk and Continuity requirements must be expressed as a Probability of Missed Detection (P_{MD}) and a Probability of False Alarm (P_{FA}) respectively.

7.5.1 Vertical Alert Limit (VAL)

The vertical alert limit is set in the Required Navigation Performance requirements for different phases of flight. In this analysis the following thresholds are used:

- 20m VAL for APV-II, and for comparison with Galileo SAS specifications;
- 15m VAL for the upper allowable band of Category I precision approach requirements;
- 12m VAL as a general limit for Category I precision approach requirements

7.5.2 Probability of False Alarm (P_{FA})

The Probability of a False Alarm, P_{FA} , caused by the RAIM detection threshold being exceeded in a fault-free case has been taken directly from the Continuity requirements.

For the precision approach operations considered in this study (APV-I, APV-II and Cat I), the NSE Continuity requirement in all cases is $1 - (8 \times 10^{-6})$ in any 15 seconds. Although updates to the GNSS navigation system may be received at a rate of the order of 1 Hz, the correlation time for the components of noise on the system will be significantly longer than 15 seconds [43], therefore it is assumed that there is only one independent sample in any 15 second period. With this assumption, the allowable probability of false alarm is equal to one minus the Continuity requirement, i.e.:

For Precision Approach, maximum P_{FA} is assumed to be 8×10^{-6} .

Note that the recommendations in [43] are that P_{FA} is set to 8.33×10^{-6} for en-route navigation. Since no value is specified for precision approach we shall use the derived value of 8×10^{-6} .

7.5.3 Probability of Missed Detection (P_{MD})

The method for setting the value to be used for P_{MD} in the RAIM algorithms under test is a matter of debate. At one extreme it is argued that where the Integrity requirement is stated as $1-(2 \times 10^{-7})$ per approach, the allowable probability of missed detection should be taken to be:

$$P_{MD} \text{ (conservative estimate)} = 2 \times 10^{-7}$$

However, this is generally regarded as an overly conservative approach. A counter argument is to recognise that P_{MD} is a conditional probability – the integrity risk is the product of P_{MD} x the integrity failure occurrence probability of the navigation solution, per approach. This is the more common approach, and indeed is used as the definition of P_{MD} in [43].

7.5.3.1 WAAS MOPS Approach

In order to determine the required probability of missed detection, as a conditional probability, the integrity failure occurrence probability for a single satellite must be assumed.

From [15], the integrity failure occurrence probability for the GPS position solution, assuming on average 8 satellites in view, is 10^{-4} per hour, which is approximately equal to 4.17×10^{-6} per approach (assuming an approach is 150 seconds, as defined in the RNP Integrity specifications[19]). [43] uses this assumption and states that for precision approach:

- P_{MD} in the single constellation RAIM-only case (8 in view) =

$$2 \times 10^{-7} / (150 \times 10^{-4} / 3600) = 0.05;$$

- P_{MD} in the Galileo + GPS RAIM-only case (20 in view) =

$$2 \times 10^{-7} / (150 \times 2.5 \times 10^{-4} / 3600) = 0.02.$$

7.5.3.2 Signal in Space Integrity Failure Occurrence Probability

The overall integrity failure occurrence probability is the combination of probabilities for Signal in Space Error (SISE) and local effects induced error.

From [45], the SISE integrity failure occurrence probability for Galileo is **3.6×10^{-5} per hour per satellite**. Assuming 9 satellites in view (i.e. one

third of the nominal constellation, as in the GPS case), this is approximately equal to **1.35×10^{-5} per approach**.

At first glance this implies that Galileo is expected to be approximately 3 times worse than GPS in this respect. However, great care must be taken in understanding these assumptions. The figure quoted for GPS is the probability of a gross integrity failure, which may be assumed to be the probability of a SIS error leading to a position solution with an inaccuracy greater than 150m. The Galileo figure has been derived from an analysis which regards a SIS error as one which leads to hazardously misleading information. This would be expected to be more stringent than the GPS case

7.5.3.3 Local Effects Integrity Failure Occurrence Probability

In this analysis, the probability of an Integrity failure caused by “local effects” such as meteorological effects, multipath, interference, etc. has been taken from [45]:

Probability of occurrence of local effect leading to hazardously misleading information =

$$7.2 \times 10^{-5} \text{ per hour} = 3.0 \times 10^{-6} \text{ per 150s}$$

In addition, the user equipment integrity risk probability has been taken from [45] as 3.0×10^{-8} per 150s.

NB Both of these figures are assumed to be independent of the number of satellites in view.

7.5.3.4 Conditional P_{MD}

Using these integrity failure occurrence probabilities presented above the probability of an integrity failure (local + non-local) for Galileo only, with no ground integrity channel, is 1.653×10^{-5} per approach. Taking these assumptions:

$$P_{MD} \text{ (Galileo only, conditional case)} = 2.0 \times 10^{-7} / 1.653 \times 10^{-5} = 0.012$$

Using the same references, the probability of an integrity failure for Galileo with no ground integrity channel, plus GPS is 1.77×10^{-5} per approach. Taking these assumptions,

$$P_{MD} \text{ (Galileo+GPS, conditional case)} = 2.0 \times 10^{-7} / 1.77 \times 10^{-5} = 0.011$$

However, taking a more conservative approach, in which it is assumed that Galileo and GPS both have integrity failure rates of 3.6×10^{-5} per hour per satellite, and assuming up to 20 satellites in view at any time, the probability of an integrity failure for Galileo with no ground integrity channel, plus GPS is 3×10^{-5} per approach. Taking these assumptions:

$$P_{MD} (\text{Galileo+GPS, conditional case}) = 2.0 \times 10^{-7} / 3.0 \times 10^{-5} = 0.0067$$

7.5.3.5 P_{MD} Conclusion

The weakness in this analysis is the difficulty in estimating the probability of SISE and local effects leading to hazardously misleading information, given the current immaturity of the Galileo design. Using the best data currently available regarding these probabilities for Galileo and GPS, the resulting P_{MD} for both the Galileo only and Galileo+GPS case is, intuitively, too high. It is unlikely that a safety case could be made, for example for Galileo only RAIM using a P_{MD} value of 0.012, which equates to an acceptable missed detection rate of one in 83 occurrences.

Intriguingly, in the conclusions presenting the final list of recommended parameters and variables to be used in RAIM analyses, [43] concludes that for both single and combined constellation activities the value to be used for this parameter is:

$$P_{MD} = 4 \times 10^{-4}$$

This figure is presented with no justification; however, it represents a reasonable compromise between the overly conservative approach presented initially and the values derived using unsubstantiated assumptions regarding the predicted integrity failure rates for Galileo and GPS. This figure is therefore used in all subsequent simulations in this thesis.

7.5.4 Satellite Availability Rates and Outage Occurrence Probabilities

In order to calculate the overall availability of RAIM, the “state probabilities” for the constellations have to be assumed. In this context, “state probability” means the probability of all of the satellites in the nominal constellation operating and providing a service, or of having one, two or more satellites off-line for any reason. Note that this relates to the chances of a satellite being unavailable; it is entirely separate from the probability of an integrity failure, which was discussed earlier.

Assumed Satellite Availability Rates and Outage Occurrence Probabilities are taken from [45] as follows:

Constellation state	State probability
27 operational satellites	0.98
26 operational satellites	0.019
25 operational satellites	0.001
24 or less operational satellites	0

Table 7-6: Galileo Constellation State Probability

	Duration	Unit
Short term MTTF	259	days
Short term MTTR	12.2	hour
Long term MTTF	6.25	Year
Long term MTTR	1.25	month
Manoeuvres	none	

Table 7-7 : GPS MTBF & MTTR

These have been consolidated to provide the following assumed combined constellation state probabilities.

Constellation state	State probability
51 operational satellites	0.96
50 operational satellites	0.038
49 operational satellites	0.002
48 or less operational satellites	0

Table 7-8 : Galileo + GPS Combined Constellation State Probability

8. DETAILED PROCESSING MODEL

8.1 Basic Functions

The tools used in this part of the thesis use some or all of the following basic functions:

- Calculation of Satellite to User Geometry;
- Generation of Observation Matrix;
- Simulation of Pseudorange Errors;
- Calculation of Navigation Solution and Position Errors;
- Application of RAIM algorithms.

These basic functions and their underlying equations are discussed in the following subsections.

8.2 Calculation of Satellite to User Geometry

At the heart of the Service Volume Simulator and the NavEng tool is a set of routines to calculate the position of the satellites in cartesian coordinates, the position of the user in the same Earth-centred, inertial reference frame, the true distance between the user and each satellite in view, and the matrix of unit vectors in local North, East, Up coordinates from the user to each visible satellite. The underlying equations to generate this user geometry are presented in the following subsections.

8.2.1 Satellite position in ECI Cartesian Coordinates

This function extracts the time (epoch) at which the required snapshot calculation is to be performed and calculates the position of each satellite in x , y , z co-ordinates. The transformation from Keplerian elements to Earth-centred, inertial (ECI) cartesian co-ordinates is performed using a standard “3-1-3” transformation [38]. This transformation is simplified, since the eccentricity of each satellite’s orbit is assumed to be zero. In this case there is no “argument of perigee” component in the Keplerian elements, so the transformation of any satellite’s position to ECI Cartesian coordinates is described below:

Given:

- Semi-major axis length (a);

- Right Ascension of Ascending Node (RAAN), Ω ;
- Orbital inclination, i ;
- Mean Anomaly, M ;
- Orbital Rate, R (degrees/minute);
- Time from the coordinate system epoch, T (minutes).

Calculate the true anomaly (i.e. position around the orbit) from the expression $\omega = (M + RT)$;

Calculate the x component from the expression

$$x_{sv} = a (\cos \Omega \cos \omega - \sin \Omega \sin \omega \cos i)$$

Equation 8-1

Calculate the y component from the expression

$$y_{sv} = a (\sin \Omega \cos \omega + \cos \Omega \sin \omega \cos i)$$

Equation 8-2

Calculate the z component from the expression

$$z_{sv} = a \sin \omega \sin i$$

Equation 8-3

This transformation has been validated using “Satellite Tool Kit” (STK©). A new scenario was created in STK and a satellite created with the classical elements corresponding to GPS satellite SV1 in Table 7-4. The scenario time and epoch time were both set 01 January 1990 00:00 UTC, which is the epoch time for the coordinate system definition. The orbit propagator type was set to “Two Body”.

Using the STK Report “J2000 ECI Position Velocity” function a report was produced showing the Cartesian coordinates and velocity of the satellite. This was saved as a comma-delimited file and imported to Excel. The format of the results was then set to display two decimal places, with the results for the first 90 minutes shown in Table 8-1.

Time (UTCG)	x (km)	y (km)	z (km)	vx (km/sec)	vy (km/sec)	vz (km/sec)
01/07/1990 00:00	-6602.95	-14311.95	-21379.80	3.07	-2.29	0.59
01/07/1990 00:10	-4740.90	-15632.01	-20944.95	3.14	-2.10	0.86
01/07/1990 00:20	-2842.56	-16832.45	-20349.82	3.19	-1.90	1.12
01/07/1990 00:30	-922.47	-17904.08	-19598.96	3.21	-1.67	1.38
01/07/1990 00:40	1004.67	-18838.71	-18698.13	3.21	-1.44	1.62
01/07/1990 00:50	2924.13	-19629.18	-17654.22	3.18	-1.19	1.85
01/07/1990 01:00	4821.21	-20269.43	-16475.21	3.14	-0.94	2.07
01/07/1990 01:10	6681.40	-20754.58	-15170.13	3.06	-0.68	2.27
01/07/1990 01:20	8490.46	-21080.91	-13748.96	2.96	-0.41	2.46
01/07/1990 01:30	10234.55	-21245.92	-12222.57	2.85	-0.14	2.63

Table 8-1: ECI Coordinates from Satellite Tool Kit for SV1

Table 8-2 presents the same case extracted from the “Cartesian” worksheet on the “RAIM Availability” spreadsheet. It demonstrates agreement in the position coordinates to within 10 metres This has been taken as validation of this coordinate transformation.

Time	x	y	z
0	-6602.95	-14311.95	-21379.80
10	-4740.90	-15632.01	-20944.95
20	-2842.56	-16832.45	-20349.82
30	-922.48	-17904.08	-19598.97
40	1004.67	-18838.71	-18698.14
50	2924.13	-19629.17	-17654.22
60	4821.21	-20269.43	-16475.21
70	6681.39	-20754.58	-15170.13
80	8490.45	-21080.91	-13748.96
90	10234.54	-21245.92	-12222.58

Table 8-2: ECI Coordinates from “RAIM Availability” spreadsheet for SV1

8.2.2 Calculate True User Cartesian Coordinates

This function takes the user latitude and longitude for which the required snapshot calculation is to be performed and calculates the position of the user, at the epoch, in the same ECI x, y, z co-ordinate frame as was used for the satellites. A major simplification used at this point is that the earth is treated as a sphere. It has been assumed that given the nature of the subsequent RAIM analyses, the effect of this simplification on the results is negligible.

The transformation is performed as follows:

Given:

- Radius of the Earth, taken as 6378 km in all directions;
- Rate of rotation of the Earth, $P = 0.25069$ degrees/minute;
- User Latitude;
- User Longitude;
- User Altitude;
- The epoch at which the ECI coordinate system is defined;
- Time from the coordinate system epoch, T (minutes);
- The angular offset between the x-axis of the ECI coordinate system and the Earth's prime meridian. In this case this is equal to 81.09° .

The ECI coordinate system used in this analysis is set by the definition of the GPS nominal constellation as presented in Section 7.2.2, which has an epoch of 01 July 1990 00:00 UTC. In order to find the coordinates of a user on the Earth's surface in the same coordinate system at some point in time, the angular offset between the x-axis defined at this epoch and an axis pointing through the Earth's Prime Meridian at this epoch is required. Using STK it was found that a satellite in circular orbit with $RAAN = 0^\circ$ and $Mean\ Anomaly = 0^\circ$ is found, at $Time = 0$ to have a sub-satellite longitude of 81.09° .

However, this is not a critical step for the analysis. It merely fixes the longitude of the calculated points for when the output is overlaid on a map of the Earth. Any errors at this point would merely result in the resulting plots being offset to the East or the West by a fixed amount, which will not affect the overall results being derived in this analysis.

1. Calculate the angle ϕ , equal to the user longitude minus the angular offset discussed above;
2. Calculate the angle θ , equal to the user latitude;
3. Calculate the x component from the expression:

$$x_u = (\text{Radius} + \text{Alt}) \cdot \cos(\phi + \text{PT}) \cos \theta$$

Equation 8-4

4. Calculate the z component from the expression

$$z_u = (\text{Radius} + \text{Alt}) \cdot \sin \theta$$

Equation 8-5

5. Calculate the y component to make a right-handed set from the expression:

$$y_u = (\text{Radius} + \text{Alt}) \cdot \cos \theta (\sin(\phi + \text{PT}))$$

Equation 8-6

6. Calculate the True Distance and Elevation to each satellite

The true distance, TD_i , to each satellite is easily found:

$$TD_i = ((x_{sv} - x_u)^2 + (y_{sv} - y_u)^2 + (z_{sv} - z_u)^2)^{1/2}$$

Equation 8-7

Next, evaluate the components Dx , Dy and Dz of the unit vector from the user to each visible satellite:

$$Dx_i = (x_{sv} - x_u) / TD_i$$

$$Dy_i = (y_{sv} - y_u) / TD_i$$

$$Dz_i = (z_{sv} - z_u) / TD_i$$

Equation 8-8

These are then transformed to North, East and Up components of a unit vector by performing a 3-2-3 co-ordinate transformation [38] from the ECI coordinate system to local user cartesian coordinates:

$$\text{Up} = (\text{Dx} \cos \theta \cos \phi) + (\text{Dy} \cos \theta \sin \phi) + (\text{Dz} \sin \theta)$$

$$\text{East} = \text{Dy} \cos \phi - \text{Dx} \sin \phi$$

$$\text{North} = (-\text{Dx} \sin \theta \cos \phi) - (\text{Dy} \sin \theta \sin \phi) + (\text{Dz} \cos \theta)$$

Equation 8-9

The Up component represents the tangent of the elevation angle of each satellite relative to the horizon, from the user location's local reference frame.

Satellite Tool Kit has been used to validate the preceding steps, by comparing the estimated azimuth, elevation and range from a fixed point on the Earth to a number of satellites. Table 8-3 presents the output from STK using the "AER" (Azimuth/Elevation/Range) reporting tool, from a facility at 0° latitude, 0° longitude to satellites SV2, SV3, SV4, SV5 and SV6, at 16:40 UTC on 1 July 1990. As before, a two-body propagator has been used.

Facility1-To-SV2				
No Access Found				
Facility1-To-SV3				
	Time (UTCG)	Azimuth (deg)	Elevation (deg)	Range (km)
1 Jul 1990	16:40:00.00	227.548	56.136	21026.755783
Facility1-To-SV4				
No Access Found				
Facility1-To-SV5				
	Time (UTCG)	Azimuth (deg)	Elevation (deg)	Range (km)
1 Jul 1990	16:40:00.00	344.203	31.292	22683.787801
Facility1-To-SV6				
	Time (UTCG)	Azimuth (deg)	Elevation (deg)	Range (km)
1 Jul 1990	16:40:00.00	129.345	14.315	24255.784514

Table 8-3: STK Az/EI/Range Report for Facility 0°Lat 0°Long

Table 8-4 presents an extract from the output from the "Table" worksheet, for the same case. Time was set to 1000 minutes, which corresponds to 16:40 UTC on 1 July 1990.

	SV1	SV2	SV3	SV4	SV5	SV6
Azimuth	-----	-----	227.5	-----	344.2	129.4
Elev	-50.6	-28.7	56.1	-33.5	31.3	14.3
Vis	Blocked	Blocked	Access	Blocked	Access	Access
Range	31184	29027	21029	29545	22679	24259

**Table 8-4: Az/EI/Range output from “Table” for Facility 0°Lat 0°Long
Time = 1000 minutes**

These results show complete agreement (to 1 decimal place) for the azimuth and elevation angles, although the Range values differ by three to four kilometres. This is because the spreadsheet application has assumed a spherical Earth, whereas STK uses a high-fidelity model of the shape of the Earth.

Table 8-5 and Table 8-6 repeat the analysis for a point with a higher elevation, in this case 70° latitude, 30° longitude. Again the azimuth and elevation angles compare very closely, although the discrepancy in range has increased to about 10 kilometres (greater than for the previous example, because the effect of the spherical Earth assumption is more pronounced at higher latitudes, due to the oblateness of the Earth).

Facility1-To-SV2				
Time (UTCG)	Azimuth (deg)	Elevation (deg)	Range (km)	
1 Jul 1990 02:30:00.00	197.415	27.643	22996.707086	
Facility1-To-SV3				
Time (UTCG)	Azimuth (deg)	Elevation (deg)	Range (km)	
1 Jul 1990 02:30:00.00	49.890	9.908	24726.668330	
Facility1-To-SV4				
No Access Found				
Facility1-To-SV5				
Time (UTCG)	Azimuth (deg)	Elevation (deg)	Range (km)	
1 Jul 1990 02:30:00.00	91.045	34.482	22438.913847	
Facility1-To-SV6				
No Access Found				

Table 8-5: STK Az/EI/Range Report for Facility 70°Lat 30°Long

	SV1	SV2	SV3	SV4	SV5	SV6
Azimuth	-----	197.4	49.9	-----	91.0	-----
Elev	-0.3	27.6	9.8	-70.8	34.5	-14.1
Vis	Blocked	Access	Access	Blocked	Access	Blocked
Range	25818	22995	24717	32501	22428	27383

Table 8-6: Az/EI/Range output from “Table” for Facility 70°Lat 30°Long, Time = 150 minutes

These results demonstrate the validity of the preceding steps in the analysis. The differences in range from the “true” values provided by STK are irrelevant for the purposes of the subsequent analyses, since the absolute range value is not important.

8.2.3 Generation of the Observation Matrix

The Observation Matrix is given the annotation **G** in this thesis. With N satellites in view, the **G** matrix is simply an $N \times 4$ matrix in which the first three columns contain the North, East and Up components of the unit vector previously derived, and the fourth column contains “1”, which represents the existence of a clock offset.

The number of satellites in view, N , is a function of the minimum mask angle. All satellites with an elevation angle greater than the user-defined masking angle are included in **G**, unless they have been set to “disabled” by the user.

8.3 Simulation of Pseudorange Errors

Each satellite input file includes a table which defines how UERE varies with elevation angle for each satellite (i.e. as a satellite gets closer to the horizon, the noise on the measurement increases). The first step in the simulation of pseudorange errors is to evaluate the UERE for each visible satellite, from its elevation angle, using a lookup table and linear interpolation.

The next step is to produce a Weighting Matrix, **W**. **W** is a diagonal matrix with values on the leading diagonal equal to the value of the corresponding satellite’s UERE.

For Service Volume Simulations no further simulation of errors is required. However, for the Navigation Engine Monte Carlo simulations, random noise (assumed to have a zero-mean Gaussian distribution, with standard deviation equal to the UERE) is applied to each signal.

For each satellite in view, a pseudorange (i.e. distance to the satellite, as measured by the receiver) is simulated as follows:

$$\text{Pseudorange} = \text{True Distance}_i + (\text{UERE}_i \times \text{Noise}) + \text{Bias}_i + \text{Clock Bias}$$

Equation 8-10

Where Noise is a randomly generated number representing a number of standard deviations taken from a normal distribution. The function used to generate noise in C++ implementations requires two random numbers, U1 and U2, each taking values between 0 and 1. In Excel appropriate random number and normal distribution functions are used.

$$\text{Noise} = [(-2 \times \ln(\text{U1})) \times \cos(2\pi \times \text{U2})]^{1/2}$$

Equation 8-11

“Bias” is a user-definable parameter that applies a fixed range error to one or more ranging signals.

8.4 Calculation of Navigation Solution and Position Errors

The basic linearized measurement equation [26] is

$$\mathbf{y} = \mathbf{G} \cdot \mathbf{x} + \boldsymbol{\varepsilon}$$

Equation 8-12

where \mathbf{x} is the four dimensional position vector (north, east, up and clock) about which the linearization has been made, \mathbf{y} is an N dimensional vector containing the raw pseudorange measurements minus the expected ranging values based on the location of the satellites and the initial estimated location of the user (\mathbf{x}), \mathbf{G} is the observation matrix and $\boldsymbol{\varepsilon}$ is an N dimensional vector containing the errors in \mathbf{y} .

The weighted least squares solution for \mathbf{x} can be found by

$$\mathbf{x}_{ls} = (\mathbf{G}^T \mathbf{W} \mathbf{G})^{-1} \mathbf{G}^T \mathbf{W} \cdot \mathbf{y} = \mathbf{K} \cdot \mathbf{y}$$

Equation 8-13

where \mathbf{W} is the inverse of the covariance matrix and \mathbf{K} is the weighted pseudo-inverse of \mathbf{G} . The diagonal elements of \mathbf{W} are the inverses of the variances (σ_i^2) corresponding to each satellite. We assume that the error sources for each satellite are uncorrelated with the error sources for any other satellite. Therefore, all off-diagonal elements are set to zero. While this assumption may not be strictly true, it should be a reasonably good

approximation. In the absence of any information regarding cross-correlation, it is recommended to treat \mathbf{W} as a diagonal matrix [50].

\mathbf{x}_{Is} is a 4 x 1 vector which contains the difference between the old estimated user position and the new estimated user position. However, \mathbf{x}_{Is} is in local (North, East, Up) co-ordinates, whereas user position is in an Earth-centred co-ordinate reference frame, therefore in order to calculate vertical and horizontal position errors it is necessary to:

1. Extract the first three elements of \mathbf{x}_{Is} into a 3 x 1 position vector (the fourth element being the estimate of user clock offset, which is not a function of the co-ordinate system being used);
2. Multiply this vector by a 3 x 3 Direction Cosine Matrix (DCM) to convert from local co-ordinates to a reference frame with axes parallel to the Earth-centred co-ordinate system in which user estimated position is defined;
3. Add the transformed matrix to the previous estimated user position to yield the new estimated user position vector;
4. Subtract the new estimated user position vector from the “true” user to yield the position errors, in the reference frame parallel to the Earth-centred co-ordinate system. This is referred to as the True Error Vector, TEV;
5. Multiply the True Error Vector by a DCM to convert back to local (North, East, Up) co-ordinates. This DCM is the inverse of the DCM used in Step 2;

$$\text{North Error} = \text{TEV}_x \sin \theta - \text{TEV}_z \cos \theta$$

$$\text{East Error} = (\text{TEV}_x \cos \theta \sin \phi) + (\text{TEV}_y \cos \phi) - (\text{TEV}_z \sin \theta \sin \phi)$$

$$\text{Vertical Error} = (\text{TEV}_x \cos \theta \cos \phi) - (\text{TEV}_y \sin \phi) - (\text{TEV}_z \sin \theta \cos \phi)$$

Equation 8-14

6. The third element of this new vector represents the Vertical Error;
7. The vector sum of the first two elements of this vector represent the Horizontal Error.

8.5 Application of RAIM Algorithms

In the Service Volume Simulations analysis, the SVS simulation engine provides to the RAIM algorithms under test:

- **G** matrix;
- **W** matrix;
- P_{MD} ;
- P_{FA} .

The RAIM algorithms return:

- Vertical Protection Limit;
- Test Statistic Threshold (or thresholds, where more than one independent test statistic is generated).

In the Navigation Engine simulations, the NavEng simulation engine provides to the RAIM algorithms under test:

- **G** matrix;
- **W** matrix;
- **y** vector;
- P_{MD} ;
- P_{FA} .

The RAIM algorithms return:

- Vertical Protection Limit;
- Test Statistic Threshold;
- Test Statistic value.

The NavEng simulation engine also provides:

- Vertical Navigation System Error (VNSE);
- Horizontal Navigation System Error (HNSE).

8.6 Calculation of Availability, Including Satellite Outage Probability

The Service Volume Simulator provides a plot of RAIM availability overlaid on a map of the specified service area. It provides a single consolidated value for the availability of RAIM over the entire service area, weighted to take into account the variation in service area with

latitude for a given latitude step size. The value of the lowest availability occurring at a point in the service area, along with that point's latitude and longitude, is also provided.

The SVS also allows the user to undertake an analysis with one or more satellites treated as "disabled". However, it does not automatically provide a figure for the overall RAIM availability given a specified probability of satellite outage. In order to produce such a figure the output from the SVS needs to be post processed.

As an example, consider a Galileo-only case. In Section 7.5.4 the state probability for Galileo having 27, 26 and 25 satellites operational at any time are given as 98%, 1.9% and 0.1% respectively. In order to calculate the overall availability of RAIM taking these figures into account, a baseline degraded case needs to be assumed; for a single satellite outage it is irrelevant which satellite is considered to have failed because the constellation is symmetrical. However, for multiple failures a baseline case needs to be defined. The cases to be used are currently undefined for Galileo, although they are defined in RTCA standards for GPS degraded states.

By running the Galileo-only case with 27, 26 and 25 satellites available, an approximate overall availability is produced thus:

$$\text{Overall availability} = [\text{Avail}(27 \text{ sat}) \times 0.98] + [\text{Avail}(26 \text{ sat}) \times 0.019] + [\text{Avail}(25 \text{ sat}) \times 0.001]$$

The Service Volume Simulator allows the user to produce a table of availability for each grid location in the test case, using a specified VAL. The relationship given above can then be used to derive the availability at every point in the sample, taking into account the probability of satellite outage, using the SVS Post processor spreadsheet.

9. LEAST SQUARES RESIDUALS (LSR) RAIM METHOD

9.1 Weighted Position Solution and Vertical Accuracy

The Least Squares Residual or LSR RAIM technique modelled in this thesis is based on that presented in “Weighted RAIM for Precision Approach” [26]. The approach is a standard snapshot RAIM technique, and the methods are well known and widely utilised.

The position solution is found by solving the basic linearized measurement equation (Equation 8-12), by use of the standard least squares method defined in Equation 8-13.

By introducing the **W** matrix to account for the unequal weighting to be given to each satellite’s ranging measurement, we can no longer separate the expected positioning errors into a Dilution of Precision (DOP) and a user ranging accuracy (UERE, or σ , common to all satellites), which was the common approach to estimating the accuracy of a satellite navigation position solution up until the removal of Selective Availability on GPS in May 2002. Instead these values are combined into expected positioning confidences:

$$\sigma_v \equiv \sqrt{[(G^T W G)^{-1}]_{33}}$$

Equation 9-1

$$HRMS \equiv \sqrt{\{[(G^T W G)^{-1}]_{11} + [(G^T W G)^{-1}]_{22}\}}$$

Equation 9-2

Equation 9-1 gives the 1σ expected accuracy in the vertical dimension, and Equation 9-2 gives the 2-dimensional RMS expected accuracy in the horizontal dimensions. The accuracy of these measures depends upon the accuracies of the satellite covariances in the **W** matrix.

9.2 Weighted RAIM Test Statistic

In order to assess the accuracy of the least squares fit we need to consider the positioning error ($\mathbf{x}_{ls} - \mathbf{x}$).

Clearly, it is not generally possible to obtain a direct measurement of this quantity; if we did, the positioning problem would be trivial, because it implies that we have prior access to a better estimate of the true position. However, we can examine the overall consistency of the solution.

Provided we have more than four measurements, the system is overdetermined and cannot be solved exactly. Since all of the conditions realistically cannot be met exactly, there is a remaining error residual to the fit. By quantifying how closely the observations agree, we can produce some test statistic relating to the consistency of the measurements. If this test statistic shows the measurements to be consistent (i.e. the fit is good), we assume that the error in position is most likely small. This is the foundation for RAIM.

The first step in the production of the required test statistic is rearrange Equation 8-12, using the least squares position solution:

$$\boldsymbol{\varepsilon}_{1s} = \mathbf{y} - \mathbf{G}\mathbf{x}_{1s}$$

Equation 9-3

N residuals are then formed in the measurement domain, grouped together as the N x 1 vector \mathbf{x}_{1s} , formed by substituting Equation 8-13 into Equation 9-3, as follows:

$$\boldsymbol{\varepsilon}_{1s} = \mathbf{y} - \mathbf{G}(\mathbf{K} \cdot \mathbf{y}) = (\mathbf{I} - \mathbf{G}\mathbf{K}) \cdot \mathbf{y} = (\mathbf{I} - \mathbf{P}) \cdot \mathbf{y}$$

Equation 9-4

This is the linear transformation that takes the range measurement \mathbf{y} into the resulting residual vector. From these error estimates we define a scalar measure to which we will refer henceforth as the Weighted Sum of Squared Errors (WSSE):

$$\begin{aligned} \text{WSSE} &= \boldsymbol{\varepsilon}_{1s}^T \cdot \mathbf{W} \cdot \boldsymbol{\varepsilon}_{1s} = [(\mathbf{I}-\mathbf{P}) \cdot \mathbf{y}]^T \cdot \mathbf{W} \cdot [(\mathbf{I} - \mathbf{P}) \cdot \mathbf{y}] \\ &= \mathbf{y}^T \cdot \mathbf{W} \cdot (\mathbf{I}-\mathbf{P}) \cdot \mathbf{y} \end{aligned}$$

Equation 9-5

If ε_i is a normally distributed zero mean random variable with a standard deviation of σ_i for all N satellites in view, WSSE is a χ^2 distributed variable with N-4 degrees of freedom.

The square root of WSSE ($\sqrt{\text{WSSE}}$) plays the role of the basic observable in this RAIM method, because this yields a linear relationship between a satellite bias error and the associated induced test statistic. ($\sqrt{\text{WSSE}}$ is observable whereas the positioning error of the least squares solution ($\mathbf{x}_{1s} - \mathbf{x}$) is not). Therefore, for integrity purposes we want to use the statistic to flag bad position solutions. Typically, a certain threshold is selected. If the statistic exceeds that threshold the position fix is

assumed to be unsafe. However if the statistic is below the threshold, then the position fix is assumed to be valid.

The fault detection plane is broken up into four regions consisting of: normal operation points, missed detections, successful detections and false alarms, as shown in Figure 9-1. This figure shows the results for 1000 samples with Gaussian noise for a single geometry with 18 satellites in view.

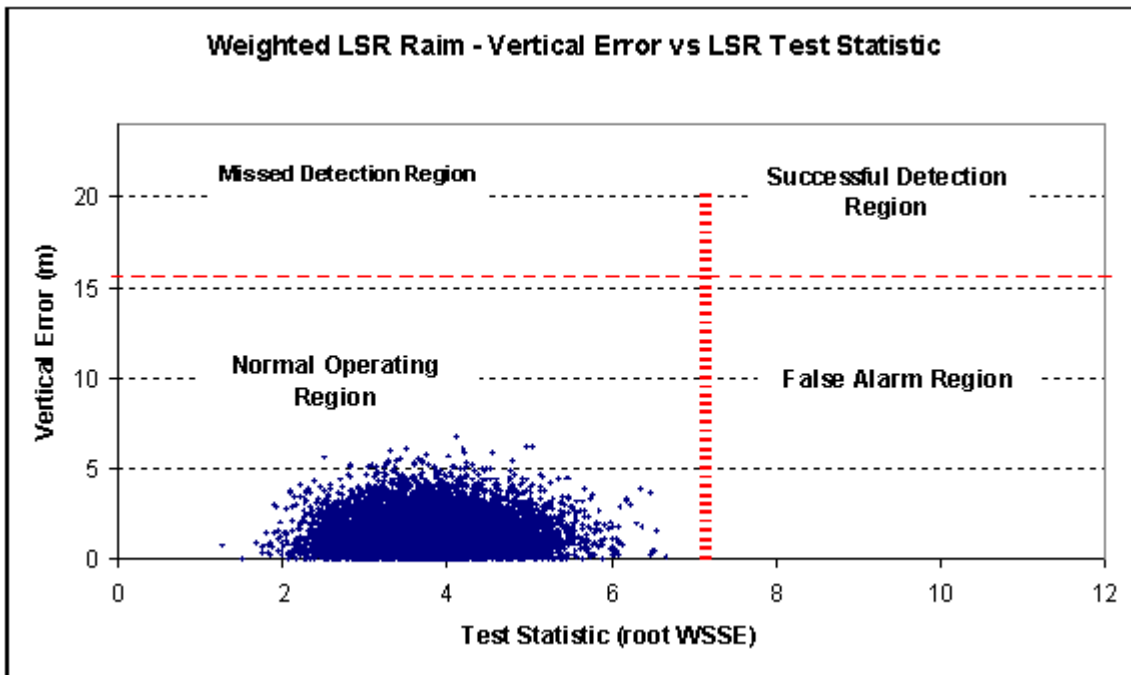


Figure 9-1 : Typical distribution of vertical errors and RAIM test statistic for normal operations (Gaussian noise, no bias)

The test statistic threshold is chosen such that the probability of false alarm is commensurate with the continuity requirement for precision approach. With WSSE being a χ^2 distributed variable, the threshold T can be selected analytically. $T(N, P_{FA})$ will only be a function of the number of satellites (N) and the desired probability of false alarms (P_{FA}). By examining the distribution it is possible to find the value $T(N, P_{FA})$ such that, for normal conditions, the statistic only has a probability of P_{FA} of exceeding it. The threshold may be found by inverting an incomplete gamma function. In practice the values for $T(N, P_{FA})$ can be easily computed off-line using an iterative root finding process and stored for use later by a RAIM algorithm, either from a lookup table or in a mathematical functions library.

9.3 Protection Levels

The N errors in the vector ϵ are mapped into two orthogonal spaces; one of dimension 4 corresponding to the position solution error and one of dimension N-4 corresponding to the distribution of WSSE (hence WSSE has N-4 degrees of freedom). Thus, in the general case, the statistic cannot be used absolutely to indicate a bad or a good position solution.

However, Brown [36] showed that for every satellite in view there is a characteristic straight line relationship between the magnitude of the vertical error and the value of the test statistic,

$$V_{SLOPE\ i} \equiv \frac{|K_{3i}| \sigma_i}{\sqrt{1 - P_{ii}}}$$

Equation 9-6

where K_{3i} represents the item on the third row of the K matrix associated with satellite i. This value represents the relationship between an applied bias on satellite i and the induced vertical position error, in the absence of any other bias or noise on any other satellite.

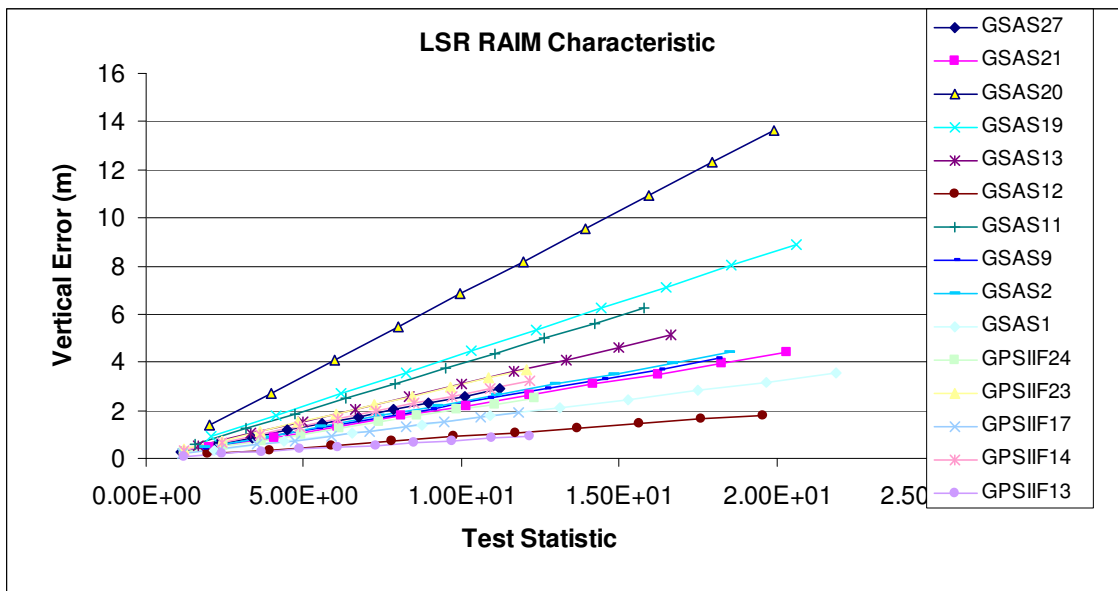


Figure 9-2 : LSR RAIM Test Statistic Characteristic

With a single satellite failure, it is possible to restrict the satellite geometries such that a large bias that is mapped into a position error is also mapped into the statistic WSSE with certainty. Thus, for this failure mode we can guarantee that the position error will not grow too large

without a corresponding growth in the statistic. Figure 9-2 shows this “Test Statistic Characteristic” for a particular Galileo + GPS case (18 satellites in view).

If there is a fault on the signal received from a single satellite which causes a bias to be added to the UERE of the ranging signal, the expected distribution of operation points in the statistic-vertical error plane is still an ellipse with roughly the same contours as in the absence of failures. The difference is that now the ellipse has moved out along the line with the corresponding V_{slope} for the failed satellite (see Figure 9-3). How far it moves along the line depends on the magnitude of the bias.

From Figure 9-3 we can see that the Vertical Protection Limit (VPL) available for any given satellite geometry has two major components:

- The product of the Test Statistic threshold (a function of the desired probability of false alarms (P_{FA}) and the number of satellites in view) and the maximum value of V_{slope} ;
- The product of the number of standard deviations corresponding to the specified probability of missed detection (P_{MD}), and the 1σ accuracy in the vertical direction (σ_v).

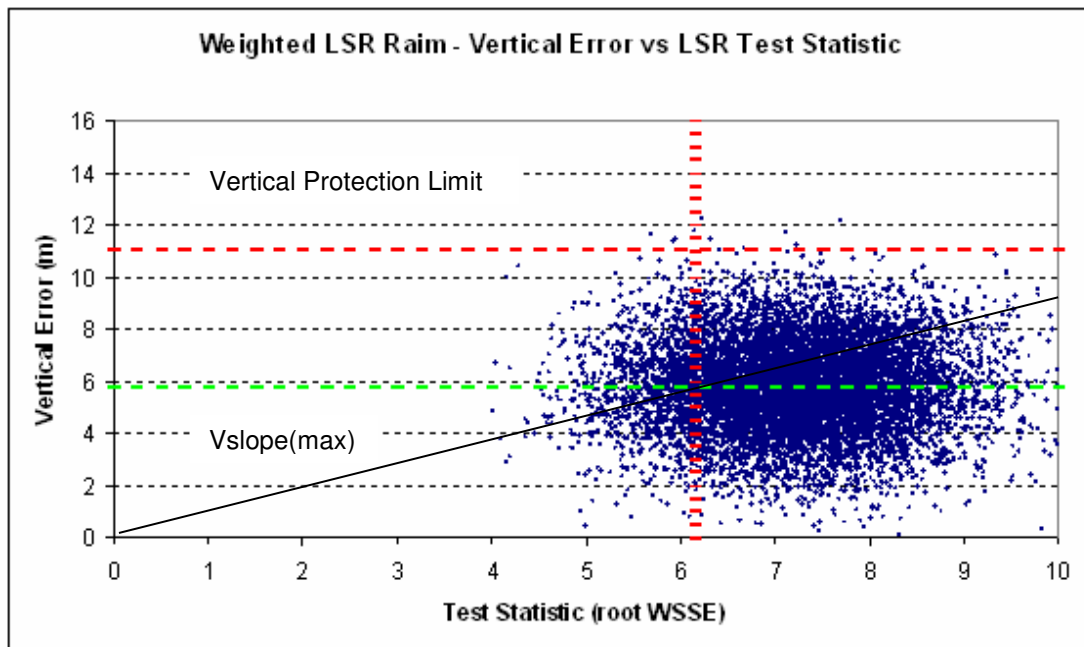


Figure 9-3 : Typical distribution of vertical errors and RAIM test statistic with critical bias on failed satellite (Gaussian noise on all satellites)

The vertical protection limit can now be calculated using Equation 9-7:

$$VPL \equiv \max[V_{SLOPE}]T(N, P_{FA}) + k(P_{MD})\sigma_V$$

Equation 9-7

9.4 Underlying Assumptions

This method contains a number of implicit assumptions that typically produce a conservative estimates of the VPL for a given satellite geometry. The major factors that lead to an over-estimate of VPL are discussed briefly below:

There is an implicit assumption that any failure causing a ranging bias will occur on the satellite which, by virtue of geometry, is the most sensitive to errors, i.e. the satellite on which a ranging error causes the greatest vertical shift error per unit increase in test statistic ($V_{slope(max)}$). Making this assumption gives this technique increased integrity, but at the cost of decreasing RAIM availability;

The noise on each measurement is likely to be closer to a “clipped Gaussian” than a true Gaussian distribution, because various system monitoring elements (not associated with the integrity determination system) are likely to detect and prevent broadcast of a large proportion of gross errors [51]. However, given that the tails are relatively weak on Gaussian distributions, this clipping effect is unlikely to have a significant effect on the validity of this RAIM approach.

As the number of satellites in view increases, so does the number of degrees of freedom, and hence so does the detection threshold $T(N, P_{FA})$. At some point, each additional satellite adds less to the increase in the accuracy of the position solution than it does to increasing the detection threshold. As a result, the vertical protection limit is *less* once these satellites are excluded than when they are kept in the solution. Figure 9-4 presents the SVS snapshot case window, showing the same case as in Figure 6-1, but this time with five satellites disabled from the analysis.

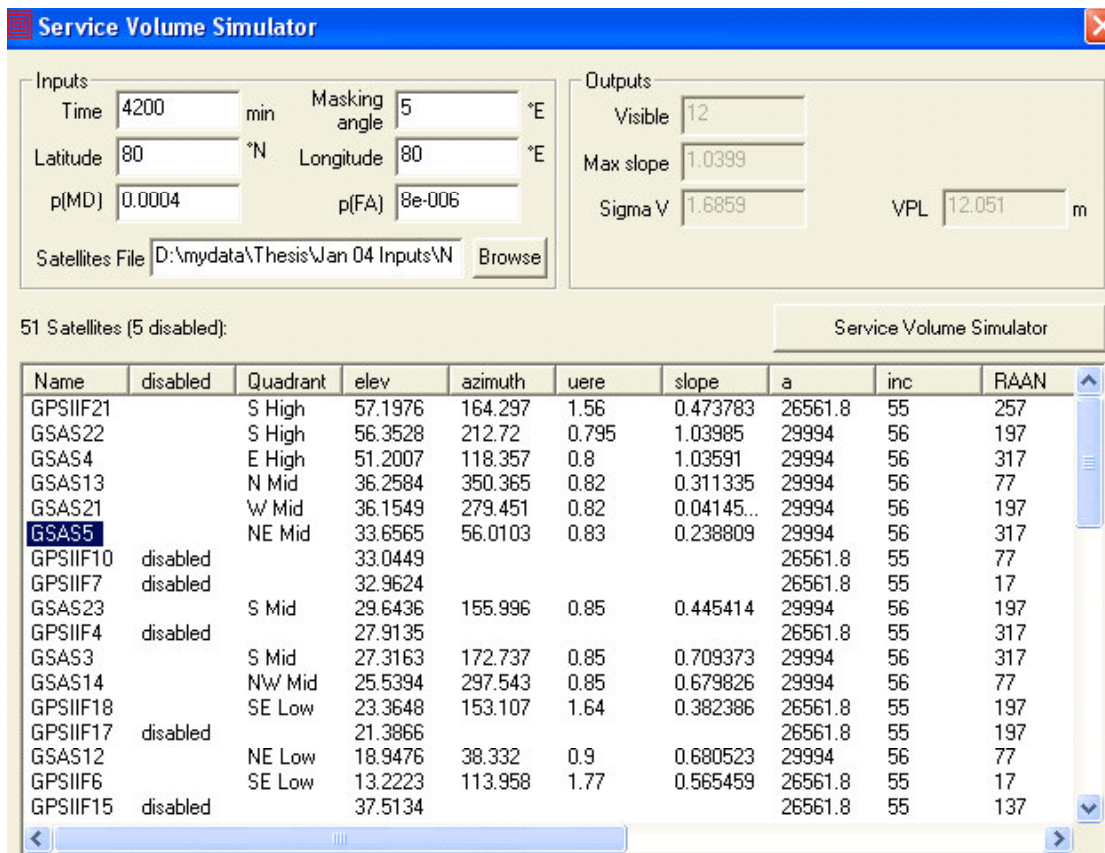


Figure 9-4: Improvement in VPL with Satellites Disabled

Number of sats visible :	17	12
$V_{\text{Slope(max)}}$:	1.0162	1.0399
σ_v :	1.6435	1.6859
LSR VPL :	12.51m	12.05m

Note that even though σ_v is slightly lower with seventeen satellites in view compared with twelve, the LSR Vertical Protection Limit is improved by nearly 0.5m by removing five satellites at medium elevation angles. This appears to be a novel observation, for which the author has found no other reference in published literature.

It is of course possible to identify, for any particular satellite geometry, which satellites can be removed to optimise the VPL calculation. However, the computational effort associated with this optimisation was not felt appropriate for this thesis. Nevertheless, any real applications of the LSR RAIM algorithm with big constellations would benefit from investigation into this point.

The method of least squares solution implicitly assumes that the observation matrix \mathbf{G} is known, and that all measurement errors (clock bias, ephemeris errors, atmospheric delay, multipath, etc.) may be lumped together into a single UERE. The weighted least squares solution then minimises the weighted residual of these errors to find a position solution. In practice, the observation matrix is itself subject to perturbations associated with ephemeris errors and user's position errors. Although this assumption does not in itself result in errors in using the LSR method, as will be shown when discussing the EIV technique, recognising this assumption results in a more effective RAIM test metric.

10. “ERRORS IN VARIABLES” (EIV) RAIM METHOD

10.1 Introduction to EIV

The Errors in Variables or EIV method described in the following sections is adapted from work produced by Professor Jyh-Ching Juang at the National Cheng Kung University in Taiwan [30].

In Section 9 the least squares solution of the linearized measurement equation (Equation 8-12) was demonstrated. Implicit in the least squares positioning solution is the assumption that the observation matrix is known, and that all errors can be lumped together as a user equivalent range error. The Errors in Variables method recognises that ephemeris errors will perturb the \mathbf{G} matrix, and that the positioning model is better solved as a linear equation with errors in both the observation matrix and the measurement error vector.

To solve this new linear equation a “Total Least Squares” (TLS) method is used, based on a matrix manipulation technique known as Singular Value Decomposition (SVD). Although the positioning solution produced by the TLS method will not in general be more accurate than that found using standard least squares techniques, the TLS method is of interest in the context of RAIM because the singular value decomposition yields quantitative measures of the mismatches in both the error vector and the observation matrix. Thus, with two independent observable metrics for measurement consistency, it is possible to construct a RAIM algorithm that, for given false alarm and missed detection probabilities, has far higher availability than the LSR algorithm previously discussed. However, as will be shown, in order to achieve this improved performance in receivers using the EIV RAIM algorithm, the underlying position algorithm requires a degree of management of the user clock offset. The detailed definition of the EIV technique is discussed in the following sections.

10.2 Total Least Squares Positioning Solution

In Equation 8-12 as previously discussed, \mathbf{x} is the four dimensional position vector about which the linearization has been made, \mathbf{y} is an N dimensional vector containing the raw pseudo-range measurements minus the expected ranging values based on the broadcast location of the satellites and the assumed location of the user (\mathbf{x}), \mathbf{G} is the observation matrix and $\boldsymbol{\epsilon}$ is an N dimensional vector containing the errors in \mathbf{y} . The resulting least squares solution, presented in Equation 8-13, minimises the objective function $\|\boldsymbol{\epsilon}\|^2$ (i.e. the norm of the error vector).

In practice, both the pseudo-range measurements and the broadcast position of each satellite are subject to errors. Therefore, we can

introduce a new matrix **H** to represent the errors associated with the observation matrix, and a vector **e** (replacing ϵ in Equation 8-12) to represent the errors not associated with the observation matrix. The resulting linear matrix equation then becomes:

$$\mathbf{y} = (\mathbf{G} + \mathbf{H}) \cdot \mathbf{x} + \mathbf{e}$$

Equation 10-1

The matrix **H** may be used to account for errors in broadcast navigation data, user linearization point, or differences in synchronisation between clocks across the visible constellation. Of course, at any instant the extent of the errors in **H** and **e** are unknown. Therefore, to solve Equation 10-1 to provide a best estimate of **x** requires both **H** and **e** to be minimized together; i.e. the idea is to find a vector **x** that best fits the model in Equation 10-1, with the model mismatch characterised by **H** and **e** as small as possible. In mathematical terms, the objective function to be minimized in this process is the Frobenius norm⁷ of the augmented matrix [**H e**].

The approach taken to solve this equation is commonly referred to as the Total Least Squares method. The method is significantly different from the standard Least Squares method previously discussed, because the objective function is a full matrix, not a vector. The main computational step in the TLS method is a matrix manipulation technique known as Singular Value Decomposition. This technique is discussed in Appendix D, using an explanation presented in [52].

The matrix to be decomposed by the SVD process is the matrix [**G y**], i.e. the N x 5 matrix formed by co-joining the observation matrix with the **y** vector. Before decomposition this matrix is pre- and post-multiplied by two new matrices **C** and **D**. Both **C** and **D** are compatible, non-singular, diagonal weighting matrices. **C** is an N by N matrix, whose entries are used to weight the significance of the different satellite range measurements. **D** is a 5 x 5 matrix, whose diagonal entries are related to the relative importance of satellite North, East and Up position, user clock and pseudo-range errors. Thus the **D** matrix allows the user to “tune” the errors-in-variables model to emphasise vertical positioning error, horizontal positioning error or clock bias, as required.

The matrix resulting from this pre- and post-multiplication is subsequently referred to as the “augmented matrix”, and the objective function to be minimised becomes $||\mathbf{C}[\mathbf{H}\mathbf{e}]\mathbf{D}||$.

⁷ The Frobenius Norm of a matrix is the square root of the sum of the squares of all elements.

The first step in the TLS process is the singular value decomposition of the augmented matrix $\mathbf{C}[\mathbf{G} \ \mathbf{y}]\mathbf{D}$ such that:

$$\mathbf{C}[\mathbf{G} \ \mathbf{y}]\mathbf{D} = \mathbf{U}\mathbf{\Sigma}\mathbf{V}^T$$

Equation 10-2

In which \mathbf{U} is an $N \times 5$ column-orthogonal matrix, \mathbf{V} is a 5×5 orthogonal matrix and

$$\mathbf{\Sigma} = \begin{bmatrix} \sigma_1 & 0 & 0 & 0 & 0 \\ 0 & \sigma_2 & 0 & 0 & 0 \\ 0 & 0 & \sigma_3 & 0 & 0 \\ 0 & 0 & 0 & \sigma_4 & 0 \\ 0 & 0 & 0 & 0 & \sigma_5 \end{bmatrix}$$

NB \mathbf{U} is termed “column orthogonal” rather than orthogonal because the “Thin SVD” process (see Appendix D) has been employed, and hence it has no inverse.

The smallest singular value, σ_5 , represents the amount of model mismatch that characterises the compatibility between the observation matrix \mathbf{G} and the measurement vector \mathbf{y} . The next step is to partition the \mathbf{U} , \mathbf{V} , $\mathbf{\Sigma}$ and \mathbf{D} matrices such that:

$$\mathbf{U} = \left| \begin{array}{c|c} \mathbf{U}_1 & \mathbf{U}_5 \\ \hline (N \times 4) & (N \times 1) \end{array} \right|$$

$$\mathbf{V} = \left| \begin{array}{c|c} \mathbf{V}_{11} & \mathbf{V}_{15} \\ \hline (4 \times 4) & (4 \times 1) \\ \mathbf{V}_{51} & \mathbf{V}_{55} \\ \hline (1 \times 4) & (1 \times 1) \end{array} \right|$$

$$\mathbf{\Sigma} = \left| \begin{array}{c|c} \mathbf{\Sigma}_1 & \mathbf{0} \\ \hline (4 \times 4) & (4 \times 1) \\ \mathbf{0} & \sigma_5 \\ \hline (1 \times 4) & \end{array} \right|$$

$$\mathbf{D} = \begin{vmatrix} \mathbf{D}_1 & \mathbf{0} \\ (4 \times 4) & (4 \times 1) \\ \mathbf{0} & d_5 \\ (1 \times 4) & \end{vmatrix}$$

The Total Least Squares position solution, derived in [52] is given by:

$$\mathbf{x}_{tls} = -(\mathbf{D}_1 \mathbf{V}_{15}) (\mathbf{V}_{55} d_5)^{-1}$$

Equation 10-3

This is shown In Section 10.3.2 to be related to the Weighted Least Squares estimate.

This approach to estimating the user's position is of limited value, since the error ellipse associated with the TLS estimate will in general be larger than the error ellipse using the standard least squares approach. However, the value of this technique will become apparent in the next section when discussing integrity monitoring.

Using the matrix partitions defined above, the mismatches in the \mathbf{H} matrix and \mathbf{e} vector may be expressed [30] as follows:

$$[\mathbf{H}_{tls} \ \mathbf{e}_{tls}] = -\sigma_5 \mathbf{C}^{-1} \mathbf{U}_5 [\mathbf{V}_{15}^T \ \mathbf{V}_{55}^T] \mathbf{D}^{-1}$$

Equation 10-4

Thus the linear matrix equation becomes:

$$\mathbf{y} = (\mathbf{G} + \mathbf{H}_{tls}) \cdot \mathbf{x}_{tls} + \mathbf{e}_{tls}$$

Equation 10-5

10.3 Setting the Weighting Matrices

The paper which first introduced the idea of using an Errors in Variables approach to RAIM [30] presented its analysis using Identity matrices for the \mathbf{C} and \mathbf{D} weighting matrices introduced above. At the time of writing this paper Selective Availability was still in operation, which of course dominated the noise on GPS measurements (irrespective of elevation angle), making the use of a weighting matrix on standard GPS position solutions irrelevant. Although this simplified the problem in that the values used for these matrices did not have to be justified, the underlying distribution for the resulting test statistics is demonstrated to be extremely complex.

A key finding from this thesis is that it is possible to set the **C** and **D** matrices such that test statistics are produced which are readily applicable for a real RAIM application. This means producing test statistics which:

- Have a simple (ideally linear) relationship between applied bias and test statistic, and hence between navigation system error and test statistic (such as the straight line characteristics described previously for the LSR method);
- Have an underlying statistical distribution which is easily defined, and hence readily provides a detection threshold given a specified false alarm probability.

The following sections present the approach used in this research to setting these weighting matrices which appears to provide test statistics with these properties. The mathematical and analytical basis for these results is presented to the extent appropriate to support the objectives of this thesis. However, it should be noted that the approach presented here has been derived empirically, with the aim of demonstrating that the EIV algorithm could be developed into a RAIM application for safety of life services. To fully develop and validate such an application a more rigorous analytical justification would be required.

10.3.1 Setting the **C** matrix

Being an N by N matrix, the **C** matrix allows weightings to be applied to each observation individually. In this way it acts like the **W** matrix introduced earlier in the LSR method, and the intention here is to set the weightings such that the Total Least Squares solution is weighted in a way which is analogous to the Least Squares solution.

Equation 9-3 showed how in the LSR method a range residual vector is produced which, using Equation 9-5, can be used to produce a Weighted Sum of Squared errors test statistic. When the Total Least Squares position solution is derived, as from Equation 10-3, a TLS range residual vector (r_{tls}) can be formed in the same way:

$$r_{tls} = y - Gx_{tls}$$

Equation 10-6

[52] shows that manipulation of Equation 10-3 and Equation 10-4 yields:

$$r_{tls} = (\sigma_5 C^{-1} U_5) / (d_5 V_{55})$$

Equation 10-7

In a manner analogous to Equation 9-5, [30] shows that a modified Sum of Squared Errors (SSE') statistic is formed from:

$$SSE' = \mathbf{r}_{t|s}^T \mathbf{r}_{t|s}$$

Equation 10-8

which has a statistical distribution that is

“...a summation of four Gamma distributions with different parameters (due to different weights) and an n-4 degrees of freedom chi-squared distribution...”

To set a detection threshold given a specified false alarm probability would require either evaluating this function using convolutions, or employment of simulation or some other numerical method, neither of which is convenient for a real-time safety-critical application.

Where **C** is an Identity matrix, using the fact that **U**₅ is a unit vector the modified, unweighted SSE' is seen to be

$$USSE' = \sigma_5^2 / (d_5^2 \mathbf{V}_{55}^2)$$

Equation 10-9

This still has the computationally prohibitive statistical distribution mentioned previously, and does not consider the application of weightings to the different observations.

By analogy with Equation 9-5, a modified Weighted Sum of Squared Errors, WSSE' can be formed

$$WSSE' = \mathbf{r}_{t|s}^T \mathbf{W} \mathbf{r}_{t|s}$$

Equation 10-10

This is seen to be identical to SSE' in Equation 10-8 above if the elements of the **C** matrix are set to be equal to the square root of the corresponding elements of the **W** matrix. Thus, for all subsequent analysis the **C** matrix in the EIV method is set to equal the square root of the **W** matrix used in the Least Squares positioning solution, since this provides a TLS equation which is directly comparable to a weighted Least Squares linear equation.

10.3.2 Setting the D matrix

[30] shows that where both the TLS and LS solutions are unweighted, the position estimates are related by:

$$\mathbf{x}_{tls} = [\mathbf{I}_4 + \sigma_5^2 (\mathbf{G}^T \mathbf{G} - \sigma_5^2 \mathbf{I}_4)^{-1}] \mathbf{x}_{ls}$$

Equation 10-11

Thus the error ellipse of the TLS solution is larger than that for the LS solution, diverging with the square of σ_5 . Furthermore the two solutions tend to converge as σ_5 tends to zero. The singular value σ_5 characterises how close the rank of the augmented matrix is to 4. It is a measure of the compatibility of the linear matrix equation.

Consider the constituent elements of the augmented matrix before multiplication by the **C** and **D** matrices, i.e. the 5 x n matrix **[Gy]**. The **D** matrix provides the means to weight the five columns of the augmented matrix as required. Clearly the effect of the fifth diagonal term, d_5 , is to control the order of magnitude of the measurement residuals column of the augmented matrix.

Note that σ_5 always represents the lowest singular value resulting from the decomposition. It is not fixed to characterise the compatibility of the fifth column compared with the first four. If we assume (as is valid for the subsequent simulations) that measurement residuals are expressed in metres, and given the measurement variances/USEREs previously discussed, elements of the **y** vector would typically be of the order one to ten metres. If the **D** matrix is set to be an Identity matrix the fifth column of the augmented matrix would dominate the Singular Value Decomposition process to the extent that σ_5 would not, generally, relate to the compatibility of the Total Least Squares solution, but could have some spurious meaning with no obvious physical significance. It is important therefore that d_5 is set to some value less than the terms d_1 to d_4 to ensure that the output from the process is meaningful.

The first three columns of this matrix constitute elements of unit vectors, therefore the value of every element will be something between 0 and 1. The unit vector indicates the direction from the User to a specific spacecraft. Any Galileo or GPS spacecraft in contact will be around 24,000-30,000 km from the user. Thus, the impact of a small change to any component of the unit vector implicitly changes the assumed location of the spacecraft by a much larger amount (magnified by a factor of around 24-30 x 10⁶). The new geometry matrix produced by the SVD process is not used in the position fix, but the fitting process (and the metrics that are based upon its outcome) should take account of the physical meaning of the terms. In other words, the weighting in the **D**

matrix should reflect the physical meaning of each column in the **[Gy]** matrix.

The fourth column, being the clock offset component, is set by default to equal 1 for all elements. The physical interpretation of this column is as follows: We are measuring time in terms of distance, based on the constancy of the speed of light. Setting this value to '1' states that a unit change in the clock bias (measured in metres), leads to a unit change in the pseudo-range error (also in metres). This is true for all observations, so the value is set to '1' for each spacecraft (row) in the observation matrix. A 1m change in clock bias leads to a 1m change in pseudo-range. Changing this value implies a change in the relationship between time and distance travelled. If it is set to, say, 1.5 then that is the equivalent of saying that a 1m change in clock bias leads to a 1.5m change in pseudo-range error. Clearly, changes to this column should be strongly suppressed if physical realism is to be maintained.

The values of the elements in the fifth column, representing the measurement residuals, require some consideration. This column represents the difference between the expected range to a spacecraft and the measured distance. So long as changes are kept relatively small (i.e. centimetres to a few metres), a change in this column might simply represent measurement noise. Unlike the previous columns, it does not represent a scaling factor – it is a measured value. The expected value of a pseudorange error is on the order of 1-20m. Thus, a realistic change (say, 1m) represents a much larger fraction than for the previous four columns.

Having reviewed the meaning of the terms in the **D** matrix, it should be noted that the position solution gained from the SVD process is NOT used as the navigation solution. For that, we still rely upon the Least Squares Residuals fit. The purpose of undertaking the SVD process is to gain another 'goodness of fit' metric, via the **[H e]** matrix. Thus, strictly, we do not need to treat the **[G y]** matrix in a physically rigorous way ; we are only interested in deriving a metric which responds linearly to induced bias.

If physical interpretation was of greatest importance, then typically, the **D** matrix may be set to something like the following:

$$\mathbf{D} = \begin{vmatrix} 1 & & & & \\ & 1 & & & \\ & & 1 & & \\ & & & 1 & \\ & & & & 100 \\ & & & & & 3 \times 10^{-5} \end{vmatrix}$$

i.e. changes to the unit vector are scaled, in accordance with their effect on the assumed spacecraft position. Changes to the 'clock' column are heavily suppressed, as these are deemed to be unrealistic (or, at least, only susceptible to very small variations). Changes to the pseudorange column (column 5) are, in contrast, much easier to allow since there is a one-to-one relationship between the perturbation and its effect on the signal timing.

If this approach is adopted, the result is a strongly non-linear response to bias. This is of little use in the current application, and so the **D** matrix given above is a poor choice for EIV RAIM.

In fact, the primary criterion for a good **D** matrix is that it provides a linear response to signal bias. Without that property, the process of estimating vertical error from test statistic value becomes much more complex. In practice, the best way to achieve that behaviour is to apply weighting such that the clock and pseudo-range columns absorb most of the changes. The reasons for doing this are as follows:

- i) **Suppressing changes to the unit vector (d_{1-3})** – As mentioned earlier, changes to the unit vector component must be suppressed, to allow for the large effect that a change in direction can have on the implied spacecraft position. Also, the SVD process takes no account of the relationship between these three components. It does not treat them as components of a unit vector, but rather as independent values. Thus, in general, it will change them in a way that changes the length of the vector. The impact of a change varies depending upon the specific geometry. For a spacecraft directly overhead, a change to the 'Up' component has a different effect on the projected spacecraft location than a change to the North or East components. Thus, its effect on the H/e metric will tend to be non-linear. For all these reasons, it is best to keep changes to the vector columns relatively small.
- ii) **Time and Distance (d_{4-5})** – As described earlier, the d_4 term allows the SVD process to introduce changes to the timing of received signals, relative to the clock bias. The d_5 term has a very similar role, since it measures the time/distance difference between expected and received signals. Thus, these two values can be seen as describing similar properties. We can use the **D** matrix to encourage an even distribution of ranging error between these two columns, while simultaneously keeping corrections to the unit vector small. This leads to a much more linear relationship between applied bias and induced H/e test statistic.

The following sections discuss the test statistics used by the EIV method, and show how the D matrix is set to provide desirable characteristics for these metrics. Note that no attempt is made at this point to provide an analytical method for the determination of the appropriate terms of the D matrix. Rather, the discussion above is distilled into the following simple rules, which provide the basis for a “trial and error” approach to finding an appropriate set of values:

- a) The weighting associated with the physical dimensions North, East and Up should all be the same, therefore set these values to be equal to one;
- b) The d_5 term should have the largest value possible, whilst remaining small enough to ensure that the singular value associated with this column of the augmented matrix will always be the lowest singular value of the SVD process;
- c) The d_4 term should be set to some value that provides test statistic characteristics such as shown in Figure 10-12 which are apparently linear over the range of biases under consideration, and which can be extrapolated to pass close to the origin on the test characteristic plot;
- d) When running a simulation of a typical satellite-to-user geometry, the test statistic probability density should closely match the ideal probability density as shown in Figure 10-6.

It may be necessary to iterate around the values of d_4 and d_5 to optimise the test statistic characteristic and probability density. At this point it is not possible to make a statement regarding how linear or how close to the origin the extrapolated characteristics should run, nor how well the simulated probability density should correlate with the ideal. The figures in Section 10.4 and 10.5 give an impression of the quality of fit that was readily achievable through trial and error for the cases analysed in this thesis, and the subsequent experimental results suggest that this is adequate for this level of analysis.

Section 13.4, in the Discussion for this thesis, presents comments on the physical significance of the parameters used in setting the D matrix, which has become apparent from the experimentation and simulation presented in subsequent sections.

10.4 EIV RAIM Test Statistics

10.4.1 Unweighted EIV Fault Detection Plane

As discussed in Section 10.3.1, a test statistic based on the sum of squared errors for the TLS position solution is readily formed. However, [30] demonstrates that this has two disadvantages compared with the standard LSR test statistic:

1. The underlying distribution is very complex, hence setting thresholds and calculating protection limits is computationally very demanding;
2. The distribution itself has a smaller hump and longer tail than the χ^2 distribution used in the LSR method, therefore at the very low false alarm probabilities demanded by RAIM applications this test statistic is likely to require a detection threshold which offers no improvement in protection limit compared with LSR RAIM.

[30] goes on to demonstrate alternative candidates for use as test statistics, which take advantage of the very important feature of the EIV method that it produces more than one independent test statistic. In the case where the **C** and **D** matrices are identity matrices, as analysed in the reference, it is shown that a fault detection plane can be drawn in which the axes represent e_{tls} and H_{tls} , as previously defined. A line from a point on this plane to the origin has a length equal to (σ_5 / V_{55}) and, obviously, makes an angle with the x-axis equal to (H_{tls} / e_{tls}) . It is shown that the length of this vector and its angle can be used as independent test statistics, i.e. each increases when a bias is applied to an observation.

Although this indicates that some fault detection scheme could be developed using this technique, it leaves the problem of defining the underlying distributions for these two test statistics open, and it does not attempt to consider the added complexity of applying weighting matrices **C** and **D** such that the TLS solution is comparable with the Least Squares position solution.

10.4.2 \sqrt{USSE} Test Statistic

One would assume that by introducing the **C** and **D** matrices to the TLS problem (i.e. if they are no longer identity matrices) the situation regarding setting appropriate test statistics and defining thresholds would become even more complicated. However, there appears to be a remarkable effect when **C** is equal to the square root of the **W** matrix, as discussed in Section 10.3.1, and the d_5 term is sufficiently small, as discussed in 10.3.2.

In Section 10.3.1 expressions were presented for the unweighted (i.e. \mathbf{C} is Identity) and weighted ($\mathbf{C} = \mathbf{W}^{1/2}$) modified Sum of Squared Errors statistic, and it was stated that the underlying distribution is a summation of four Gamma distributions with different parameters and an N-4 degrees of freedom χ^2 distribution, which is very difficult to deal with analytically. In Section 10.4.1 it was stated that in the unweighted case the term (σ_5 / V_{55}) can be used as a test statistic on the fault detection plane. This clearly has a similarity with the unweighted modified Sum of Squared Errors (USSE') defined in Equation 10-9; the difference being the inclusion of the d_5 term in the denominator of USSE'.

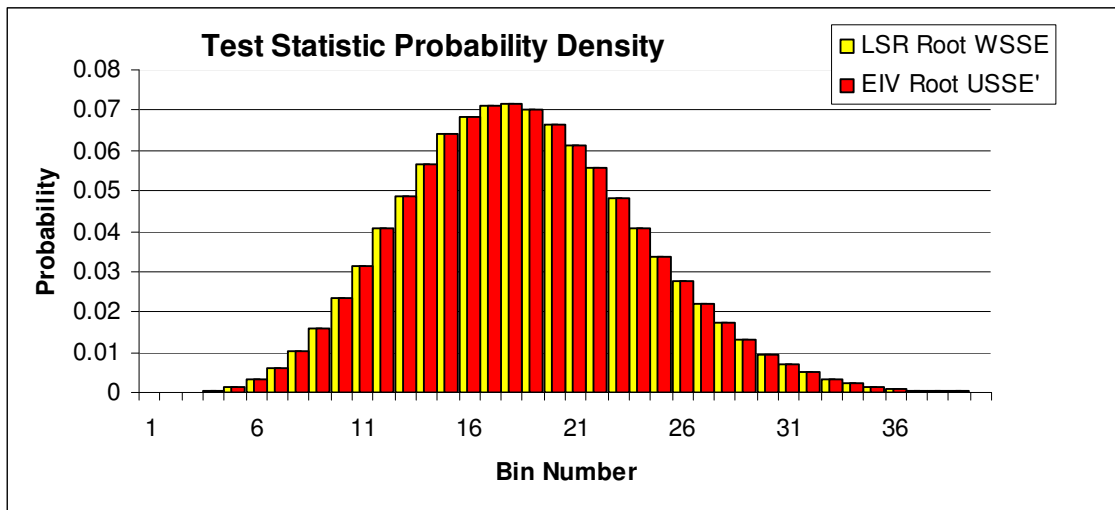


Figure 10-1 : Comparison of $\sqrt{\text{USSE}'}$ with $\sqrt{\text{WSSE}}$

Figure 10-1 presents the output from a run using the NavEng tool, in which the square root of USSE' is used as a test statistic for the EIV algorithm. The run comprised one million samples. The range between the lowest and highest value of test statistic for both $\sqrt{\text{USSE}'}$ and $\sqrt{\text{WSSE}}$ is split into 50 equal sized "bins" and the number of samples falling into each bin is counted. The resulting plot shows the probability density for the test statistic in question. In this case the probability density of $\sqrt{\text{USSE}'}$ appears identical to that of $\sqrt{\text{WSSE}}$. Indeed, using the "Correl" function in Excel to find the correlation on the first 10,000 samples from this run found a perfect correlation between the two.

Therefore, although no rigorous mathematical justification is presented, it appears that when the \mathbf{C} matrix introduced in Equation 10-2 is set to *the square root of the \mathbf{W} matrix*, and d_5 is sufficiently small, $\sqrt{\text{USSE}'}$ is equal to the LSR test statistic $\sqrt{\text{WSSE}}$. Setting fault detection thresholds for a required false alarm probability therefore requires precisely the same process as for the LSR method.

Furthermore, Figure 10-2 shows the Test Statistic Characteristic for $\sqrt{\text{USSE}}$, for the same case as was used to generate the equivalent characteristic for the LSR RAIM case in Figure 9-2. These characteristics can be seen to be identical, again demonstrating the direct relationship between $\sqrt{\text{USSE}}$ and $\sqrt{\text{WSSE}}$.

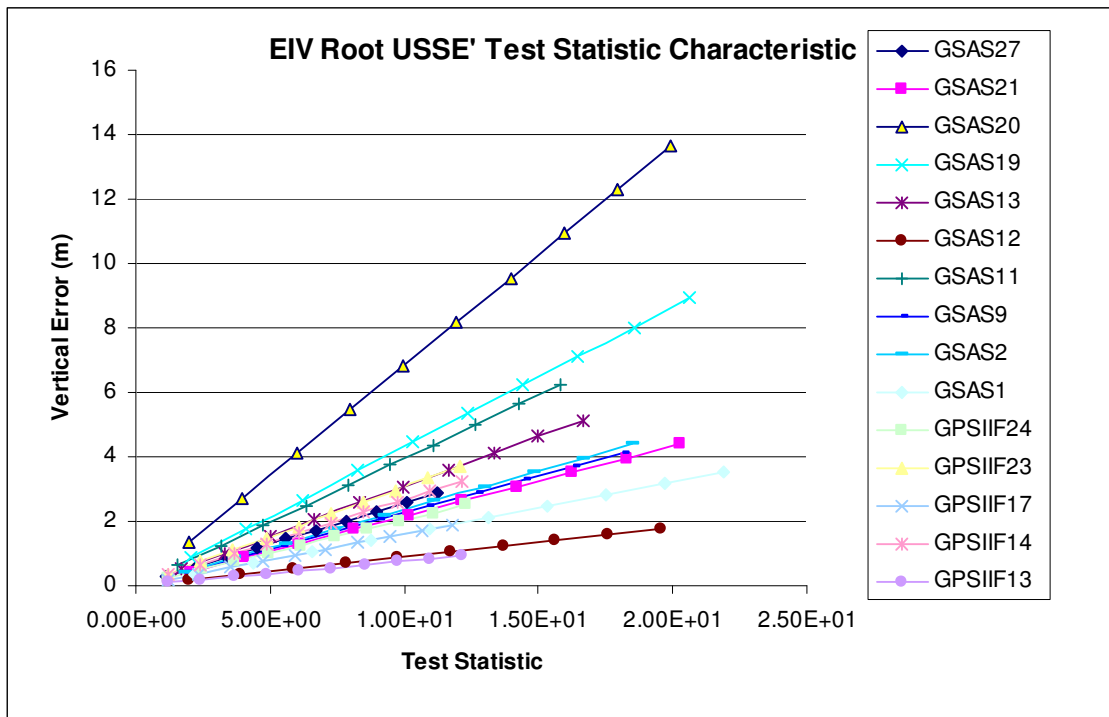


Figure 10-2 : $\sqrt{\text{USSE}}$ Test Statistic Characteristic

It should be noted that the value of the $\sqrt{\text{USSE}}$ test statistic is dominated by the σ_5 term. When d_5 is small, the term V_{55} tends toward unity, and so it appears that σ_5 is itself approximately proportional to $\sqrt{\text{WSSE}}$, with $1/d_5$ acting as the constant of proportionality. Indeed this was the relationship which was originally observed to have the underlying χ^2 distribution, although on closer analysis it became apparent that the V_{55} term had to be included to provide the very high correlation with $\sqrt{\text{WSSE}}$ described above.

10.4.3 H/e Test Statistic

When discussing the unweighted EIV case previously it was stated that if $\|H_{t|s}\|_F$ (the Frobenius norm of $H_{t|s}$) and $\|e_{t|s}\|$ (the vector norm of $e_{t|s}$) are used as axes for a fault detection plane, both the distance of a point to the origin and the angle that this line makes with the x-axis act as independent test statistics. The $\sqrt{\text{USSE}}$ term defined above represents the distance to the origin and, being exactly equal to $\sqrt{\text{WSSE}}$ is in fact a measure of the overall consistency of the set of measurements.

Rather than consider the angle of the line drawn from a point on the plane to the origin, we can more conveniently consider the ratio of H_{tls} and e_{tls} . This comparison of the two mismatches provides an assessment of the extent of ephemeris error and pseudo-range error

The ratio of these scalar values (i.e. $\|H_{\text{tls}}\|_F / \|e_{\text{tls}}\|$) thus provides a test statistic that represents the extent to which the Total Least Squares position solution has allocated errors to the model (**H**) or to the measurements (**e**). For brevity we shall refer to the ratio of these norms as H/e, i.e. by definition,

$$H/e = \|H_{\text{tls}}\|_F / \|e_{\text{tls}}\|$$

Equation 10-12

Note from Equation 10-4 that both H_{tls} and e_{tls} are directly related to σ_5 , V_{55} and d_5 . However, because they are both directly related to all of these terms, the ratio $\|H_{\text{tls}}\|_F / \|e_{\text{tls}}\|$ is entirely uncorrelated with $\sqrt{\text{USSE}}$. This is a very important point; being uncorrelated, $\sqrt{\text{USSE}}$ and H/e may be used as two independent test statistics.

The independence of the two statistics may be further understood, by considering *what* they are measuring. These two statistics represent two different properties of the mismatches between the total least-squares solution and the measurement data. The $\sqrt{\text{USSE}}$ term represents the summed *magnitude* of mismatches between the observation data and the least-squares solution. The H/e statistic, on the other hand, tell us something about where those mismatches occurred. In particular, it tells us the ratio of error attributed to pseudorange measurement (i.e. parallel to the observation vectors) versus error attributed to the Geometry matrix (i.e. error in the observation unit vector itself). This explanation gives some insight into the response of the H/e statistic. The example in Appendix D of a singular value decomposition of a 2-dimensional matrix provides additional insight into the relationship between these two test statistics.

If the errors are mostly found to be ‘along’ the observation vectors, H will be small and e will be large – so, H/e will be a small number. Conversely, if significant errors are attributed to the Geometry matrix and the pseudoranges are judged to be good, H/e will be large.

The implications of this are worth some consideration. The H/e statistic will be quite insensitive to errors which do not induce large changes in the Geometry matrix. Fortunately, the $\sqrt{\text{USSE}}$ statistic *is* sensitive to these errors. The use of a ‘backstop’ $\sqrt{\text{USSE}}$ threshold will be discussed later. Furthermore, consider that the majority of spacecraft visible at any given time are most likely to be found at mid to low elevations. This will

generally be so, since the area of the sky below 45° represents almost $2\frac{1}{2}$ times the area of sky above 45° elevation. Thus, the 'up' direction for a receiver is generally oblique to the majority of observation vectors, i.e. a *vertical* error will induce changes in the geometry of a larger number of spacecraft than a *horizontal* error. The H/e statistic is therefore particularly well suited to detection of vertical error.

Figure 10-3 illustrates the point:

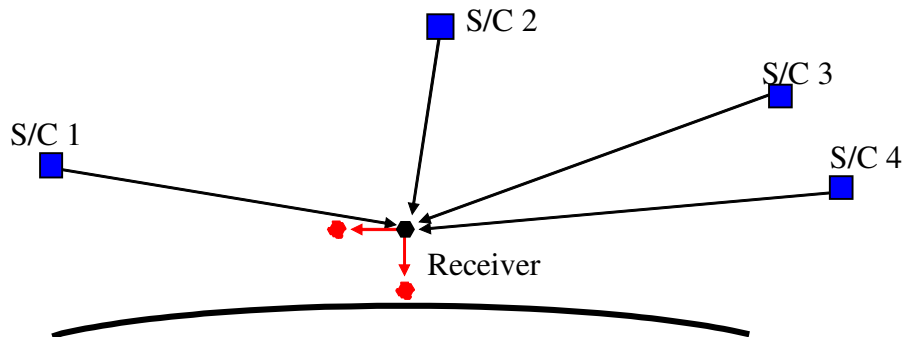


Figure 10-3 Geometry change with vertical displacement

As described, a vertical change in receiver position produces large changes in the vectors to spacecraft 1, 3 and 4. By contrast, spacecraft 2 experiences little change in direction, since the motion has a large component along the observation vector. In contrast, a horizontal change only induces significant change in the direction of the vector to Spacecraft 2, which is high in the sky.

Given the very different nature of errors to which the two test statistics, H/e and $\sqrt{\text{USSE}}$, respond, it is intuitively clear that the two are linearly independent. They measure fundamentally different properties.

For completeness, the correlation between (H/e) and $\sqrt{\text{USSE}}$ was calculated using the first 10,000 samples from the NavEng simulator run which was used to produce Figure 10-1. In this case it was found to be -0.02, which is an extremely weak correlation, of the order of what is found when comparing two lists of 10,000 random numbers.

Figure 10-4 presents the distribution of lateral error vs H/e test statistic, and Figure 10-5 presents the distribution of vertical error vs H/e test statistic for the same set of data. This shows that the H/e test statistic is reasonably strongly correlated with vertical error. In fact the value of this correlation was found to be 0.83. In contrast, the statistic does not respond strongly to lateral error..

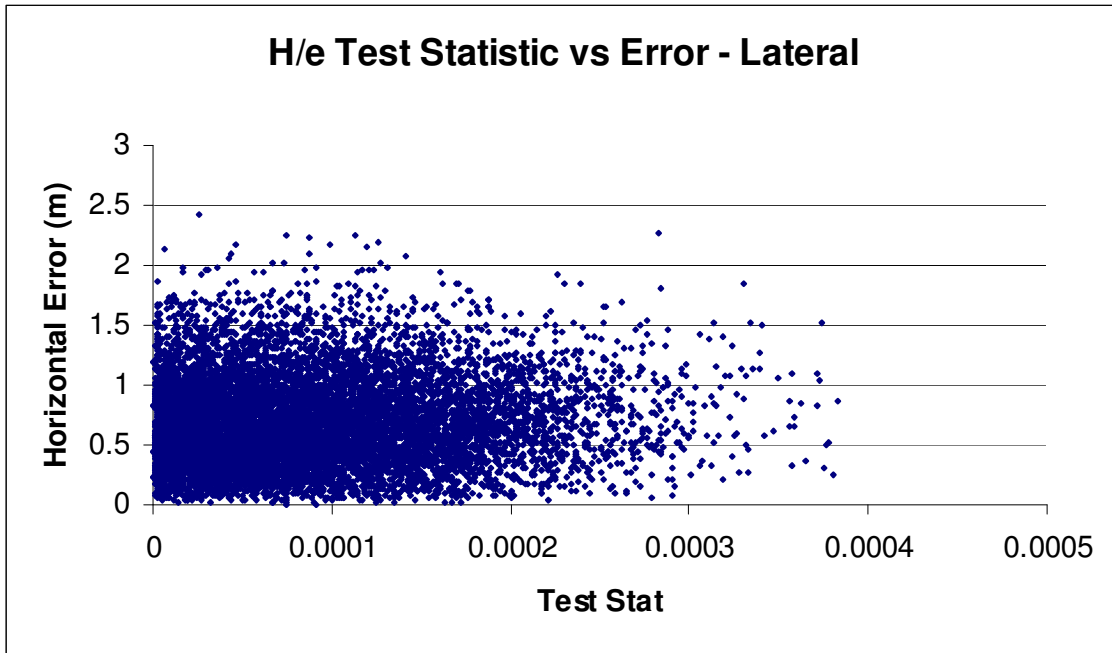


Figure 10-4 : H/e Test Statistic Distribution vs Horizontal Error

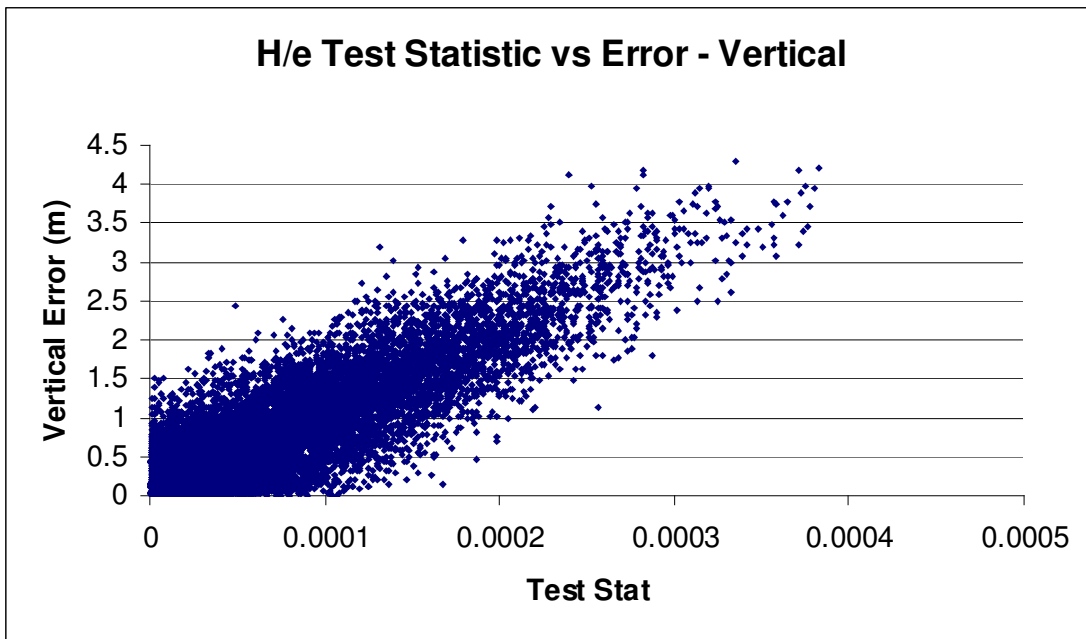


Figure 10-5: H/e Test Statistic Distribution vs Vertical Error

Figure 10-6 presents the probability density for the H/e test statistic. Note how closely this distribution matches the theoretical curve for a “Half-Normal Distribution”. A Half-Normal Distribution is effectively a zero-mean normal distribution folded around the mean, so that all values are positive. The correlation in this case is found to equal 0.99997.

This is a very important result, because it greatly simplifies the task of setting the detection threshold for this test statistic. If the standard deviation of the distribution is determined, the appropriate threshold for a given alarm rate is readily determined. The major investigation to be undertaken on the EIV method is therefore to formulate a method for setting the **D** matrix such that the distribution of the H/e Test Statistic is bounded by a Half-Normal distribution, and that the standard deviation of this distribution may be evaluated analytically.

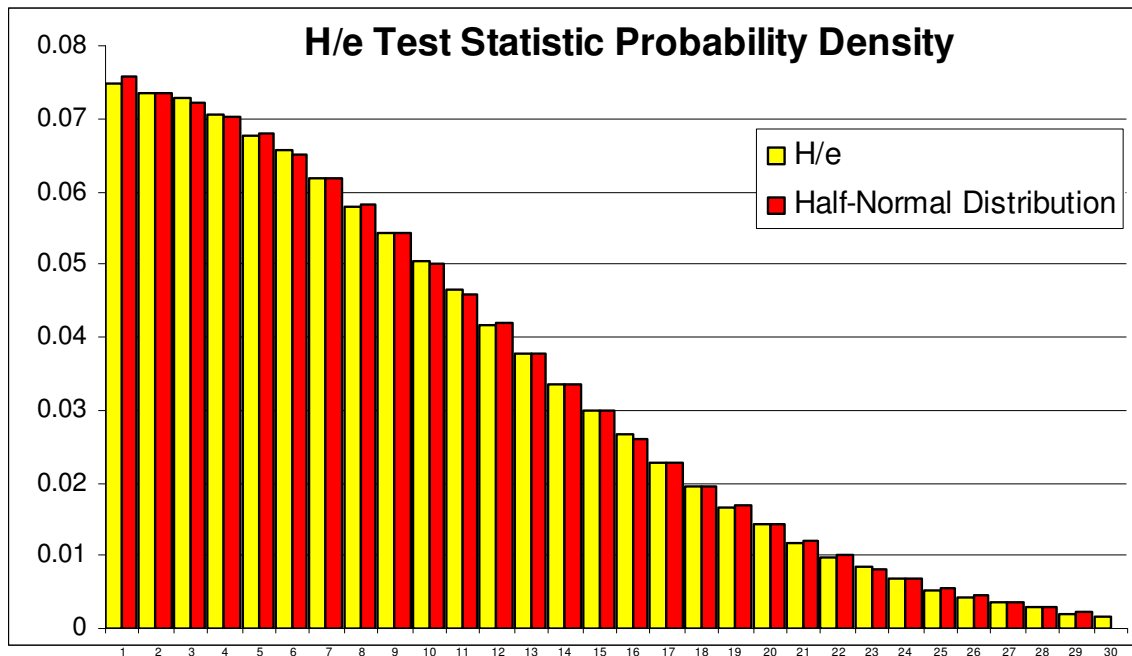


Figure 10-6 : Ideal H/e Test Statistic Probability Density

The technique used to estimate the standard deviation of this distribution is described in Section 10.5.2.

10.5 Combining Two Test Statistics

10.5.1 Overall Concept

Either of the test statistics described in the previous sections could potentially be used as the fault detection mechanism in a RAIM algorithm. However using either $\sqrt{\text{USSE}}$ or H/e on its own would not provide any significant advantage over other RAIM algorithms. The power of the EIV method becomes apparent when using both test statistics together, i.e. so that a fault condition is declared only when both test statistics exceed specified thresholds.

Consider the simplified case in which the continuity requirement leads to a specified probability of false alarm of 1×10^{-6} . The LSR RAIM threshold would need to be set to yield no more than one alarm per one million

independent samples. Using the EIV approach, the $\sqrt{\text{USSE}}$ threshold could be set to yield one detection per thousand samples, as long as the H/e threshold is also set to the same alarm rate. Because they are entirely uncorrelated the overall probability of false alarm would be 1×10^{-6} , as required. Clearly, the P_{FA} component of VPL derived from this method would be significantly smaller than the P_{FA} component of VPL using the LSR method.

Figure 10-7 shows two sets of 10,000 samples generated by the NavEng tool and displayed graphically using the “3d Grapher” tool [53]. The horizontal axis (“x”) represents the $\sqrt{\text{USSE}}$ threshold and the vertical axis (“z”) represents the vertical error derived from a least squares navigation solution.

The first set of data represents an unbiased sample, i.e. only zero-mean Gaussian noise is applied to each measurement. The second set of data represents the case where a bias is applied to the most critical satellite in view. As described previously for the LSR algorithm, the test statistic distribution increases in value in both the vertical error and test statistic domains.

The vertical line on this figure represents the detection threshold for the specified false alarm rate (in this case set to 1×10^{-4} , so that around ten samples would be expected to exceed this threshold). The horizontal line represents the vertical protection limit calculated using the LSR method for this P_{FA} and a P_{MD} also of 10^{-4} .

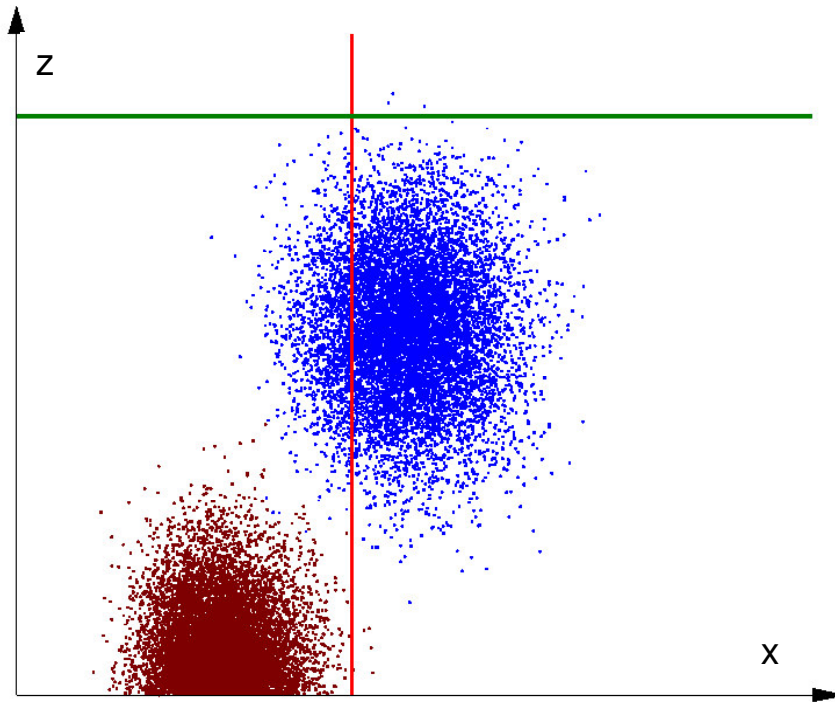


Figure 10-7 : Vertical Error (z-axis) vs $\sqrt{\text{USSE}}$ Test Statistic (x-axis)

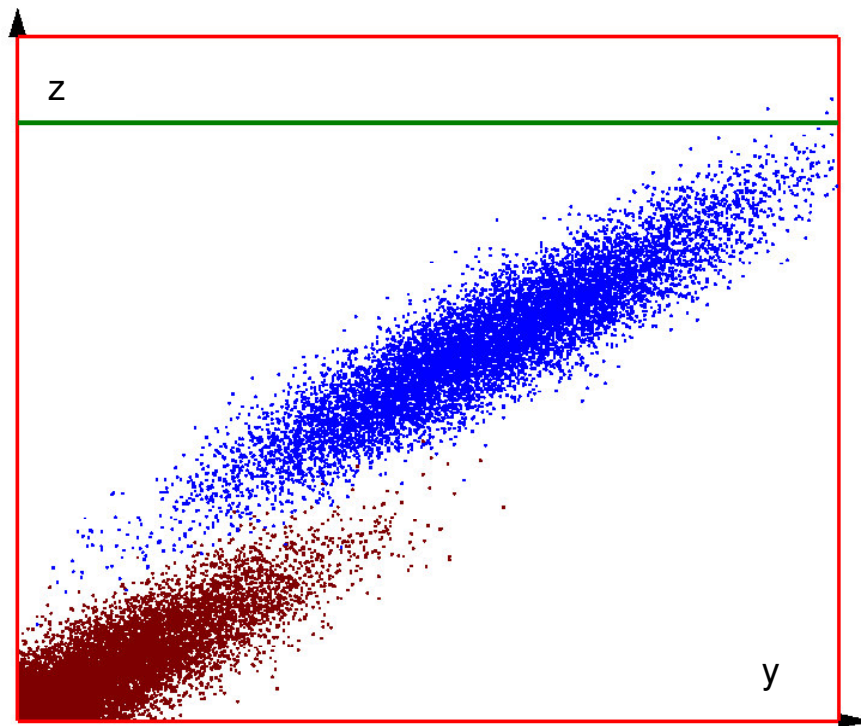


Figure 10-8 : Vertical Error (z-axis) vs H/e Test Statistic (y-axis)

Figure 10-8 presents the same data, viewed along the x-axis so that this figure represents the distributions of vertical error against H/e test

statistic for the unbiased and biased cases. The horizontal line again represents the VPL derived from the LSR method.

Figure 10-9 presents the data for the unbiased case alone, viewed along the z-axis to show the relationship between the $\sqrt{\text{USSE}}$ Test Statistic (x-axis) and the H/e Test Statistic (y-axis). As with Figure 10-7 the vertical line represents the detection threshold using the LSR method. This figure also includes a region in the top right hand corner marked by the H/e detection threshold and the $\sqrt{\text{USSE}}$ detection threshold. These values have been set to yield the same combined detection rate as the LSR detection threshold.

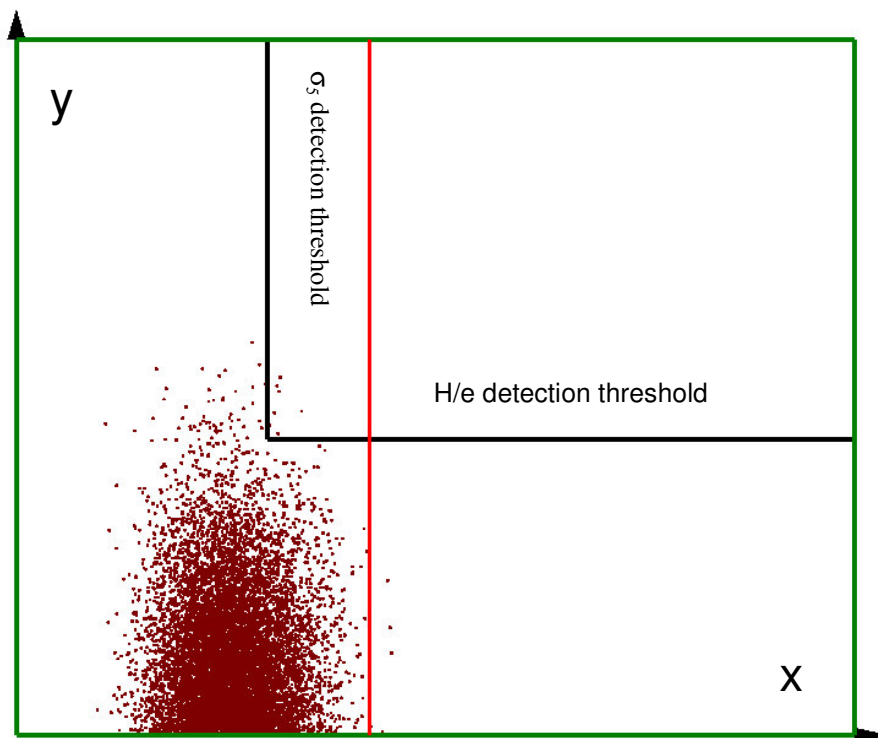


Figure 10-9: $\sqrt{\text{USSE}}$ Statistic (x-axis) vs H/e Test Statistic (y-axis)

Figure 10-10 presents the same information as Figure 10-7, but now also showing the vertical protection limit as calculated using the EIV algorithm. This is approximately 15% lower than the VPL calculated using the LSR method.

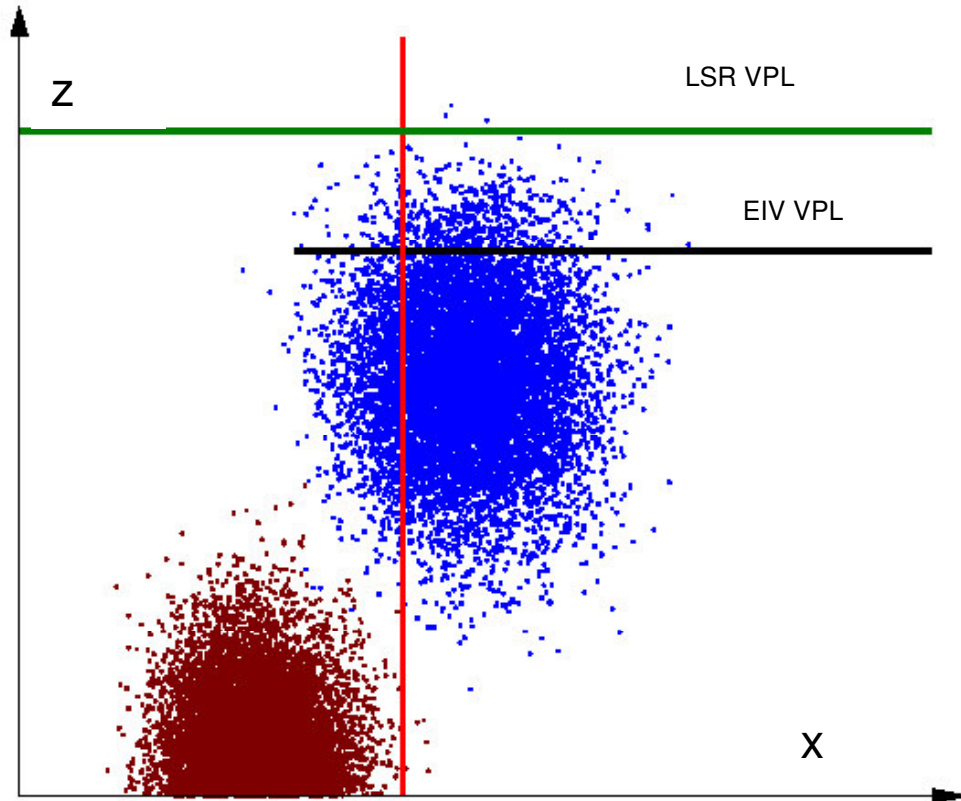


Figure 10-10 : Vertical Error vs $\sqrt{\text{USSE}}$ Statistic, showing EIV VPL

Finally, Figure 10-11 attempts to present these data in a three dimensional perspective view. The higher horizontal plane is the LSR VPL, whilst the lower plane represents the EIV VPL and its associated detection thresholds.

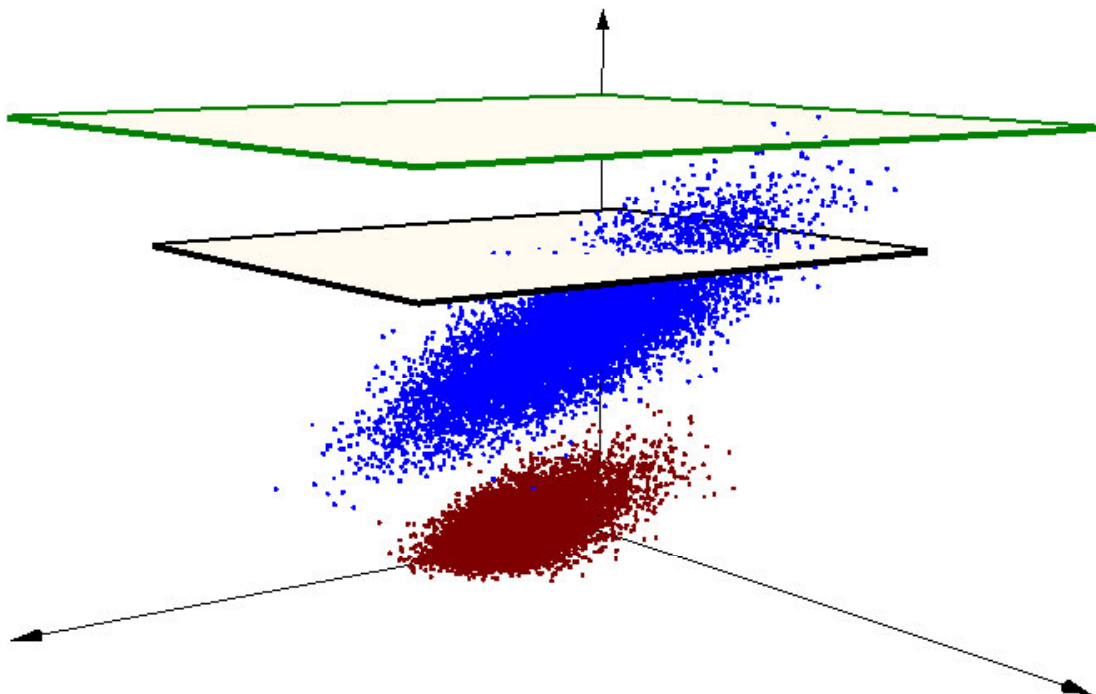


Figure 10-11 : EIV Test Statistic Distribution in 3 dimensions

10.5.2 H/e Test Statistic Standard Deviation

In order to set a detection threshold for the H/e test statistic, the probability density function (i.e. the probability that the value of this statistic exceeds a given value) for the unbiased case needs to be evaluated. In Figure 10-6 it was shown that when correctly set up H/e displays a Half-Normal distribution; given the standard deviation for this distribution a detection threshold is readily evaluated.

The standard deviation can be evaluated for any case using Monte Carlo simulation techniques, but this is likely to be too time-consuming to be applicable to real-time safety-critical applications. An analytical approach is therefore required. Based on the results from simulation and experimentation, there appears to be a reasonably simple way of producing a good estimate of the standard deviation.

The H/e statistic responds linearly to an induced bias – this is one of the fundamental properties that we sought when tuning the **D** matrix. In a non-biased case, each pseudo-range measurement will be subject to Gaussian noise which is, in effect, a sequence of small biases. Thus, holding all other measurements constant, if the pseudorange has a Gaussian distribution, the H/e test statistic must also have a Gaussian distribution.

With noise present on all of the 'n' observations, the H/e test statistic can then be approximated by a sum of 'n' Gaussian distributions. The sum of two independent Gaussian distributions is, itself, a Gaussian distribution, with variance equal to the vector sum of the variances of the component distributions. Thus, taking the approximation that the contributions from each spacecraft are independent, it follows that the distribution of H/e can be found.

The approach taken here is to consider each observation (i.e. each satellite in view) in isolation. If a bias is applied to this satellite of magnitude equal to its UERE (i.e. the 1σ expectation of range error on a signal), with no noise or bias on any other satellite, a value for H/e can be determined. If the values arising in this way, by considering each satellite in turn, are arranged as a vector, the Norm of this vector (i.e. the square root of the sum of the squares of the elements of this vector) represents the standard deviation of H/e for this case.

Figure 10-12 shows the H/e test statistic characteristic for the same case for which the LSR and \sqrt{USSE} characteristics were presented earlier. These plots show how vertical error and test statistic are related for a known bias applied to each satellite in turn. Given the UERE for each observation, it is a simple task to evaluate the expected (1σ) value of H/e test statistic from each satellite. The vector summation of these values provides the estimate of the overall standard deviation. This entire process is expressed linearly in Section 10.6.

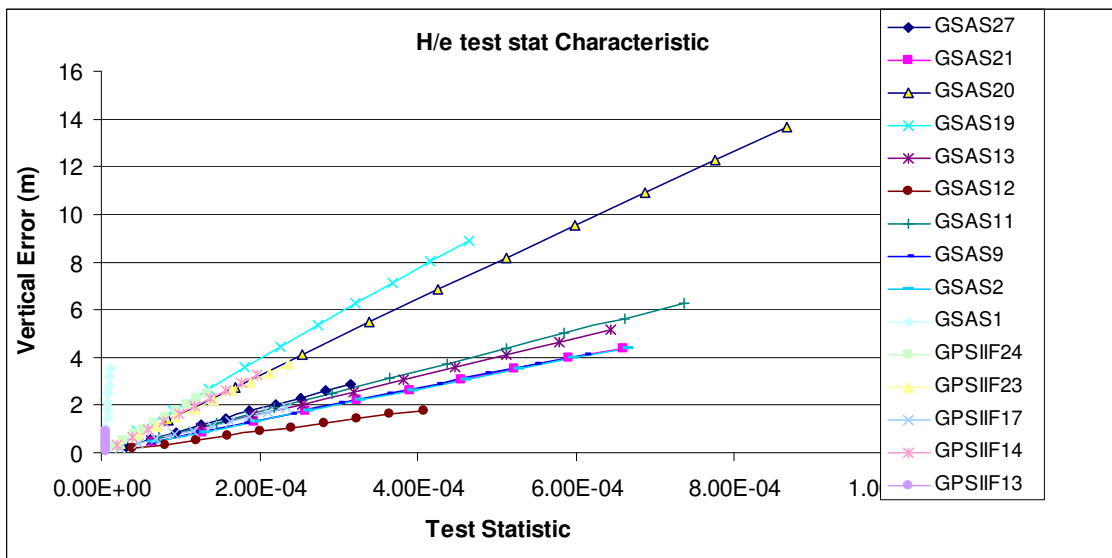


Figure 10-12 : H/e Test Statistic Characteristic

For the case represented by this figure, the standard deviation is calculated to be approximately 9.69×10^{-5} . In comparison, the standard

deviation calculated by looking at ten thousand samples from the navigation engine for this case is found to equal 9.55×10^{-5} , i.e. the estimation technique appears to agree with the observations to within about 1.5%.

10.5.3 Backstop Threshold

The EIV method has an additional element of complexity which needs to be taken into account when developing an operational RAIM algorithm. Notice on Figure 10-12 that on this characteristic the satellite which has the greatest vertical error for a given applied bias (satellite GSAS20 in this example) does not have the steepest slope on the characteristic; in this example there are three satellites for whom a large applied bias on either one could lead to large vertical error without generating a large value of H/e test statistic.

In the LSR method, the satellite with the steepest characteristic slope is by definition the Critical Satellite, i.e. the satellite whose characteristic effectively determines the VPL, because in setting the VPL it is assumed that any feared event will occur on this satellite's signal. This is also the case for the $\sqrt{\text{USSE}}$ test statistic of course, but is not generally true for the H/e test statistic.

In the EIV method we identify the Critical Satellite from the $\sqrt{\text{USSE}}$ characteristic (i.e. it is the same as the LSR critical satellite). Therefore, in order to provide with certainty that a bias on any satellite will be detected by the EIV RAIM algorithm without exceeding the evaluated VPL, for specified values of P_{FA} and P_{MD} , it is necessary to add a secondary test threshold, acting only on the $\sqrt{\text{USSE}}$ test statistic, which if exceeded will generate an alarm regardless of the value of the H/e test statistic.

The process used to set this backstop threshold is as follows:

- Identify the Critical Satellite from the $\sqrt{\text{USSE}}$ test statistic characteristic (GSAS20 in the case above);
- From the H/e test statistic characteristic, identify every satellite whose characteristic is steeper than that of the Critical Satellite (in this case, GSAS 19, GSAS1 and GPSIIF13);
- Identify the satellite from this list which has the maximum slope on the $\sqrt{\text{USSE}}$ test statistic characteristic (GSAS19);
- Use the slope of this satellite's characteristic in the subsequent "Threshold Balancing" process.

10.5.4 Threshold Balancing

Having established the probability density functions of the two test statistics ($\sqrt{\text{USSE}}$ ' and H/e) the next step is to evaluate values for the detection thresholds on each test statistic such that the P_{FA} requirement is met and the VPL is minimised. This requires the characteristics of each test statistic (i.e. the relationship between vertical error and test statistic) to be taken into consideration.

For the $\sqrt{\text{USSE}}$ ' test statistic the relationship is identical to the approach used in the LSR method.

For the H/e characteristic the situation is more complex. As discussed above, Figure 10-12 presents the test statistic characteristic for the H/e test statistic, for the same case analysed using LSR RAIM in Figure 9-2 previously. The characteristics are still linear (at least over the relatively low range of biases covered by this example), and pass through the origin. Given these characteristics the relationship between vertical error and H/e test statistic can be readily evaluated by finding the value of H/e generated by applying a unit bias in turn to each observation.

Once the test statistic characteristic has been evaluated for both $\sqrt{\text{USSE}}$ ' and H/e the final step is to “balance” the $\sqrt{\text{USSE}}$ ', H/e and Backstop thresholds.

When a value for a threshold is multiplied by a value for the corresponding test statistic characteristic (i.e. the slope of vertical error against test statistic) the product is some value of vertical error. This value is effectively the component of VPL associated with the alarm rate for this test statistic. “Balancing” is the process by which thresholds are set such that:

- The combined probability of either
 - exceeding the thresholds on both $\sqrt{\text{USSE}}$ ' and H/e simultaneously, or;
 - exceeding the Backstop threshold

is no greater than the required P_{FA} ;

- The VPL component derived from $\sqrt{\text{USSE}}$ ' and H/e test statistic methods are equal;
- The VPL component derived from the Backstop is less than or equal to the VPL component derived in the previous step.

Note that in some cases it is impossible to satisfy all these conditions. Figure 10-13 shows the $\sqrt{\text{USSE}}$ characteristic and Figure 10-14 shows the H/e characteristic for such a special case. In fact the geometry leading to this case occurs at the same geographical location, 100 minutes earlier, than the characteristics previously discussed.

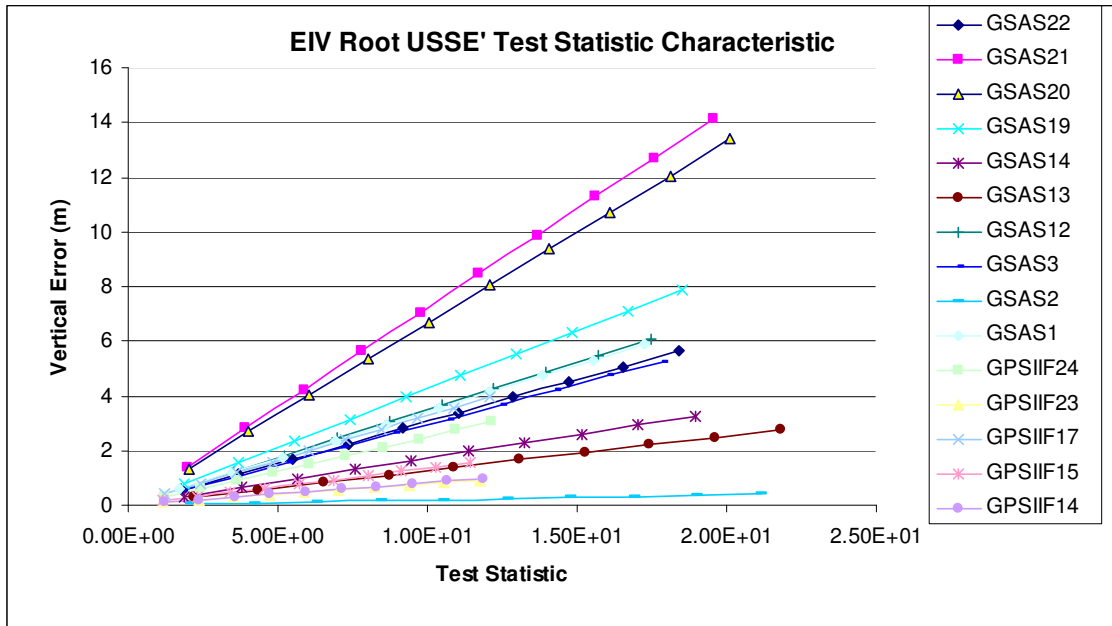


Figure 10-13 : Root USSE' Characteristic (Special Case)

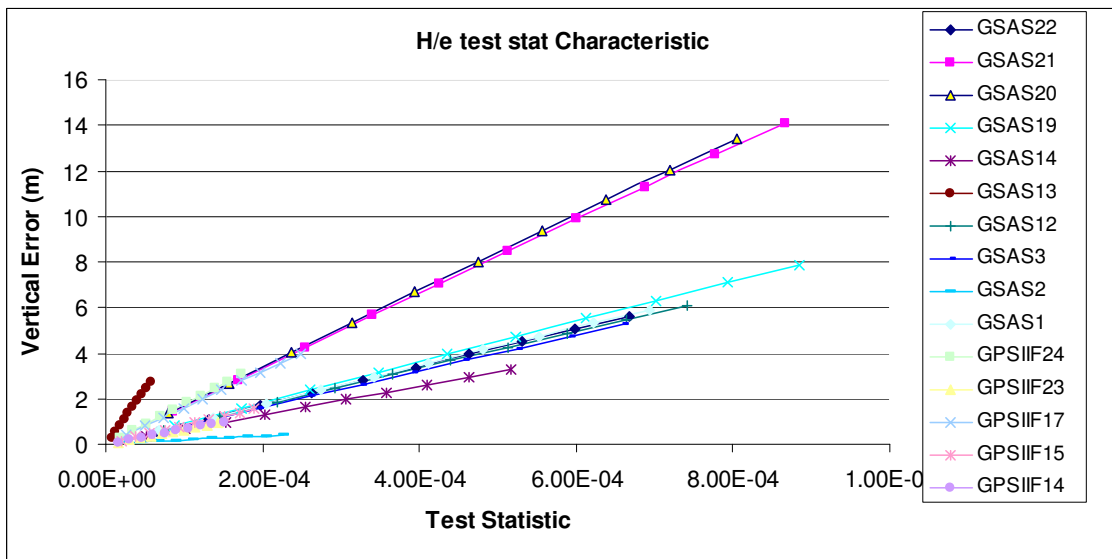


Figure 10-14 : H/e Characteristic (Special Case)

In this case the Critical Satellite is seen to be GSAS21. However, it can be seen that satellite GSAS20 has a slightly less steep $\sqrt{\text{USSE}}$ characteristic, but a marginally steeper H/e characteristic than the

Critical Satellite. The Backstop threshold in this case will therefore be set to cater for the case of a feared event occurring on GSAS20. Because the $\sqrt{\text{USSE}}$ slope for this satellite is so close to that of the Critical Satellite, it is impossible to balance fully the thresholds in the manner described above. In this case the VPL component calculated by multiplying the slope of the GSAS20 $\sqrt{\text{USSE}}$ characteristic by the Backstop threshold is always larger than the VPL component derived by balancing the other two thresholds. In this case the VPL solution is said to be “Backstop Limited”.

10.6 Calculate the Vertical Protection Limit

In the LSR RAIM method, calculating the VPL is based on an assumption that the worst case bias (i.e. the bias which when applied to the critical satellite causes a missed detection probability exactly equal to P_{MD}) is that bias which, in the absence of noise on any satellites, would just cause the LSR RAIM detection threshold to be exceeded. This simplifies the task of setting the VPL⁸.

In the EIV method the situation is more complicated, because the worst case bias is not found from some simple general relationship. Instead an iterative method is required (or, at least has been assumed for this implementation, since a closed-form solution to the problem is not obviously apparent), which determines the worst case bias given the $\sqrt{\text{USSE}}$ Threshold and H/e Threshold values. The following steps describe the logic used to find the worst case bias, and hence to set the Vertical Protection Limit using the EIV method.

1. Consider a case where no bias is applied to any satellite, but each measurement is subject to random noise with a variance as defined by the assumed UERE value for that satellite. In this case the $\sqrt{\text{USSE}}$ Test Statistic has a central χ^2 distribution, with N-4 degrees of freedom.
2. Now consider the same case, but with a bias applied to the Critical Satellite. The test statistic distribution is now a non-central χ^2 distribution, with a non-centrality parameter which can be derived as follows:
 - Given that Equation 9-6 presents the relationship between LSR Test Statistic and Vertical error, and the K_{3i} term represents the relationship between applied bias and vertical

⁸ Although as we shall demonstrate this assumption is false.

error, the value of Test Statistic for a given applied bias, in the absence of any noise on any signals, is readily found.

- By assuming that this value would be the central value for the new distribution, the value of the non-centrality parameter is easily derived.
3. As an increasing bias is applied to the Critical Satellite, the “cloud” representing its distribution moves along the line representing the Critical Characteristic in Figure 10-15. For any particular applied bias, there is some probability of measurements having a value of $\sqrt{\text{USSE}}$ Test Statistic less than the derived $\sqrt{\text{USSE}}$ Threshold. We refer to this probability as “P(subUSSE)”.

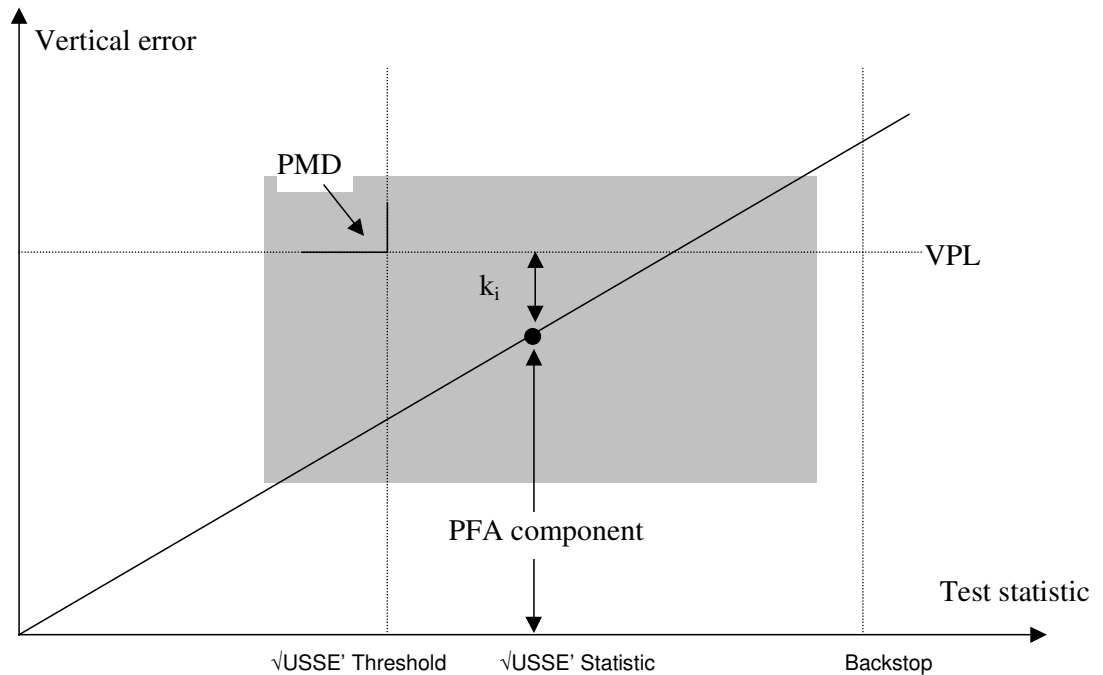


Figure 10-15 : Calculation of EIV Worst case Bias

4. Given all the terms required to define a non-central χ^2 distribution for a given applied bias, the value of P(subUSSE’) is readily derived as a function of applied bias.
5. In the absence of noise, the assumed applied bias will induce a vertical error which we refer to us as the “P_{FA} Component” since this is the component of VPL which is a function of the detection threshold, which is in turn a function of P_{FA}. This is shown in Figure 10-15.

6. When noise is applied to each measurement, the distribution of vertical navigation system error will have a normal distribution, with a mean equal to “ P_{FA} Component” and a standard deviation equal to σ_v , the 1σ vertical error derived previously. The term “ k_i ” in Figure 10-15 represents the number of standard deviations associated with a given probability, which when multiplied by σ_v yield a term we refer to as the “ P_{MD} Component”, since this is related to the required Missed Detection probability.
7. For any assumed applied bias, it is possible to calculate a value for k_i such that the region marked as “PMD” in Figure 10-15 represents the probability of the random noise exceeding the threshold represented by k_i , whilst simultaneously being below the \sqrt{USSE} Threshold. This area should be, by definition, equal to P_{MD} , since this represents a Missed Detection.

In the implementations of the algorithm used in this thesis an iterative process is used to find the maximum value of Vertical Protection Limit that meets these constraints.

10.7 EIV Method - Processing Logic Pseudocode

This section presents the EIV method in a format that can be used to implement the algorithm into computer code. Rather than use formal mathematical language, the names of functions commonly found in C++ mathematical libraries or Matlab are used. For example “normcdf” represents the cumulative density function of the Normal Distribution and “chi2inv” represents the inverse of the χ^2 cumulative distribution function.

10.7.1 Initialise the algorithm

This algorithm has the following inputs:

- **G** matrix;
- **W** matrix;
- **y** vector;
- P_{FA} :
- P_{MD} ;
- Number of satellites in view (N).

The first stage of the process is identical to the standard LSR RAIM process. We need the following outputs from the LSR algorithm:

- $V_{\text{slope(max)}}$;
- Critical Satellite;
- σ_V ;
- k (the number of standard deviations associated with P_{MD} , found from the lookup table or statistics function used by the LSR algorithm);
- Calculate the square root of $(1 - P_{ii})$ (where P_{ii} is the diagonal element of the P matrix associated with the satellite under consideration. See Equation 9-5). These values (the square root of $(1 - P_{ii})$) are arranged as a new vector BiasRatesVect.

10.7.2 Calculate the Test Statistics

- Form the \mathbf{C} matrix, as a diagonal matrix with each element equal to the square root of the elements on the diagonal of the \mathbf{W} matrix;
- Get the \mathbf{D} matrix from an external “Dmat” file.
- Put the fifth diagonal element of this matrix until a variable called “ d_5 ”;
- Form the augmented matrix $\mathbf{C}[\mathbf{G} \ \mathbf{y}]\mathbf{D}$;
- Perform the Singular Value Decomposition (SVD) of the matrix $\mathbf{C}[\mathbf{G}\mathbf{y}]\mathbf{D}$;
- Partition the \mathbf{U} , $\mathbf{\Sigma}$ and \mathbf{V} matrices as per Section 10.2.
- Produce the Test Statistic $\sqrt{USSE'} = (\sigma_5^2 / d_5^2 V_{55}^2)^{1/2}$
- Produce the new matrix $[\mathbf{H}_{tIs} \ \mathbf{e}_{tIs}] = -\sigma_5 \mathbf{C}^{-1}\mathbf{U}_5 [\mathbf{V}_{15}^T \ \mathbf{V}_{55}^T] \mathbf{D}^{-1}$
- Produce the H/e Test Statistic, $H/e = \|\mathbf{H}_{tIs}\|_F / \|\mathbf{e}_{tIs}\|$

10.7.3 Calculate the Detection Thresholds

- Assume a value which represents the largest bias which needs to be detected using this algorithm (i.e. for which this algorithm has to have linear characteristics). In this case it has been assumed to equal 20m;
- For Satellite = 1 to N;
 - Get the value from the diagonal of the \mathbf{W} matrix corresponding to this satellite. Call this “ b ”;

- Make a vector \mathbf{q} , in which every element is set to zero except the element corresponding to this satellite, which is set to 20;
- Produce the new $n \times 5$ augmented matrix $\mathbf{C}[\mathbf{G} \ \mathbf{q}]\mathbf{D}$;
- Perform the Singular Value Decomposition of the matrix $\mathbf{C}[\mathbf{G} \ \mathbf{q}]\mathbf{D}$;
- Run through the same steps as previously for the EIV algorithm, to decompose the matrices, etc.
- Store the value of $(\| \mathbf{H}_{\text{tls}} \|_F / \| \mathbf{e}_{\text{tls}} \|) \times (b / 20)$ (i.e. the ratio of these two values) in an array EIV_TS_Vector .
- This represents the H/e test statistic associated with a bias equal to this satellite's UERE; the 20m term is used to minimise non-linearity effects of the characteristic close to the origin.
- Store, in a new array EIV_Slope_Vector the value from :
 - $(K_{3i} \times b) / \text{EIV_TS_Vector}(i)$
 - This represents the slope of the $(\| \mathbf{H}_{\text{tls}} \|_F / \| \mathbf{e}_{\text{tls}} \|)$ test statistic with respect to satellite bias.
- Next Satellite.
- Evaluate the Norm (i.e. square root of the sum of the squares of the elements) of EIV_TS_Vector . Call this value EIV_TS_Sigma . This is the estimate of the Standard Deviation of the H/e test statistic.
- Get the value from the EIV_Slope_Vector that corresponds to the Critical Satellite from the LSR calculation. Call this value $\text{EIV_Critical_Characteristic}$;
- Derive $\text{Vslope}(2)$ – this is the highest value of “Slope”, i.e. the LSR test statistic characteristic, for a satellite **which has a steeper EIV test statistic characteristic than the critical satellite**. If no satellite has a steeper EIV TS characteristic than the Critical Satellite, $\text{Vslope}(2)$ equals the second highest slope on the LSR characteristic.

 The next few steps are quite complicated, and require detailed explanation through the following statements:

- The total allowable false alarm rate is driven by the specification P_{FA} ;
- An alarm can be generated in one of two ways:
 - By the \sqrt{USSE} ' Threshold and H/e Threshold both being exceeded simultaneously; or
 - By the Backstop Threshold being exceeded.
- The \sqrt{USSE} ' Test Statistic has a χ^2 distribution, with N-4 degrees of freedom;
- The H/e Test Statistic has a Half-Normal distribution;
- In order to set the \sqrt{USSE} ' and H/e thresholds correctly, we must find values that meet the following constraints:
 - $[\sqrt{USSE}' \text{ Threshold} \times V_{\text{slope(max)}}] = [\text{H/e Threshold} \times \text{EIV_Critical_Characteristic}]$;
 - The combined probability of false alarm (taking into account the probability of exceeding the Backstop Threshold) is equal to P_{FA} . Thus, P_{FA} has two components:
 - The probability of the \sqrt{USSE} ' Threshold being exceed (P_{subUSSE}) and H/e Threshold being exceeded ($P_{H/e}$) occurring simultaneously
 = $[P_{\text{subUSSE}} \times P_{H/e}]$;
 - The probability of the Backstop being exceeded without the $P_{H/e}$ threshold being exceeded (otherwise an alarm would already have occurred)
 = $[(1 - P_{H/e}) \times P_{\text{Backstop}}]$,
 - The value of P_{subUSSE} can therefore be found by solving⁹ the following convoluted expression for $F(x) = 0$:

$$F(x) = P_{FA} - (x \times P_{H/e}) - ((1 - P_{H/e}) \times P_{\text{Backstop}})$$

⁹ NB This function requires a robust numerical method. The nature of the function changes significantly as the observation geometry changes, and is itself worthy of further investigation. For this thesis a modified version of a Brent solver was used in the C++ and Matlab implementations of this algorithm, with bespoke subroutines added to cater for conditions when the Backstop factor was either insignificant or dominant.

Equation 10-13

Given that:

$$P_{H/e} = 2 \times \text{normcdf} \left(\frac{\text{Vslope}(\text{max}) \times (\text{chi2inv}(1-x, N-4))^{1/2}}{\text{EIV_TS_sigma} \times \text{EIV_critical_characteristic}} \right)$$

Equation 10-14

Where “normcdf” represents the cumulative density function of the Normal Distribution and “chi2inv” represents the inverse of the χ^2 cumulative distribution function.

Having found the required probabilities for the two EIV RAIM detection thresholds to be exceeded in order to meet the required P_{FA} specification, the detection thresholds are readily found:

- $\sqrt{\text{USSE}'_Threshold} = (\text{chi2inv}(1 - P_{\text{subUSSE}'}, N-4))^{1/2}$
- $\text{EIV_H_over_e_Threshold} = \text{EIV_TS_sigma} \times \text{abs}(\text{norminv}(P_{H/e} / 2))$
- $\text{Backstop} = (\text{chi2inv}(1 - P_B, N-4))^{1/2}$

10.7.4 Calculate the VPL

This function requires an iterative process to determine the EIV worst case bias, i.e. the bias which, if applied to the Critical Satellite, would generate a missed detection probability equal to the specified P_{MD} . The process is described algorithmically in Section 10.6.

The VPL calculated by evaluating the worst case bias on the $\sqrt{\text{USSE}'}$ threshold is then compared with the VPL arising from the Backstop threshold. The larger of the two values is returned as the Vertical protection Limit.

10.7.5 Calculate Fault Detection State

The fault detection logic for the algorithm now becomes:

- If $[(\sqrt{\text{USSE}'} > \sqrt{\text{USSE}'_Threshold}) \text{ AND } ((\| \mathbf{H}_{\text{tls}} \|_F / \| \mathbf{e}_{\text{tls}} \|) > \text{EIV_H_over_e_Threshold})]$ OR $(\sqrt{\text{USSE}'} > \text{Backstop})$ then declare an alarm.

11. NUMERICAL EXAMPLES FOR LSR AND EIV METHODS

This section presents a numerical example of the calculation of Vertical Protection Limit, detection thresholds and test statistics for the Least Squares Residuals and Errors in Variables RAIM methods previously described. The condition analysed is that of a Galileo-only constellation¹⁰, with a UERE characteristic as defined in Section 7.1.2.

The input conditions are:

- Latitude 52°, Longitude 0°;
- Time = 100 mins;
- 10° Masking Angle;
- $P_{FA} = 8 \times 10^{-6}$;
- $P_{MD} = 0.0004$.

This leads to the user-satellite visibility geometry shown in Table 11-1.

Sat ID	North	East	Up	Elev (Deg)	UERE (m)
GS20	0.0147	0.1871	0.9822	79.2	0.79
GS19	0.2021	-0.6081	0.7677	50.2	0.8
GS1	-0.1998	0.6385	0.7432	48.0	0.805
GS21	-0.1713	0.8362	0.5210	31.4	0.83
GS2	0.5640	0.6527	0.5058	30.4	0.83
GS9	-0.8459	0.2739	0.4575	27.2	0.85
GS12	0.2311	-0.8812	0.4124	24.4	0.88
GS13	-0.5035	-0.8239	0.2601	15.1	0.96
GS11	0.8429	-0.4804	0.2426	14.0	0.99

Table 11-1: Satellite Visibility and UERE

11.1 Calculate LSR VPL

The Observation Matrix (**G**) is easily formed by augmenting the columns containing the North, East and Up components of the unit direction vectors with a column of ones to represent the existence of an unknown user clock offset.

¹⁰ For clarity a case with only 9 satellites in view has been chosen. A combined Galileo/GPS constellation would have around twice as many satellites in view, making the example more complicated to demonstrate.

$$\mathbf{K} = \begin{bmatrix} 0.0111 & 0.0672 & -0.0779 & -0.0397 & 0.3559 & -0.4313 & 0.0586 & -0.2506 & 0.3067 \\ -0.0671 & -0.2713 & 0.1500 & 0.2709 & 0.2655 & 0.0522 & -0.2148 & -0.1727 & -0.0127 \\ 1.0627 & 0.7031 & 0.2671 & -0.3521 & -0.3512 & -0.3234 & -0.1303 & -0.3924 & -0.4836 \\ -0.4783 & -0.2696 & -0.0327 & 0.3115 & 0.3097 & 0.2972 & 0.1849 & 0.3184 & 0.3590 \end{bmatrix}$$

The absolute values of the highlighted terms on the third row are the elements $|\mathbf{K}_{3i}|$ that appear in Equation 8-13. Similarly, as from Equation 9-4,

$$\mathbf{P} = \mathbf{G.K} =$$

$$\begin{bmatrix} \mathbf{0.5532} & 0.3712 & 0.2566 & 0.0157 & 0.0197 & -0.0171 & 0.0175 & -0.1030 & -0.1139 \\ 0.3807 & \mathbf{0.4487} & 0.0654 & -0.1316 & -0.0494 & -0.0701 & 0.2273 & 0.0715 & 0.0574 \\ 0.2665 & 0.0663 & \mathbf{0.2772} & 0.2307 & 0.1471 & 0.1763 & -0.0608 & -0.0335 & -0.0698 \\ 0.0174 & -0.1417 & 0.2453 & \mathbf{0.3614} & 0.2878 & 0.2462 & -0.0727 & 0.0124 & 0.0439 \\ 0.0217 & -0.0531 & 0.1564 & 0.2878 & \mathbf{0.5061} & -0.0756 & 0.0118 & -0.1342 & 0.2791 \\ -0.0198 & -0.0791 & 0.1965 & 0.2582 & -0.0793 & \mathbf{0.5283} & 0.0169 & 0.3035 & -0.1253 \\ 0.0218 & 0.2750 & -0.0727 & -0.0817 & 0.0132 & 0.0181 & \mathbf{0.3339} & 0.2508 & 0.2416 \\ -0.1521 & 0.1030 & -0.0476 & 0.0166 & -0.1795 & 0.3872 & 0.2985 & \mathbf{0.4848} & 0.0892 \\ -0.1789 & 0.0879 & -0.1056 & 0.0624 & 0.3970 & -0.1699 & 0.3058 & 0.0949 & \mathbf{0.5063} \end{bmatrix}$$

The terms on the leading diagonal are elements \mathbf{P}_{ii} which also appear in Equation 9-6. Thus, for each satellite in view, the value of V_{slope} can be evaluated as follows:

SV	\mathbf{K}_{3i}	\mathbf{P}_{ii}	Slope
GS20	1.063	0.553	1.256
GS19	0.703	0.449	0.758
GS1	0.267	0.277	0.253
GS21	-0.352	0.361	0.366
GS2	-0.351	0.506	0.415
GS9	-0.323	0.528	0.400
GS12	-0.130	0.334	0.140
GS13	-0.392	0.485	0.525
GS11	-0.484	0.506	0.681

The satellite most sensitive to a bias is clearly GS20, which sets the value of maximum slope, $V_{\text{slope(max)}}$, to 1.256.

We now have all the information required to calculate the LSR VPL which is available from the satellite geometry. However, in order to calculate VPL we also need the factors $T(N, P_{FA})$ and $k(P_{MD})$ which appear in Equation 9-6. As previously discussed, these are functions of

the number of satellites in view, the required false alarm rate, and the acceptable missed detection probability.

Taking the false alarm probability specified for both Cat I and APV II specifications of 8×10^{-6} , with 9 satellites in view, $T(N, P_{FA}) = 5.60$. This is the detection threshold for the LSR RAIM algorithm.

Assuming a missed detection probability of 4×10^{-4} (see Section 7.5 for a discussion on the setting of this parameter), $k(P_{MD})$ is found from an inverse of the normal distribution for this probability level, $k(P_{MD}) = 3.353$.

$$\text{LSR RAIM VPL} = (1.256 \times 5.598) + (3.353 \times 1.303) = \underline{\underline{11.40 \text{ m}}}$$

Figure 12-15 in Section 12.2.1.1 shows the Navigation Engine configured for a simulation of this case, which confirms the VPL calculated above.

11.2 Calculate LSR Test Statistic

Consider a case in which a 6m bias exists on the measurement on satellite GS20, with all other observations being normal. A typical set of measurement residuals might be:

Satellite	Residual (m)
GS20	6.82
GS19	0.50
GS1	0.59
GS21	0.14
GS2	-0.68
GS9	0.28
GS12	-0.79
GS13	1.34
GS11	-0.80

Table 11-2: Example set of pseudorange residual errors

These residuals are arranged into the vector \mathbf{y} .

As shown in Equation 9-5, the LSR Weighed Sum of Squared Errors is equal to $\mathbf{y}^T \cdot \mathbf{W} \cdot (\mathbf{I} - \mathbf{P}) \cdot \mathbf{y}$

Subtracting the **P** matrix from an Identity matrix:

$$(\mathbf{I-P}) = \begin{bmatrix}
 0.4468 & -0.3712 & -0.2566 & -0.0157 & -0.0197 & 0.0171 & -0.0175 & 0.1030 & 0.1139 \\
 -0.3807 & 0.5513 & -0.0654 & 0.1316 & 0.0494 & 0.0701 & -0.2273 & -0.0715 & -0.0574 \\
 -0.2665 & -0.0663 & 0.7228 & -0.2307 & -0.1471 & -0.1763 & 0.0608 & 0.0335 & 0.0698 \\
 -0.0174 & 0.1417 & -0.2453 & 0.6386 & -0.2878 & -0.2462 & 0.0727 & -0.0124 & -0.0439 \\
 -0.0217 & 0.0531 & -0.1564 & -0.2878 & 0.4939 & 0.0756 & -0.0118 & 0.1342 & -0.2791 \\
 0.0198 & 0.0791 & -0.1965 & -0.2582 & 0.0793 & 0.4717 & -0.0169 & -0.3035 & 0.1253 \\
 -0.0218 & -0.2750 & 0.0727 & 0.0817 & -0.0132 & -0.0181 & 0.6661 & -0.2508 & -0.2416 \\
 0.1521 & -0.1030 & 0.0476 & -0.0166 & 0.1795 & -0.3872 & -0.2985 & 0.5152 & -0.0892 \\
 0.1789 & -0.0879 & 0.1056 & -0.0624 & -0.3970 & 0.1699 & -0.3058 & -0.0949 & 0.4937
 \end{bmatrix}$$

$$(\mathbf{I-P})\mathbf{y} = \begin{bmatrix}
 2.787 \\
 -2.224 \\
 -1.466 \\
 -0.013 \\
 -0.158 \\
 -0.393 \\
 -0.898 \\
 1.778 \\
 1.268
 \end{bmatrix}$$

$$\mathbf{W}(\mathbf{I-P})\mathbf{y} = \begin{bmatrix}
 4.466 \\
 -3.475 \\
 -2.262 \\
 -0.019 \\
 -0.230 \\
 -0.543 \\
 -1.159 \\
 1.929 \\
 1.294
 \end{bmatrix}$$

Therefore $\mathbf{y}^T \cdot \mathbf{W} \cdot (\mathbf{I-P}) \cdot \mathbf{y} = \text{WSSE} = 29.85$

Hence the LSR RAIM Test Statistic, $\sqrt{WSSE} = \sqrt{29.85} = 5.46$

Since this is less than the detection threshold calculated for this case (5.60), this would not generate an alarm.

11.3 EIV Method

Setting the detection thresholds, and hence evaluating the protection limits, using the EIV method requires repetition of the same process that is used to calculate the test statistic for a set of measurements. Therefore in this worked example we shall first calculate the test statistics, and then calculate the thresholds and VPL.

11.3.1 Define Weighting Matrices

Set the **C** matrix to be equal to the square root of the **W** matrix:

$$\mathbf{C} = \begin{bmatrix} 1.266 & 0 & 0 & 0 & 0 & 0 & 0 & 0 \\ 0 & 1.250 & 0 & 0 & 0 & 0 & 0 & 0 \\ 0 & 0 & 1.242 & 0 & 0 & 0 & 0 & 0 \\ 0 & 0 & 0 & 1.205 & 0 & 0 & 0 & 0 \\ 0 & 0 & 0 & 0 & 1.205 & 0 & 0 & 0 \\ 0 & 0 & 0 & 0 & 0 & 1.176 & 0 & 0 \\ 0 & 0 & 0 & 0 & 0 & 0 & 1.136 & 0 \\ 0 & 0 & 0 & 0 & 0 & 0 & 0 & 1.042 \\ 0 & 0 & 0 & 0 & 0 & 0 & 0 & 0 \\ 0 & 0 & 0 & 0 & 0 & 0 & 0 & 0 \\ 0 & 0 & 0 & 0 & 0 & 0 & 0 & 0 \\ 0 & 0 & 0 & 0 & 0 & 0 & 0 & 0 \\ 0 & 0 & 0 & 0 & 0 & 0 & 0 & 0 \\ 0 & 0 & 0 & 0 & 0 & 0 & 0 & 0 \\ 0 & 0 & 0 & 0 & 0 & 0 & 0 & 1.010 \end{bmatrix}$$

Next, define a **D** matrix. In this example, the matrix below has been used:

$$\mathbf{D} = \begin{bmatrix} 1 & 0 & 0 & 0 & 0 & 0 \\ 0 & 1 & 0 & 0 & 0 & 0 \\ 0 & 0 & 1 & 0 & 0 & 0 \\ 0 & 0 & 0 & 0.07 & 0 & 0 \\ 0 & 0 & 0 & 0 & 0.00085 & 0 \end{bmatrix}$$

11.3.2 Calculate the EIV Test Statistics

Using the same **y** matrix as was defined above, the augmented matrix becomes:

$$C[Gy]D = \begin{bmatrix} 0.0186 & 0.2368 & 1.2433 & 0.0886 & 7.33E-03 \\ 0.2526 & -0.7601 & 0.9597 & 0.0875 & 5.29E-04 \\ -0.2482 & 0.7932 & 0.9232 & 0.0870 & 6.21E-04 \\ -0.2063 & 1.0075 & 0.6277 & 0.0843 & 1.48E-04 \\ 0.6795 & 0.7864 & 0.6094 & 0.0843 & -6.96E-04 \\ -0.9952 & 0.3222 & 0.5383 & 0.0824 & 2.82E-04 \\ 0.2627 & -1.0013 & 0.4687 & 0.0795 & -7.64E-04 \\ -0.5244 & -0.8583 & 0.2709 & 0.0729 & 1.19E-03 \\ 0.8514 & -0.4852 & 0.2450 & 0.0707 & -6.83E-04 \end{bmatrix}$$

Undertake Singular Value Decomposition, and produce \mathbf{U} , $\mathbf{\Sigma}$ and \mathbf{V} matrices:

$$\mathbf{U} = \begin{bmatrix} 0.3996 & 0.4069 & -0.0106 & -0.4788 & -0.6446 \\ -0.0087 & 0.6111 & -0.0193 & -0.2723 & 0.5095 \\ 0.5121 & 0.0975 & -0.0650 & -0.0338 & 0.3334 \\ 0.5012 & -0.0709 & 0.0100 & 0.3242 & 0.0021 \\ 0.3672 & 0.0819 & 0.5106 & 0.3225 & 0.0342 \\ 0.3106 & 0.0060 & -0.5759 & 0.3167 & 0.0838 \\ -0.2143 & 0.4959 & -0.0291 & 0.2034 & 0.1862 \\ -0.1680 & 0.2945 & -0.4723 & 0.3823 & -0.3398 \\ -0.1462 & 0.3272 & 0.4230 & 0.4455 & -0.2354 \end{bmatrix}$$

$$\mathbf{\Sigma} = \begin{bmatrix} 2.3915 & 0 & 0 & 0 & 0 \\ 0 & 2.0491 & 0 & 0 & 0 \\ 0 & 0 & 1.5896 & 0 & 0 \\ 0 & 0 & 0 & 0.0876 & 0 \\ 0 & 0 & 0 & 0 & 0.00464 \end{bmatrix}$$

$$\mathbf{V} = \begin{bmatrix} -0.1579 & 0.2227 & 0.9620 & 0.0005 & -0.0008 \\ 0.7656 & -0.5876 & 0.2617 & 0.0114 & -0.0006 \\ 0.6210 & 0.7727 & -0.0769 & -0.1064 & 0.0066 \\ 0.0579 & 0.0895 & -0.0117 & 0.9933 & -0.0426 \\ 0.0013 & 0.0015 & -0.0009 & -0.0430 & -0.9991 \end{bmatrix}$$

Therefore the $\sqrt{\text{USSE}}$ Test Statistic, $|(\sigma_5 / d_5 V_{55})| =$

$$|0.00464 / (0.00085 * -0.9991)| = \underline{\underline{5.46}}$$

which, as expected, is the same as the LSR $\sqrt{\text{WSSE}}$ test statistic.

From Equation 10-4, $[\mathbf{H}_{\text{tls}} \ \mathbf{e}_{\text{tls}}] = -\sigma_5 \mathbf{C}^{-1} \mathbf{U}_5 [\mathbf{V}_{15}^T \ \mathbf{V}_{55}^T] \mathbf{D}^{-1}$

$$[\mathbf{H}_{\text{tls}} \ \mathbf{e}_{\text{tls}}] = \begin{bmatrix} 1.87\text{E-}06 & 1.37\text{E-}06 & -1.57\text{E-}05 & 1.44\text{E-}03 & 2.777 \\ -1.50\text{E-}06 & -1.10\text{E-}06 & 1.26\text{E-}05 & -1.15\text{E-}03 & -2.223 \\ -9.86\text{E-}07 & -7.23\text{E-}07 & 8.27\text{E-}06 & -7.57\text{E-}04 & -1.464 \\ -6.48\text{E-}09 & -4.75\text{E-}09 & 5.43\text{E-}08 & -4.97\text{E-}06 & -0.010 \\ -1.04\text{E-}07 & -7.65\text{E-}08 & 8.74\text{E-}07 & -8.00\text{E-}05 & -0.155 \\ -2.62\text{E-}07 & -1.92\text{E-}07 & 2.20\text{E-}06 & -2.01\text{E-}04 & -0.389 \\ -6.02\text{E-}07 & -4.42\text{E-}07 & 5.05\text{E-}06 & -4.62\text{E-}04 & -0.894 \\ 1.20\text{E-}06 & 8.79\text{E-}07 & -1.01\text{E-}05 & 9.20\text{E-}04 & 1.779 \\ 8.56\text{E-}07 & 6.28\text{E-}07 & -7.18\text{E-}06 & 6.58\text{E-}04 & 1.271 \end{bmatrix}$$

- $\|\mathbf{H}_{\text{tls}}\|_F$, Frobenius Norm of $\mathbf{H}_{\text{tls}} = 0.00235$
- $\|\mathbf{e}_{\text{tls}}\|$, Vector Norm of $\mathbf{e}_{\text{tls}} = 4.533$

Therefore, the **H/e Test Statistic** = $0.00235 / 4.533 = \underline{\underline{5.18 \times 10^{-4}}}$

11.3.3 Calculate the H/e Standard Deviation

The first step needs to be performed separately for each satellite in view. Only a single example (for satellite GS20) is presented here.

- Produce a vector \mathbf{q} , which is a null vector, except for the term relating to the satellite in question, which is set to 20;
- Produce the Augmented Matrix $\mathbf{C[Gq]D}$

$$\mathbf{C[Gq]D} = \begin{bmatrix} 0.0186 & 0.2368 & 1.2433 & 0.0886 & 2.15E-02 \\ 0.2526 & -0.7601 & 0.9597 & 0.0875 & 0.00E+00 \\ -0.2482 & 0.7932 & 0.9232 & 0.0870 & 0.00E+00 \\ -0.2063 & 1.0075 & 0.6277 & 0.0843 & 0.00E+00 \\ 0.6795 & 0.7864 & 0.6094 & 0.0843 & 0.00E+00 \\ -0.9952 & 0.3222 & 0.5383 & 0.0824 & 0.00E+00 \\ 0.2627 & -1.0013 & 0.4687 & 0.0795 & 0.00E+00 \\ -0.5244 & -0.8583 & 0.2709 & 0.0729 & 0.00E+00 \\ 0.8514 & -0.4852 & 0.2450 & 0.0707 & 0.00E+00 \end{bmatrix}$$

- Decompose using SVD and calculate H/e , as above. In this case $H/e = 0.00145$
- This is the value of the test statistic for a 20m bias. The UERE for this signal is 0.79m. Therefore, the 1σ expectation of H/e test statistic for measurements on this signal = $(0.00145 \times 0.79) / 20 = 5.726 \times 10^{-5}$.
- Repeat for all satellites in view, and arrange results as a vector:

Satellite	$1\sigma H/e$
GS20	5.726E-05
GS19	3.289E-05
GS1	4.087E-06
GS21	3.948E-05
GS2	3.895E-05
GS9	3.817E-05
GS12	2.477E-05
GS13	4.602E-05
GS11	5.340E-05

- Calculate the norm of this vector, = 1.204×10^{-4} . This is the estimate of the **standard deviation of the H/e Test Statistic**.

11.3.4 Calculate the Detection Thresholds

- Produce the H/e Test Statistic Characteristic, and calculate the slope of the characteristic of the Critical Satellite (GS20). NB This can be performed in parallel with the previous step by utilising the fact that the vertical error induced by a 20m bias on observation i is equal to K_{3i} . Therefore the slope for GS20 = $(20 \times 1.0627)/0.00145 = 14,660$. This is the **EIV Critical Characteristic**.
- Identify the satellite on which the Backstop Threshold should be applied. GSAS19 and GSAS1 both have H/e characteristics steeper than that of GS20. Of these, GSAS19 has the steepest $\sqrt{\text{USSE}}$ characteristic slope (equal to 0.758, as found above in the LSR method)

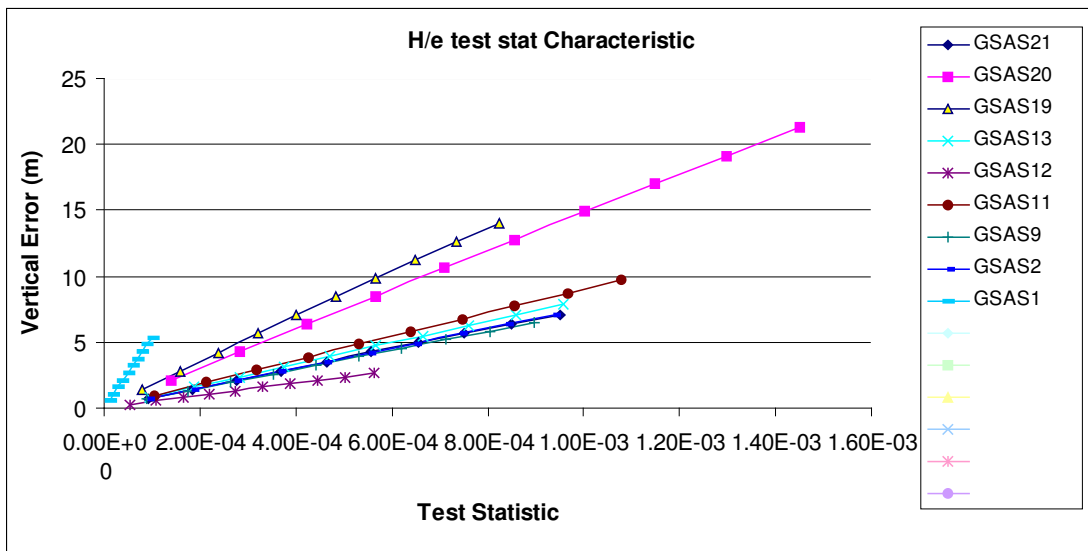


Figure 11-1: H/e Test Statistic for Worked Example

- The next step requires an iterative solution of Equation 10-13 and Equation 10-14, using an appropriate numerical method. This is best explained by stepping through the derived solution:
 - Assume that the required probability of exceeding the $\sqrt{\text{USSE}}$ Detection Threshold = 3.05×10^{-3} ;
 - With 9 satellites in view, therefore 5 degrees of freedom, the square root of the χ^2 distribution at this probability is:
$$\sqrt{\text{USSE}} \text{ Detection Threshold} = 4.233$$
 - From the LSR method, $V_{\text{slope(max)}} = 1.256$. Therefore the component of VPL that would derived from a threshold of 4.233 is:
$$\sqrt{\text{USSE}} \text{ VPL Component} = 4.233 \times 1.256 = 5.31 \text{ m}$$

- Because the $\sqrt{\text{USSE}}$ characteristic slope of the Backstop satellite is not very close to that of the Critical Satellite, assume that the Backstop Threshold can be set to correspond to 1% of the desired P_{FA} , i.e. $P_{\text{Backstop}} = 8 \times 10^{-8}$. With 5 degrees of freedom, the Backstop Threshold is calculated to be 6.43. Multiplying this by the $\sqrt{\text{USSE}}$ characteristic slope of the Backstop satellite, 0.758, yields:

$$\text{Backstop VPL Component} = 4.88 \text{ m}$$

- The probability of exceeding the H/e threshold is therefore required to be $(8 \times 10^{-6} - 8 \times 10^{-8}) / 3.05 \times 10^{-3} = 2.60 \times 10^{-3}$. This equates to 3.01 standard deviations on a Half-Normal distribution;
- Given the H/e Test Statistic Standard Deviation = 1.204×10^{-4} , the Threshold associated with this probability is

$$\text{H/e Detection Threshold} = 1.204 \times 10^{-4} \times 3.01 = \mathbf{3.624 \times 10^{-4}}$$

- The component of VPL that would derived from this threshold of 4.233 is:

$$\text{H/e VPL Component} = 3.624 \times 10^{-4} \times 14660 = \mathbf{5.31 \text{ m.}}$$

Therefore, the system is balanced with a H/e Detection Threshold of 3.624×10^{-4} , a $\sqrt{\text{USSE}}$ Detection Threshold of 4.233 and a Backstop Threshold of 6.43.

11.3.5 Calculate the EIV VPL

As with calculating the detection thresholds, setting the VPL is an iterative process that is easiest demonstrated by starting with the solution and working backwards.

- Assume that the Worst Case Bias on the Critical Satellite = 7.0m;
- Multiplying this by the k_{3i} term for the critical satellite gives the vertical error, in the absence of any noise on this or any other satellite, which would be induced: $7.0 \times 1.0627 = 7.439\text{m}$;
- Given the $\sqrt{\text{USSE}}$ Slope for this satellite = 1.256, the test statistic that would be induced is $7.439 / 1.256 = 5.923$;
- When noise is added to the signals, the residuals will have a non-central χ^2 distribution with non-centrality parameter λ equal to

$$5.923^2 = 35.08$$

- With a $\sqrt{\text{USSE}}$ Detection Threshold of 4.233, the χ^2 test threshold is $4.233^2 = 17.918$;
- With 5 degrees of freedom, $\lambda = 35.08$ and $x = 17.92$, the probability of a random sample have a test statistic less than the $\sqrt{\text{USSE}}$ Detection Threshold is 0.0183;

- Given the required P_{MD} of 0.0004, the VPL should be set such the probability of exceeding the VPL limit with this applied bias

$$= 0.0004 / 0.0183 = 0.0219;$$
- k_i , the number of standard distributions associated with this probability = 2.02;
- Given $\sigma_v = 1.303$ m, the component of VPL due to the missed detection probability = $2.02 \times 1.303 = 2.63$;
- VPL for this bias is therefore $7.44 + 2.63 = \mathbf{10.07m}$

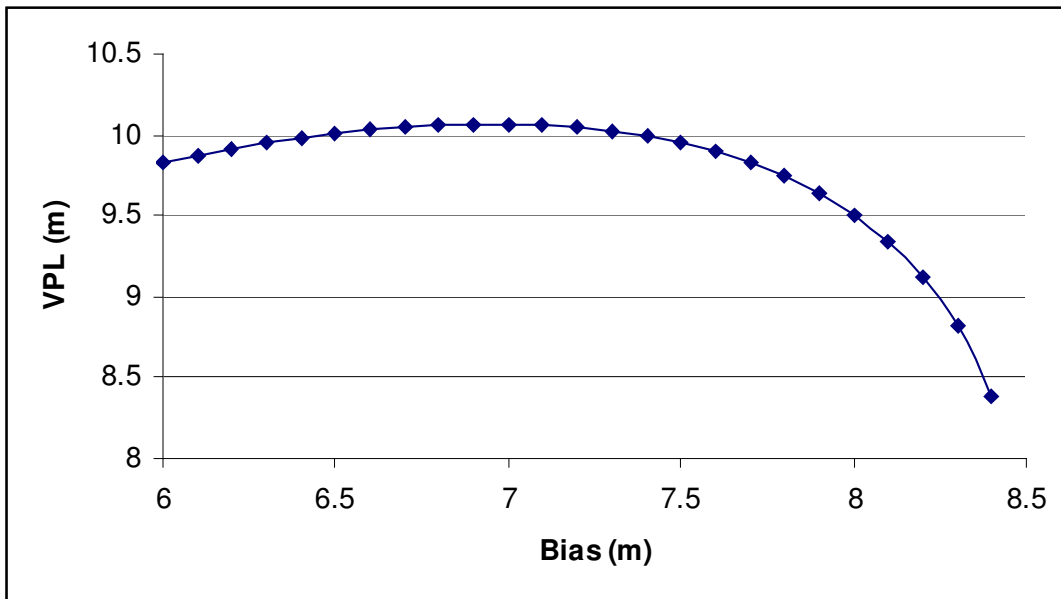


Figure 11-2 : Curve of VPL against Bias for a Fixed P_{MD}

Figure 11-2 shows how results from repeating this process for a range of values of bias, which confirms that the worst case bias in this example is 7.0m.

The VPL returned from this algorithm is therefore **10.07m**.

Note that this is approximately 12% lower than the VPL calculated using the LSR method.

Note also that with a 6m bias applied, the test statistics are 5.46 and 5.18×10^{-4} for \sqrt{USSE} and H/e respectively. These are both greater than the calculated detection thresholds of 4.233 and 3.624×10^{-4} respectively, therefore in this example an alarm would be generated by the EIV algorithm but not by the LSR algorithm, demonstrating the improved detection capability of the EIV method.

12. RAIM EXPERIMENTATION RESULTS

This section provides the results from the RAIM simulation experimentation, under the following headings:

1. Service Volume Simulation Results,
 - LSR and EIV RAIM algorithms
 - Galileo only, with 10° mask angle;
 - Galileo+GPS, with 10° mask angle;
 - Galileo only, with 5° mask angle;
 - Galileo+GPS, with 5° mask angle;
 - Galileo SISA/IF integrity algorithm (WAAS equation, with three critical satellites constraint).
2. Navigation Engine Simulation Results
3. Flight Trials Simulation Results
 - LSR and EIV RAIM algorithms
 - Response to Step Bias Feared Events;
 - Response to Ramp Bias Feared Events;
 - Response with Fault Detection and Exclusion incorporated.

12.1 Service Volume Simulation Results

Initial results from the SVS are presented in the following subsections. The following parameters are common to all SVS runs reported in this section:

- $P_{FA} = 8 \times 10^{-6}$;
- $P_{MD} = 0.0004$;
- Time Step = 2 mins;
- Time steps = 2160 (gives total of 72 hours repeat period);

- Spatial Resolution = 2° in Latitude and 2° in Longitude.

UERE curves as below, shown graphically in Figure 12-1:

Elevation Angle (degrees)	5	10	15	20	30	40	50	60	90
GPS IIF (EUROCAE Baseline) (m)	2.27	1.86	1.71	1.64	1.59	1.57	1.56	1.56	1.56
Galileo Test Case Baseline (m)	1.66	1.14	0.96	0.88	0.83	0.81	0.8	0.79	0.79

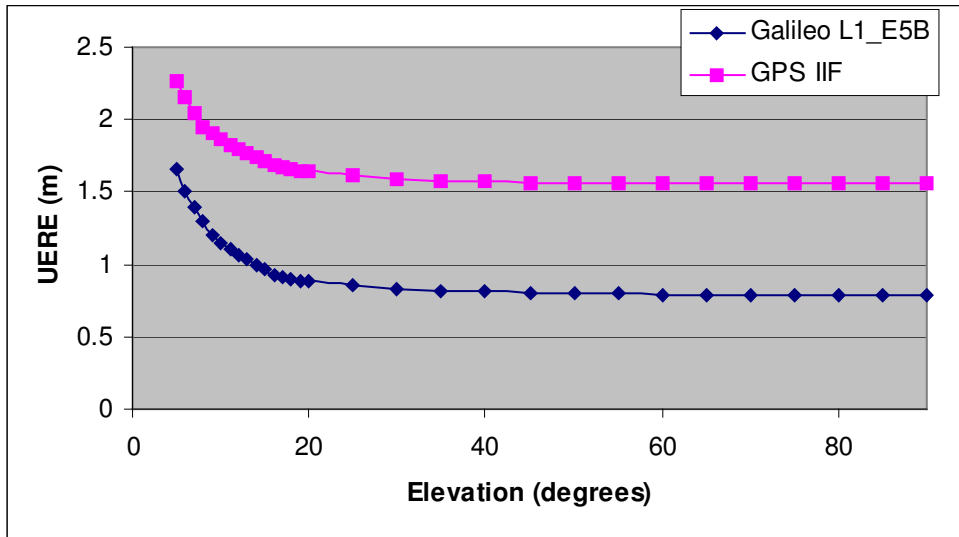


Figure 12-1 : Baseline GPS and Galileo UERE curves for RAIM analysis

For combined Galileo+GPS constellation analysis, the constellations have been configured such that the Galileo planes are co-planar with the GPS planes. This configuration has been demonstrated to be the “worst case” condition taken as a global average and when considering worst-case locations.

For all charts in this section the key representing availability of Integrity to the specified VAL is as presented below:

	99.9% - 100%
	99.5% - 99.9%
	97% - 99.5%
	<97%

Figure 12-2 : Key (RAIM Availability Percentage) for SVS Output Graphs

The availability of RAIM Integrity, at the specified Vertical Alert Limit (VAL) given the conditions specified above are presented in the following sections. In each case, the availability has been calculated three times, covering the cases of all satellites available, one satellite disabled, and two satellites disabled. The state probabilities for these three cases differ depending upon whether it is a Galileo-only case or a Galileo + GPS case, as specified below:

	All satellites available	One disabled	Two disabled
Galileo only	0.98	0.019	0.001
Galileo + GPS	0.96	0.038	0.002

Table 12-1 : Constellation State Probabilities

The availability results from each case are multiplied by the corresponding state probability and then added together to give an overall estimate of the availability of integrity.

For each Vertical Alert Limit used to evaluate availability, results are presented under headings which have the following meanings:

- “Global Average, all OK” – This is the average availability of integrity for the case with no satellites disabled. Note that this is a geographically weighted average, i.e. it takes into account the variation in the actual surface area associated with each spatial measurement (because a 2° x 2° cell close to the equator covers a much greater surface area than a 2° x 2° cell close to the poles);
- “Global Average, One Disabled” – Again, a weighted average, for the case with one satellite removed from the simulation;
- “Global Average, Two Disabled” – Again, a weighted average, with two satellites removed. For the combined constellation cases, this is one GPS satellite and one Galileo satellite;
- “Consolidated Average” – This is the weighted average when the three cases above are combined taking into account the appropriate state probabilities;
- “Minimum Availability” – This is the lowest availability found in any single cell, following consolidation of the three states. The Latitude and Longitude of the central point of this cell is also specified;

- “Minimum in ECAC” – This is the lowest availability found in any single cell, above 30°N Latitude and below 75°N Latitude, following consolidation of the three states. Note that Longitude limits have not been taken into account, since the actual longitude of these results is arbitrary (the constellation parameters have not been fixed relative to any specified ground track).

12.1.1 Galileo Only, LSR RAIM, 10° Masking

Vertical Alert Limit	20m
Global Average, all OK	97.05%
Global Average, One Disabled	90.73%
Global Average, Two Disabled	83.29%
Consolidated Average	96.92%
Minimum Availability	86.47% 71S 141E
Minimum in ECAC	86.56%

Table 12-2 : Galileo only LSR RAIM Availability, 10° Mask

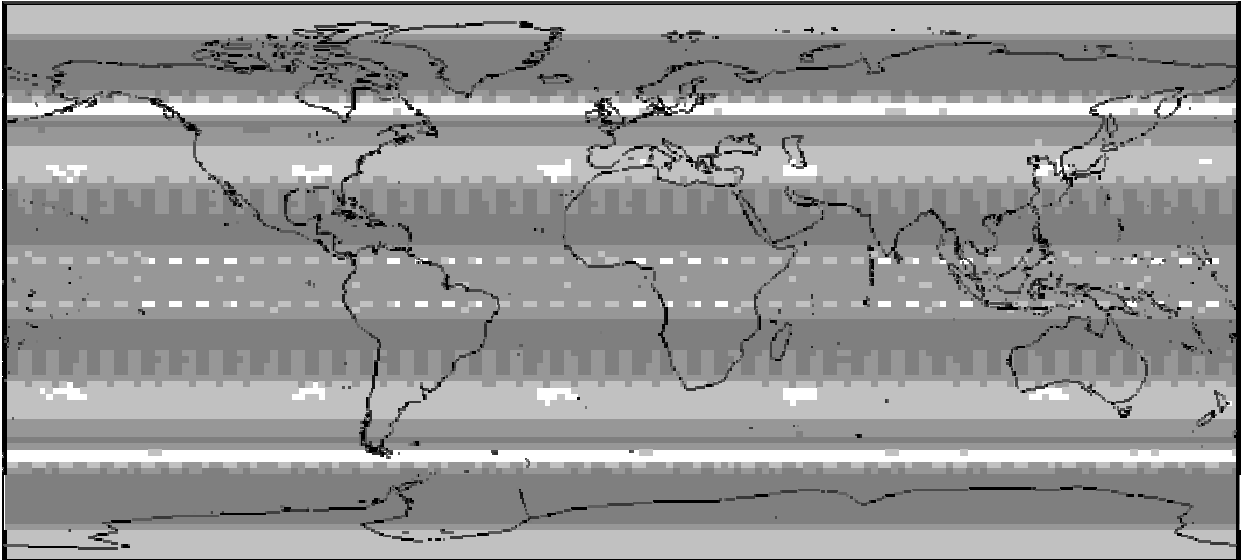


Figure 12-3 : Galileo only, LSR RAIM Availability, 10° Mask, 20m VAL

12.1.2 Galileo Only, EIV RAIM, 10° Masking

Vertical Alert Limit	20m
Global Average, all OK	99.75%
Global Average, One Disabled	95.75%
Global Average, Two Disabled	89.65%
Consolidated Average	99.67%
Minimum Availability	96.78% 28S 161W
Minimum in ECAC	97.99%

Table 12-3 : Galileo only EIV RAIM Availability, 10° Mask

Table 12-3 presents a particularly interesting result, in that the Consolidated Average Availability for the EIV RAIM algorithm at 20m VAL exceeds the availability requirement for the Galileo Safety of Life Service, if the availability requirement is taken to be a global average. If the specification is for the availability requirement to be met at the worst user location (in this case at around 29°N) then the Galileo Safety of Life Service specification cannot be met by EIV RAIM alone.

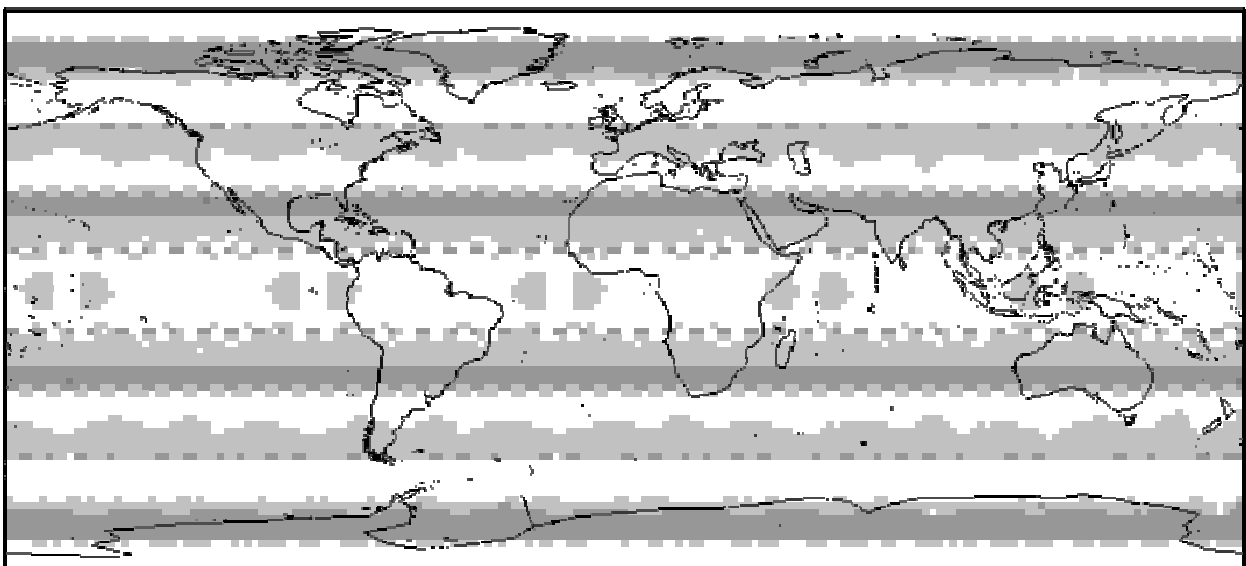


Figure 12-4: Galileo only, EIV RAIM Availability, 10° Mask, 20m VAL

12.1.3 Galileo + GPS, LSR RAIM, 10° Masking

Vertical Alert Limit	20m	15m
Global Average, all OK	99.96%	97.89%
Global Average, One Disabled	99.74%	95.95%
Global Average, Two Disabled	99.59%	95.01%
Consolidated Average	99.95%	97.81%
Minimum Availability	97.48% 69N 135E	95.82% 71N 117E
Minimum in ECAC	97.48%	85.82%

Table 12-4 : Galileo+GPS LSR RAIM Availability, 10° Mask

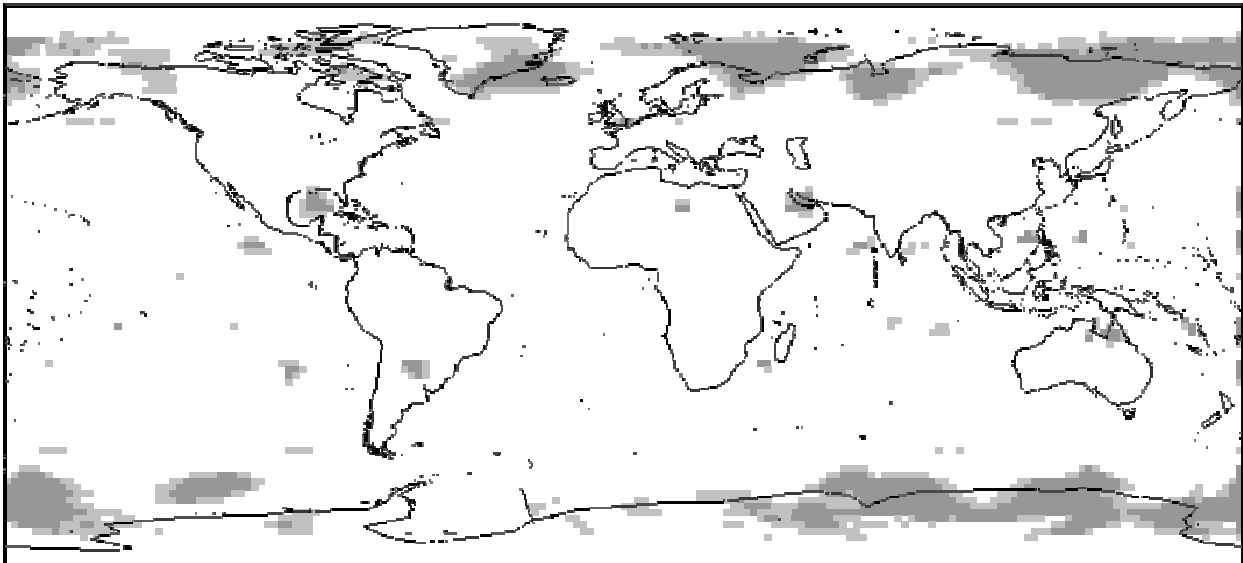


Figure 12-5 : Galileo+GPS LSR RAIM Availability, 10° Mask, 20m VAL

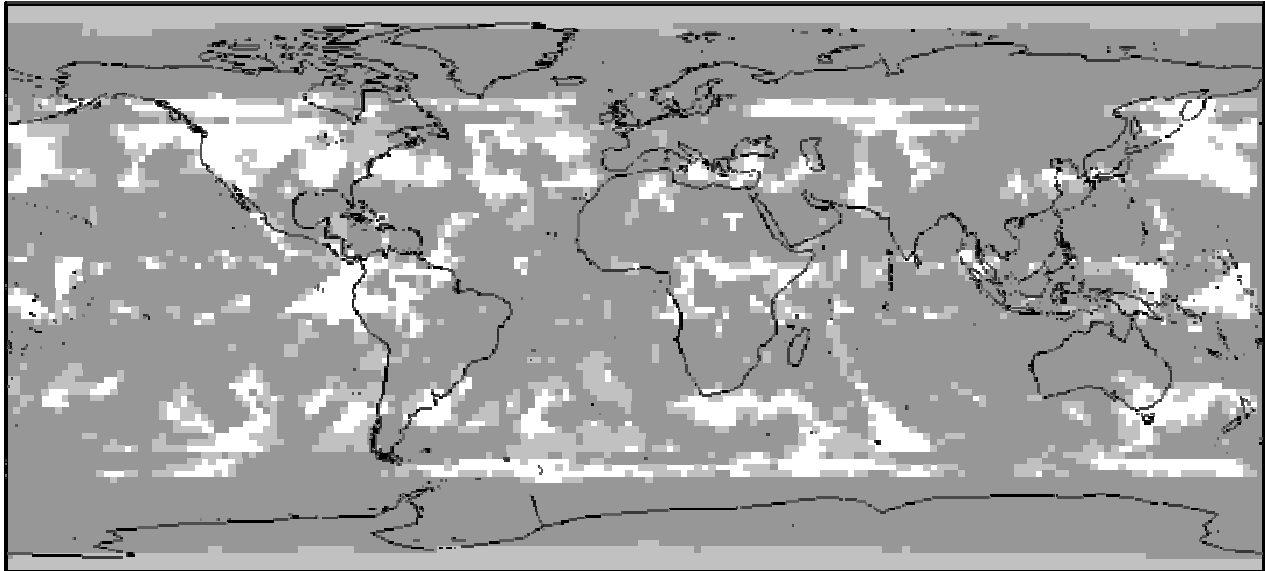


Figure 12-6: Galileo+GPS LSR RAIM Availability, 10° Mask, 15m VAL

12.1.4 Galileo + GPS, EIV RAIM, 10° Masking

Vertical Alert Limit	20m	15m	12m
Global Average, all OK	100%	99.89%	96.23%
Global Average, One Disabled	99.98%	99.40%	92.89%
Global Average, Two Disabled	99.93%	98.70%	90.38%
Consolidated Average	99.999%	99.87%	96.09%
Minimum Availability	99.78% 67S 65E	96.37% 71N 133E	80.97% 85S 13E
Minimum in ECAC	99.80%	96.37%	81.52%

Table 12-5 : Galileo+GPS EIV RAIM Availability, 10° Mask

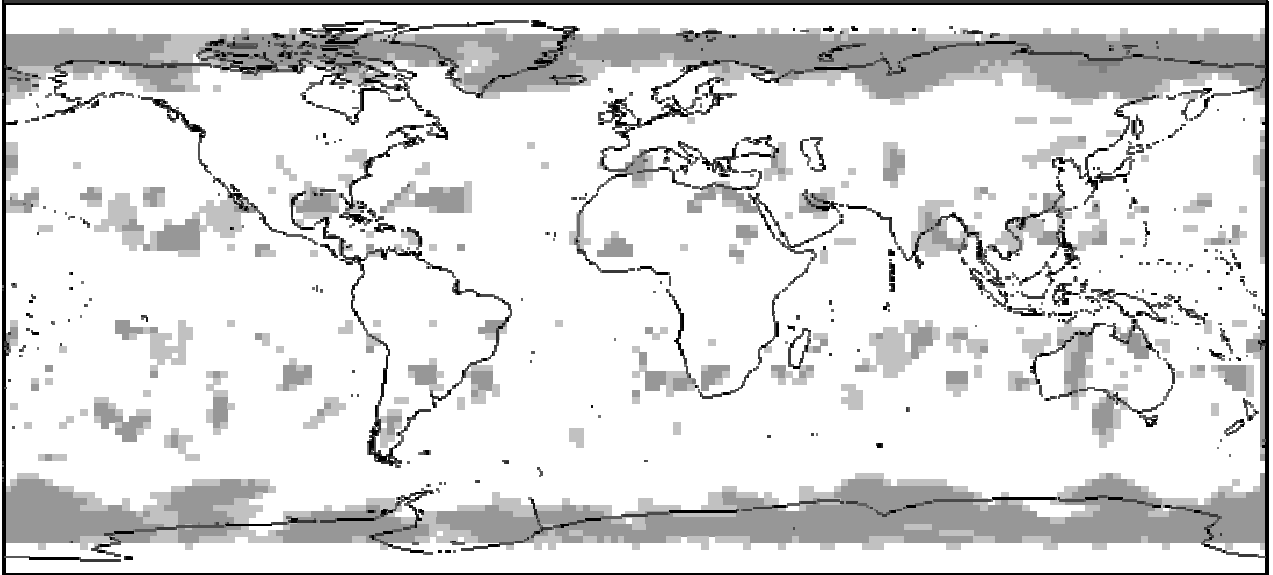


Figure 12-7: Galileo+GPS EIV RAIM Availability, 10° Mask, 15m VAL

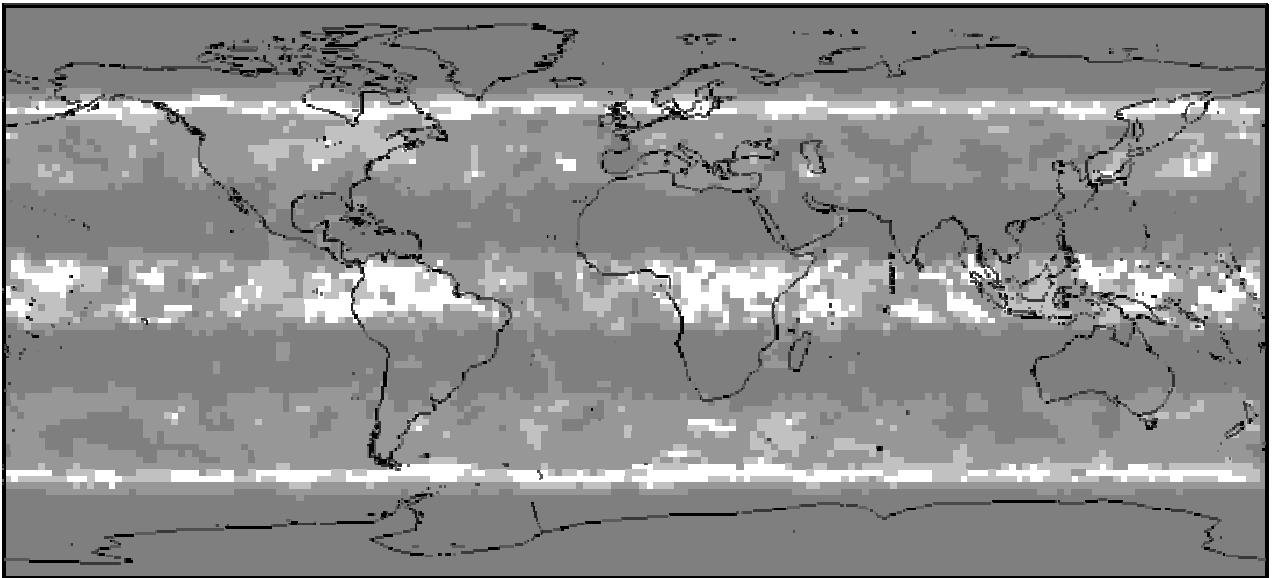


Figure 12-8 : Galileo+GPS EIV RAIM Availability, 10° Mask, 12m VAL

12.1.5 Galileo Only, LSR RAIM, 5° Masking

Vertical Alert Limit	20m	15m
Global Average, all OK	99.96%	91.30%
Global Average, One Disabled	98.07%	85.15%
Global Average, Two Disabled	94.16%	78.64%
Consolidated Average	99.92%	91.17%
Minimum Availability	98.55% 17S 31E	80.50% 71S 63W
Minimum in ECAC	99.36%	80.53%

Table 12-6 : Galileo only LSR RAIM Availability, 5° Mask

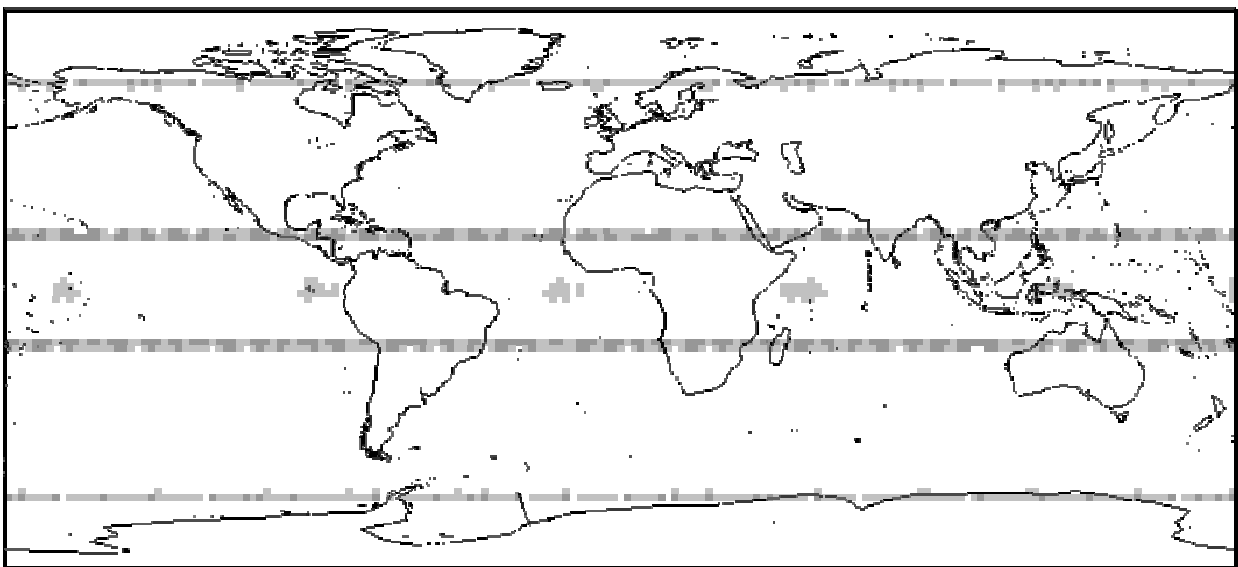


Figure 12-9 : Galileo only, LSR RAIM Availability, 5° Mask, 20m VAL

12.1.6 Galileo Only, EIV RAIM, 5° Masking

Vertical Alert Limit	20m	15m
Global Average, all OK	100%	98.26%
Global Average, One Disabled	99.31%	94.73%
Global Average, Two Disabled	96.53%	89.0%
Consolidated Average	99.98%	98.19%
Minimum Availability	99.94% 23N 67E	91.82% 23N 23W
Minimum in ECAC	99.95%	95.21%

Table 12-7 : Galileo only EIV RAIM Availability, 5° Mask

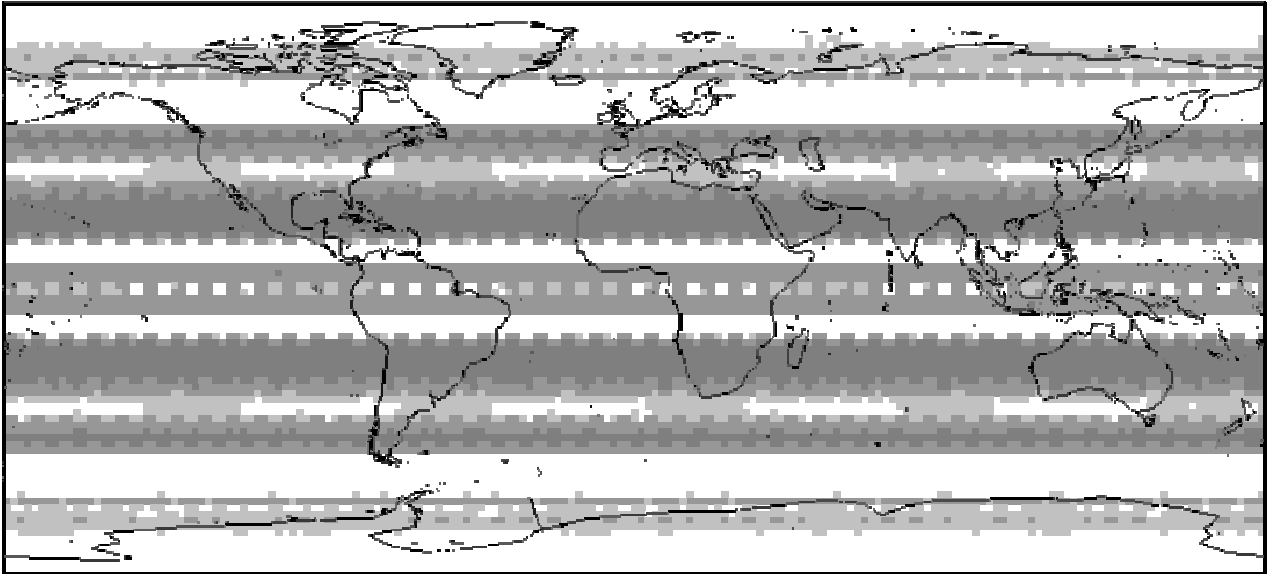


Figure 12-10 : Galileo only, EIV RAIM Availability, 5° Mask, 15m VAL

12.1.7 Galileo + GPS, LSR RAIM, 5° Masking

Vertical Alert Limit	20m	15m	12m
Global Average, all OK	100%	99.97%	95.77%
Global Average, One Disabled	99.98%	99.69%	93.67%
Global Average, Two Disabled	99.97%	99.45%	92.69%
Consolidated Average	99.999%	99.95%	95.68%
Minimum Availability	99.7% 67N 161E	97.88% 69N 139E	78.94% 73N 149W
Minimum in ECAC	99.7%	97.88%	78.94%

Table 12-8 : Galileo + GPS LSR RAIM Availability, 5° Mask

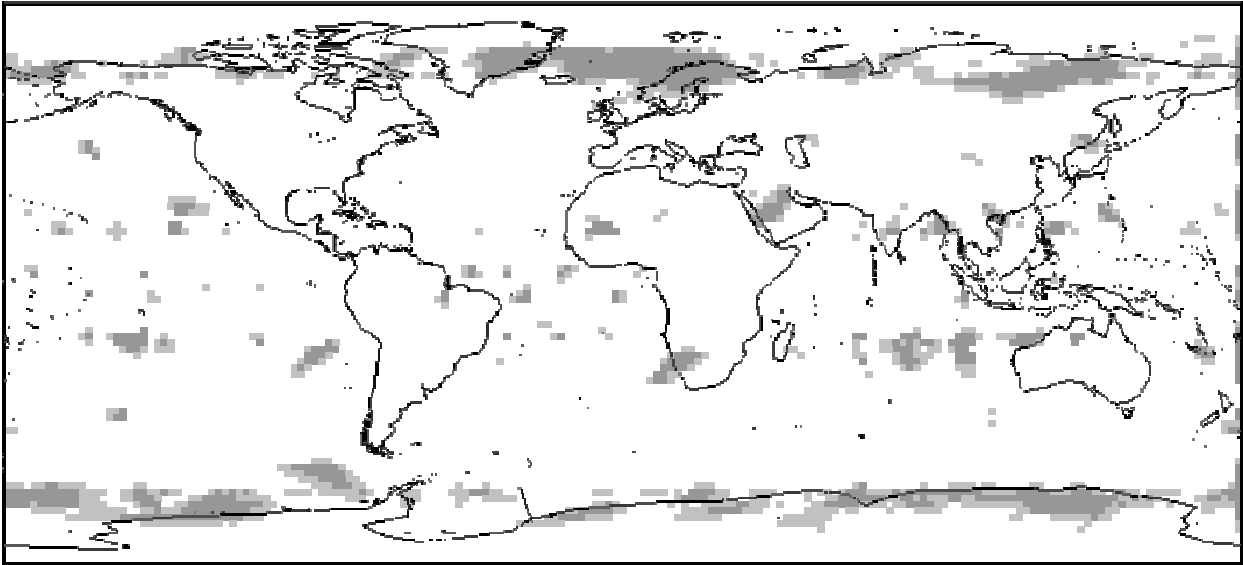


Figure 12-11 : Galileo+GPS LSR RAIM Availability, 5° Mask, 15m VAL

12.1.8 Galileo + GPS, EIV RAIM, 5° Masking

Vertical Alert Limit	20m	15m	12m
Global Average, all OK	100%	100%	99.84%
Global Average, One Disabled	100%	99.97%	99.46%
Global Average, Two Disabled	100%	99.95%	99.21%
Consolidated Average	100%	100%	99.83%
Minimum Availability	100%	99.61% 71S 61E	96.56% 21N 109E
Minimum in ECAC	100%	99.7%	97.05%

Table 12-9 : Galileo + GPS EIV RAIM Availability, 5° Mask

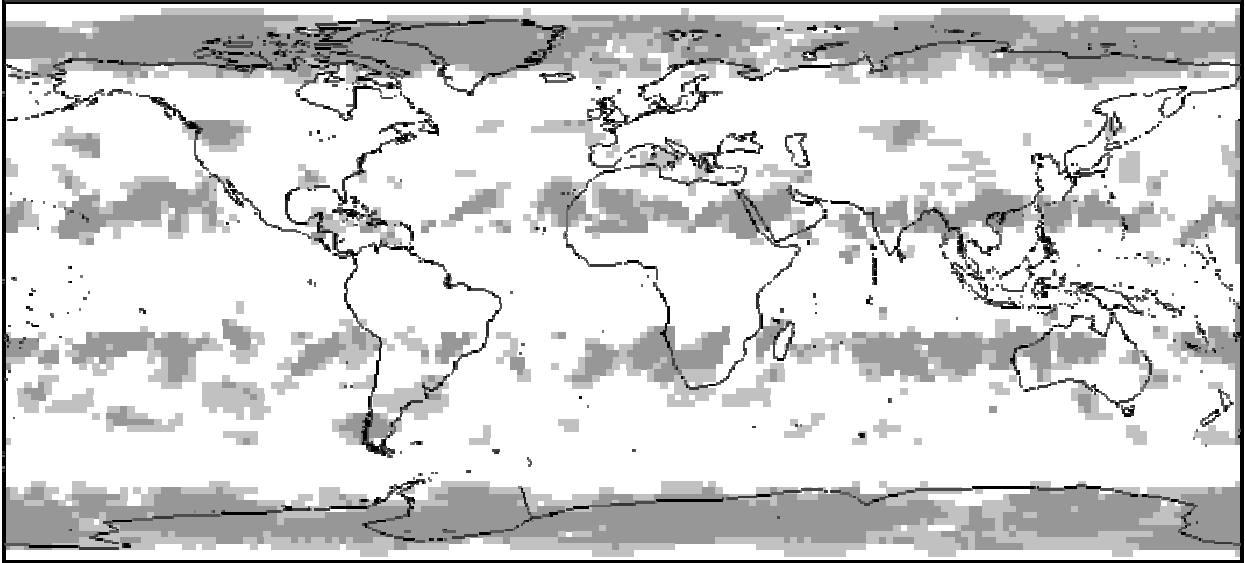


Figure 12-12 : Galileo+GPS EIV RAIM Availability, 5° Mask, 12m VAL

12.1.9 Galileo SISA/IF (WAAS Equation, 3 Critical Satellites), 10° Masking

This section provides results for a Service Volume Simulation performed on an algorithm modelling a simplified form of the Galileo SISA/IF availability function. In this case, availability is defined as:

VPL (calculated as $5.33 * \sigma_v$, as per [15], referred to as the “WAAS Equation”),

And

No more than 3 “Critical Satellites”, where such a satellite is defined as:

“If a satellite in view above the specified masking angle would, if removed from navigation solution, cause the VPL to exceed the VAL it is classified as a Critical Satellite”.

NB This is not the definitive Galileo SISA/IF availability algorithm; however, it is the working assumption taken at the time of this experimentation.

Vertical Limit	Alert	20m	15m	12m
Global Average, all OK		100%	99.93%	89.81%
Global Average, One Disabled		99.84%	98.11%	85.95%
Global Average, Two Disabled		97.95%	95.02%	80.88%
Consolidated Average		99.99%	99.89%	89.72%
Minimum Availability		99.97% 19N 115 E	97.89% 11N 7E	76.3% 23N 71E
Minimum in ECAC		99.98%	99.92%	78.07%

Table 12-10 : Galileo only SISA/IF Availability, 10° Mask

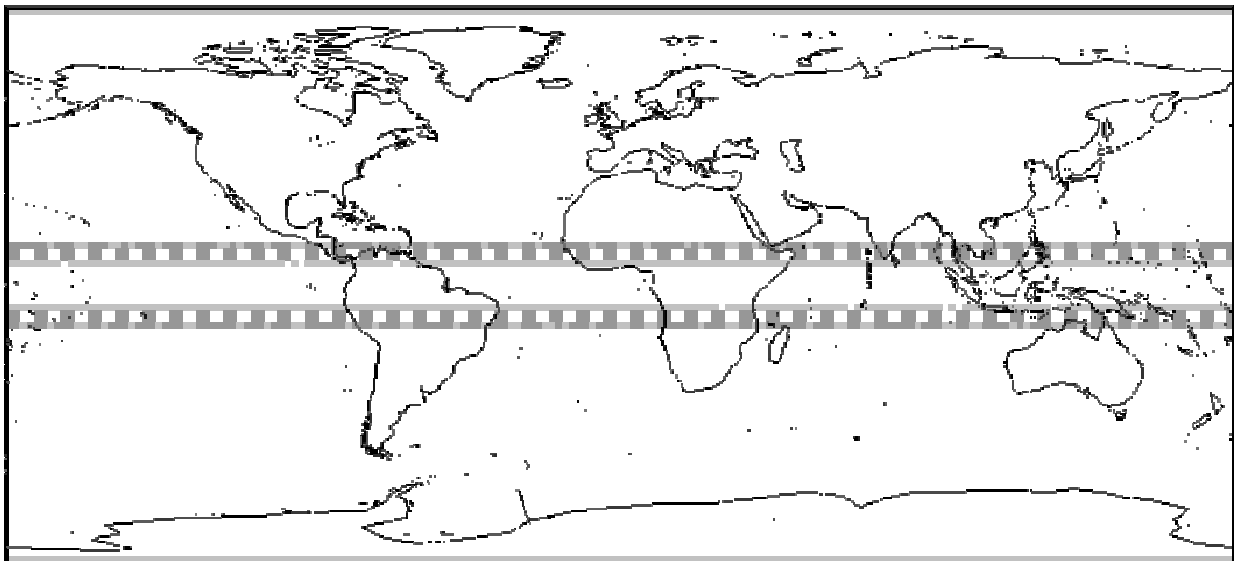


Figure 12-13 : Galileo only SISA/IF Availability, 10° Mask at 15m VAL

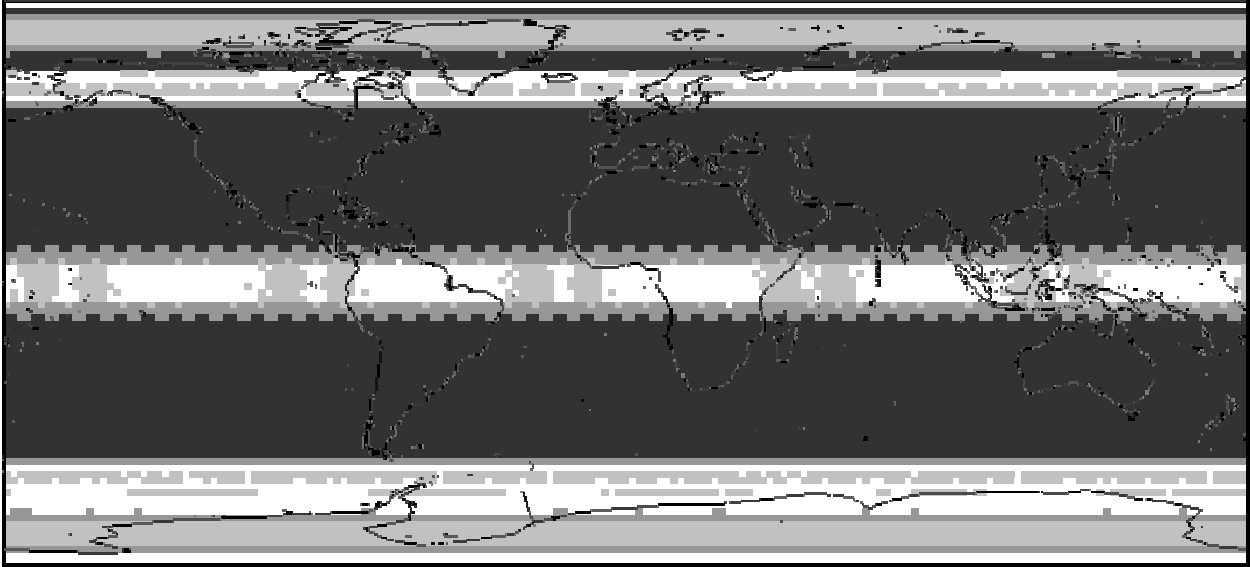


Figure 12-14 : Galileo only SISA/IF Availability, 10° Mask at 12m VAL

12.2 Navigation Engine Simulation Results

This section presents two examples of the use of the Navigation Engine Simulator (NavEng) to verify that the Errors in Variables RAIM algorithm can meet the specified False Alarm and Missed Detection probabilities whilst also yielding a lower VPL than that evaluated using standard LSR RAIM.

The NavEng is a Monte Carlo simulation¹¹. For each sample, a true range and a pseudorange is generated for each satellite in view, with the pseudorange error having a distribution defined by the relevant UERE curve and calculated elevation angle. The RAIM algorithm calculates a navigation solution and RAIM test statistics, and the navigation state is updated accordingly.

NB This simulation models a fixed receiver, with a large number of samples taking place with a fixed satellite geometry. It does not simulate a trajectory or a fixed user with a moving constellation; instead it is used to produce statistical data regarding the RAIM algorithm's performance for many samples of a fixed use case.

Two cases are described below:

¹¹ NB The "random" numbers used to generate noise in these simulations are taken from a list of pseudorandom numbers which is reinitialised when the tool is loaded, therefore runs of different cases can be performed using an identical set of "random noise" data.

- Galileo only, 10° masking angle – corresponding to the standard Galileo use case defined for GSTBv1 experimentation [45];
- Galileo + GPS, 5° masking angle – corresponding to the use case for combined constellations specified in [43].

In both cases the geometry has been defined as that occurring at Latitude 52° Longitude 0° Time 100 minutes, as defined within the NavEng tool. This has been selected arbitrarily as the default values for this tool, and has no particular significance (other than the location being close to the location of the precision approach trials data used in the Flight Trials simulation runs described in Section 12.3). For the Galileo-only case, it also corresponds to the numerical example presented in Section 11.

P_{FA} has been set to 8×10^{-6} and P_{MD} has been set to 0.0004, as specified earlier in the discussion of SVS parameters. Runs are performed with no applied bias (in order to demonstrate the false alarm performance of the algorithms), and with an applied bias (in order to demonstrate the missed detection performance of the algorithms).

The “No Bias” runs are performed with ten million samples. With this specified P_{FA} one would expect around 80 samples to generate false alarms. If the assumptions regarding the underlying distributions of the test statistics are correct, and if the thresholds are correctly set to generate a false alarm probability of 8×10^{-6} , using a binomial distribution¹² one would expect the number of alarms N generated in such a simulation to be $62 < N < 97$, with 95% probability.

Since the specified Missed Detection probability is far less stringent than the false alarm constraint, fewer samples are required to provide a statistically significant validation of this parameter. With P_{MD} set to 0.0004, one million samples would be expected to generate around 400 missed detections, if a critical bias is applied. Again using a binomial distribution analysis, one would expect $360 < N < 439$ missed detections, with 95% probability.

The UERE curves in both cases are as shown in Figure 12-1.

¹² Because the BINOMDIST function in MS Excel cannot handle probability values and sample sizes of 8×10^{-6} and 1×10^7 respectively, an on-line resource was used to set these limits [55]. Using this tool it was found that for a cumulative binomial distribution probability of 2.5%, 62 alarms would be expected. Similarly, to set the 97.5% cumulative probability threshold, 97 alarms would be expected. Therefore these values define the boundary of experimental values expected with 95% probability.

12.2.1 Galileo Only, RAIM Results

12.2.1.1 Unbiased Case

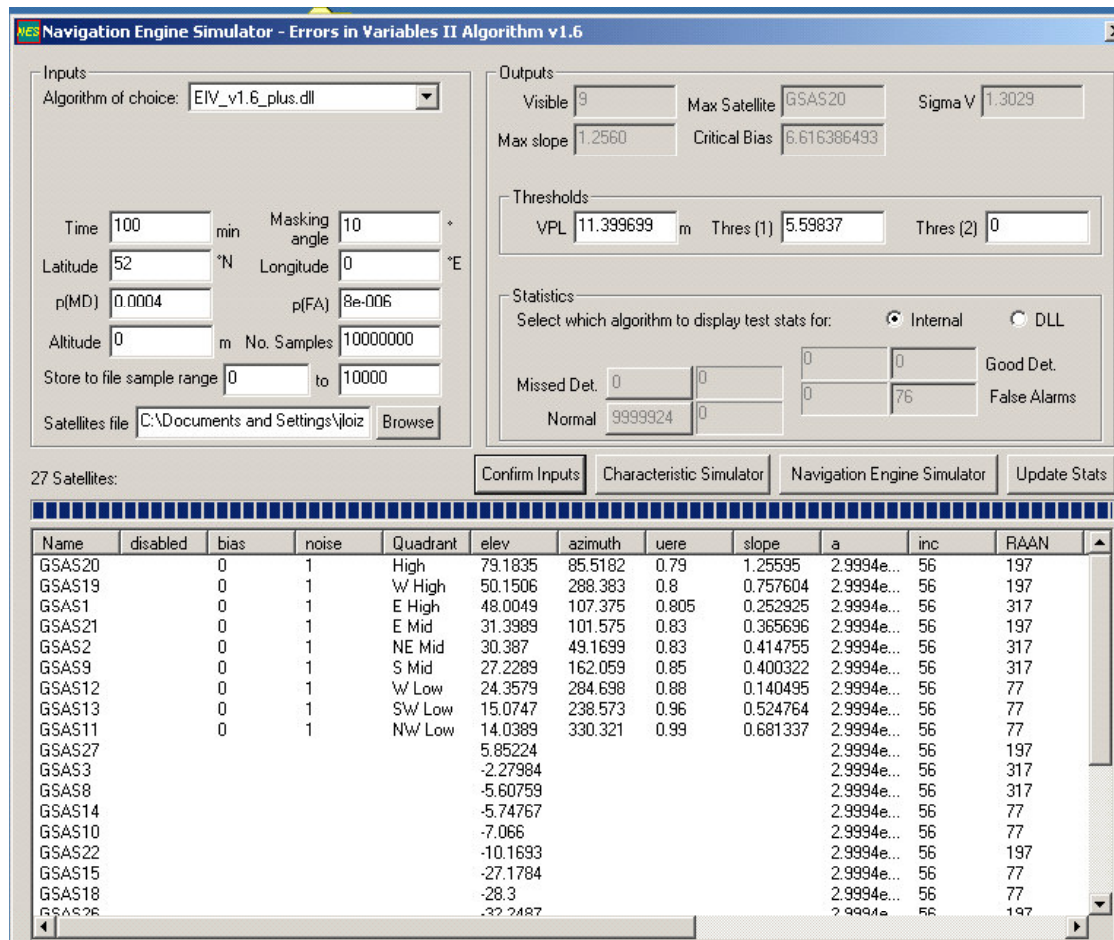


Figure 12-15 : NavEng Run for Galileo Only, LSR RAIM, no Bias

This screenshot (Figure 12-15) from the NavEng tool shows the results from a run with no bias, processed using the LSR RAIM algorithm. The VPL is evaluated as 11.4m, and the number of false alarms is 76, which matches well with the expectation of 80 alarms for the specified P_{FA} and sample size. This suggests that the tool provides a reasonable simulation of the expected distribution of errors on each measurement, by giving the expected central χ^2 distribution for the LSR test statistic.

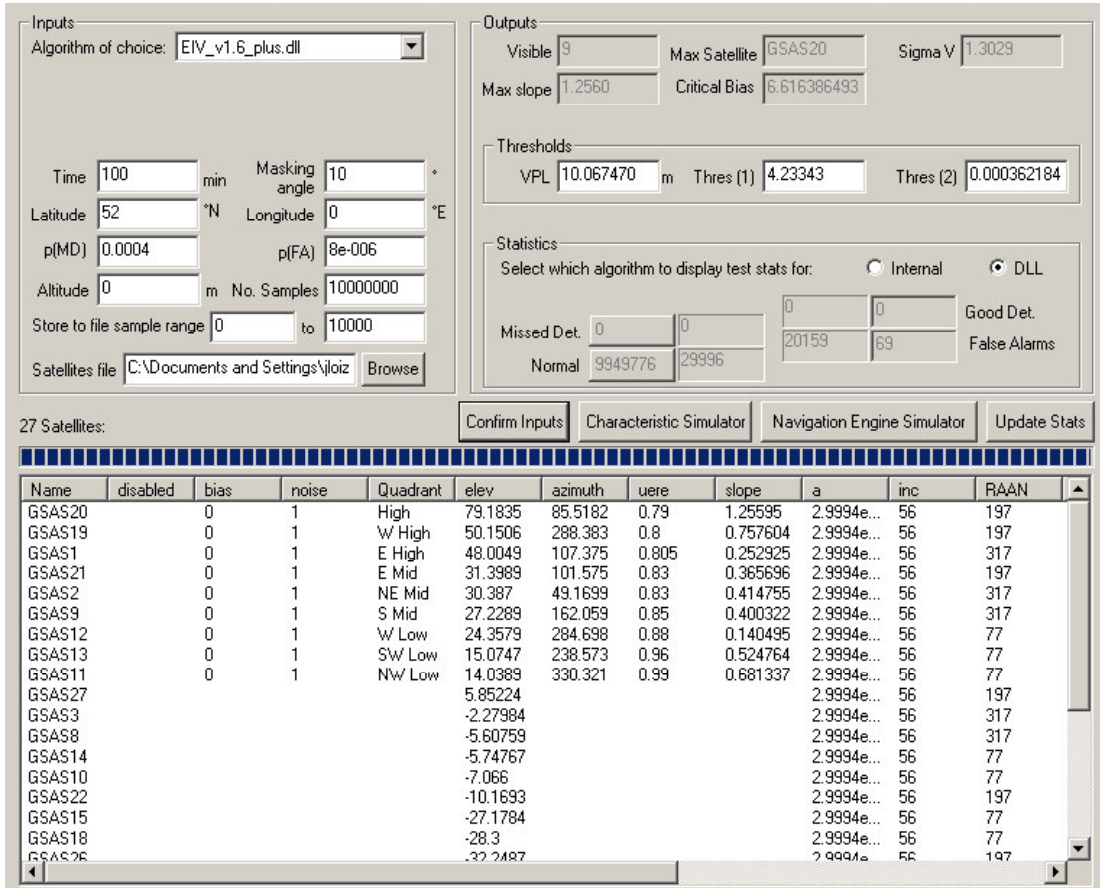


Figure 12-16 : NavEng Run for Galileo Only, EIV RAIM, no Bias

Figure 12-16 presents the same data processed using the EIV RAIM algorithm. In this case the VPL is 10.1m (about 12% less than the LSR VPL), and the number of false alarms is 69 (i.e. slightly fewer than the LSR case, but still within the expected experimental limits).

Note that a false alarm is only generated when both detection thresholds are exceeded. In this case there are 29,996 instances of the \sqrt{USSE} threshold being exceeded but the H/e statistic remaining below its threshold, and 20,159 instances where H/e exceeds its threshold but no alarm is generated because \sqrt{USSE} remains below limits. These values are shown in the figure above.

12.2.1.2 Biased Case

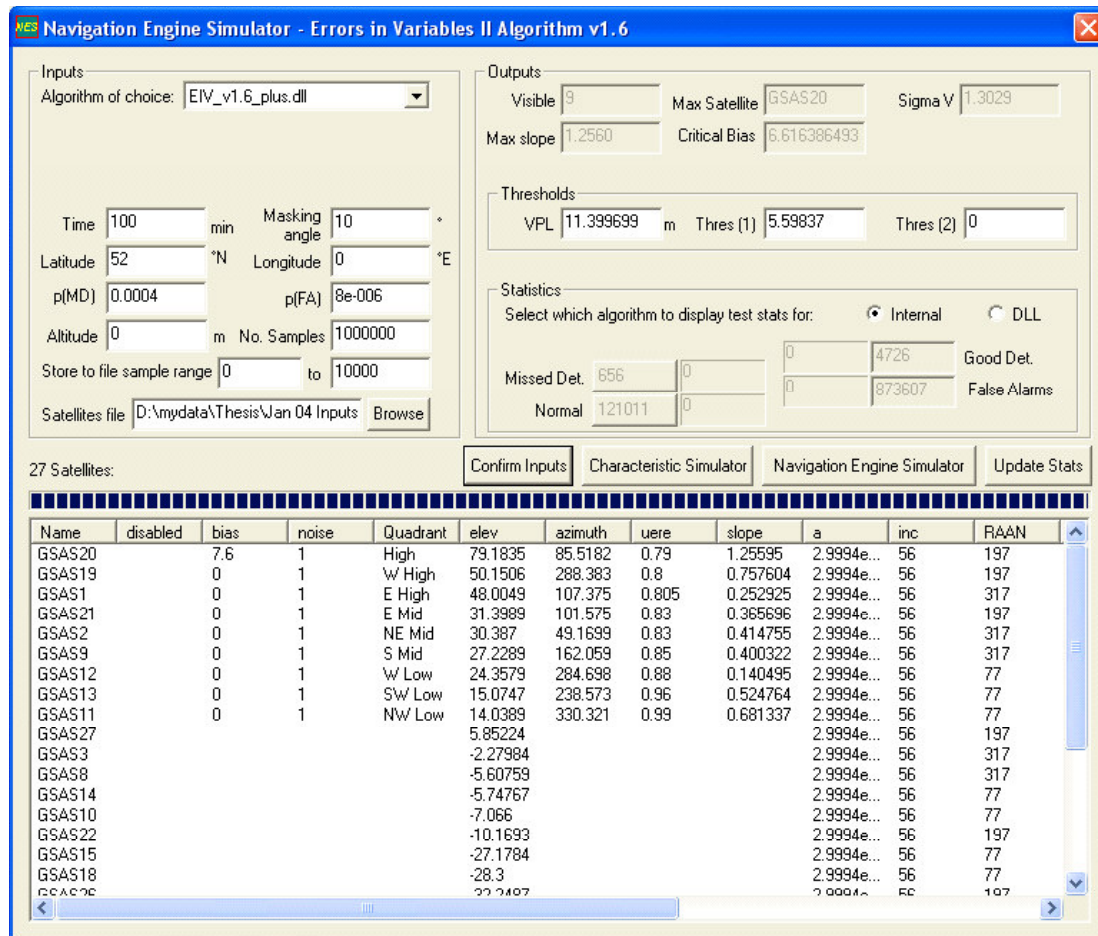


Figure 12-17 : NavEng Run for Galileo Only, LSR RAIM, with Bias

Figure 12-17 presents the Galileo-only case with a worst case bias applied, processed using LSR RAIM. This figure shows that 4,726 samples had a navigation error that exceeded the VPL but which generated a correct alarm (Good Detections) whilst 656 samples exceeded the protection limit without an associated alarm (Missed Detections). This value is higher than the expectation, and considerably beyond experimental limits. This suggests that the standard LSR algorithm under-estimates the vertical protection limit under certain circumstances.

This is a very significant result that is worthy of further investigation, but is beyond the scope of the current analysis. It is emphasised that the result shown in Figure 12-17 is not an anomaly, but is a repeatable result for this particular geometry case.

Note that the bias applied in this case (7.6m on satellite GSAS 20) is greater than the Critical Bias displayed in the NavEng tool control window (6.616m), which is the Critical Bias for the LSR algorithm (i.e. the bias which, if applied in the absence of any noise, would be just enough to trigger the LSR RAIM alarm). The worst case bias is calculated numerically, by evaluating the bias which, if applied to the critical satellite, would have the largest probability of a sample having VNSE exceeding the VPL and an LSR test statistic lower than the LSR threshold. The Critical Bias is less than the worst case bias, and does not, in general generate as many missed detections as the worst case bias.

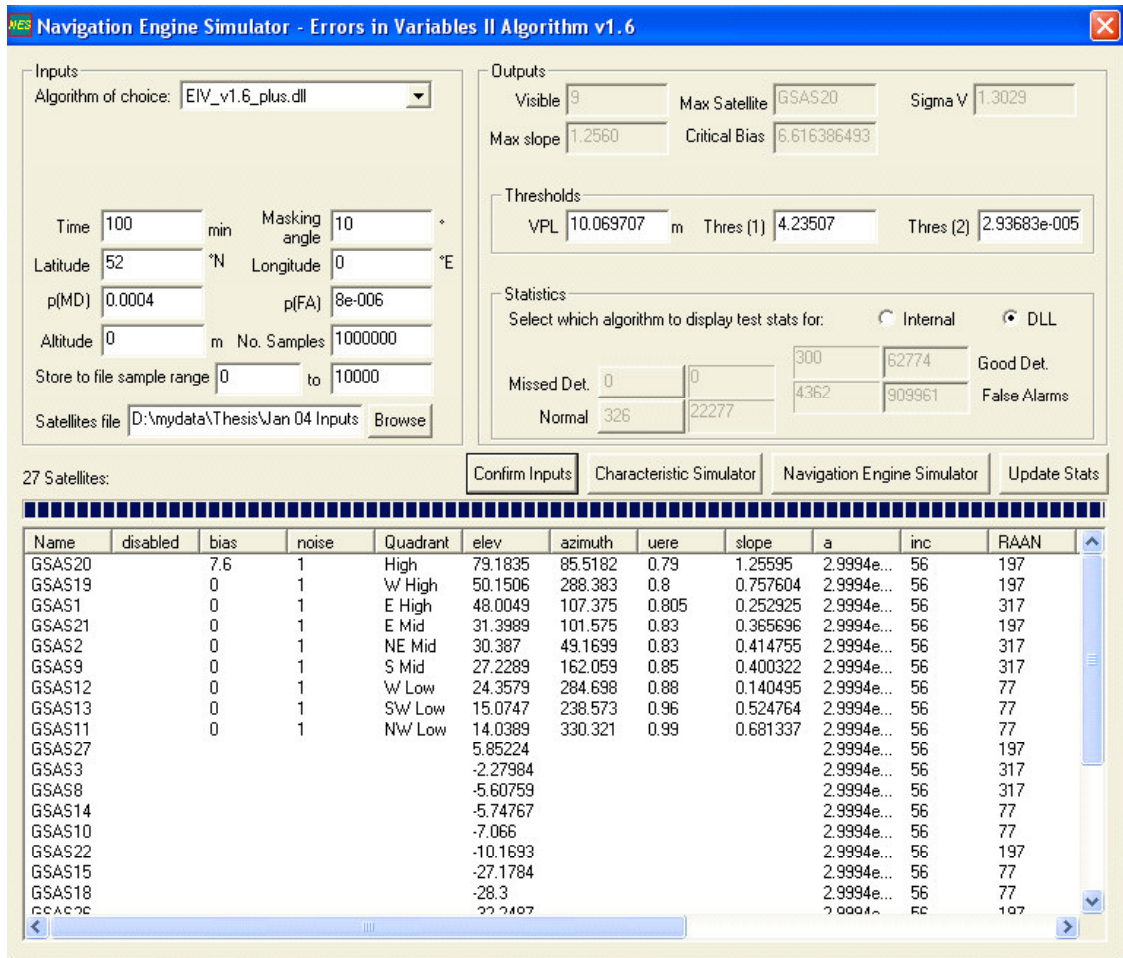


Figure 12-18 : NavEng Run for Galileo Only, EIV RAIM, with LSR worst case Bias

Figure 12-18 shows the same data processed using the EIV algorithm. As discussed above, the applied bias is the Worst Case Bias for the LSR algorithm. In this case, the observed number of missed detections is 300, which is much lower than the number of missed detections using LSR. This is as expected, since this applied bias is higher than the worst

case bias for the EIV algorithm, causing more samples to fall into the region of Good Detections for the EIV algorithm.

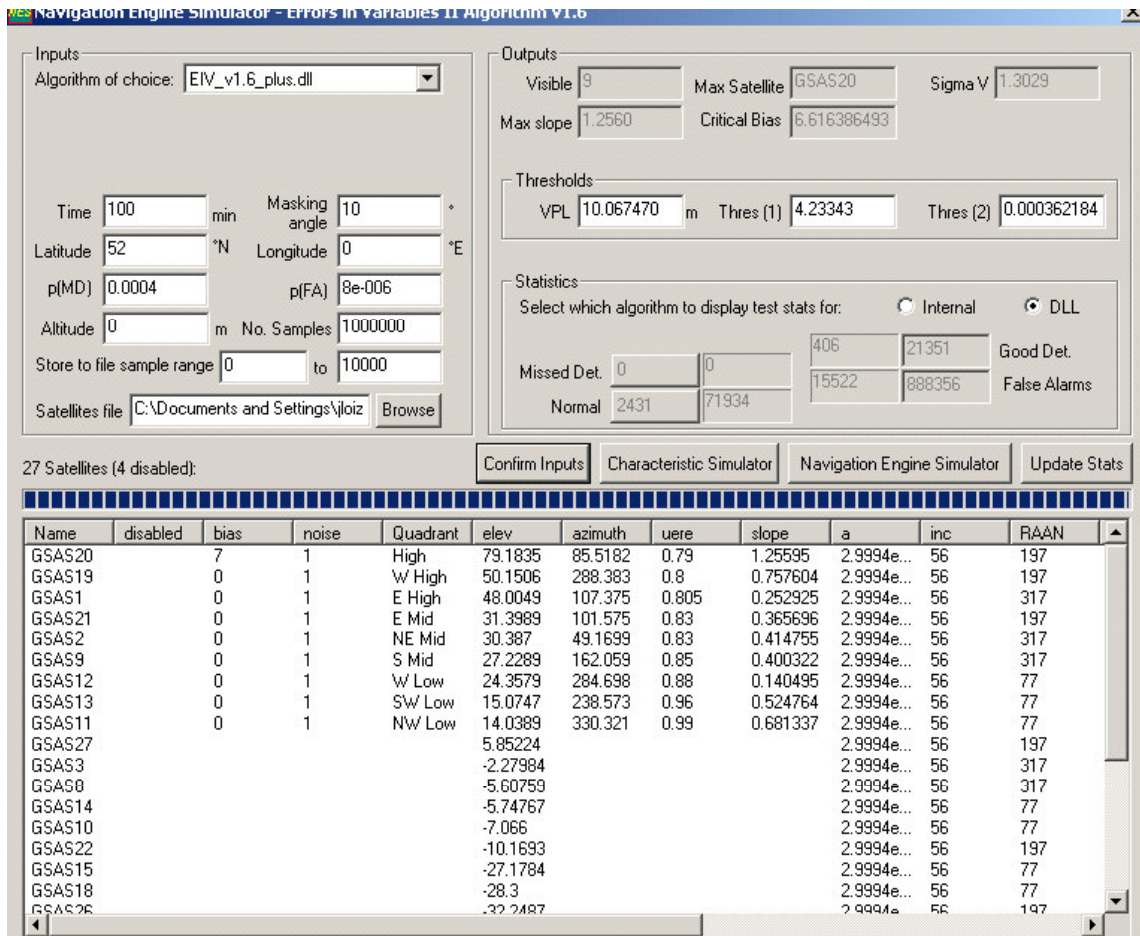


Figure 12-19: NavEng Run for Galileo Only, EIV RAIM, with EIV worst case Bias

Figure 12-19 shows the performance of the EIV algorithm under the worst case base for this algorithm. As discussed previously, this bias is evaluated numerically, by finding the bias which when applied to the critical satellite has a probability equal to P_{MD} of any sample having a VNSE larger than the VPL¹³, and simultaneously having either or both of its test statistics below their specified threshold. This requires a numerical convolution of a non-central χ^2 distribution (for the \sqrt{USSE} test statistic) a half-normal distribution (for the H/e statistic) and a normal distribution (for the vertical error distribution). Note that this bias is smaller than the worst case bias for the LSR algorithm. This is not surprising, since the detection threshold for the \sqrt{USSE} statistic is lower

¹³ NB This is how VPL is set in the EIV algorithm, so the worst case bias is an artefact of the EIV method, as demonstrated in Section 11.3.5 in the numerical example.

than the equivalent threshold for the LSR test statistic, therefore one would expect the worst case bias for EIV to occur at a slightly lower value than for LSR.

In this case, 406 missed detections were observed, which closely matches the expectation of 400 given the specified P_{MD} and sample size. This suggests that the VPL calculated by the EIV algorithm correctly represents the protection limit, given the specified missed detection specification and the calculated detection thresholds.

12.2.2 Galileo + GPS, RAIM Results

12.2.2.1 Unbiased case

The screenshot displays the NavEng tool interface for a Galileo + GPS simulation. The 'Inputs' section shows the algorithm set to 'EIV_w1_E_plus_d1'. Simulation parameters include a 100-minute duration with a 5-degree masking angle. The protection level (VPL) is calculated as 8.303076 meters. The number of missed detections is 0, and the number of false alarms is 85. The 'Statistics' section shows that the 'Internal' algorithm was used for test state display.

The '51 Satellites' table provides detailed RAIM data for each satellite:

Name	disabled	bias	noise	Quadrant	elev	azimuth	usec	slope	a	inc	RAIM
GSAS20	0	1		High	73.1835	85.5182	0.79	0.684349	2.9994e...	56	197
GPSIF23	0	1		High	75.8052	289.718	1.56	0.306217	2.69618...	55	257
GPSIF24	0	1		E High	83.7085	83.071	1.56	0.204206	2.69618...	55	257
GPSIF14	0	1		W High	81.968	282.481	1.56	0.267413	2.69618...	55	137
GSAS19	0	1		W High	50.1506	288.383	0.8	0.432642	2.9994e...	56	197
GSAS1	0	1		E High	48.0049	187.375	0.805	0.161161	2.9994e...	56	317
GPSIF13	0	1		NW Mid	37.4224	384.103	1.58	0.07578	2.69618...	55	137
GSAS21	0	1		E Mid	31.3889	181.575	0.83	0.216344	2.9994e...	56	197
GSAS2	0	1		NE Mid	30.387	49.1689	0.83	0.237326	2.9994e...	56	317
GSAS9	0	1		S Mid	27.2289	162.058	0.85	0.227365	2.9994e...	56	317
GPSIF17	0	1		E Mid	26.0389	182.453	1.61	0.160115	2.69618...	55	197
GPSIF2	0	1		S Low	24.5489	163.245	1.64	0.125474	2.69618...	55	317
GSAS12	0	1		W Low	24.3579	284.688	0.88	0.09172	2.9994e...	56	77
GSAS13	0	1		SW Low	15.0747	238.573	0.96	0.308402	2.9994e...	56	77
GSAS11	0	1		NW Low	14.0389	330.321	0.99	0.390061	2.9994e...	56	77
GPSIF10	0	1		SW Low	7.04533	225.113	2.05	0.206629	2.69618...	55	77
GSAS27	0	1		W Low	5.05204	284.908	1.65	0.257607	2.9994e...	56	197
GPSIF1	0	1		SE Low	4.118	76.3823	2.27	0.277055	2.69618...	55	317

Figure 12-20 : NavEng Run for Galileo + GPS, LSR RAIM, no Bias

This screenshot (Figure 12-20) from the NavEng tool shows the results from a run for Galileo + GPS with no bias, processed using the LSR RAIM algorithm. The VPL is evaluated as 8.3m, and the number of false alarms is 85, which matches well with the expectation of 80 alarms for the specified P_{FA} and sample size.

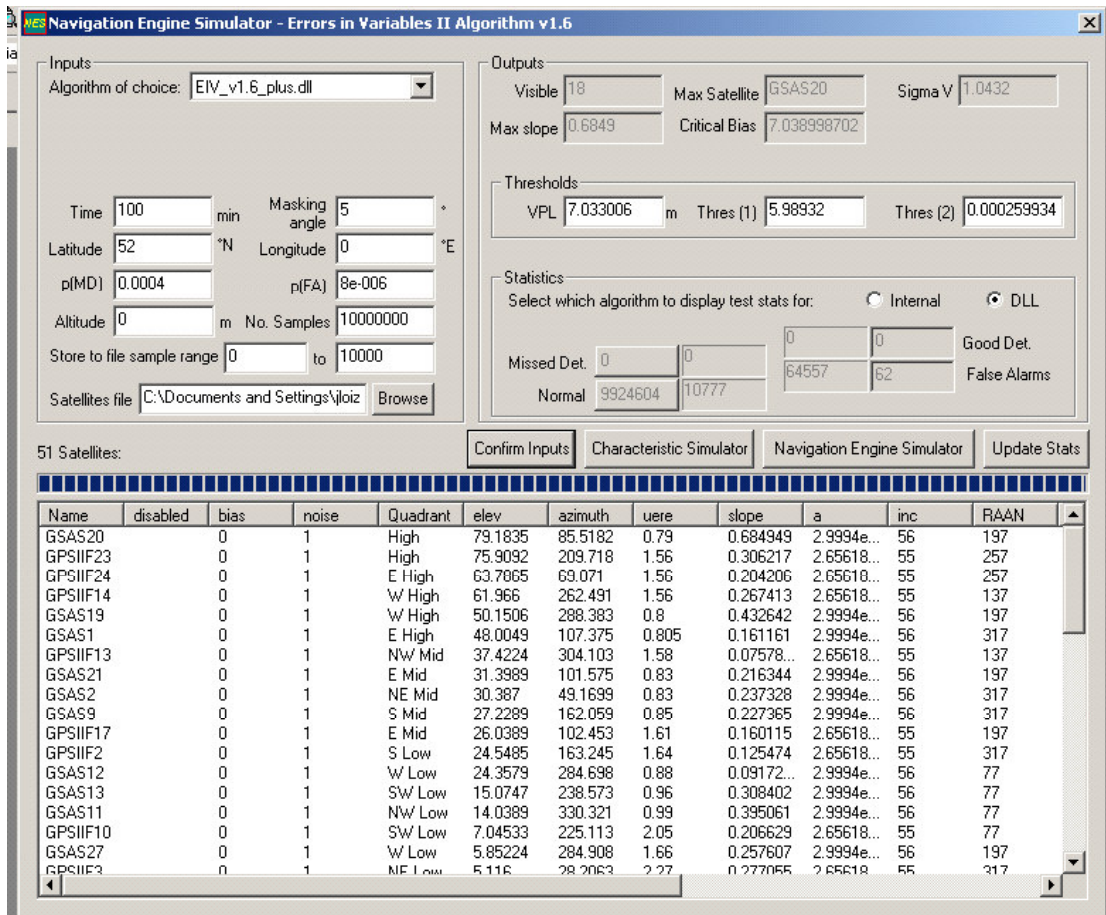


Figure 12-21 : NavEng Run for Galileo + GPS, EIV RAIM, no Bias

Figure 12-21 presents the same data processed using the EIV RAIM algorithm. In this case the VPL is 7.0m (about 18% less than the LSR VPL), and the number of false alarms is 62 which is within the expected experimental limits. Note that a false alarm is only generated when both detection thresholds are exceeded. In this case there are 10,777 instances of the \sqrt{USSE} threshold being exceeded but the H/e statistic remaining below its threshold, and 64,557 instances where H/e exceeds its threshold but no alarm is generated because \sqrt{USSE} remains below limits. These values are shown in the figure above.

This suggests that the EIV algorithm can provide a significantly lower VPL than LSR RAIM, whilst maintaining the specified false alarm specifications. It also suggests that the underlying assumptions regarding the distribution of EIV test statistics (that the \sqrt{USSE} statistics has a χ^2 distribution whilst the H/e distribution is half-normal) are reasonable, since the detection rates closely match the expectations for thresholds based upon these assumptions.

12.2.2.2 Biased Case

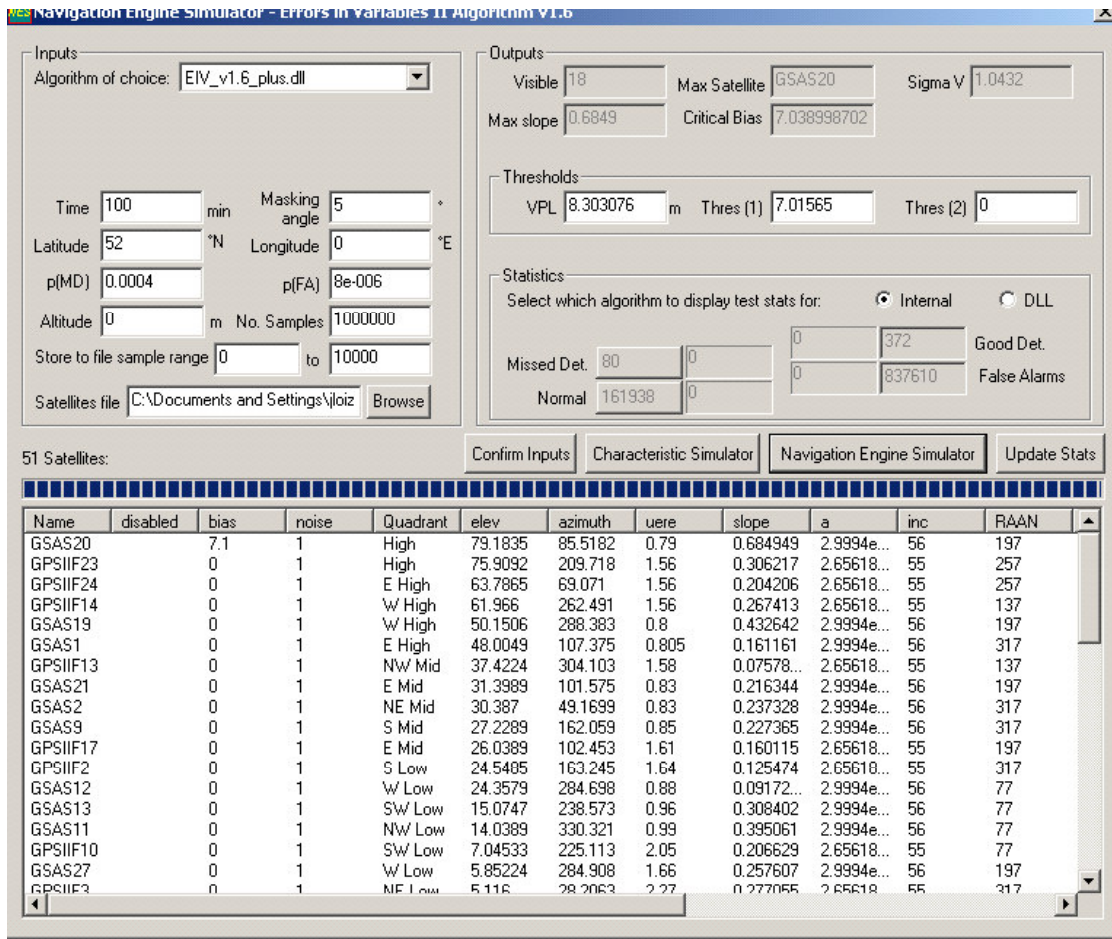


Figure 12-22 : NavEng Run for Galileo + GPS, LSR RAIM, with Bias

Figure 12-22 presents the Galileo+GPS case with a worst case bias applied, processed using LSR RAIM. This figure shows that 80 samples exceeded the protection limit without an associated alarm (Missed Detections). This value is considerably lower than the expectation, and well outside experimental limits.

This suggests that in cases with a large number of satellites in view (as is the case with combined constellations), the LSR algorithm may significantly overestimate the VPL.

Figure 12-23 demonstrates an interesting shortcoming with the LSR method when used with a combined constellation. It appears that with a large number of satellites in view some satellites contribute more to increasing the required detection threshold (because each additional satellite in view adds a degree of freedom that increases the threshold for a χ^2 test statistic), than it does to improving the accuracy of the

position solution. These satellites are seen to be those which have the lowest slopes on the LSR RAIM test statistic characteristic (identified under the heading “slope” in the NavEng tool lower window). Although the VPL calculated in the case above is found to be 8.30m, it can be seen in Figure 12-23 that by disabling the four satellites with the lowest values of “slope” (GSAS 12, and GPS2, GPS13 and GPS17), and hence reducing the degree to which the system is overdetermined, the VPL calculated by the LSR algorithm actually decreases by about 2.5%, to 8.1m. In this case, for the same applied bias as was used to generate Figure 12-22, the number of missed detections has increased to 154. This is still well within the P_{MD} specifications.

This demonstrates that the LSR algorithm is not optimal when used with large numbers of satellites in view, and that it can be improved simply by including a routine to select some subset of the satellites in view for calculation of RAIM integrity.

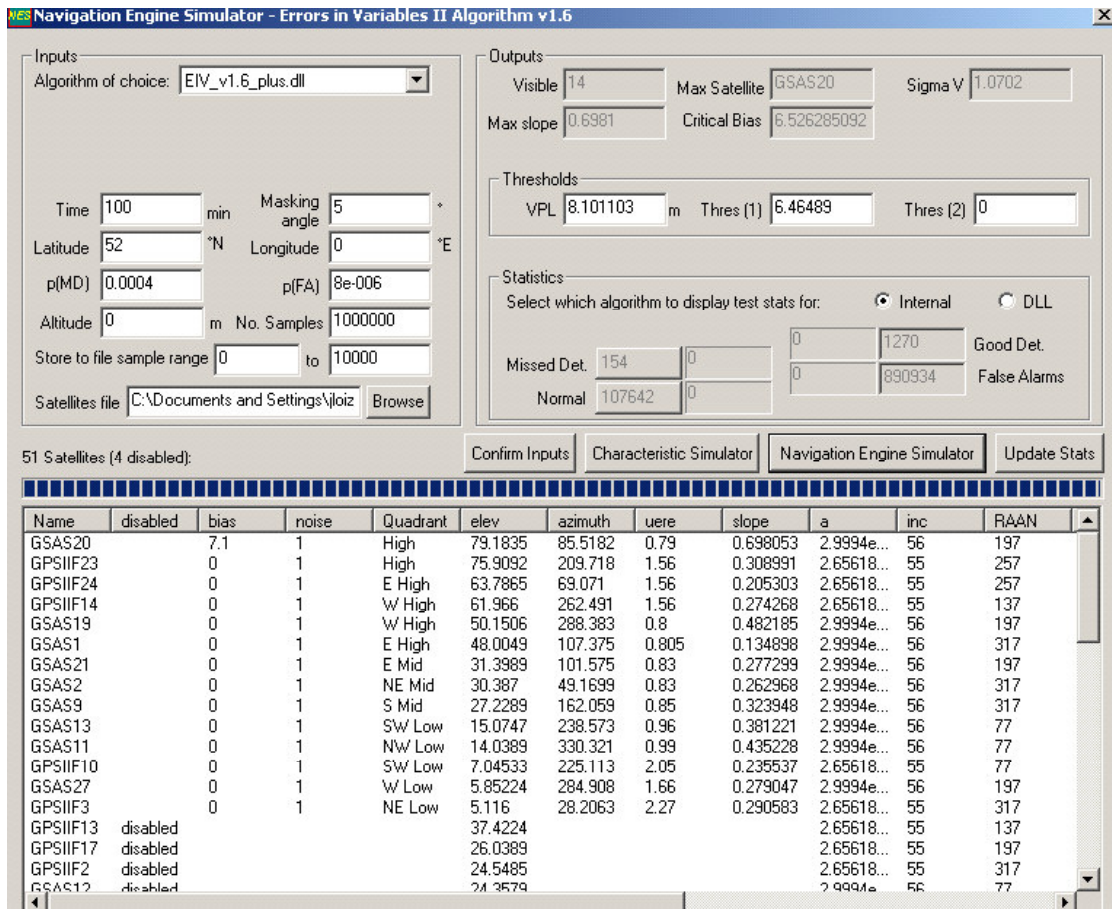


Figure 12-23 : NavEng Run, LSR RAIM, with Bias and satellites disabled

Note that this effect of apparently improving VPL as satellites are removed from the RAIM processing does not appear to occur with the

EIV algorithm, which suggests that EIV is closer to an optimal RAIM solution than the LSR method. In fact for the case shown in Figure 12-23 the EIV RAIM VPL is increased from 7.04m to 7.14m, with an incremental increase as each satellite is disabled.

Finally in this section, Figure 12-24 shows the output from the navigation engine simulator for the combined GPS + Galileo constellation using EIV RAIM, with the EIV worst case bias applied. This demonstrates a Missed Detection rate of 373 samples out of one million, which is within the expected 95% experimental bounds.

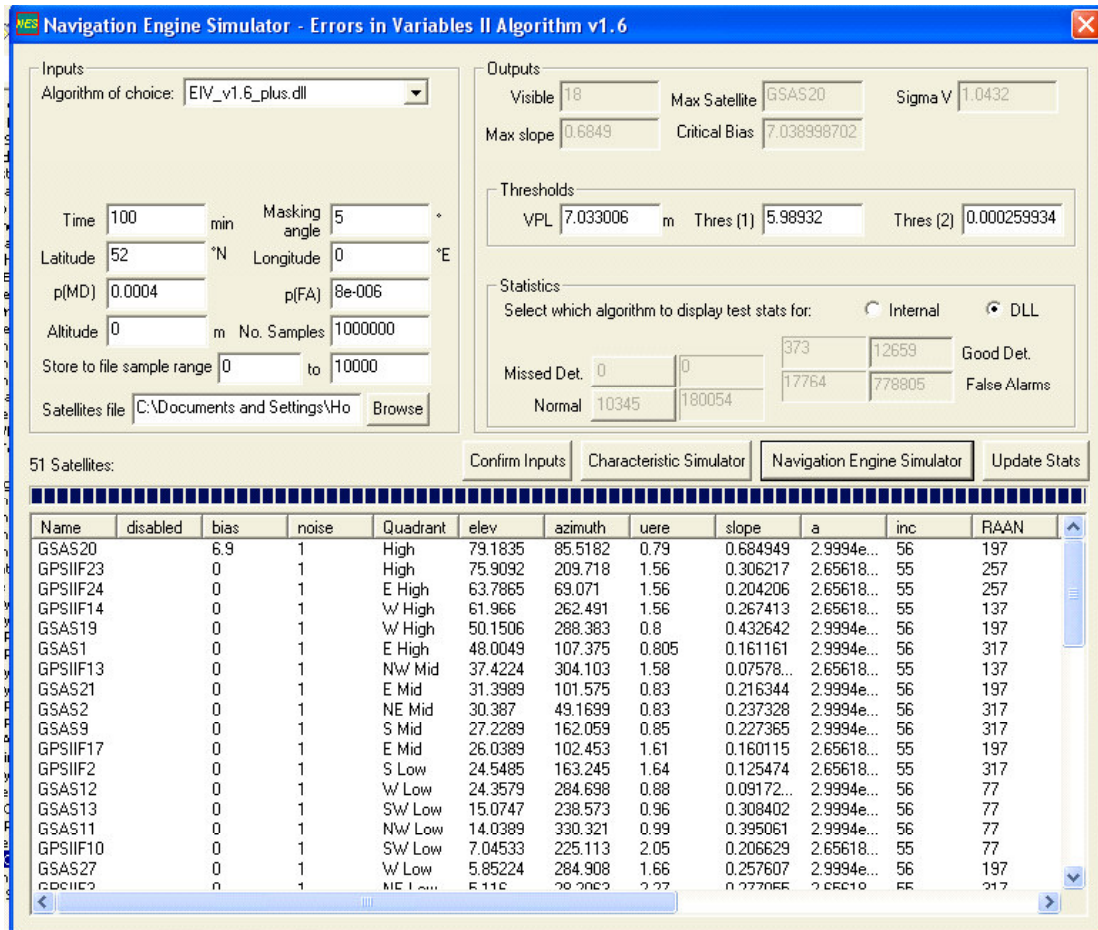


Figure 12-24 : NavEng Run for Galileo + GPS, EIV RAIM, with Bias

These results appear to demonstrate that the EIV RAIM algorithm provides a significantly lower VPL than the LSR RAIM algorithm, whilst also meeting the missed detection and false alarm specifications. They also demonstrate that the EIV algorithm appears to be closer to an optimal algorithm for VPL than the commonly implemented LSR method.

12.3 Flight Trials Simulation Results

This section presents the results from Matlab-based Flight Trials simulations. The following plots are based on a simulation of a combined Galileo/GPS constellation, being used to provide RAIM-based integrity to an airborne receiver whilst the aircraft is undertaking a final approach to land.

Each plot presents a series of traces which are explained in the accompanying text. The bottom trace in all cases represents the “Alarm State” for the RAIM algorithm, represented numerically. The values plotted have the following meanings:

- **Alarm State = 0 means Nominal Operations** – Vertical Error is below VPL, and the RAIM algorithm has not declared an alarm;
- **Alarm State = 1 means False Alarm** – Vertical Error is below VPL, but the RAIM algorithm has declared an alarm;
- **Alarm State = 2 means Good Detection** – Vertical Error is above VPL, and the RAIM algorithm has correctly declared an alarm;
- **Alarm State = 3 means Missed Detection** – Vertical Error is above VPL, but the RAIM algorithm has not declared an alarm. This is clearly undesirable.

The following parameters are used to configure the simulation:

- $P_{FA} = 8 \times 10^{-6}$;
- $P_{MD} = 0.0004$;
- Masking Angle = 5° ;
- Undeclared offset between Galileo and GPS system time¹⁴ = 5 nanoseconds;
- 1-sigma OD&TS Error for Galileo = 0.715 m (65cm, plus 10% margin);
- 1-sigma OD&TS Error for GPS = 1.5 m.

¹⁴ It is expected that some mechanism would be available to disseminate the time offset between Galileo and GPS system times, either broadcast through either of the systems or provided from some other source. However, for the purpose of these simulations it is assumed that there will always be some residual time offset error not completely accounted for in this broadcast offset, and that this error has a maximum value of 5 ns [48].

- UERE curves as below, shown graphically in Figure 12-1.

NB Each simulated satellite has been given a “true” almanac and a “broadcast” almanac. This allows for Orbit Determination & Time Synchronisation (OD&TS) errors to be modelled for each satellite, as components of its clock offset, semi-major axis, inclination, right ascension of ascending node (RAAN) and mean anomaly. The values of each of these components were randomly selected from a distribution which would yield an overall OD&TS ranging error component of about 0.72 m (0.6m clock error and 0.4 m due to errors in semi-major axis, inclination, RAAN and mean anomaly) for Galileo and 1.5 m (0.8m random clock and 1.25m in position) for GPS IIF [54]. Once set, these OD&TS errors remain fixed for all simulation runs.

The simulation is performed with 1 second epochs. The precise receiver-to-satellite geometry is determined by the data file which is used to provide the simulated aircraft trajectory in the simulation. Note that the true position of the receiver has been extracted from actual instrumented flight trials data provided by NATS; this trajectory represents a genuine precision approach into Boscombe Down airfield by a BAC 1-11 aircraft. In the cases presented, the start time is exactly 50,000 seconds after midnight (i.e. 13:53:20). At this instant the receiver has a location (on WGS-84 coordinates) of 51.198161N -1.665454E 527.6572m Altitude. The satellite positions are readily determined by propagating the orbits defined in Section 7.2 (i.e. take the epoch at which the orbits are defined as being midnight on the day of the flight trial, and propagate them forward by 50,000 seconds to find their positions at the start of the analysis).

At each epoch an “environmental” component of UERE (tropospheric, ionospheric, multipath, receiver additive white gaussian noise), consistent with the UERE curve, taking into account the OD&TS component already modelled, is added to each ranging measurement. This “environmental” component is produced by setting a randomly selected Zenith Tropospheric Delay (ZTD, which is fixed for all epochs), from which individual tropospheric delays are calculated as a function of elevation angle. To the tropospheric component is added (vector sum) ionospheric delay, multipath jitter, and AWGN receiver noise. These components, other than the tropospheric component, are therefore treated as being uncorrelated between epochs.

A Pseudorange Vector is then produced at each epoch by adding the satellite clock error, receiver clock error and environmental noise error to the true distance from the user to each satellite. As and when required, a bias representing a Feared Event is also added to this vector. This Pseudorange Vector is used by simulated receiver algorithms which use unfiltered Least Squares algorithms to estimate the user position, and

various test RAIM algorithms to detect the occurrence of these Feared Events.

12.3.1 LSR RAIM, Step Bias

Figure 12-25 demonstrates the ability of the LSR RAIM algorithm to detect a step bias. A step bias is initiated 60 seconds into the simulation (approximately 60 seconds before touchdown of the simulated aircraft). The bias has a ranging error magnitude of 12 m, is held for 21 seconds and then released completely. It is applied to the Critical Satellite, i.e. the satellite which has the steepest LSR RAIM characteristic at that epoch. No FDE is used, i.e. satellites are NOT excluded on detection of an alarm condition.

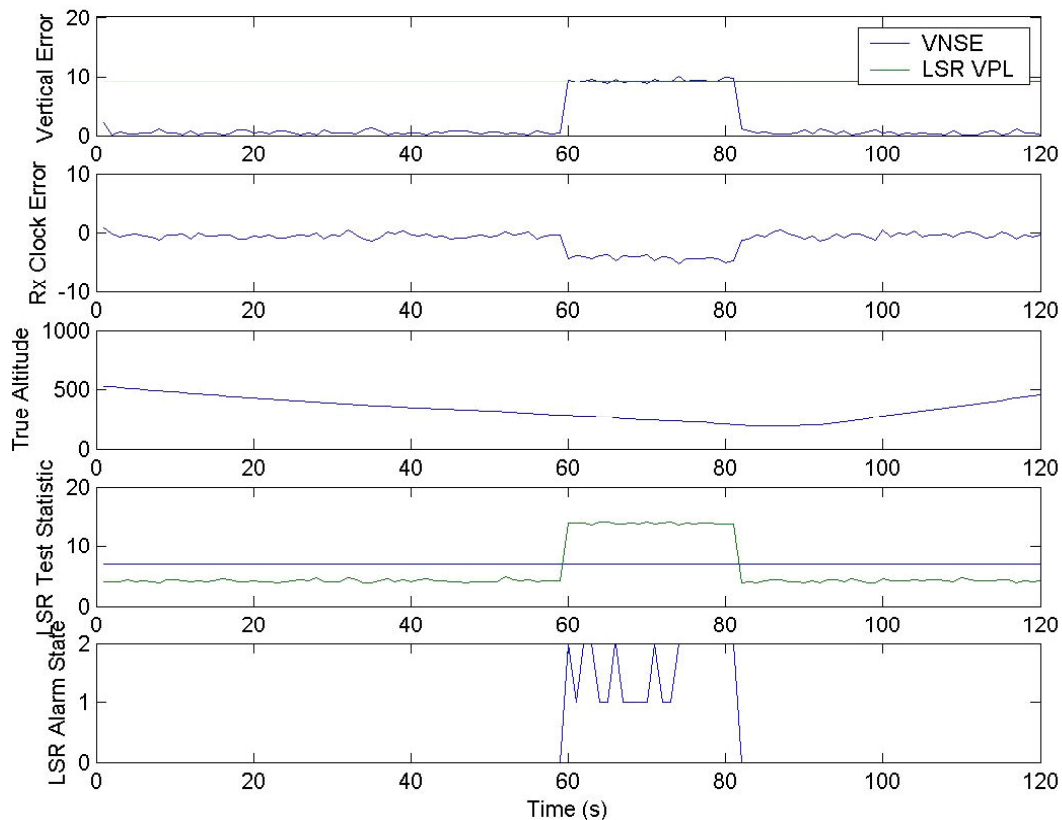


Figure 12-25 : LSR RAIM Response to Step Bias

The top trace show how the Vertical Navigation System Error (VNSE) responds to this step bias, with VNSE fluctuating around the VPL calculated by the LSR RAIM algorithm.

The second trace shows how the user receiver clock error responds to this step bias. The 12m ranging error effectively increases the user clock

error by around 4m. Note that in this case the user clock is updated on an epoch-by-epoch “snapshot”, i.e. there is no filtering of the user clock. Note also that the clock update comes from the least squares position and timing solution derived from the combined Galileo/GPS measurements. As a result, this trace shows the user clock error demonstrates a step function similar to the VNSE (and the input bias function).

The third plot shows the simulated true altitude of the receiver during the two-minute simulation period. Note that the true position of the receiver has been extracted from actual instrumented flight trials data provided by NATS; this trajectory represents a genuine precision approach into Boscombe Down airfield by a BAC 1-11 aircraft.

The fourth plot shows how the LSR Test Statistic responds to this step bias. The statistic rises above the detection threshold at the same as the VNSE rises.

The bottom plot shows the alarm state derived from the LSR RAIM algorithm. The numerical state values have the meanings defined in Section 12.3. For the majority of the run the state has a value of 0, meaning nominal operations. However, when the bias is applied the alarm state varies between one and two, which shows that the RAIM is triggered for the entire duration of the applied bias, and the state fluctuates between False Alarm and Good Detection as the VNSE fluctuates relative to the VPL.

12.3.2 EIV RAIM, Step Bias, Snapshot User Clock

Figure 12-26 demonstrates the ability of the EIV RAIM algorithm to detect a step bias. Conditions are as defined in the previous section.

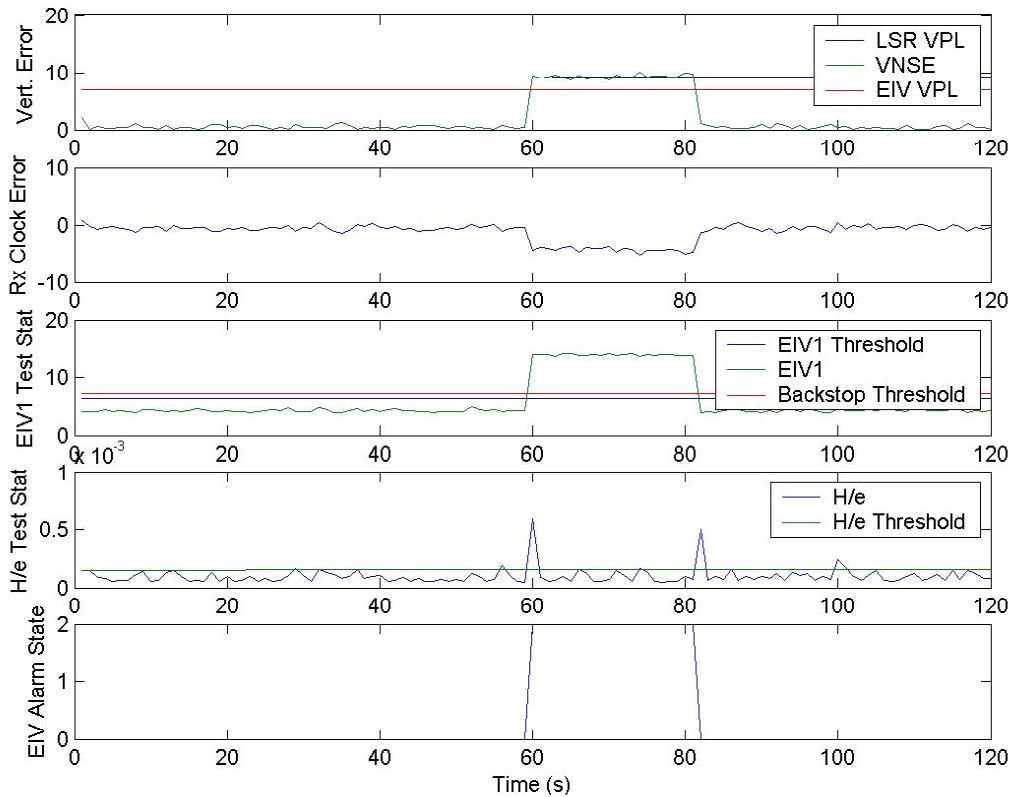


Figure 12-26 : EIV RAIM Response to Step Bias

The top trace show how the VNSE responds to this step bias, with VNSE fluctuating around the VPL calculated by the LSR RAIM algorithm, and above the VPL calculated by the EIV algorithm. Note that the VPL calculated by EIV RAIM is approximately 2m lower than the LSR RAIM VPL.

The second trace shows the clock error for the user clock used by this implementation of the EIV algorithm. In this case it is identical to that shown previously for the LSR method.

The third trace shows the EIV $\sqrt{\text{USSE}}$ Test Statistic¹⁵ (labelled “EIV1”) and its relation to the primary detection threshold for this statistic, and the Backstop threshold. As expected, this trace has the same characteristic as the LSR RAIM test statistic. As a reminder at this point, in the EIV algorithm an alarm is generated if the Backstop threshold is exceeded by $\sqrt{\text{USSE}}$, regardless of the status of the H/e test statistic,

¹⁵ Note that in order to avoid confusion with the $\sqrt{\text{WSSE}}$ statistic used for weighted Least Squares RAIM, the $\sqrt{\text{USSE}}$ test statistic is labelled “EIV1” in all of these plots.

although the standard process is for $\sqrt{\text{USSE}}$ and H/e both to exceed their corresponding thresholds for an alarm to be generated.

The fourth trace shows the EIV “H/e” Test Statistic and its relation to the detection threshold for this statistic, and demonstrates a very important feature of the EIV algorithm. Unlike the $\sqrt{\text{USSE}}$ statistic that remains above its threshold for the duration that the Feared Event is active, this statistic exceeds its detection threshold in this period on three short periods only:

- At the start of the FE, when the bias is applied and the VNSE and clock error both rise rapidly;
- At the end of the FE, when the bias is removed and the VNSE and clock error both drop rapidly;
- At one other point between these events, due to random noise fluctuations, which can be seen to be correlated with a small peak in VNSE.

The bottom trace shows that the alarm status is nominal outside of the FE start and stop times, and set to a value of two (“Good Detection”) for the duration of the FE. Note that this detection is due to $\sqrt{\text{USSE}}$ exceeding the Backstop threshold. If the Backstop were not employed the EIV algorithm would detect the FE only at the points at which H/e exceeds its threshold. The observations in between these spikes would be Missed Detections.

In this case, as a result of the satellite geometry, the Backstop is quite close to the $\sqrt{\text{USSE}}$ threshold, so it is unlikely that an FE would occur that exceeds the $\sqrt{\text{USSE}}$ threshold only. However, in general there may be cases in which the Backstop is significantly higher than the $\sqrt{\text{USSE}}$ threshold. In this case, the behaviour of the H/e Test Statistic shown above would be unacceptable, as this could easily lead to Hazardous Misleading Information.

The following section presents an approach to mitigating this problem.

12.3.3 EIV RAIM, Step Bias, Filtered User Clock

Figure 12-27 repeats the case discussed above, but this time with a filter applied to the use clock such that user time is taken to be an unweighted average of the last fifty one-second epochs.

The traces are identical to those shown in Figure 12-26 except the second trace demonstrates how the user clock has been smoothed by this filter (the decay in the first 50 seconds is settling time for this filter from its initial state) and the fourth trace shows that in this case H/e more

closely follows the VNSE and input Feared Event functions. In this case the EIV RAIM algorithm would correctly detect the step bias Feared Event even if the Backstop threshold were not exceeded.

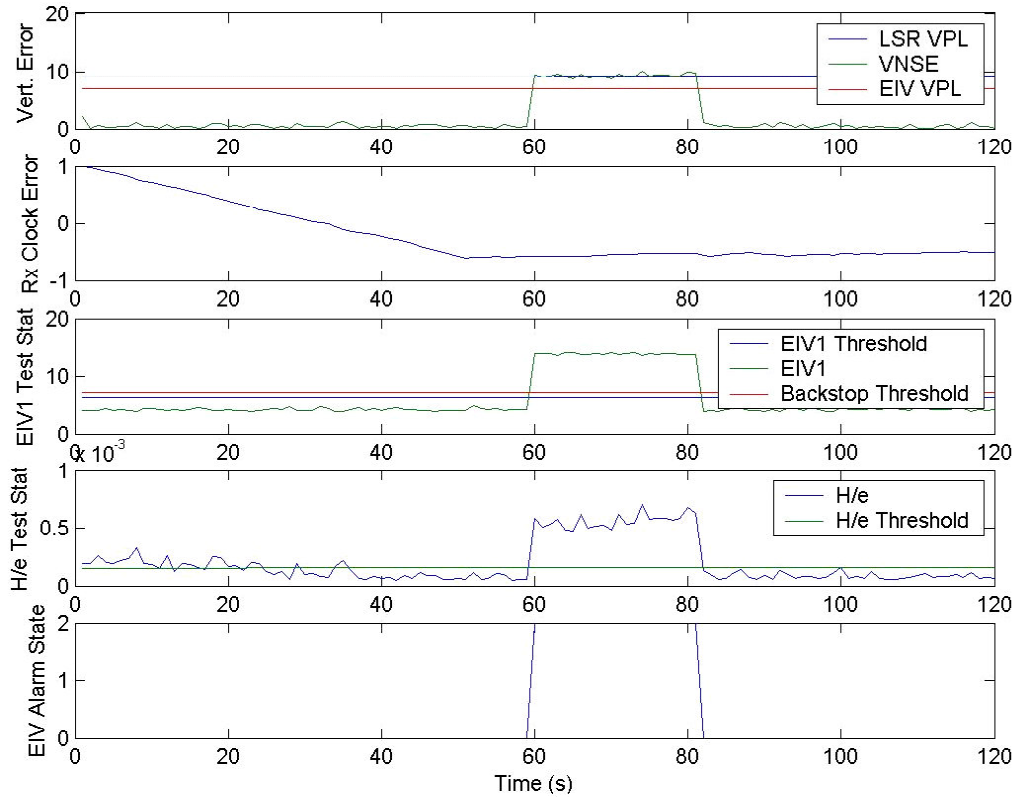


Figure 12-27 : EIV RAIM response to Step Bias, with Filtered Clock

12.3.4 LSR RAIM, Ramp Bias

Figure 12-28 demonstrates the ability of the LSR RAIM algorithm to detect a ramping bias. A ramp bias is initiated 60 seconds into the simulation (approximately 60 seconds before touchdown of the simulated aircraft), on the critical satellite. The bias increases at a rate of 1 m/s, and lasts for 12 seconds. It is held for 10 seconds and then released completely. No FDE is used, i.e. satellites are NOT excluded on detection of an alarm condition.

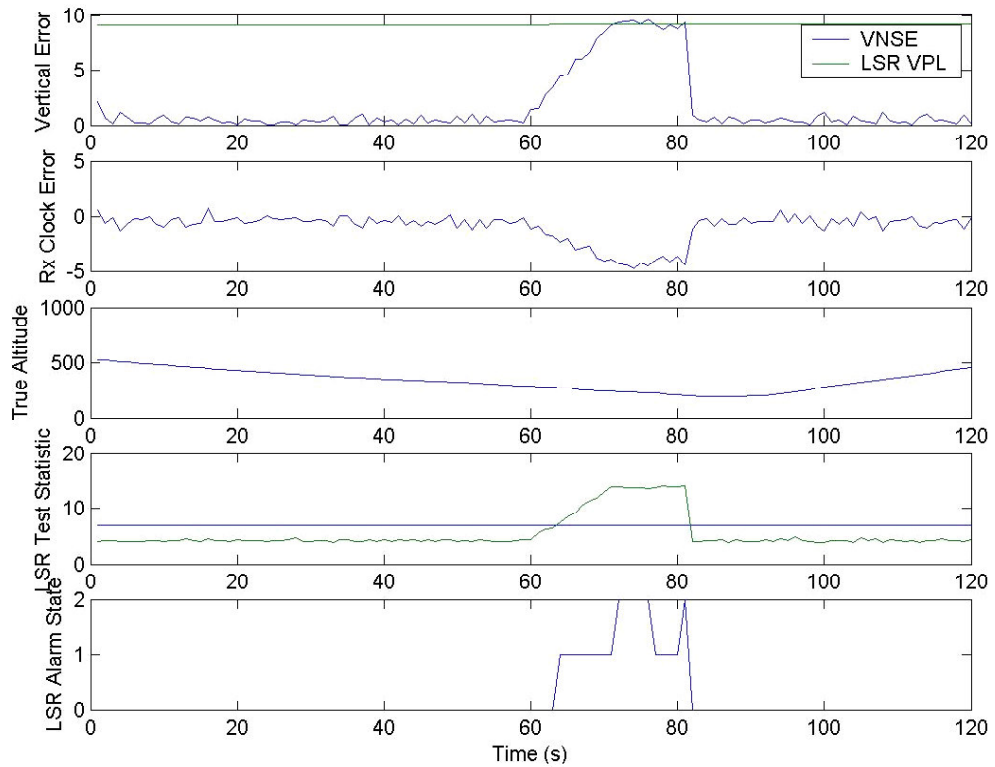


Figure 12-28 : LSR RAIM Response to Ramp Bias

These traces show how VNSE, clock error and LSR Test Statistic ramp up as the bias is applied and held. As expected, the RAIM algorithm detects the FE before the VPL is exceeded, and maintains that detection throughout the duration of the FE.

12.3.5 EIV RAIM, Ramp Bias, Snapshot User Clock

Figure 12-29 shows the same Ramp Bias case as for Figure 12-28, as processed by the EIV algorithm with a snapshot user clock approach.

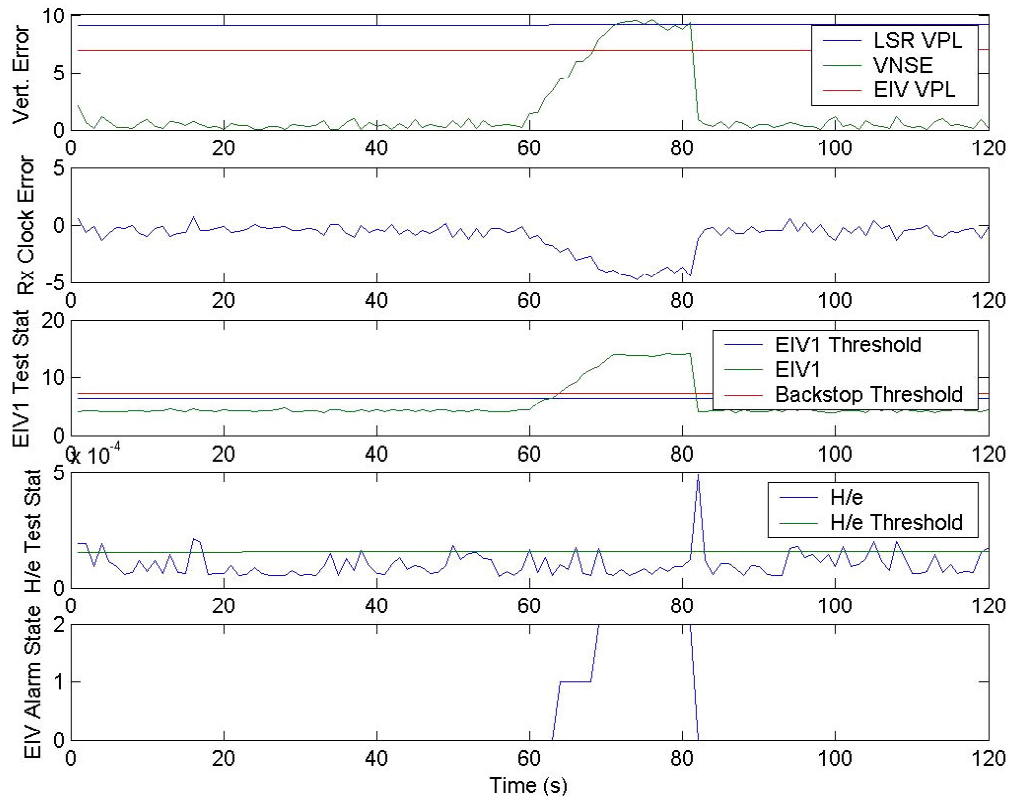


Figure 12-29 : EIV RAIM Response to Ramp Bias

The point to note here is demonstrated by the fourth trace, in which the H/e Test Statistic is fluctuating around its detection threshold. In particular note that this statistic does not appear to react to the applied bias in any prominent way, except for the point where the bias is removed (as a step function), where the H/e trace displays a sharp spike.

Although there are no missed detection in this case, this is entirely due to the backstop threshold providing the required integrity.

These plots suggest that for Feared Events with an increasing bias (which provide the characteristics against which current RAIM receivers for aeronautical applications are defined [56]) the EIV algorithm in itself would not be acceptable, if a snapshot approach is used to update the user receiver clock.

12.3.6 EIV RAIM, Ramp Bias, Filtered User Clock

Figure 12-30 shows the same Ramp Bias case as for Figure 12-28, as processed by the EIV algorithm with a filtered user clock approach. As with the Step Bias case, these plots suggest that applying a simple filter

to the user clock allows the H/e Test Statistic to more closely trace the characteristic of the input FE and applied noise.

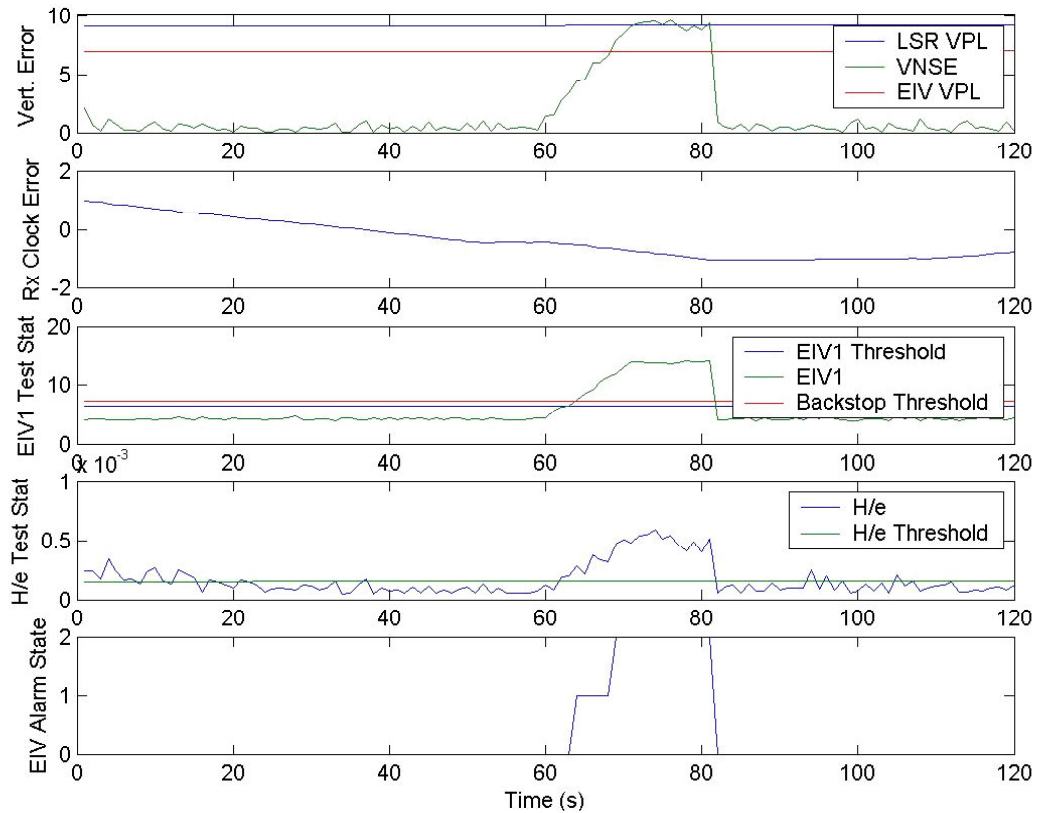


Figure 12-30 : EIV RAIM Response to Ramp Bias (Filtered Clock)

12.3.7 EIV RAIM, Ramp Bias, System-Switchable User Clock

Figure 12-31 represents a similar analysis to that shown in Figure 12-30, but using an alternative approach to mitigate the effect of the Feared Event contaminating the user clock estimate, and hence causing the H/e test statistic not to track the VNSE. This technique is referred to as the “System-Switchable User Clock” technique, and it takes advantage of the fact that when using combined Galileo and GPS constellations for RAIM, each system can provide an independent estimate of the user clock error. It is therefore possible to provide user clock error estimates based on Galileo-only, GPS-only and combined system measurements simultaneously. In the event of a Feared Event occurring, these three measurements will diverge in some way. By providing some thresholds for this divergence it is relatively simple to set up some switching logic such that the user clock is slaved to one of these three update sources at any time.

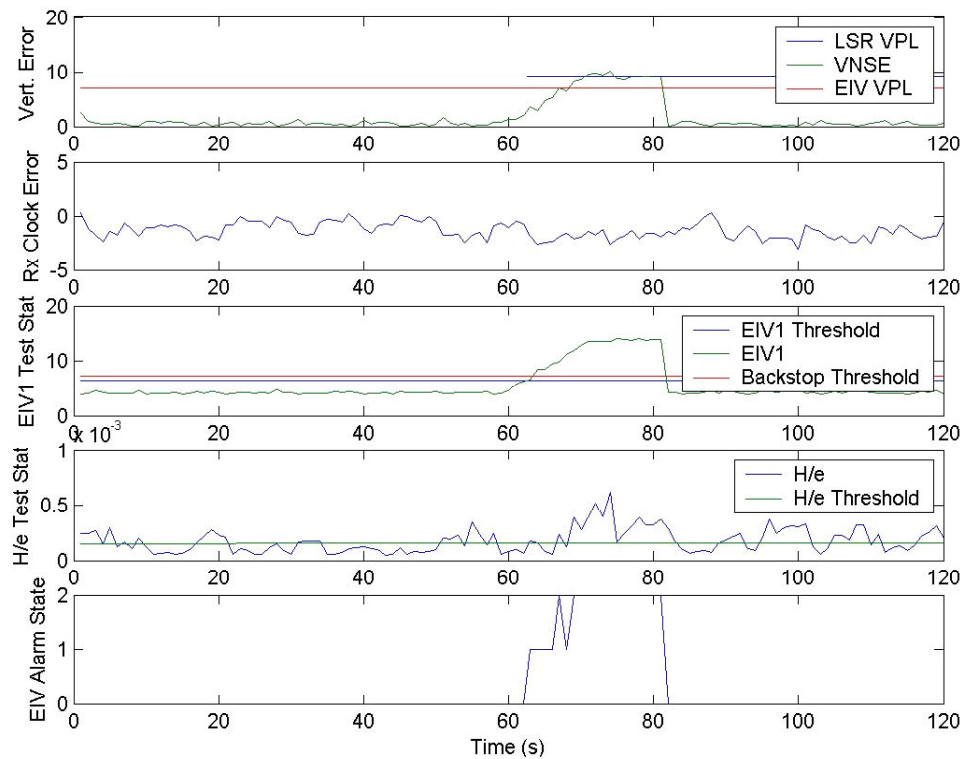


Figure 12-31 : EIV RAIM Response to Ramp Bias (Switchable Clock)

In Figure 12-31 a system has been modelled in which the user clock is nominally updated by the clock error estimate coming from the combined GPS/Galileo navigation solution. However, the clock error estimate from GPS-only and Galileo-only solutions are compared at every epoch, and if these disagree by more than twice σ_T then¹⁶ the Executive Clock becomes either the GPS or Galileo-slaved clock, depending upon which is closer to the previous clock error estimate.

Figure 12-32 demonstrates the activity of this Executive Clock selection function. Before the start of the Feared Event the clock update estimate derived from Galileo alone is very close to the estimate from the combined constellation (i.e. the clock estimate is dominated by the Galileo satellites in view). As the bias ramp begins to take effect (which in this case occurs on a particular Galileo satellite which is the dominant satellite for both vertical accuracy and user clock estimate), the Galileo and combined system clock estimates begin to diverge from the GPS-only estimate.

¹⁶ where σ_T is the standard deviation of the time accuracy from the combined system, derived from the 4th element of the diagonal of the Dilution of Precision matrix, analogous to σ_V discussed previously.

At some critical point, relatively early in the rise of the VNSE, the two single-system clock estimates diverge beyond the set threshold, and GPS time is selected as the Executive Clock to update the user clock. This is shown by the trace labelled “Executive” being superimposed on the GPS trace from approximately 65 seconds into this graph, as shown by the arrow.

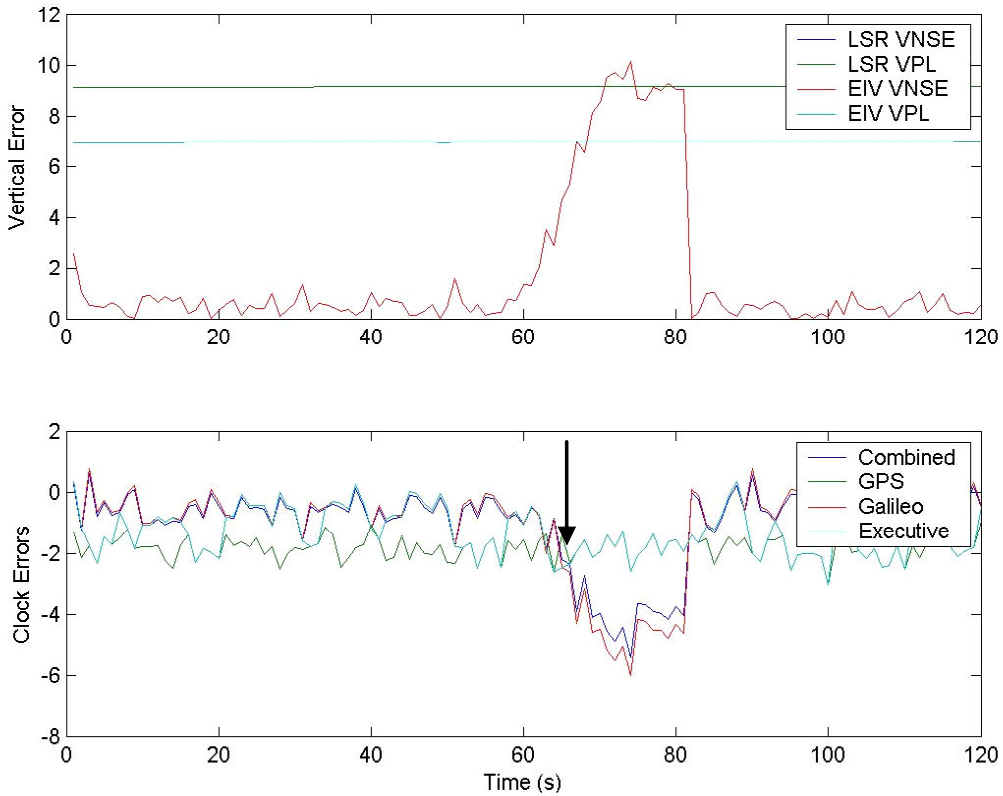


Figure 12-32 : Selection of Executive Clock

This technique appears to provide an alternative to filtering as a method for overcoming the shortcoming in the EIV method regarding user clock contamination due to a biased measurement. However it is only applicable for use with a combined constellation – the System-Switchable User Clock technique cannot be used for Galileo-only applications.

12.3.8 EIV RAIM, Ramp Bias, Ideal Clock

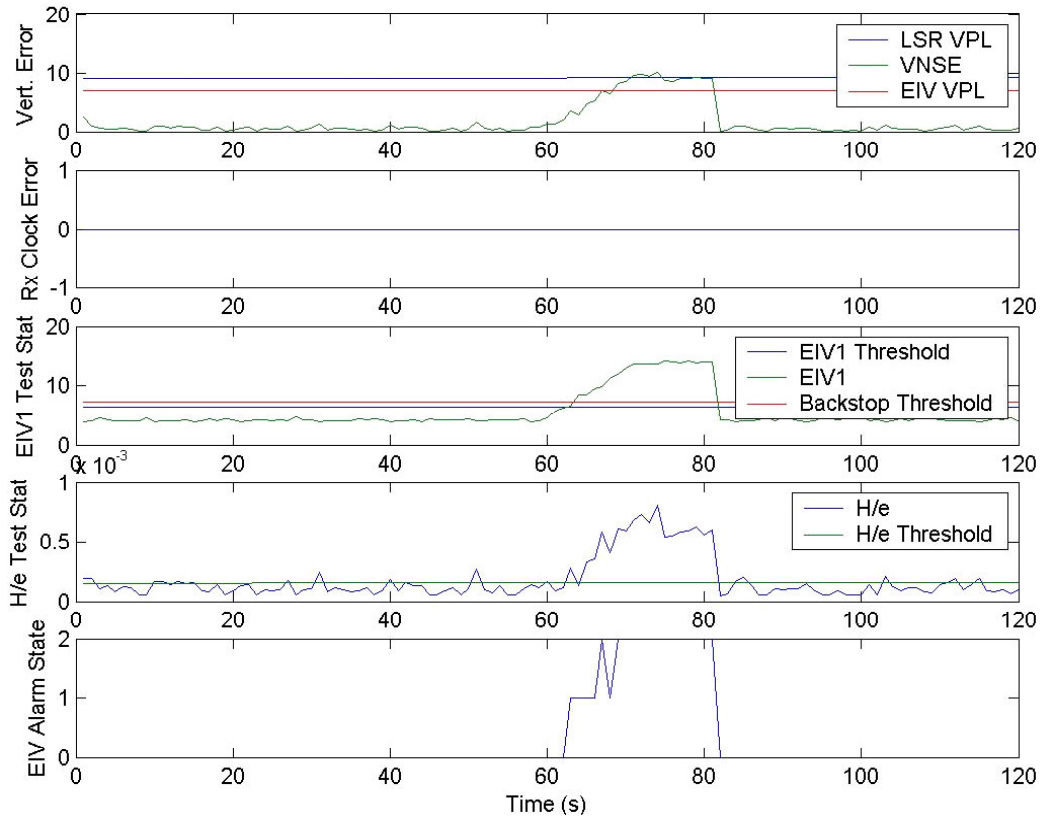


Figure 12-33 : EIV RAIM Response to Ramp Bias (Ideal Clock)

Figure 12-33 represents a similar analysis to that shown in Figure 12-30, but using an alternative approach to mitigate the effect of the Feared Event contaminating the user clock estimate, and hence causing the H/e test statistic not to track the VNSE. Instead of relying on clock filtering or the use of two independent systems whose time references can be compared, this technique assumes that a user has a clock which is sufficiently stable that it can be held fixed for the duration of the final approach, without any clock updates from the navigation solutions. With recent advances in atomic clock technology, rubidium atomic frequency standard (RAFS) clocks of size, weight and cost applicable to avionics applications are now becoming available. By using such a clock as part of the Galileo/GPS receiver and holding the clock during the approach, it appears to be possible to use the EIV algorithm in a way which allows H/e to track the VNSE even more closely than with either the filtered clock or system-switchable clock methods.

12.3.9 EIV RAIM, Step Bias, with FDE

The cases analysed previously have all assumed that no Fault Detection and Exclusion (FDE) algorithms are employed. Figure 12-34 presents the results for the EIV RAIM with unfiltered clock response to a step function (the same Step FE used in previous cases), but in this case a simple FDE algorithm has been used. When the RAIM algorithm generates an alarm, an FDE subroutine is called which calculates the LSR RAIM test statistic for every case with one of the satellites in view excluded (i.e. with 17 satellites in view 17 values of test statistic are evaluated). It is assumed that the satellite which has been excluded in the case which produced the lowest value of LSR RAIM test statistic is the satellite on which the bias causing the alarm to be generated is applied. The broadcast almanac for this satellite is then set to “Not Use”, and it is excluded from the rest of the run.

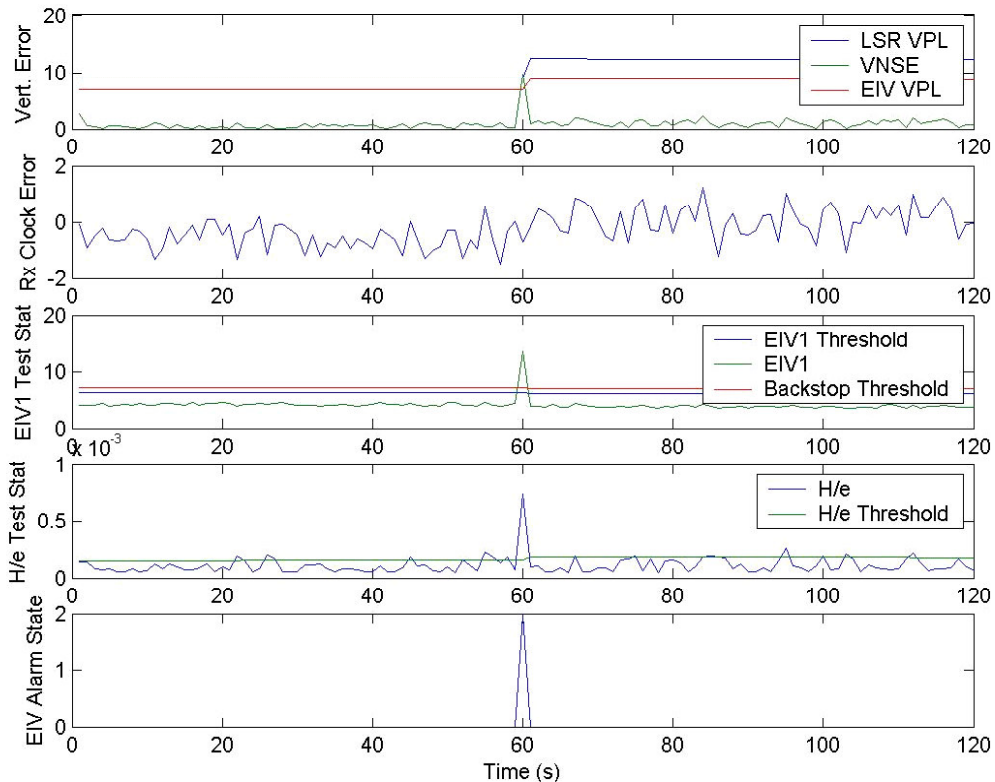


Figure 12-34 : EIV RAIM response to Step Bias, with FDE Active

The point at which the satellite is excluded is clearly indicated by the increase in VPL for both LSR and EIV RAIM methods in the uppermost plot. As soon as the satellite is excluded the $\sqrt{\text{USSE}}$ and H/e test statistics both return to normal levels from their spikes at the time of alarm.

12.3.10 EIV RAIM, Ramp Bias, with FDE

Figure 12-35 presents the results for the EIV RAIM with unfiltered clock response to a ramp function (the same Ramp FE used in previous cases), with the FDE subroutine described in the previous section applied. This shows similar characteristics to the Step function response discussed previously, but in this case the FDE subroutine and RAIM have clearly been triggered by the $\sqrt{\text{USSE}}$ statistics exceeding the Backstop threshold. With no filtering of the clock the H/e statistic does not appear to register the occurrence of the ramp Feared Event.

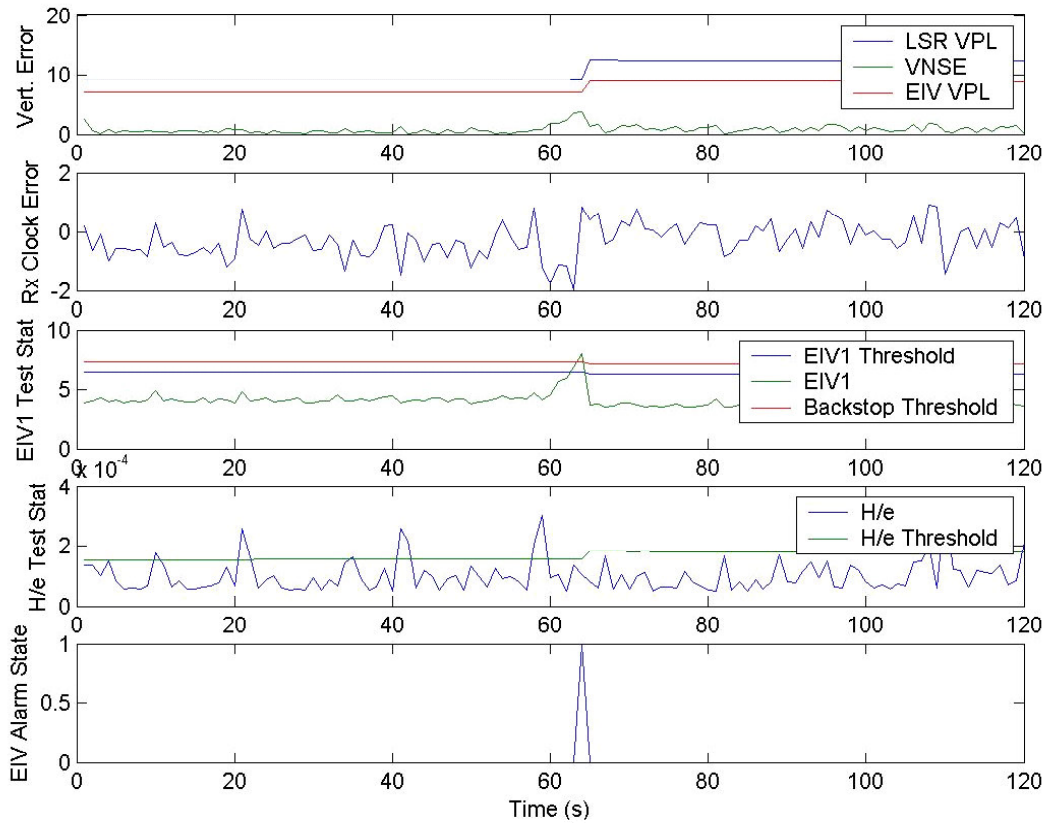


Figure 12-35 : EIV RAIM response to Ramp Bias, with FDE Active

13. DISCUSSION

This section discusses the results from the RAIM study presented in the previous section, and attempts to integrate these results with the conclusions from the Integrity Justification study.

13.1 Service Volume Performance

The results in Section 12.1 demonstrate the following main points:

1. If Galileo is used alone, with a 10° masking angle and standard Least Squares Residuals RAIM, the minimum availability of RAIM integrity to a Vertical Alert Limit of 20m is about 86%. This is far short of the availability requirement of 99.5% specified for the Galileo Safety of Life Service (SoL).
2. If instead the EIV algorithm is used, worst case availability is about 97%. However, the global weighted average availability is about 99.8%. Since the loss of RAIM availability (“RAIM Holes”) is entirely deterministic (i.e. the presence of a RAIM hole over a destination airfield may be predicted at the time of filing a flight plan) it may be possible to make a case that weighted average availability greater than 99.5% is sufficient to meet the SoL specifications.
3. There is often a significant difference between weighted average availability and worst case availability, and for the Galileo-only cases this worst case availability often occurs in tropical regions, well away from the European Civil Aviation Conference (ECAC) region. Constraining the Galileo design such that the performance availability specifications must be met at the worst location globally, rather than as a global average, may significantly increase the difficulty of the task, possibly with little benefit. It is recommended that the impact that the current definition of availability will have on the Galileo element performance specifications should be identified as a matter of urgency.
4. Using the EIV algorithm with Galileo only, the availability of RAIM at the worst user location is estimated to be around 99.95% for a 20m VAL, if a masking angle of 5° is used. This would meet the SoL specifications if the masking angle is taken to correspond to the recommendations of the EUROCAE Galileo Working Group, rather than the 10° constraint used in the standard Galileo use case.
5. The minimum masking angle therefore has a very significant impact on the overall availability of integrity. It is recommended that the impact that the current definition of masking angle will have on the

Galileo element performance specifications should be identified as a matter of urgency. In particular, for the Galileo SoL service whose specification is closely aligned with the requirements for aviation precision approach, the justification for using a more demanding masking angle than that usually specified by the aviation community should be very well justified, given the impact that this constraint may have on Galileo system design.

6. When considering Galileo + GPS combined constellation performance, the additional level of over-determination of the navigation solution provides a very significant improvement in RAIM availability.
7. With a 10° masking angle, a combined constellation system using EIV RAIM should easily exceed the specifications for the SoL service (99.8% availability at the worst user location, for a 20m VAL);
8. With a 5° masking angle, Cat I performance may be considered, with worst case availability to 15m VAL of 99.6%, and global average availability to 12m VAL of 99.8%.
9. The SISA/IF system, assuming the constraint of no more than 3 critical satellites is applied for integrity to be available, should easily meet the specifications for the SoL service at the worst user location. However, the worst case availability to 15m VAL of around 97% suggests that it might be quite difficult to improve the system to the point where it might be considered for Cat I globally. However, within ECAC Cat I levels may be achievable, since the drop-off in availability at 15m VAL occurs in a very narrow equatorial band.
10. For all the Galileo-only analyses, the availability of integrity drops off significantly when considering the states with one and two disabled satellites. This is especially true for the SISA/IF case, where the reduction in the number of satellites in view is made worse by the constraint of having no more than three critical satellites in the navigation solution. This makes the results presented for the Galileo-only cases quite sensitive to the assumptions made regarding the state probabilities for one and two satellite disabled cases. The current assumption of 0.98 state probability for all satellites operating translates into an average downtime per operational satellite of about 6 hours per year. Although the SISA/IF performance to 20m VAL has sufficient margin that the SoL specification should be met even if the average Galileo downtime is significantly higher than this, the validity of the other Galileo-only performances discussed above should be treated with care. However, the Galileo + GPS case results are relatively insensitive to the state probabilities applied for single and double satellite outage cases.

13.2 Navigation Engine Performance

The Navigation Engine tool has provided a useful method for demonstrating that the EIV algorithm gives an improved VPL compared with LSR RAIM, whilst simultaneously confirming that the assumptions made in developing the EIV algorithm are valid. Specifically, the EIV algorithm assumes:

- The Total Least Squares position solution can be manipulated to yield two test statistics, $\sqrt{\text{USSE}}$ and H/e, that are independent of each other, and that each have a linear relationship with vertical navigation system error;
- When the **C** matrix in the EIV method is correctly configured, the $\sqrt{\text{USSE}}$ test statistic has a χ^2 distribution and hence detection thresholds can be set using a similar approach to that for LSR RAIM;
- When the **D** matrix in the EIV method is correctly configured, the H/e statistic has a half-normal distribution;
- The standard deviation of this half-normal distribution can be readily evaluated based on the characteristics of the H/e statistic.

The results for the EIV algorithm from the NavEng tool have all been entirely consistent with these assumptions.

In all cases examined the false alarm rate has been consistent with the specification, which suggests that the thresholds on the two test statistics have been set correctly, which in turn implies that the underlying distributions of these statistics have been correctly modelled. This has been demonstrated to be true even at the very low probability levels required to demonstrate RAIM algorithms, by using simulation runs with 10^7 samples, against a P_{FA} of 8×10^{-6} .

The detection capability for a step bias has been clearly demonstrated, with a missed detection performance consistent with the specification. Since the EIV VPL is evaluated by using a numerical method to find the worst case bias, given the assumed distributions of the test statistics and the vertical navigation system error, any flaws in the assumptions regarding these distributions would be readily apparent. As it stands, the results match expectations very closely.

The performance of the LSR RAIM algorithms show two interesting features:

1. Under certain conditions, the LSR algorithm appears to underestimate, the VPL, in that a worst case bias can be found that

can be applied to significantly exceed the specified missed detection requirement;

2. Under certain conditions (in particular with a large number of satellites in view, some of which are relatively close together from the perspective of the user) the VPL evaluated by the RAIM algorithm can be improved by removing some of these satellites from the navigation solution. This is because they add little to the accuracy of the navigation solution, but increase the required detection threshold, and hence the VPL.

Thus it is quite easy to demonstrate that the LSR algorithm is less than optimal and that, therefore, there is merit in investigating more sophisticated RAIM algorithms, such as EIV.

13.3 Flight Trials Simulation Performance

The results from the Matlab Flight Trials simulations provide a useful addition to the NavEng experimentation. In particular, these runs enabled the following points to be validated:

- The performance of the LSR and EIV algorithms when dealing with signals in which the components of OD&TS error, tropospheric error and other environmental error are modelled separately, rather than just as a combined noise source with a normal distribution;
- The performance of these algorithms with a combined GPS/Galileo constellation on which there is some undeclared system clock offset;
- The performance of these algorithms with step and ramp feared events.

The main result arising from this phase of experimentation is that the EIV algorithm cannot be treated as a “snapshot” RAIM algorithm in the same way as LSR.

With the LSR algorithm, the magnitude of the RAIM test statistic is not affected by a bias in the user clock. Since such a bias applies a common error to each received measurement, the magnitude of the bias does not affect the magnitude of the range residuals. Therefore, the magnitude of an LSR test statistic depends entirely on the consistency of the received measurements, and is independent of the user model (i.e. the accuracy of the user linearisation point and clock bias).

EIV RAIM, on the other hand, is very much dependent upon the user model, since the H/e test statistic is a measure of the ratio of changes that are made to the user model compared with the range residuals. An

initial clock bias at the time of initiation of a Feared Event will therefore affect the ability of the RAIM algorithm to detect errors.

This manifests itself differently with a ramp bias compared with a step bias feared event.

With a step bias feared event, assuming that before its application the system was operating nominally and so the user clock has no outstanding bias, the H/e test statistic initially detects the bias in the same way as the LSR test statistic. However, if the system does not use Fault Detection and Exclusion, so the biased measurement is not immediately rejected, the effect of this step error will be to add some bias to the user clock estimate. This will effect the user model used at the next epoch by the EIV algorithm, so that whilst the bias is sustained the H/e component of the EIV algorithm no longer detects a problem. The test statistic then drops away back to normal levels, and so the normal H/e component response to a step bias is a short spike at the time of application, and again on removal of the bias. This is shown very clearly in Figure 12-26.

With a ramping error feared event, the effect is more insidious. Because the clock error increases gradually, epoch by epoch, the H/e test statistic of the EIV algorithm may not detect the change in the user model at all. This is shown clearly in Figure 12-29, where the ability of the EIV algorithm to detect the feared event is due entirely to the Backstop threshold on the $\sqrt{\text{USSE}}$ test statistic, whilst the H/e statistic shows no indication of the presence of a bias until the bias is removed as a step function.

In fact, although we have only discussed the effect of errors in the clock estimate on the response of the H/e statistic, in theory the EIV algorithm is sensitive to any errors in the user model, the amount depending upon the terms in the **D** matrix and hence the extent to which the “H” term is allowed to admit errors in the user model in each dimension.

This puts a significant restriction on the use of EIV for RAIM: in effect, *the EIV RAIM algorithm is only useful for detecting faults occurring in a given epoch, if the linearization point derived from the previous epoch is known to be “good”.*

Because of this feature of the EIV algorithm, great care must be used in its implementation. However, as was seen in Figure 10-4 and Figure 10-5, simulations using the Navigation Engine suggest that there is little or no correlation between lateral errors and H/e test statistic, whereas there is a very strong correlation between vertical error and H/e.

In theory, the techniques demonstrated for controlling the contamination of clock error should be adequate to protect against vertical errors in the

linearization point as well. The reason for this is similar to the argument illustrated by Figure 10-3, which shows how changes in the vertical component of the linearization point manifests itself differently in the pseudorange errors to different satellites, depending upon their elevation. If one considers for example a receiver with a 10m bias in its estimate of clock error, this would have a fairly small impact on the estimate of lateral position, because the error would appear in measurements from a variety of directions in azimuth, yet it would have a significant impact on vertical error, since all measurements come from above the user. As a result, clock error and vertical error are closely linked. Therefore, in theory, as long as the clock error component of the user model is managed to prevent it being contaminated by ramping biases, the EIV algorithm should be useable as a valid RAIM technique to protect vertical position solutions derived from a standard least squares fit algorithm.

Three different techniques have been demonstrated to show that the EIV algorithm can be used as a powerful RAIM system, as long as measures are taken to prevent the clock error component of the user model being contaminated by the feared event which the RAIM algorithm is intended to protect against. These methods are:

- Use some form of clock filtering technique, such that the user clock estimate used by the EIV algorithm is not updated on an epoch-by-epoch basis, but is instead updated with some filtered estimate of the clock error, with a time constant sufficiently long that it would enable the detection of any proscribed ramping bias;
- Use some form of selective switching technique, such that the consistency of clock state estimates are compared using different sources, and some logic is applied as to which source becomes the “Executive Clock” in the event that the sources diverge beyond some set limits. The most obvious example of this is where Galileo and GPS are used together, so that a user has two independent clock error estimates, along with one combined navigation solution estimate, which can be compared against the user clock. This technique appears to provide quite strong defence against contamination of the user clock estimate, and hence would be a good solution for combined GPS/Galileo RAIM implementations;
- Use a very stable clock such as an avionics-grade RAFC as part of the receiver equipment, and use a clock-coasting mode when entering phases of flight requiring high integrity, such as precision approach. Such a technique would require some significant safeguards to ensure that the clock state is not corrupted in the moments before entering clock-coasting mode, but offers the solution with the best overall performance.

One additional benefit of using the latter approach is that when clock coasting, the navigation equations could be modified to solve for just the three unknowns of spatial position. This would yield a solution with a smaller σ_v and one more degree of freedom, and hence one would expect an improvement in the VPL that would be evaluated in these circumstances. This is an interesting point, but is beyond the scope of the current research activity.

13.4 Comments on the Physical Implementation of the EIV Method

At this point it was worth returning to the analytical treatment of the EIV method presented earlier to gain more understanding of what the H/e statistic represents. These terms were introduced in Equation 10-1 as:

$$\mathbf{y} = (\mathbf{G} + \mathbf{H}) \cdot \mathbf{x} + \mathbf{e}$$

From which we can make the expansion

$$\mathbf{H}_i \mathbf{x} = \mathbf{H}_{i1} \mathbf{x}_1 + \mathbf{H}_{i2} \mathbf{x}_2 + \mathbf{H}_{i3} \mathbf{x}_3 + \mathbf{H}_{i4} \mathbf{x}_4$$

Thus the perturbation matrix \mathbf{H} operates on the difference between the actual position/time state and the linearization point. If the pseudorange on observation on the i^{th} observation has a significant bias then the above components of \mathbf{H} can be used to cancel out this bias in the TLS position solution. The greater the size of the components of \mathbf{x} the smaller the components of \mathbf{H} need to be to achieve the same effect, since the corrected bias is the product of \mathbf{H} and \mathbf{x} .

In Section 10.2 it was stated that the objective function to be minimised is $\|\mathbf{C}[\mathbf{H}\mathbf{e}]\mathbf{D}\|$. From the descriptions of the \mathbf{C} and \mathbf{D} matrices discussed earlier it is seen that this objective function F can be expanded as follows:

$$\begin{aligned} F &= \|\mathbf{C}[\mathbf{H}\mathbf{e}]\mathbf{D}\|_F \\ &= \left(\frac{H_{11}d_1}{\sigma_1} \right)^2 + \dots + \left(\frac{H_{i1}d_1}{\sigma_i} \right)^2 + \left(\frac{H_{i2}d_2}{\sigma_i} \right)^2 \\ &\quad + \left(\frac{H_{i3}d_3}{\sigma_i} \right)^2 + \left(\frac{H_{i4}d_4}{\sigma_i} \right)^2 + \left(\frac{e_i d_5}{\sigma_i} \right)^2 \\ &\quad + \dots + \left(\frac{e_n d_5}{\sigma_n} \right)^2 \end{aligned}$$

Thus, the σ_i terms normalise the contributions corresponding to each satellite's pseudorange measurement, and the d_j terms weight each component of the vector containing offset (three position components and clock) and pseudorange residual. Therefore, if d_j is small the corresponding components of the vector contribute little to the cost function F , and the solution will permit relatively large values of H_{ij} or e_i as appropriate. Conversely, if d_j is large then that component of the vectors will probably dominate the cost function, and so will be tightly minimised.

When discussing setting the \mathbf{D} matrix in Section 10.3.2 it was shown that for our purposes we choose to use a matrix in which the first three terms have a unity value, the fourth term has a value some two orders of magnitude reduced, and the fifth term is reduced by 5 or 6 orders of magnitude on unity. These values minimise the components of \mathbf{H} corresponding to position offsets, allow moderate values for clock offset, and admit a large amount of latitude for the residuals.

By setting the terms of the \mathbf{D} matrix in this way we are implicitly recognising the following points:

1. Clock errors and height errors are very closely linked. As mentioned above and by referring back to Figure 10-3 it can be seen that a clock bias is very similar moving the antenna along the vertical axis, in terms of the impact on the pseudorange measurements. A clock bias adds or subtracts the same amount to each pseudorange, while moving the antenna vertically changes the pseudorange in the same direction, but not equally. Hence there is a very strong correlation between the "clock" and "up" error states;
2. Because of the relatively high drift rate in the type of crystal oscillator typically used in GNSS receivers, errors in the linearization point are likely to be dominated by the clock component;
3. For aviation precision approach, vertical protection is more demanding than lateral protection, therefore we wish to optimise the algorithm for vertical protection.

Based on the argument developed above for the effects of the weighting matrices on the EIV solution, $\|\mathbf{H}\|$ will be dominated by the \mathbf{H}_{i4} values (corresponding to the receiver clock offset), whilst $\|\mathbf{e}\|$ will be almost equal to the norm of the least squares residuals vector. Because of the minimisation used the values of \mathbf{H}_{i4} obtained will depend on the values of d_4 and \mathbf{x}_4 .

Thus the sensitivity of the EIV method to errors in the clock component of the linearization point is related to the value chosen for the d_4 term. This suggest that a larger (i.e. closer to unity) value for this term would

make the algorithm less sensitive to clock errors, but would also make the H/e statistic less useful as a RAIM statistic. Conversely, making the d_4 term even smaller would admit larger values of clock offset into the value of $\|H\|$, potentially making the H/e statistic more sensitive, but also making the task of managing the errors in the linearization point more difficult. In practice the values to be used in tuning the D matrix would need to be set based upon parameters such as the drift rate of the receiver's clock and the method being used to manage the receive clock estimate for the linearization point.

The approach taken to setting the D matrix in this thesis has effectively "tuned" the process to make a RAIM algorithm sensitive to clock errors, and has then taken advantage of the correlation between clock error and vertical error to use the algorithm for vertical protection during precision approach. It should be noted that this was not a deliberate process when undertaking the simulation trials described earlier; This understanding of the relationship between the terms of the D matrix and the sensitivity to errors in the linearization point has arisen from analysis of the results of the simulations.

Therefore, although the EIV method has been shown to offer significant improvements compared with LSR RAIM when evaluated in a strictly defined simulation environment, a great deal of practical experimentation would be required to show that the shortcomings previously discussed can be suitably managed. In the previous section it was stated that the EIV RAIM algorithm is only useful for detecting faults occurring in a given epoch, if the linearization point derived from the previous epoch is known to be "good". How "good" this has to be depends upon issues such as the drift rate of the receiver clock, the dynamics of the receiver (such as the rate of change of vertical position) and effects of filtering in the receiver on both clock and position. These effects will place constraints on the errors in the linearization point that the EIV algorithm would have to deal with from epoch to epoch.

13.5 RAIM in the Context a of Global Integrity Service

The results from the Integrity Justification Study and the RAIM Study can be summarised in the following two statements:

1. The Galileo Integrity Determination System will cost much more to develop, deploy and operate than it is ever likely to recoup in commercial revenues, therefore its inclusion in the Galileo system architecture cannot be justified on commercial grounds;
2. Given the predicted future performance of Galileo and GPS free to air signals, RAIM algorithms will offer users an integrity monitoring capability at least as good as that from the Galileo IDS.

Although the demonstration of these points is adequate to meet the objectives of this thesis as presented in the problem statement at Section 1.3, a number of other questions have arisen in the course of this work that deserve some brief discussion, to provide a context for these conclusions.

13.5.1 Context of Galileo Integrity Service

Over the duration of the research activities leading to this thesis the case against the inclusion of an Integrity service in the Galileo system has grown significantly; indeed, in February 2004 the Chief Engineer of the UK's National Air Traffic Services (NATS) stated publicly [57] that the operators of the US WAAS system and the Japanese MSAS system intend to provide integrity for Galileo through their own systems, at a stroke taking away a large fraction of the previously assumed market for Galileo integrity services. Furthermore, progress continues to be made on other regional augmentation systems, in Australia and India for example, further weakening the potential market for a global integrity service. Yet, at the time of writing, the Galileo Joint Undertaking, the quasi-Governmental body responsible for taking the Galileo programme from public to private operational management, remains committed to specifying a Safety of Life service and an encrypted integrity-based Commercial Service in the Galileo high-level system requirements.

The Galileo Working Group of the European Organization for Civil Aviation Equipment Manufacturers (EUROCAE) has also undertaken a number of studies [58] into possible concepts for operations for the use of Galileo to assist aviation precision approach. It is interesting to note that these studies consistently note the potential for a combined GPS/Galileo RAIM system as a backup integrity barrier, yet equally consistently reject the notion of using RAIM as an alternative to the Galileo IDS. One could postulate a number of reasons for this resistance, from an unwillingness to knock down one of the pillars on which Galileo was "sold" to politicians, to the commercial self interest of certain companies involved in these discussions, to a more human, instinctive unwillingness to conclude that airborne avionics can be entrusted with determining the integrity of a navigation position solution during final approach.

The author believes that a perfectly sound concept of operations is possible using RAIM, in conjunction with GPS and space-based augmentation systems other than the Galileo IDS. If we consider an environment in which EGNOS, WAAS and MSAS are all providing an integrity service for both GPS and Galileo, a suitably equipped user could have integrity adequate for precision approach, given any two from three from GPS, Galileo and SBAS. If either GNSS (GPS or Galileo) were for any reason unavailable integrity would still be provided by the

other system through SBAS. If SBAS were unavailable, the two GNSS would provide adequate integrity through RAIM, as demonstrated in this thesis. This should provide sufficient redundancy for even the most demanding safety of life user groups, without the need for a Galileo IDS.

The sticking point in such discussions is the possibility that some feared events may exist which RAIM cannot protect against. There may potentially be some failure mode for Galileo which can cause hazardous misleading information to an airborne receiver, whilst not generating a RAIM alarm. Examples of such failure modes are difficult to come by, but they cannot be dismissed out of hand. The author's response to this argument is that it doesn't make sense to build an expensive IDS at this stage of the programme, to protect against unknown failure modes. It would be wiser to develop and deploy the Galileo system without in-built integrity, and add an integrity system at some later point, when the behaviour of the system is better characterised. This would have the additional benefit of shifting the capital expenditure for this aspect to the programme much closer to the point at which revenues might be expected, hence improving the internal rate of return on the programme, as discussed in the Integrity Justification Study.

13.5.2 Time To Alarm – A Problem for Galileo

In Section 5.6.2 a brief discussion of the constraint that the Time to Alarm (TTA) requirement puts on the Galileo IDS was presented. Over the duration of the development of this thesis it has become apparent that the TTA specification is arguably the single biggest cost driver on Galileo, as currently defined. Indeed, the entire system architecture has effectively been driven by this single requirement.

As currently defined, the Galileo satellites have no inter-satellite links. In order for the ground segment to communicate with any satellite, direct contact has to be established between the satellite and an uplink station. Had inter-satellite links been employed then it would be possible to use any satellite in contact with the ground as a relay, so that telemetry, telecommand and, in particular, navigation data messages could be passed up and down using the satellites themselves as a communications network. The use of links was discussed early in the system engineering phase of Galileo, and rejected on the grounds that it would be too difficult to ensure that the 6 second TTA requirement could always be met with such an architecture.

As a result, the Galileo architecture now includes a network of around 30 Uplink Stations used exclusively for uplinking navigation and integrity data messages to the satellites in the constellation (which is entirely distinct from the network of telemetry, tracking and commanding stations used for spacecraft monitoring and control), along with a high integrity, high speed mission data network linking all of these stations to two hot

redundant control centres. This complex and costly “Mission Segment” is driven entirely by the 6 second TTA requirement. Without this requirement there is little doubt that the early trade-offs on Galileo would have included inter-satellite links (as is the case for the GPS satellites currently being launched to replenish the constellation) in the baseline architecture, and greatly simplified the Mission Segment.

Yet although TTA has such a profound impact on the design of Galileo’s IDS, for RAIM it is almost irrelevant. It is inconceivable that a receiver using RAIM would struggle to meet a 6 second TTA. This point hasn’t been analysed in this thesis – it is very difficult to demonstrate, and adds little value to testing the problem statement – but it should be considered in any discussions regarding the future evolution of the Galileo system.

13.5.3 RAIM as a Solution to the Integrity Problem

The introduction to this thesis referred to the often observed phenomenon that if there is a way to get a useful service for free, somebody will find a way to get it. In this context, the “useful service” is the high-integrity navigation solution, and the way to get it “for free” is by using RAIM.

This provides two kinds of problem: Firstly, for the Galileo system designers, the Galileo and GPS free-to-air signals will “cannibalise” their market, which affects the business case for development of the IDS, as previously discussed. Secondly, it provides a problem for developers of RAIM algorithms – specifically, how to have their algorithm accepted by the user community and, ideally, how to make money from the process.

This thesis has concentrated on aviation precision approach as the target audience for the integrity systems under comparison. One important feature of the aviation market that is worthy of note is that all air navigation systems must be based on accepted standards, and all such standards must be in the public domain. This means that it is impossible for any individual or organisation to patent a new RAIM algorithm, get it accepted as a new international standard for airborne GNSS receivers, and hold a monopoly on the rights for its use.

At present the LSR RAIM algorithm is enshrined within ICAO standards as the standard RAIM algorithm to be used, where RAIM is applicable (i.e. as a backup to SBAS, for detecting local errors). For EIV, or any other better-performing RAIM method to usurp LSR as the designated standard would take an enormous amount of work, be it analytical, experimental and even political in terms of the lobbying that is required to make such a fundamental change to ICAO standards. Without some underlying business case, nobody is likely to take up this battle.

13.5.4 Further Development of EIV

This then leaves us in a position in which we have demonstrated a new RAIM algorithm which appears to provide significantly better performance than the LSR method, and which provides a strong argument against the further development and deployment of the Galileo IDS. However, EIV has some significant weaknesses, in that it needs to be used as part of an integrated system to protect against gradually ramping biases, perhaps using stable on board clocks, barometric aiding or inertial sensors. This takes it away from being a true RAIM algorithm and is more properly an “Assisted Autonomous Integrity Monitoring” (AAIM) method.

The author expects the integration of navigation systems with other sensors to be a major area for growth in the coming years, both in academic circles and for commercial applications. Given the barriers mentioned above to the commercial exploitation of a new RAIM algorithm through international standards, perhaps the most promising route to developing a business case for EIV is through the development of some integrated sensor suite, incorporating the principles of EIV RAIM in some way.

13.5.5 The Future for the Galileo IDS

At the time of writing, as Europe prepares to enter the Full Development, Initial Deployment and Initial Operations (Phase C/D/E1) Phase of Galileo, the Safety of Life Service remains within the service requirements for the system, and hence the IDS (more accurately, the Integrity components of the Galileo Mission Segment) remain enshrined in the system architecture. Unsurprisingly, the estimated costs to complete the programme continue to climb, mainly in the area of the Mission Segment, and the integrity requirements continue to provide the greatest technical challenges.

Yet there is still no evidence that the market drivers for high-integrity navigation solutions, such as the airlines, actually want the solution being offered by Galileo.

The consortia putting together their bids to operate Galileo under a public/private partnership will no doubt undertake their own detailed cost benefit analyses and, it is hoped, will propose system architectures which best meet the requirements of the market for Galileo services. A comparison of the conclusions of these analyses with those presented within this thesis offers an opportunity to assess how well the problem statement has been addressed. This will be the “acid test” for the arguments presented in this thesis.

14. CONCLUSIONS AND RECOMMENDATIONS

14.1 Conclusions

The first part of this thesis, the Integrity Justification Study, demonstrates that the inclusion of a ground-based integrity system in Galileo is incompatible with the desire to fund the deployment and operation of Galileo through private investment. For safety-of-life and other users that require a certified, high-availability integrity signal, the existence of EGNOS, WAAS and other overlay systems will restrict the market for Galileo integrity-based services such that there is no viable business case for significant private investment. Based on the results and conclusions from this study, the Integrity Determination System as currently specified adds considerable cost to the Galileo programme, but offers no obvious benefit. Regardless of any other conclusions from this study concerning likely RAIM performance, one should question the arguments to commit well over one billion Euros on a system which would not meet Cat I precision approach requirements, and offers little over WAAS and EGNOS.

The second part of this thesis, the RAIM Study, demonstrates that the performance that can be expected from Galileo receivers using autonomous integrity monitoring techniques is broadly equivalent to that currently defined for the Galileo safety-of-life service. Furthermore, when GPS and Galileo signals are combined, the performance may approach that required for aviation Category 1 precision approach, i.e. significantly better than that intended for the Galileo Safety of Life service.

A novel RAIM algorithm, based on a Total Least Squares (TLS) solution of the navigation problem linear equations, under certain, well-controlled conditions, offers potentially better performance than the standard Least Squares approach. This improvement is possible because the TLS approach provides two apparently uncorrelated RAIM test statistics. Because each test statistic has the necessary characteristic of increasing in proportion to the applied bias (and hence to the induced vertical positioning error) it is possible to set a fault detection logic based on detection thresholds for both statistics being simultaneously exceeded. This allows lower detection thresholds for a given false alarm probability than for the standard Least Squares RAIM approach, which in turn leads to significantly improved RAIM availability. However, this novel approach also has significant issues regarding its physical implementation, making it more likely to be used as part of an Assisted Autonomous Integrity Monitoring system, rather than pure RAIM, therefore the comparison with Least Squares RAIM is not entirely fair.

If Galileo and GPS provide dual frequency free-to-air signals with ranging error performances as currently predicted, professional and safety-of-life users may be able to exceed IDS integrity specifications using RAIM. This has a significant impact on the case for private investment in Galileo; given the expected performance from a combined free signal constellation, the scope for the Galileo operator to raise revenues by selling access to encrypted parts of the navigation message is doubtful.

14.2 Recommendations for Further Research

This thesis attempts to consider a commercial question, regarding the value for money offered to investors in Galileo by developing an integrity determination system, and a more detailed technical evaluation of a novel RAIM algorithm. As a result, there is a danger of it falling between two stools, being neither a complete cost/benefit analysis for the Integrity system nor a rigorous evaluation of the EIV RAIM technique. At each stage of the analysis a number of questions have arisen which, although both relevant and interesting, have been deemed to be out of scope for this research, in order to keep the thesis within reasonable bounds. This section attempts to highlight those questions for which additional research would provide useful complementary results to this thesis.

Perhaps the most obvious direction for additional research is in the formal definition of the Errors in Variables RAIM algorithm. This thesis has shown that both of the test statistics derived for the EIV method appear to be directly proportional to applied biases, and hence have a linear relationship with vertical position error. Furthermore, the underlying statistical distributions for these test statistics resemble very well known functions, thus making the task of setting detection thresholds and calculating protection limits relatively simple.

These statements are made based on the results from simulations. Although a logical process is presented in this thesis which builds on the paper which first introduced the EIV method [30], to cover the case where observations are weighted according to their assumed variances, the conclusion that the H/e test statistic follows a half-normal distribution is driven by the results of Monte Carlo simulations, rather than by a rigorous mathematical analysis. It is recommended that further research is undertaken into the mathematical principles underlying the EIV method, ideally by someone with a stronger grounding in linear algebra and statistics than the author of this thesis. In particular, the methods used for setting the terms in the \mathbf{D} matrix described in this thesis would benefit from more rigorous analysis.

An additional area of research, perhaps for someone seeking to make an operational implementation of the EIV algorithm, is to consider how best

to manage the user clock in an EIV-enabled receiver, to mitigate the problems discussed previously regarding detection of ramping errors if the user clock is unfiltered. Recent advances in rubidium atomic frequency standards (RAFS) mean that atomic clocks with exceptional short-term stability are, or soon may be, sufficiently small, cheap and robust to be considered for avionics applications. It is conceivable that an EIV RAIM receiver using such a clock would be able to “clock coast” for the duration of the terminal approach phase of flight, and in this time the navigation receiver would have to solve for three unknowns, instead of the four unknowns solved for presently. This would simultaneously improve the accuracy of the navigation solution, and provide an additional degree of freedom for the RAIM algorithm to be used in assessing integrity.

Alternatively, there is scope for significant research into the opportunities offered through Galileo and GPS having independent timing references. This was shown to provide an elegant solution to the problem of avoiding contamination of the user clock estimate as required by the EIV algorithm; a user of a combined Galileo/GPS constellation can at any time compare the receiver clock estimate against a Galileo-only solution, a GPS-only solution and a combined constellation solution. By providing rules for the actions to be taken if the consistency between these measurements exceeds specified limits, it is conceivable that this may lead to alternative approaches to combined system RAIM. Inevitably there will be other applications which can be exploited by taking advantage of this property, and this is likely to be a fruitful area of research.

Finally, and perhaps most significantly, there remains a major requirement for the business case for the Integrity functions within Galileo to be analysed dispassionately and for the system architecture and deployment schedules to be revised accordingly.

15. REFERENCES

1. TECHNOMAR, VEGA, Metamarket., Structural Analysis Of The European Satellite Navigation Application Segment, Final Report, October 2000 (unpublished)
2. European Commission DG TREN, GEMINUS Study – Final Summary Report (Deliverable D8.2), March 2001 (unpublished)
3. Ammour, N, Thieboult, V., Galileo Overall Architecture Definition – Integrity, Alcatel Space Industries report GALA-ASPI-DD-013 Issue 2.1. 21 July 2000 (unpublished)
4. PriceWaterhouseCoopers, Inception Study to Support the Development of a Business Plan for the GALILEO Programme, TREN/B5/23-2001, 14 November 2001 (unpublished)
5. European Commission DG TREN, Galileo Definition Phase, Initial Results 7 June 2000 (unpublished)
6. Morgan-Owen G., Jenkins B., et al., Galileo Overall Architecture Definition – Market Research Methods and Overall Results, Racal Tracs Ltd report GALA-RACAL-DD-005 Issue 2.0., 12 October 2000 (unpublished)
7. Pullen, S.P., Pervan., B.S., Parkinson, B.W., A New Approach to GPS Integrity Monitoring Using Prior Probability Models and Optimal Threshold Search, Department of Aeronautics and Astronautics, Stanford University, 1999.
8. Ochieng, W, Cross, P., Galileo System Definition – GPS Integrity Monitoring Assessment, GALA WP 2.2.2.4, 21 July 2000 (unpublished)
9. Gallimore, J., Galileo Overall Architecture Definition – Cost Benefit Analysis, Astrium Ltd report GALA-ASTL-DD-021 Issue 2 (unpublished)
10. RBCNews press release, ECOFIN – Some Ministers Concerned About Financial Aspects of Galileo Project, 4 December 2001
11. Lyons, P.K., [Ed.], EC Inform – Transport, No. 56, January 2002.
12. National Air Traffic Services Ltd, (NATS) private communication with EC DG TREN, 2002 (unpublished)
13. GalileoSat Definition Study, Final Presentation, ESTEC, March 2001 (unpublished)

14. Wide Area Augmentation System (WAAS) Independent Review Board Report, Institute of Defense Analyses, 18 January 2001
15. Minimum Operational Performance Standards for Global Position System/ Wide Area Augmentation System Airborne Equipment – RTCA/Do-229C
16. Diesel, J.W., Huddle, J.R., Advantages of Autonomous Integrity Monitored Extrapolation Technology for Precision Approach ION GPS '97
17. Ochieng, W.Y., Sheridan K.F., Han, X., Cross, P.A., Lannelongue, S., Ammour, N., Petit, K., Integrity Performance Models for a Combined Galileo/GPS Navigation System, Journal of Geospatial Engineering (May/June, 2001).
18. Loizou, J.D., Navigation System Integrity Monitoring and Fault Detection Process, UK Patent Publication GB2380819, 16 April 2003
19. Minimum Operational Performance – Required Navigation Performance for Area Navigation RTCA/Do-236
20. AN-WP/7556 Addendum No.1 Appendix, draft amendment to annex 10 of the convention on international civil aviation, Volume I – Radio Navigation Aids, International Standards and Recommended Practices (SARPS)
21. Galileo Mission High Level Definition (HLD), 13 February 2001, ESA/EC Document No. 107/00050/2001 (not published)
22. European Space Agency, Galileo System Requirements Document (SRD), Issue 2.0 (not published)
23. Alcatel Space Industries, IDS Requirements Specifications (IDS-Req), Issue 1.0 (not published)
24. Claes, P and Dinwiddy, S.E., Galileo Integrity Implementation Options, Galileo's World magazine, AdvanStar Communications, Summer 2001.
25. Galati, G., Mariani, V., Dellago, R., Lisi M., The Integrity Requirement in Satellite Navigation: System Design Trade-Offs, 18th AIAA International Communications Satellite Systems Conference, Oakland, CA, 10-14 April 2000.
26. Walter, T., and Enge, P., Weighted RAIM for Precision Approach. Proceedings of ION GPS 95, Palm Springs, CA, September 1995, pp1995-2004

27. Cross, P.A., Advanced Least Squares Applied to Position Fixing, Department of Land Surveying, university of east London, Working Paper 6, April 1983
28. Ochieng, W.Y., Sheridan K.F., Sauer, K., Cross, P.A., Iliffe, J., Lannelongue, S., Ammour, N., Petit, K., Potential Performance Levels of a Combined Galileo/GPS Navigation System, RIN Journal of Navigation (July 2001).
29. Martin-Peiro, A.B., Mozo-Garcia, A., Romay-Merino, M.M., New Integrity Concept at User Level for a Future Galileo and GPS Environment, Proceedings of GNSS 2001, Seville, May 2001.
30. Juang, Jyh-Ching. On GPS Positioning and Integrity Monitoring. IEEE Transactions on Aerospace and Electronic Systems, Vol. 36, No. 1 Jan 2000.
31. Hahn, J., Discussion paper on the Galileo Integrity Concept, ESA-APNNG-TN/00391-JH, November 2003.
32. Brown, R.G. Hwang, P.Y.C., GPS Fault Detection by Autonomous Means Within the Cockpit, Proceedings of the Annual meeting of the Institute of Navigation (Seattle, WA), June 1986
33. Lee, Y.C., Analysis of Range and Position Comparison Methods as a means to Provide GPS Integrity in the User Receiver, Proceedings of the Annual meeting of the Institute of Navigation (Seattle, WA), June 1986
34. Parkinson, B.W., Axelrad, P., Autonomous GPS Integrity Monitoring Using the Pseudorange Residual, Navigation, Vol.35 No.2, 1988
35. Sturza, M.A., Navigation System Integrity Monitoring Using Redundant Measurements, Navigation, Vol.35 No.4, 1989
36. Brown, R.G., A Baseline RAIM Scheme and a Note on the Equivalence of Three RAIM Methods, Proceedings of the National Technical Meeting of the Institute of Navigation, January 1992.
37. Volpe National Transportation Systems Centre, Vulnerability Assessment of the Transportation Infrastructure Relying on the Global Positioning System, 29 August 2001.
38. Hughes, Peter C., Spacecraft Attitude Dynamics, John Wiley & Sons, 1986
39. PopTools add-in for Excel, <http://www.dwe.csiro.au/vbc/poptools/>,
40. gMatVec C++ matrix/Vector library, downloaded from <http://www.gnu.org/software/gama>

41. Cumulative distribution functions library (dcdflib) downloaded from <http://www.netlib.org/random/index.html>
42. Press, W.H., et al., Numerical Recipes in C, 2nd Edition, Cambridge University Press, 1992.
43. Have, D., Reference Set of Parameters for RAIM Availability Simulations, EUROCAE Working Group 62 Working Paper, July 2003 (unpublished)
44. Shaw, M., Turner, D., and Sandhoo, K., GPS Modernisation. Proceedings of GNSS 2000, Edinburgh, May 4, 2000 116-1179
45. Lannelongue, S., Galileo Context Assumptions for GSTBv1 Test Cases, Galileo Industries document GSTB-ASPI-TN-09 September 2002 (unpublished)
46. Zappavigna, A., Galileo Phase B2 UERE Budget Results, Galileo programme document GB2/SE/TNO/001 May 2002 (unpublished)
47. NATO Standardization Agreement Navstar Global Positioning System: System Characteristics, 1 February 1991
48. Hahn, J., GPS/Galileo Time Offset Interface Control Document (GGTO-ICD), Draft 1.5, 29 January 2003 (unpublished)
49. Forrest, W. M., Interoperability of the GPS and Galileo System Timescales for Positioning and Metrology, MSc Thesis, University of Nottingham, 2003.
50. Walter, T., Enge, P., and Hansen, A., A Proposed Integrity Equation for WAAS MOPS, Department of Aeronautics and Astronautics, Stanford University, 2000.
51. DeCleene, B., Defining Pseudorange Integrity – Overbounding, Proceedings of ION GPS 2000, Salt Lake City, Utah, September 2000
52. Golub, G. H. and Van Loan, C. F., Matrix Computations, 3rd edition, The John Hopkins University Press 1996
53. 3-d Grapher tool v2.1, downloaded from www.romanlab.com.
54. UCLA, Cumulative Binomial Distribution Calculator used on-line from <http://calculators.stat.ucla.edu/cdf/binom/binomialcalc.php>
55. Born, G.H., Radial, In-Track and Cross-Track Variations Due to Perturbations in the Initial Conditions of Near Circular Orbits, ASEN 3200, April 2002

56. TSO-C129a, Airborne Supplemental Navigation Equipment Using the Global Positioning System (GPS)
57. Lawson, J., Address to delegates at UK Galileo Day, February 2004 (unpublished speech).
58. Jeans, R., Concept Of Operations For Combined Galileo/GPS Receivers, EUROCAE Working Group 62 Working Paper, Jan 2004 (unpublished)

16. BIBLIOGRAPHY

- a) Parkinson, B.W., and Spilker, J.J. [Eds.], Global Positioning System – Theory and Applications, AIAA Progress in Astronautics and Aeronautics Volume 164
- b) European Commission DG TREN, GEMINUS Study – Deliverable D4 “Service Definition” – Annex D to the Final Report
- c) European Commission DG TREN, GEMINUS Study – Deliverable D6 “Business Model” – Annex E to the Final Report
- d) European Commission DG TREN, GEMINUS Study – Ad-Hoc Working Paper Assessing the Commercial Opportunities for the Galileo Operator – Annex F to the Final Report
- e) European Commission DG TREN, GEMINUS Study – Deliverable D1.1.2 “GALA User Requirements Review”
- f) European Commission DG TREN, GEMINUS Study – Deliverable D2.2 “Operator’s Requirements”
- g) Ober, P. B., Integrity Prediction and Monitoring of Navigation Systems, Integricom Publications, 2003, ISBN 90-77267-0108
- h) Matlab 6.5 User Manual, The MathWorks Inc., 2002
- i) Walkenback, J., Microsoft Excel 2000 Power Programming with VBA, IDG Books Worldwide 1999
- j) Leonard, A., Blomenhofer, H, Izquierdo, I., GPS and Galileo Interoperability and Synergies, Proceedings of GNSS 2003, Graz, Austria 2003.
- k) Styles, J., Costa, N., Jenkins, B., Gabaglio, V., Market and policy drivers for the development of the navigation services in the Galileo era, Proceedings of GNSS 2003, Graz, Austria 2003.
- l) Lee, Y.C., Van Dyke, K.L., Analysis performed in Support of the Ad-Hoc Working Group of RTCA SC-159 on RAIM/FDE Issues, ION NTM 2002, San Diego, California, January 2002.
- m) Henrion, S., Zink, T., User Integrity Determination (DIL 53), Galileo project document GAL2-ASPI-TN-102, May 2002 (not published).
- n) Zink, T., Eissfeller, B., et al., Analyses of Integrity Monitoring Techniques for a Global Navigation Satellite System (GNSS-2), Proceedings of GNSS 2000.

- o) Medel, C.H., Virgili, L.P., et al., SISA Computation Algorithms and their applicability for Galileo Integrity, Proceedings of GNSS 2003, Graz, Austria 2003.
- p) Brenner, M., Implementation of a RAIM Monitor in a GPS Receiver and in Integrated GPS/IRS, Proceedings of ION GPS-90, September 1990

APPENDIX A SAMPLE RESULTS FROM GALSAS STUDY

The following sections present abridged reports from three interviews (out of seventeen conducted by the author) undertaken as part of the “Structural Analysis of the European Satellite Navigation Applications Segment” study, discussed in Section 3.2.

A.1 UK Civil Aviation Authority - Safety Requirements Group

Interviewed in June 2000.

Profile of the organisation

The role of the Safety Requirements Group (SRG) within the UK Civil Aviation Authority is to set the safety standards for all aspects of civil aviation, and ensure that they are maintained. The Group's operating costs are met entirely from charges on the industry. Unlike many countries, there is no direct Government funding for the Group's work.

Current GNSS activities

“All navigation aids fail: it's a question of whether or not they fail with integrity.” – Initial results from joint studies with the University of Leeds suggest that GPS provides a relatively consistent service, but it has occasionally suffered insidious failures which limit the scope for its widespread approval as a navigation aid.

To date, UKCAA has approved GPS for use as a component of navigation systems in civil aircraft for the following applications:

- Basic Area Navigation (B-RNAV¹⁷);
- North Atlantic crossings (to replace Omega);
- North Sea helicopters (to replace Decca Navigator).

Safety Regulatory view of GNSS

In order to approve an Air Traffic Service, the CAA SRG is required to certify the entire structure that supports this service, such as the safety management system, equipment specification, etc. This UK legal safety regulatory function cannot be discharged for GPS, because of its nature as a system owned and operated by the US DoD.

¹⁷ *B(asic)-RNAV defines European Area Navigation (RNAV) operations which satisfy a required track keeping accuracy of ± 5 NM for at least 95% of the flight time. This level of navigation accuracy is comparable with that which can be achieved by conventional navigation techniques.*

However, the CAA are keen to emphasise that GPS is not treated as an Air Traffic Service (and neither will be EGNOS or Galileo); as it only forms part of an approved integrated navigation system (e.g. airfield, lighting, airspace, procedures, etc.). For example, GNSS alone as a signal in space cannot in itself be treated as a replacement or alternative to fully approved Air Traffic Services such as Instrument Landing System (ILS).

It is proposed that EGNOS will be represented by a single authority which possesses legal personality (i.e. a focal point which accepts liability, accepts safety management and channels issues such as cost recovery). This facilitates the approval of EGNOS as a common European component for use in the air traffic services of States.

EGNOS augments the performance of GPS to achieve suitability for some aviation navigation purposes. However, as GPS is an unapproved component, it cannot be assured that all potentially catastrophic GPS anomalies can be mitigated.

However, subject to performance demands GPS can be approved, unaugmented by SBAS (e.g. EGNOS), for use in non-terminal phases of flight, and that EGNOS opens opportunities in the precision and non-precision landing phase of flight (e.g. Cat I landings) which have the potential for approval as part of a total Air Traffic Service.

It is also conceivable that a safety regulatory approach could be accepted for GPS (without breaching US sovereign and military sensitivities) which could result in the CAA accepting a higher degree of reliance on GPS in aviation despite the inability to discharge legal powers of approval (NB This is a personal opinion of the interviewee, not necessarily the official view of the UK CAA).

The UK CAA's position on the removal of GPS Selective Availability is that it makes no difference to the use of GPS as a navigation aid. Even with SA on, GPS meets the positioning requirements for non-terminal phases (e.g. B-RNAV). Furthermore, the removal of selective availability has no impact on GPS availability and integrity, the main safety related characteristics of GPS which effectively drive UK CAA policy.

Future use of GNSS

The CAA expect GPS to be increasingly included as part of integrated navigation systems in civil aviation, and over time the number of areas in which it will be approved for use will increase beyond the three currently listed by the UK CAA (see above).

The introduction of EGNOS will add terminal and approach phases to the areas which may be approved for use. From the point of view of the UK

CAA, EGNOS will meet their user community's requirements; Galileo, as presently promoted, does not add anything of value from a safety regulatory perspective. Although Galileo has the potential to permit full safety regulatory visibility (e.g. failure modes), it does not represent an Air Traffic Service, and can only be used as part of an integrated system (and hence offers negligible advantage over EGNOS).

The alleged benefits of independent GNSS constellations are potentially flawed as this presupposes that both are approved or at least accepted by safety regulatory authorities. For example GPS, unaugmented, cannot currently be regarded as an independent component providing full redundancy to Galileo for purposes for which it cannot be approved. This not the case where GPS is augmented by EGNOS, where the benefits of independence are only maintained by maintaining concurrent use EGNOS and Galileo. It is only in these circumstances where there is great potential to reduce (or even eliminate) the requirement for traditional ground based navigation aids (over a relatively long period of time, to enable an orderly transition process to a wholly satellite-based navigation system).

The current plan to make the Safety Access Service on Galileo an encrypted, "pay-to-use" signal, is unlikely to be supported by the aviation community because it introduces a set of unnecessary risks and failure modes into a safety critical service. Given that GPS augmented by EGNOS will offer a high integrity signal fulfilling a number of civil aviation navigation purposes with a free-to-air signal, acceptance of a restricted access signal on Galileo could be a major stumbling block.

Apart from airborne applications, there is a clear market for GNSS receivers on airfield support vehicles – a market which will increase both in size and importance as the number of aircraft movements increases.

GNSS Policy issues

GPS currently has a significant advantage over Galileo in that the regulations defined by the US Federal Aviation Authority (FAA) are almost always ahead of the regulations from the CAA and JAA, to the extent that many JAA regulations are effectively FAA regulations with new covers and cosmetic changes.

GPS is now regarded as a mature system, with ICAO Standards and Recommended Practices (SARPS) in place for its internationally interoperable use as a navigation aid, including the use of space and ground based augmentation systems. In order for Galileo to be readily accepted into the civil aviation community there needs to be agreement on the international compatibility and interoperability of Galileo and GPS. This effort must be co-ordinated at ICAO level and at equipment level through standards making bodies such as the Radio Technical

Commission for Aeronautics (RTCA) and the European Organisation For Civil Aviation Equipment (EUROCAE).

Reference was made to a paper by Joe Fee of the FAA outlining personal views on the value of Galileo and GPS together to the aviation community, which includes the following statement:

“First of all there should be agreement on the compatibility and interoperability of the two systems. Once this is agreed, joint action could be taken immediately to extend the existing ICAO standards for Galileo. This effort must be co-ordinated with development of equipment standards from RTCA/EUROCAE and certification from the JAA/FAA in the same time frame.

These parallel efforts must be initiated in the near future if the practical use of GNSS-2 is to occur within the next two decades. If the GNSS-2 providers agree to common standards at an early stage of development and work together towards their implementation, the standards process can be dramatically shortened.”

It is felt that at the moment EUROCAE, as a voluntary organisation with no power to set mandatory equipment standards, is powerless to prevent GPS from being accepted as the *de facto* standard for GNSS in aviation applications. The concern is that as advanced standards are introduced in the US that refer explicitly to GPS rather than to a generic GNSS, these will be taken up as European and international standards, which will present hurdles for Galileo when it is ready for introduction as a navigation system.

Conclusions

The UK CAA regard the Galileo programme as “not sufficiently user driven”. Based on their current understanding of the system, Galileo in itself does not offer any significant safety regulatory advantages over GPS with EGNOS and other augmentation systems;

- However, Galileo in conjunction with GPS/EGNOS would provide a redundant, independent GNSS, which does offer the opportunity for greater reliance on GNSS (and, potentially, a scaling down in terrestrial navigation aids);
- There is a significant concern about the use of “controlled access signals” on Galileo. Encryption of navigation signals, possibly with a “pay-to-use” mechanism for the decryption key, adds a number of failure modes and other complications to a safety-critical service which the aviation community is unlikely to support – especially given that the GPS/EGNOS signal will be free-to-air;

- There is a danger that GPS and augmented-GPS based navigation systems will become *de facto* international standards, through the way JAA and EUROCAE standards and regulations tend to follow behind equivalent American bodies. This could present a significant delay to the acceptance of Galileo by the aviation community, and in order to mitigate this risk European delegates to ICAO should ensure that as regulations are developed for the use of GPS, these should be extended to include Galileo at the same time.

A.2 BT Cellnet

Interviewed in May 2000.

Profile of the Company

“BT Cellnet, the Mobile Internet market leader, is the UK's fastest growing Mobile Internet company. Today it has over 7 million customers using its voice services and 600,000 ISP subscribers to its Genie Internet Mobile Internet service. Wholly owned by BT plc, the company is driving beyond the boundaries of voice communication to lead the Mobile Internet revolution. BT Cellnet launched the UK's first Mobile Internet Service Provider, Genie Internet in 1999, and will be the first to introduce the new generation of very high-speed mobile data services using GPRS, or General Packet Radio Services, in Summer 2000.”

Since 1998 Cellnet have offered “Traffic Line”, their first Location Service which offers users traffic information relevant to their location, which is evaluated from the users cell identification.

As from June 2000 Cellnet will offer their “Locator” service. Based on GSM cell and sector identification to estimate the user's location, this offers position accuracy of about 200m in major conurbation, degrading to up to 25 km in rural areas. Using the “Locator” service, users will be able to access information regarding the nearest facility chosen from a menu, e.g. restaurants, automatic bank teller machines, fuel stations, etc. “Traffic Line” will continue to be supported, as a subset of “Locator”.

Competitive Environment

Within the UK BT Cellnet are one of four mobile telephone operators (the others being Vodafone, Orange and One2One) who, along with NTL, have also been awarded licenses to operated the new 3G telecommunications systems. All operators have plans to offer Location Services in the near future.

Market Data

BT Cellnet's interest in the satnav market is limited to its potential for use in providing Wireless Location Services. The recent report from Strategis Group Europe was discussed, and the market projections showing around 100 Million users of cellular systems for location-based information by 2002/2003 in Europe, rising to over 200 Million by 2005, matched their own assessments.

Technology

BT Labs, the technology arm of BT plc, are currently undertaking studies regarding the various positioning technologies that may be used to support Wireless Location Services. Until the recent decision by the US to turn off GPS Selective Availability the focus of efforts had been on terrestrial base station triangulation techniques, although various forms of DGPS were also being evaluated. With SA off, the 10m accuracy offered by unaugmented GPS is regarded as sufficiently accurate to meet all foreseeable needs for Wireless Location Services, and GPS (or some other GNSS) is being seriously considered as the positioning technology for future services.

The technology on which their current location services are based (cell and sector identification) offer very poor positioning accuracy away from built-up areas, and in cities during peak times the cell switching techniques used to smooth cell loadings often lead to sudden jumps in the reported position of the user (as the cell identification changes). However, they offer better in-building performance than GPS, do not suffer "canyoning" in built up areas to the same extent as GPS, do not require any additional hardware, and have little effect on the battery life of the user terminal.

Some GSM handsets with built-in GPS receivers are now coming on to the market, and BT Cellnet are evaluating the performance of these items to determine the viability of GPS/GNSS as a technology to meet their needs.

In addition, it is envisaged that by around 2004 broadband 3G mobile telephones will have a significant market, and the current expectation is that such systems will have an inherent position location capability with an accuracy of at least 20m. The technology on which this will be based is not yet decided.

Market trends and factors

The recent proliferation in Wireless Access Protocol (WAP) enabled mobile phones has led to great interest in the ability of networks to provide information to mobile users which is relevant to their location. To

some extent the network operators such as BT Cellnet are being driven by a customer expectation that cellular systems can determine user location to much greater accuracy than is currently possible.

Cellnet believe that “E911”-type legislation for the localisation of callers of emergency numbers may be introduced by around 2003, and the accuracy required by this legislation will have a major impact on the positioning technology to be used.

Cellnet also estimate that by 2003 the majority of mobile telephones sold in the UK will have a location capability with an accuracy possibly driven by the “E911” legislation. If GPS/GNSS becomes the *de facto* standard for Wireless Location Services, required accuracy would be of the order of about 10m. The system is expected to provide location information to the user, and also to send this information on request to the network. Ideally, the network should be able to poll a user terminal in idle mode, to determine its location, and forward this data to other authorised users. For example, it is envisaged that by dialling the number of a mobile phone, preceded by some service code, it would be possible to see that the target user is on the second floor of the HMV store in Oxford Street.

In order to become a standard feature in future mobile telephones a position location technology needs to:

- add little cost and size to the terminal;
- have no recurring licensing cost;
- work well in built-up areas;
- have little impact on battery life;
- be capable of estimating position within 20/30 seconds of switch-on;
- be capable of being “pinged” by the network for its location, ideally from within idle mode, and replying within 20/30 seconds;
- provide location information that can be readily translated into inputs for various location service applications;
- be compatible with the requirements for any “E911”-type legislation.

Market reaction to the introduction of GALILEO

The current timescales for the introduction of Galileo is far too distant to come into the strategic plans of BT Cellnet. At the moment it is not yet

decided if satnav will be a major component of their plans for Wireless Location Services. The decision to turn off GPS SA has certainly been very influential, and there is a good chance that GPS receivers will be standard features in high-end mobile telephones within the next two/three years.

If GPS does become the *de facto* standard, Galileo will have to be completely compatible with GPS in order for it to be used by mobile telephone networks. The better availability offered by the Galileo constellation would make it better suited to urban users of mobile phones, but this is likely to be limited to the Open Access Service. The positioning accuracy of GPS meets all foreseen requirements for cellular users, and the other Galileo features of integrity and continuity of service are not seen as offering any marketing advantage over GPS.

It is unlikely that networks such as BT Cellnet would be interested in implementing a location service which requires decryption of the Controlled Access signal and/or payment of recurring licensing costs.

Conclusions

- Operators of cellular telephone networks in the UK see a large market for Wireless Location Services, which require some position technology to be either built into the network, or into the handset itself;
- Wireless Location Services now being introduced are based on network infrastructure (i.e. do not use satnav). With SA off, GPS offers a significant improvement in the accuracy available;
- Network operators see 10m accuracy as the limit for their requirements;
- The major growth period for this market is expected to be from 2002 to 2005;
- Although the better urban performance of Galileo compared with GPS is a marketable feature, it is unlikely that the Controlled Access Service would be implemented as the Wireless Location Services technology by cellular network operators.

A.3 CMT TechServ

Interviewed in May 2000.

Profile of the Company

CMT TechServ is a division of Communications & Measurement Technologies Ltd (CMT). Operating mainly in the UK, their activities as a value-added reseller for Trimble GPS equipment has opened some markets in the Middle East, in support of oil and gas exploration activities.

CMT's activities have a common theme of GPS and radio applications, covering: radio modems for point-to-point telemetry; service and hardware provision for GPS and Differential GPS (DGPS) (including the Focus FM UK-wide DGPS service); integrated bespoke GPS solutions; and Trimble equipment distribution. CMT originally identified a niche in the market for precise position systems some 11 years ago.

In the near-future CMT intend to expand their activities to include satellite delivered GPS corrections in collaboration with Omni-Star of Holland, and are also developing some automatic vessel identification applications for marine navigation around coastal waters.

Competitive Environment

For GPS equipment solutions, competition comes from suppliers of equipment from Leica, Ashtech, etc. For the Focus FM DGPS service, main competition comes from Racal Survey's DGPS/Real Time Kinematic (RTK) service. CMT currently have about 60% of the market in the UK for fee-paying DGPS, although this is changing rapidly.

The switch-off of GPS Selective Availability has made a huge difference to the market for DGPS services already, with the market for users requiring 10<x<100m accuracy disappearing overnight, although there is still a market for high end, <1m accuracy users.

CMT expects the market for satnav equipment to move rapidly toward greater integration with communications systems, with the market for location-based services being the driver for the global sat/nav industry in the next few years.

Market Data

CMT are currently evaluating the market for satnav services, and have no comment on the existing estimates.

Technology

CMT believe that there will be a large market for applications requiring $1 < x < 10$ m accuracy. Although some specialist/professional applications will require decimetre and centimetre accuracy, this will remain a niche market for the foreseeable future.

Other drivers for market demand will be increased robustness (i.e. sky availability), reduced cost and improved in-building performance. This latter point is recognised as a weakness of GNSS compared with terrestrial position systems based on cellular telephones, and is believed to be a large potential market for trains, etc. (which currently have poor GPS service when in stations or passing through tunnels).

Expected technological trends in GNSS systems influencing market development include increased accuracy from GPS; increase in the range of applications using GPS (possibly including integration with other systems to provide better in-building performance); increased ease of use in human/machine interfaces; and reduced power and size in GPS receivers to allow personal tracking applications to be developed. In particular, CMT expect to see a drive toward GPS receivers with 1-day active battery packs; at present, battery life presents a significant restriction to the ways in which GPS receivers are used, and hence to the applications being developed.

CMT expect a shift to occur in the near to mid-term future regarding the way in which GNSS applications are bundled. At present, new navigation and positioning applications are developed and sold as an integrated system including GPS receiver, application host electronics and user interface unit. Taking as an example the case of in-car GPS, there is a host of potential applications, including moving map/navigation systems, lost vehicle tracker systems, hazard/traffic warning systems, potentially even “black box”-type data recorders. All of these applications need only one GPS receiver, therefore CMT expect cars in the future to be fitted with a GPS/GNSS receiver as a standard feature, which has some kind of “GPS Out” feeding a data bus on to which the various applications can be connected.

This is a very significant shift in thinking – the market for GNSS applications will greatly exceed the market for GNSS receivers, and the interface standard to be used by commercial applications will soon be set. In order to be successful, Galileo receivers will therefore need to offer a compatible interface (because applications developers will not wish to develop and market separate GPS and Galileo applications).

Market trends and factors

With the removal of SA, CMT expect an increase in the interest in using GPS for low-end surveying activities. For example, Local Authorities are required to map the location of lamp posts, man-holes, fire hydrants, trees, etc., to some given accuracy, and this is currently performed using traditional surveying techniques. Although the necessary accuracy is greater than unaugmented GPS currently offers, CMT expect non-real-time positioning applications to be developed to meet similar markets which do not require the expense and complexity of DGPS. This point is expected to be amplified with the introduction of EGNOS, which will almost certainly make <10m accuracy DGPS redundant, and may become the standard tool for non-precision surveying.

Similarly, as more and more GPS receivers are used for recreational navigation (such as hiking and rambling), it is conceivable that the legal definition of boundaries and footpaths may change from a line drawn on a map to a set of co-ordinates published on a web-site which may be downloaded into a user's terminal.

CMT perceive the quality and nature of current user interfaces in GNSS applications as being a barrier to progress. For most mass-market applications, an output presented as a latitude and longitude display on a screen is of little value; users require the data to be presented in an appropriate fashion (such as voice synthesis for traffic management applications), and to be translated into some appropriate reference (e.g. a car navigation application that says "Take the first left after the church, into King Street" is more user friendly than an application that says "Take the first turning on your left, distance 120 metres").

CMT see the drivers for change in the GNSS market being integrated GNSS/comms receivers, and the increase in uptake of in-car GPS (as previously discussed).

Although CMT expect the mass market demand for accuracy to be between 1m and 10 m accuracy, they also perceive a significant market for decimetre and (potentially) centimetre accuracy, for surveying applications (e.g. oil and gas exploration). There is also likely to be a niche market for real-time, high precision positioning.

Regarding the development and launch of new products and services, CMT regard themselves as being project led, i.e. they have no plans to start developing anything either for EGNOS or Galileo as an internal investment, but will react when a project identifies a specific requirement. To this end, EGNOS full operational capability is still too far away to affect CMT's plans, and Galileo is not even on their horizon.

As the launch of Galileo becomes closer, CMT will need to see a demand for use of the CAS signals in order to begin development of dedicated Galileo products and services.

CMT expect Galileo to be compatible with, and complementary to, GPS; CMT expect to see combined GPS/Galileo receivers which process the open access signals from both systems and produce a better service than is available from either system on its own.

In order for Galileo to become a part of CMT's strategic thinking, it would have to offer a free-to-air signal with 1m<x<10m accuracy standalone (i.e. without the need for differential receivers or post-processing).

CMT foresee a small market for applications that would benefit from Galileo's signal integrity and guarantee of service.

The vast majority of applications foreseen by CMT require some communications system alongside the GNSS service, therefore an on-board data communications payload would be of interest, if its bandwidth is sufficient to enable it to be used for a large number of applications simultaneously.

Market reaction to the introduction of GALILEO

CMT expect a fairly rapid expansion in the market for GPS receivers and associated applications, with the recent removal of SA. This is expected to consolidate the position of GPS as the system of choice for medium precision positioning systems. For high-precision positioning, differential GPS (in its various forms) will remain an important, but reduced, market.

In the mid-term future, the introduction of EGNOS and other space-based augmentation systems will further reduce the market for DGPS services world-wide.

By the time Galileo is operational GPS receivers (with or without some form of augmentation) are expected to be extremely commonplace, coming as standard equipment with most cars, mobile telephones, etc. In order to make any impact on this market Galileo receivers would have to either be significantly cheaper or offer better accuracy/availability from its Open Access Service.

Conclusions

- The removal of SA is already having a profound effect on the market for DGPS services. In the mid-term future this is likely to lead to an increase in the market for GPS receivers, which can now be used for medium precision positioning tasks that previously required DGPS (e.g. in agriculture);

- The introduction of EGNOS will take this a stage further, increasing the accuracy available from standalone GPS receivers;
- CMT expect a fairly rapid surge in the number of installed GPS receivers (mobile phones, vehicles, etc.), and that the next stage in the market's development will be based around applications sold without a bundled receiver. This requires some kind of interface standard to be developed;
- Galileo must be sufficiently compatible with GPS that any applications developed and intended to use a standard "GPS interface" could also be connected to the output from a Galileo receiver;
- Galileo is too far away to have an impact on CMT's strategic thinking. From their current understanding of the system, the market for the Controlled Access Services will be very limited;
- In order to succeed, Galileo receivers need to be cheaper than GPS, or the OAS needs to offer better accuracy and availability than GPS;
- Receivers that can combine measurements from GPS and Galileo free-to-air signals are likely to meet the needs of the vast majority of users for whom either system on its own is not good enough;
- A key opportunity for improvement would be in-building performance. CMT see the in-building performance of GPS as a weakness; if Galileo can offer significantly better performance in buildings and in built-up areas, this would be a significant advantage;
- CMT see the drivers for change in the GNSS market being integrated GNSS/comms receivers, and the increase in uptake of in-car GPS.

APPENDIX B RESULTS FROM UKISC WORKING GROUP SURVEY

The following sections present consolidated reports from responses received for the UK Industrial Space Committee's Galileo Working Group survey discussed in Section 3.5.

Five responses were produced, which are broadly classified as three representing the views of "Prime Contractors" and two "Non-primes". Consolidated responses to the list in questions presented in Section 3.5 are presented below

B.1 Galileo "Prime Contractors" view

The points listed below present a synopsis of the views expressed by members of the UKISC Galileo Working Group representing large systems integrators and potential prime contractors for elements of the Galileo system infrastructure.

- 1 EGNOS could become the safety service for GPS and Galileo (i.e. The EGNOS system could just delete GLONASS and replace it with Galileo). With respect to other augmentations, you can probably do everything you want with GPS provided you find an augmentation to suit the application. What we hope Galileo can do is to make many of the diverse range of augmentations redundant. In many ways Galileo is competing with the augmentations rather than GPS. If you look at the number and cost of the hundreds of GPS augmentations, a global Galileo could well be cheaper.
- 2 GPS III appears to be aiming at a performance similar to Galileo. 3G mobile communications systems could do the job for the mass-market users, but according to a German study, the infrastructure costs in Germany alone would equal a global Galileo.
- 3 The 'free of direct user charge' service of Galileo is likely to be superior to that offered by GPS IIF due to superior signal structure (possibly 3 frequencies).
- 4 There is little technical risk in implementing Galileo especially after the successful deployment of GPS. The most significant delay has been due to a lack of an institutional/legal entity (joint undertaking) with the authority and competence to move forward.

- 5 European Governments plan to spend 1.1B Euro (tbc) on the development phase. After that, user departments will pay as they would for GPS. Beyond that, the PPP process will determine the size of public sector subsidy, if any.
- 6 Mechanisms could be related to Intellectual property Rights (IPR) – licences, royalties, etc. The only way to get commitment is to invite bids from potential PPP operators and to enter into binding contracts.
- 7 If the US government decide to 'take out' the competition with a constellation of (say) 100 GPS III satellites with a free open-access signal, then they could obviously scupper Galileo. The questions are would they, and why? The main motivation behind GPS modernisation is probably Galileo. If Galileo stopped, would the US press ahead with modernisation?
- 8 The better you make OAS, the less people will be willing to pay for CAS. The professional market for Galileo never was big and never would come close to covering much of the costs of Galileo. Tapping into the mass market has always been the only possible way of getting a reasonable commercial return on Galileo. Our own views on the potential market would have to remain confidential at the moment as this would form part of our bid to be the PPP partner.
- 9 The only way to ensure this is to make it a PPP and to invite competitive bids. The bidders would then have to put their money where their mouths were and state what public funding would be required and what their own business plans were. However, also remember that this is PPP (i.e. a partnership) and the public side can expect to shoulder some of the continuing burden through public sector service payments.
- 10 France seem to stand alone on this. No-one wants Galileo as a military system except France, who threaten they will walk away from the programme if they don't get PRS. We will just have to watch this space and see how the politicians respond.
- 11 At the moment Galileo would not have any capability like SA and the military will not have any control. Is this realistic? I think not, but who

knows.

- 12 It is our belief that Galileo will only be used as an aid to navigation. “Sole means” status is difficult to achieve, and not necessarily desirable in view of the possibility of interference or single point failure. The liability therefore may be limited to negligence.
- 13 (a) This must be through a formal competitive tender process leading to a binding contractual relationship (see 8 above). The EC should invite consortia to make proposals to deploy and operate a system to deliver a given level of service for a given period of time ('the concession contract'). The consortia would then make proposals stating what money would be required from the public sector (if any and when required, short or long term) and what their business plans were. The award would be adjudicated on the level of service offered, the confidence that it would be delivered, the robustness of the business case, the cost to the public sector etc
- 14 (b) The strategic arguments in favour of Galileo are strong enough in some countries where they already would like it to be a public procurement (e.g. France, Italy) but not in others (e.g. UK, Germany, Netherlands).
- 15 Up to the point of Galileo Initial Operational Capability, which should be brought about by an entirely publicly funded programme, there will be very limited grounds for private funds. The subsequent development of services and user equipment is where we would see genuine private investment. (A PPP provided infrastructure should ultimately be regarded as a variant of public funding).
- 16 It is a major criticism of the Galileo Programme that little participation by end users has resulted in a specification which, whilst sound, follows traditional lines, perhaps lacking innovation. The reluctance of user groups to participate should not be construed as lack of interest but as reluctance to pay before they can be sure that a well managed programme will emerge.
- 17 Airlines, including many American ones, have been positive towards the introduction of Galileo provided it does not require re-certification of the aircraft fit. Galileo plus GPS will give a level of service that should be

much more easily certifiable for aviation use than augmented GPS on its own.

B.2 “Non-Primes” view

The points listed below present a synopsis of the views expressed by members of the UKISC Galileo Working Group representing smaller companies, and/or organisations closer to the applications-end of Galileo services, rather than having major interests in Galileo system infrastructure.

- 1 There are two strong reasons to support Galileo. Firstly, GPS has become a key element of Europe’s transport, telecommunications and industrial infrastructure, and it is rapidly becoming indispensable. It is wrong for Europe to become so reliant on a system under the control of the US DoD. Secondly, a combined GPS/Galileo constellation is worth much more than the sum of its parts.

The GPS constellation was designed for military users who typically can see a lot of the sky at the same time. The GPS system performs poorly in urban areas. Similarly, EGNOS was designed primarily for aviation users and also offers little to urban users. Although Galileo on its own offers little improvement over GPS + EGNOS, on its own it provides an alternative system, and in combination with GPS it will open a huge market for consumer uses of satellite navigation.

- 2 Services are still under definition but expected to include;
 - Free GPS like service (“OAS”)
 - A free ‘safety-of-life’ service with authentication of signal to prevent spoofing (“SAS”)
 - Higher accuracy charged commercial services (“CAS”)
 - Very accurate and/or encrypted services for Government and/or paying users (“PRS”)

These will be guaranteed services. They will be comparable in accuracy with GPS upgrade; probably will have higher security available to commercial users. Probably more accurate than 3G systems

- 3 This is the current specification for the OAS. However, this causes a problem for any commercial operator of the system, because such a service, when combined with the free dual-frequency signal from

upgraded GPS, will provide such a high level of performance that this will inevitably “cannibalise” the market for the CAS (and possibly SAS) services.

- 4 On current plans, GPS will begin to deploy next generation satellites before Galileo deploys its first operational satellites. However, since Galileo is starting from scratch (rather than replacing old satellites), it should have a full operational capability with dual-frequency signals many years before GPS Block IIF.

Terrestrial networks will start to include positioning systems to support location – based services well before Galileo, but these are unlikely to offer the same degree of accuracy.

- 5 According to the official programme plan, Galileo will cost € 3.25 Billion to the end of 2008, and a further € 220 Million per annum thereafter. Of this, only € 1.8 Billion of the development costs are currently identified as a public funding contribution, the balance (and the recurring costs) should come from private investment.

It is extremely unlikely that the system will be capable of generating direct revenues sufficient to attract the required level of private investment. Therefore, if the system is developed as some form of PPP, it is almost inevitable that there will be a significant public funding contribution. Given the cost model stated above, it is estimated that a “public service” charge of around € 600 Million pa will be required in order to make Galileo a worthwhile private investment.

Assuming that the UK contributes at 15% of total costs, the cost to UK would be about € 270 M initially, with a recurring cost of € 90 M pa.

- 6 There have been no convincing arguments that any revenue mechanisms can be set up around selling access to the Commercial Access signals . Potentially there may be scope to charge a levy on each Galileo receiver chip, but this is fraught with difficulties.

Although a number of organisations have signed a commitment in principle to invest in the Galileo system, following a number of studies there has been no evidence that Galileo will attract sufficient private investment to sustain any form of PPP, unless a very substantial annual public service charge is levied.

- 7 The technical and commercial arguments supporting Galileo (i.e. the benefits to users from a bigger constellation and dual-frequency free signals) apply equally to the US and Europe. The US has a number of current generation GPS satellites on the ground, ready to replace failed satellites in orbit. The current plan is to upgrade the system gradually,

be replacing failed Block II satellites with next generation satellites as they become available. However, the GPS satellites in orbit have demonstrated service lives considerably longer than their design specifications. As a result, if the US sees a potential commercial advantage, it could launch say six additional GPS satellites at short notice, and accelerate the upgrade programme by two to three years.

This would inevitably reduce any potential market for Galileo commercial access signals. Since GPS IIF will also include free signals in the protected L5 band, such an acceleration of the programme would also allow the US to consolidate the role of GPS in aviation and safety-of-life applications.

- 8 There has been an assumption that there is a market for users requiring authentication, accountability and a guarantee of service. This market is small (by volume), and its financial value has not been determined. Such users would have a simple commercial decision: Pay for Galileo's guaranteed service, or pay an insurance premium and use the free-to-air signals. It is very unlikely that CAS can be competitive in this environment.
- 9 This is a clear weakness in the current programme structure – there is no single customer, and ESA are exploiting the lack of well-defined requirements to undertake R&D activities that should be left entirely to potential suppliers of the system.

There is no reason why Galileo could not be run as a simple procurement. The required service specifications are well-known and can be simply stated – basically they are the same performance specifications as GPS Block IIF. The EU should set up a single body charged with procuring the system against these specifications, with ESA providing technical assistance in tender evaluation.

The current confused structure cannot possibly produce a cost-effective solution.

- 10 Galileo's potential use as a military system is a great concern to the US. The "High Dynamic User" specifications defined in the Galileo System Requirements Document greatly exceed the performance of non-military GPS receivers, and would enable Galileo to be used as a guidance platform for some weapons systems.

There is an argument that if Europe is to invest in its own GNSS, it makes sense to use it to provide strategic independence from GPS. However, in this case the system must be an entirely public procurement and operation, with similar export controls to those applied by the US.

If it is not to be used for military purposes, there is no justification for the PRS service or the High Dynamic User specifications. There is also an argument that in this case the system does not need to follow the GPS/GLONASS model with clocks on-board the satellites. A much cheaper architecture would use bent-pipe satellites and closed-loop controlled clocks on the ground.

At present Galileo is a civil system, with some potential military uses. This is the worst possible option, and a decision must be made to go one way or the other. The UK position is to make it a purely civil system.

- 11 It is inevitable that Galileo will include some mechanism for jamming or deliberately degrading the signals in the event of an emergency. Galileo will not be able to offer any levels of guaranteed availability beyond those of GPS C/A code – under conditions in which GPS SA is turned on, Galileo will undoubtedly also use a degraded signal.
- 12 We have seen no evidence that any user group will use Galileo only if it offers liability cover. The costs associated with providing this cover are likely to be very high, and difficult to recover – it would be much easier and cheaper for individual users to take out their own insurance for problems associated with using Galileo. The requirement for liability cover from the system should be removed.
- 13 The strategic arguments and benefits to Europe (and the world) that Galileo offers have been identified and presented many times over. Clearly the system ought to be deployed even if private investment is not forthcoming. However, this introduces a problem for the supporters of PPP because the benefits that will accrue will come regardless of whether or not it includes private investment. Unlike a PPP for a hospital or a toll bridge, the Prime manufacturers will benefit from the construction and operation of the system, regardless of whether or not they invested in it directly. Private investment into the programme will not give them any significant commercial advantage.
- 14 There are no such plans. At some point in the future, before a PPP can go ahead, there must be some comparison of the costs using a PPP compared with a traditional public procurement (the so-called “public sector comparator” or PSC). Following on from the previous answer, the Galileo programme is in the nonsensical situation in which the promoted candidates for the PPP have a vested interest in their PPP proposals failing the PSC – the system will still be built (almost certainly by these same Prime Contractors).
- 15 The arguments against a fully publicly funded programme are dogmatic, based on a simplistic argument that since many people will make a lot of

money from the existence of Galileo, they ought to put up some of the investment, which in turn will lead to a cost-effective design and operations concept. These arguments don't stand up to scrutiny, for reasons previously discussed.

There are many arguments to support an entirely public-funded programme, but the simplest is that a PPP cannot ever be cheaper than the PSC, and there's no reason why any investors should try to make it so. Public procurement of the system is inevitable, but the price will go up the longer it takes to recognise this fact.

Mitigation techniques to survive signal loss are required even for GPS. For the UK there is extensive and growing reliance on GPS for strategic issues. Telecommunications (timing), Survey (oil and Gas exploration Ordnance Survey) and public service such as ambulance (where they are totally reliant on GPS to improve their response times to incidents, as mandated by Government). This growing reliance on GPS in the UK for strategic and public interest issues means that should Galileo go ahead it should be treated as a true public project and not PPP. Any direct revenue generation opportunities from Galileo are very low. The main revenue will come from production of receivers and value added services from which Government will then take a tax (i.e. corporation tax).

However much we 'trust' the US, it is inevitable that US national interests will be the prime concern, and for either political or commercial reasons the GPS service may be changed, degraded or removed with serious consequences in some areas. However a subset of GPS out of US control would suffice.

- 16 End-user groups have not been adequately represented. Specifically, the signal structure should best meet the requirements of end-users (in terms of performance and equipment cost), even if that means providing less than the maximum theoretical performance.

The Galileo programme has taken an "if we build it, they will come" attitude to end-users, which is true to an extent, but may lead to an imperfect solution.

- 17 WAAS and EGNOS are likely to become enshrined in civil aviation standards and practices over the next few years. Galileo's integrity determination system does not offer any performance advantages over WAAS/EGNOS and there is no evidence that the civil aviation community will reap any benefit from this system. However, the additional availability provided by Galileo's additional satellites would be strongly welcomed by all aviation users.

APPENDIX C PERFORMANCE OF MDE ALGORITHM

As has been previously discussed, the nearest comparison to the analysis presented in this thesis in currently published literature comes from work performed under [17]. This work, undertaken under the GALA Study, uses the technique of Marginally Detectable Errors (MDE) to assess RAIM availability. The MDE technique is itself based on an algorithm formalised in [27].

The steps of the MDE method may be summarised as:

1. Compute \mathbf{C}_x , the covariance matrix of the estimated parameters (position and clock error) and extract standard deviations:

$$\mathbf{C}_x = (\mathbf{G}^T \mathbf{W} \mathbf{G})^{-1}$$

Equation C- 1

2. Compute \mathbf{C}_v , the covariance matrix of the residuals:

$$\mathbf{C}_v = \mathbf{W}^{-1} - \mathbf{G}(\mathbf{G}^T \mathbf{W} \mathbf{G})^{-1} \mathbf{G}^T$$

Equation C- 2

3. For each observation i , determine the standard deviation of the residual, σ_{vi} , from the i^{th} element of the leading diagonal of \mathbf{C}_v .
4. For each observation i , determine the variance of the observation, σ_i^2 , which is the square of the UERE for satellite i , from the i^{th} element of the leading diagonal of \mathbf{W}^{-1} .
5. Calculate the ratio P_i :

$$P_i = \sigma_i^2 / \sigma_{vi}$$

Equation C- 3

6. For the specified False Alarm Probability (P_{FA}), evaluate \mathbf{a} , the number of standard distributions (from a two-tailed test) associated with this probability on a Gaussian distribution.
7. For the specified Missed Detection Probability (P_{MD}), evaluate \mathbf{b} , the number of standard distributions (from a one-tailed test) associated with this probability on a Gaussian distribution.
8. For each observation i , determine the Marginally Detectable Error (MDE_i), which is the minimum size of gross error on this observation that will be detected at the specified P_{MD} and P_{FA} :

$$\mathbf{MDE}_i = P_i(\mathbf{a} + \mathbf{b})$$

Equation C- 4

9. For each observation i , produce a vector \mathbf{b}_i , which is a null vector, except for the i^{th} element which is \mathbf{MDE}_i , for example:

$$\mathbf{b}_i^T = [0,0,0, \mathbf{MDE}_i, 0 \dots 0,0,0]$$

Equation C- 5

10. For each observation i , compute the position shift due to each \mathbf{MDE}_i

$$\mathbf{x}_i = (\mathbf{G}^T \mathbf{W} \mathbf{G})^{-1} \mathbf{G}^T \mathbf{W} \mathbf{b}_i$$

Equation C- 6

11. The Vertical Protection Limit is taken to be the largest value of $\mathbf{x}_{i(3,3)}$, i.e. the largest third diagonal element on the list of vectors \mathbf{x}_i ,

The key point that distinguishes the MDE approach from the LSR method is the way the False Alarm probability (P_{FA}) is handled. In the LSR method, k (P_{MD}) is identical to \mathbf{b} as shown in Step 7 above. However, in the LSR method, the calculation of T (N, P_{FA}), the decision threshold for alarms, reflects the assumption that the test statistic has a chi-square distribution, with $N-4$ degrees of freedom. This is the main cause of divergence between results using the two different methods.

Although superficially the LSR method seems quite different from the MDE method, in fact by following the steps through in detail it turns out that the computed vertical position shift due to $\mathbf{MDE}(\max)$ is exactly the same as $(\mathbf{a} + \mathbf{b}) \times V_{\text{slope}(\max)}$. This somewhat surprising result is because σ_{vi} (in MDE terminology) is identical to $((1 - P_{ii}) \times \sigma_i)$ (LSR terminology).

VPL calculated from the MDE method is therefore identically equal to:

$$\mathbf{VPL}_{\text{MDE}} = V_{\text{slope}(\max)} \times (\mathbf{a} + \mathbf{b})$$

Equation C- 7

Therefore there are two differences in the calculation of VPL:

1) For the Missed Detection component, MDE multiplies \mathbf{b} by $V_{\text{slope}(\max)}$, whilst the LSR method multiplies \mathbf{b} by σ_v ;

2) For the False Alarm component, MDE multiplies $V_{\text{slope}(\max)}$ by the normal distribution factor \mathbf{a} , whilst LSR multiplies $V_{\text{slope}(\max)}$ by the χ^2 distribution factor $T(N, P_{FA})$.

Where the number of satellites in view is around 6 or 7, as might be typical for applications using GPS alone with a masking angle of say 10°, the two methods will give very similar results. However, as the number of degrees of freedom increases, with up to 23 satellites in view for the dual constellation case, the divergence in results becomes dramatic, with the MDE method giving much lower VPL values.

Figure C- 1 presents the results for a simulation of the combined GPS/Galileo constellation case, for a fixed geographical position, at 5 minute intervals for 24 hours. This shows that the results from the MDE algorithm follow the same general pattern as those from the LSR algorithm, but with a reasonably consistent offset, making the MDE estimate of VPL less conservative than the LSR approach.

Figure C- 2 presents the results for the same case, re-run to use just the nominal 24 satellite GPS constellation. In this case the results from the two methods are very similar, with occasional excursions by the MDE method to large VPL values when unfavourable viewing geometries occur.

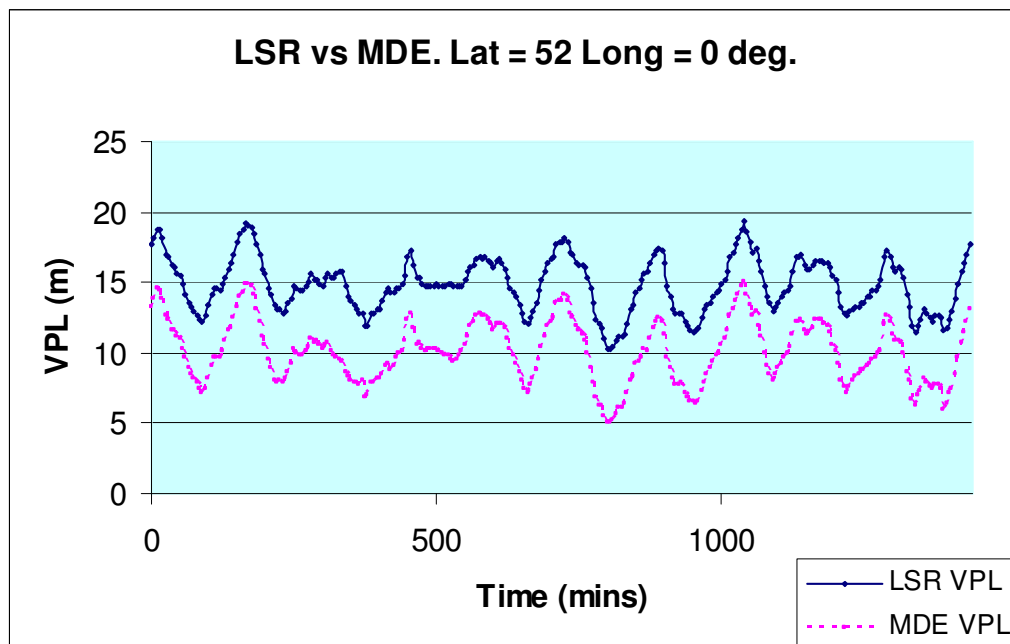


Figure C- 1: Comparison of VPL calculated using LSR and MDE approaches, for GPS+Galileo

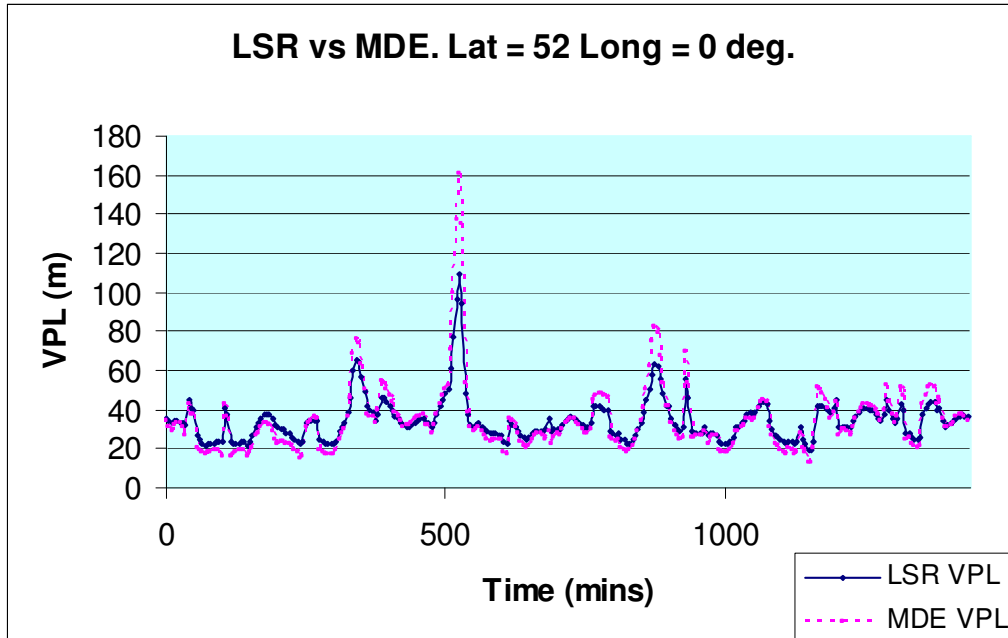


Figure C- 2: Comparison of VPL calculated using LSR and MDE approaches, for GPS-only

A Monte Carlo simulation for combined GPS/Galileo constellations was performed using the “Bias Modelling” spreadsheet described in Section 6.3, for both LSR and MDE approaches simultaneously. For a fixed geographical location and epoch (52°N latitude, 0° longitude, time = 0 minutes), one hundred thousand repetitions were made to calculate the LSR VPL, MDE VPL and actual vertical error. For each repetition, new random values for the UERE on each visible satellite were applied, based on a Gaussian distribution and the UERE/elevation curves presented previously for Galileo and GPS dual frequency services. In order to produce meaningful results with one hundred thousand repetitions, P_{MD} and P_{FA} were both set to 1×10^{-4} , so that ten false alarms would be expected in the fault-free case. For each case, each algorithm could produce one of four outcomes:

- Normal operations – vertical error is below VPL and test statistic is below test threshold;
- Alarm – vertical error is above VPL and test statistic is above test threshold;
- False Alarm – vertical error is below VPL and test statistic is above test threshold;
- Missed Detection – vertical error is above VPL and test statistic is below test threshold.

	Normal	Alarm	FA	MD
LSR	99,988	0	12	0
MDE	95,388	3	4609	0

Table C- 1: Comparison of MDE with LSR for Galileo+GPS Case

The MDE method clearly has a much higher false alarm rate than the LSR method; in fact this rate is far above the specified P_{FA} value, equivalent to a false alarm probability of 4.6×10^{-2} . It is believed that that this is because by using the normal distribution factor \mathbf{a} instead of the χ^2 factor, the MDE method effectively ignores any false alarms generated by satellites other than that identified as generating the MDE, when setting the test statistic. This is potentially an interesting area for further investigation, but is beyond the scope of this thesis.

This Monte Carlo analysis was then repeated for the GPS-only case. and The LSR results were as follows:

	Normal	Alarm	FA	MD
LSR	99,989	0	11	0
MDE	100,000	0	0	0

Table C- 2: Comparison of MDE with LSR for Galileo-only Case

These results appear to support the conclusion that the MDE approach yields similar results to the LSR approach for small constellations, but differs significantly with large constellations, to the extent that the MDE algorithm used in the GALA analysis of combined GPS/Galileo RAIM performance is invalid, since it does not provide the specified fault-free false alarm probability when dealing with large constellations. Because the results between the two methods are so similar when using the GPS constellation alone, it is conceivable that the shortcomings with the MDE method have not been previously identified, because few analyses have been performed looking at constellations larger than GPS alone.

APPENDIX D INTRODUCTION TO SINGULAR VALUE DECOMPOSITION

This introduction to the Singular Value Decomposition (SVD) process is derived from “Matrix Computations” by Golub and Van Loan [52].

SVD is a very useful way of dealing with sets of linear equations (or matrices) which are either singular or numerically very close to singular. In such situations, other decomposition techniques such as Gaussian elimination may fail. SVD is also a very powerful method for solving least-squares (LS) problems, both as an alternative to the “normal equations” method of solving the LS problem or for solving the total least squares (TLS) problem as will be demonstrated below.

For any real $M \times N$ matrix \mathbf{A} , there exist;

- An orthogonal, $M \times M$ matrix, \mathbf{U} ,
- An orthogonal, $N \times N$ matrix, \mathbf{V} ,
- A diagonal, $P \times P$ matrix, $\mathbf{\Sigma} = \text{diag}(\sigma_1, \dots, \sigma_P)$

where $P = \min(M, N)$ and $\sigma_1 \geq \sigma_2 \geq \dots \geq \sigma_P \geq 0$.

Such that:

$$\mathbf{A} = \mathbf{U}\mathbf{\Sigma}\mathbf{V}^T$$

Equation D- 1

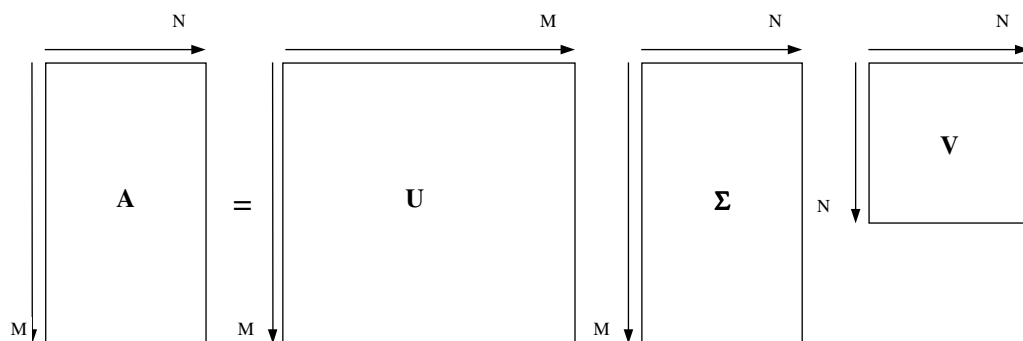


Figure D - 1: Graphical Representation of the SVD Process

The (column) vectors, \mathbf{u}_i and \mathbf{v}_i are termed the i^{th} left singular and i^{th} right singular vectors respectively. $\sigma_1, \dots, \sigma_P$ are termed, the “singular values” of \mathbf{A} and all other elements in matrix $\mathbf{\Sigma}$ are zero.

Another commonly used, trimmed-down form of the SVD is the “Thin SVD”. This is similar to the above method with the exception that the matrix, \mathbf{U} has dimensions $M \times N$ and the matrix, $\mathbf{\Sigma}$ is a square, $N \times N$ matrix. This is the type of SVD method employed in the EIV RAIM method. Matrix \mathbf{U} in this case is “column-orthogonal” as its columns are orthonormal but the matrix itself, being singular (non-square) can have no inverse.

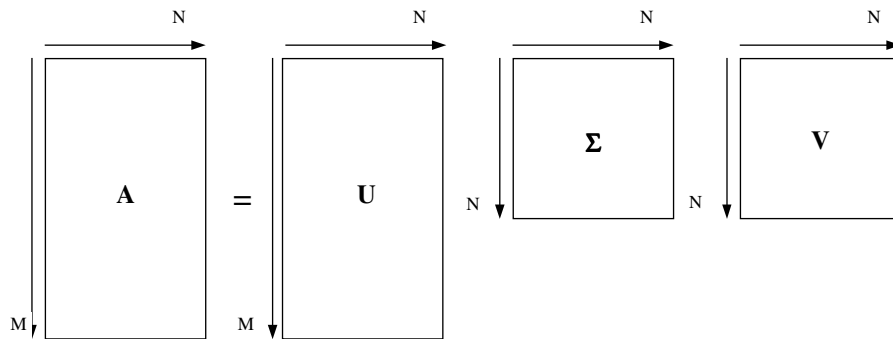


Figure D - 2: Graphical Representation of the Thin SVD Process

A transformation performed by matrix, \mathbf{A} upon the N -dimensional vector, \mathbf{x} , can be characterised in terms of the matrices \mathbf{U} , $\mathbf{\Sigma}$ and \mathbf{V} in the following way. Every matrix transformation involves a stretch and/or a rotation of the matrix or vector which is being acted upon. This can be thought of as the action of three, independent matrix transformations, namely, the action of a hanger matrix, a stretcher matrix and an aligner matrix. A hanger matrix is created by loading the vectors from a perframe into the columns of the matrix. A perframe is a set of orthonormal basis unit vectors (axes) for an N -dimensional vector space. In analogy with the SVD, the hanger matrix is represented by the matrix, \mathbf{U} . The aligner matrix is created by loading the vectors from a perframe into the rows of the matrix. In analogy with the SVD, the aligner matrix is the matrix, \mathbf{V} . The stretcher matrix defines the amount of stretch in each of the respective dimensions which will be performed by the matrix transformation. In analogy with the SVD, the stretcher matrix is the matrix, $\mathbf{\Sigma}$. For example, a stretch of amount, σ_1 will be performed in the direction of the first, perframe vector and so on. A value of zero for any of the elements of $\mathbf{\Sigma}$ will indicate that this particular dimension has collapsed and the matrix transformation is performed onto a vector

space of lower dimensionality. It is important to note that Singular Value Decomposition can be performed upon any $M \times N$ matrix.

In the transformation, $\mathbf{y} = \mathbf{A}\mathbf{x}$, where \mathbf{x} and \mathbf{y} are N -dimensional vectors a linear mapping is performed from the vector space \mathbf{x} to the vector space \mathbf{y} . If there are as many unknowns as there are simultaneous, linear equations, i.e. $M = N$ and they are not linearly dependent then matrix \mathbf{A} is non-singular and square. This means that the whole of the vector space, \mathbf{y} , can be “reached” by matrix, \mathbf{A} , i.e. the “range” of \mathbf{A} . If however, matrix, \mathbf{A} is singular (or numerically close to singular) then there will be a subspace of \mathbf{x} that is mapped to zero by the matrix transformation, i.e. $\mathbf{A}\mathbf{x} = 0$. This subspace is termed the “nullspace” and its dimension is termed the “nullity” of \mathbf{A} . The subspace of \mathbf{y} which can be reached by the matrix transformation performed by \mathbf{A} is termed the “range” of \mathbf{A} . The dimension of the range of \mathbf{A} is termed the “rank” and observes the simple relationship; Rank + Nullity = N .

In the case of an under-determined set of linear equations, i.e. $N > M$, a unique solution is not expected and the matrix transformation performed by matrix \mathbf{A} maps the vector space of \mathbf{x} into one of lower dimensionality. In this case $\sigma_1, \dots, \sigma_M$ produced by the SVD are non-zero (or non-negligible numerically) and the corresponding columns of matrix \mathbf{U} define the orthonormal basis unit vectors (perpframes) of the range of \mathbf{A} . Also in this case, $\sigma_{M+1}, \dots, \sigma_N$ are zero (or numerically negligible) and their corresponding columns in the matrix, \mathbf{V} (or rows of matrix \mathbf{V}^{-1}) define the orthonormal basis unit vectors of the nullspace.

$$\text{rank}(\mathbf{A}) = r$$

Equation D- 2

$$\text{null}(\mathbf{A}) = \text{span}\{\mathbf{v}_{r+1}, \dots, \mathbf{v}_n\}$$

Equation D- 3

$$\text{range}(\mathbf{A}) = \text{span}\{\mathbf{u}_1, \dots, \mathbf{u}_r\}$$

Equation D- 4

The SVD process is very useful for identifying problems of rank deficiency or numerically near-rank deficiency with a design matrix. If any of the components, $\sigma_1, \dots, \sigma_P$ are zero or small enough that their value is swamped by round-off error then this is the first indication that there is a problem of rank deficiency. The matrix, $\mathbf{\Sigma}$ is said to be ill-conditioned if σ_N/σ_1 is too large, i.e. its reciprocal is of the same order as the machine precision.

When considering the design matrix of the RAIM algorithms, the above situation is not likely to occur as the solution is generally over-determined by multiple (more than 4) satellites and linear dependency is likely to be precluded by the geometry of the satellite orbits. Hence the singular values $\sigma_1, \dots, \sigma_N$ will all be positive, non-zero. σ_N is a relevant value as it is the 2-norm distance from \mathbf{A} to the set of all singular matrices.

D.1 The SVD Process

SVD is a commonly used process and examples of coding implementations are easily found in the general literature. This section gives a high level description of the general processes required to implement a working SVD algorithm.

The process can be broken down into six discrete steps. As described in Equation D- 1, the matrix \mathbf{A} can be described in terms of three matrices, \mathbf{U} , $\mathbf{\Sigma}$ and \mathbf{V} . To find these matrices, follow the procedure described below:

1. Find the 'n' Eigenvalues, λ , of the matrix $\mathbf{A}^T \cdot \mathbf{A}$
2. Find the 'n' Eigenvectors, that correspond to the 'n' Eigenvalues found in step 1.
3. Form a diagonal matrix, $\mathbf{\Sigma}$, from the Eigenvalues found in step 1,

$$\mathbf{\Sigma} = \begin{pmatrix} \sigma_1 = \sqrt{\lambda_1} & & 0 & & 0 \\ & \sigma_2 = \sqrt{\lambda_2} & & & 0 \\ & & 0 & & \\ & & & \sigma_p = \sqrt{\lambda_p} & \\ & & & & \end{pmatrix}$$

where p is the smaller of m and n,

and $\sigma_1 > \sigma_2 > \dots > \sigma_p$

4. Arrange the Eigenvectors of $\mathbf{A}^T \cdot \mathbf{A}$, in the same order, to form the columns of matrix \mathbf{V} ,

$$\mathbf{V} = \left(\begin{pmatrix} \mathbf{v}_1 \end{pmatrix} \begin{pmatrix} \mathbf{v}_2 \end{pmatrix} \begin{pmatrix} \mathbf{v}_n \end{pmatrix} \right)$$

5. Find the first column vectors of the matrix \mathbf{U} , using the relationship:

$$\mathbf{u}_i = \sigma_i^{-1} \mathbf{A} \mathbf{v}_i, \text{ for } i = 1 : n$$

where \mathbf{v}_i are the column vectors of the matrix \mathbf{V}

6. Find the remaining $(m-n)$ columns of the matrix \mathbf{U} , using the Gram-Schmidt orthogonalisation process. This process is well documented in mathematical literature and will not be described here.

D.2 SVD of a 2-Dimensional Matrix

In order to demonstrate the purpose of using the Singular Value decomposition process, let us consider the SVD of a simple 2x2 matrix:

$$\mathbf{A} = \begin{pmatrix} 0.5 & 1 \\ 1 & 0.5 \end{pmatrix}$$

Using the process described above, this can be decomposed into the three matrices, \mathbf{U} , $\mathbf{\Sigma}$ and \mathbf{V} as follows:

Original Matrix, \mathbf{A}		Hang (\mathbf{U})		Stretch ($\mathbf{\Sigma}$)		Align (\mathbf{V})	
0.5	1	-0.7071	0.7071	1.5	0	-0.7071	-0.7071
1	0.5	-0.7071	-0.7071	0	0.5	-0.7071	0.7071

To understand the physical significance of these three matrices, let us consider the matrix action (i.e. the transformation) of the matrix \mathbf{A} on the points of a unit circle. This is shown in Figure D - 3, i.e. the unit circle is transformed to an ellipse/ The transformation is, therefore, a rotation about the origin of the coordinate frame, with a stretch along each of the axes of the frame.

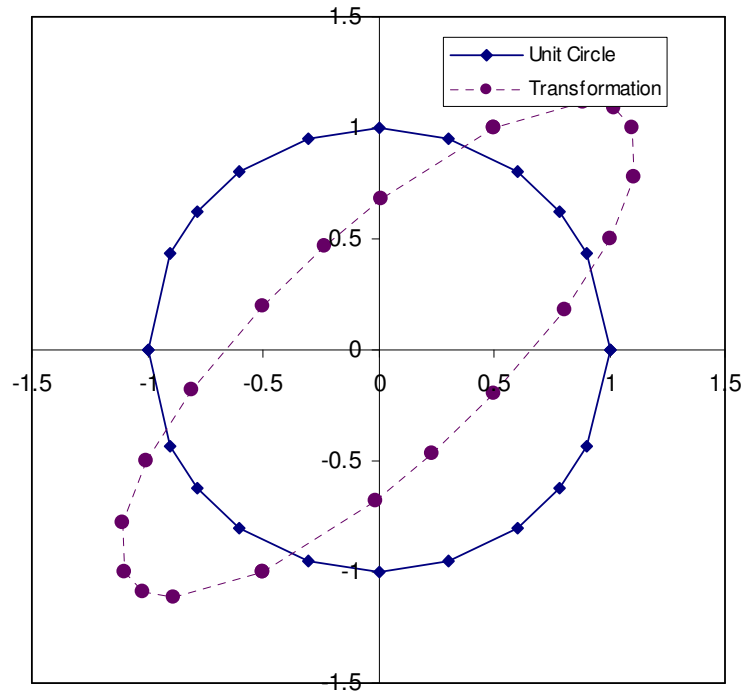


Figure D - 3: Action of Matrix A on Unit Circle

The next three figures demonstrate the effect of multiplying \mathbf{A} by the matrices, \mathbf{U} , $\mathbf{\Sigma}$ and \mathbf{V}^T in sequence, showing how this produces an identical transformation.

Figure D - 4 shows the transformation of the \mathbf{U} matrix, which is a rotation of the axes of the coordinate frame (as demonstrated by the circle and square, which mark the “before” and “after” of a single point).

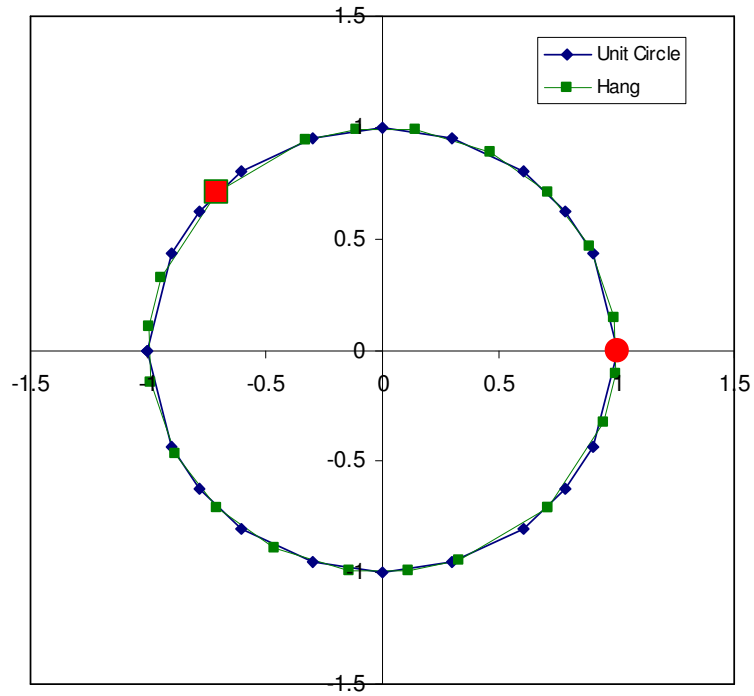


Figure D - 4: Action of U (“Hang”) Matrix on Unit Circle

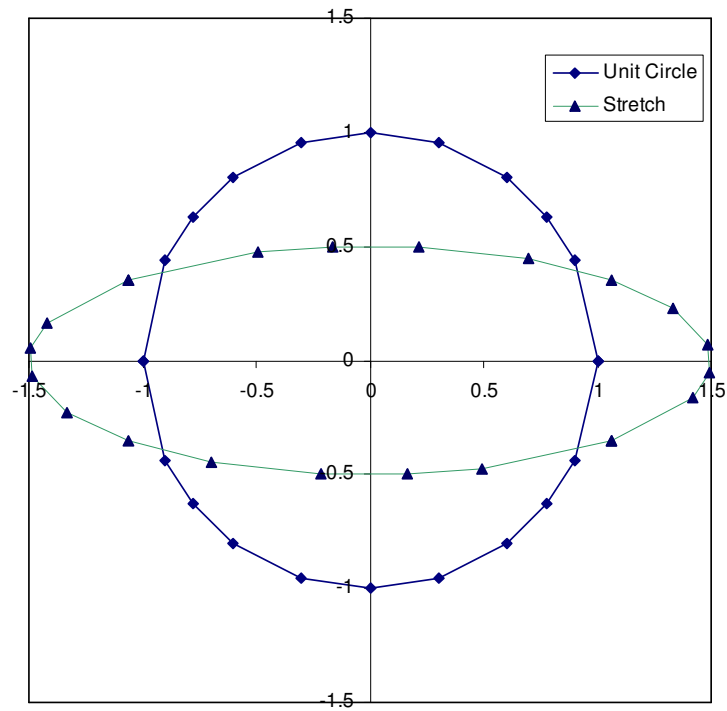


Figure D - 5 : Action of Σ (“Stretch”) Matrix on Unit Circle

Figure D - 5 shows the “stretch” along the two axes, derived from the Σ matrix. In this case the effect is to multiply the coordinates of the points of the unit circle by 1.5 in one direction and by 0.5 in the orthogonal direction.

The final step is to “align” the transformation back to the original coordinate frame, by multiplying by V^T . This yields the same ellipse as shown in Figure D - 3. We can therefore see, by following the steps of the SVD process, the basis for the transformation of the unit circle to an ellipse, aligned and stretched by matrix A .

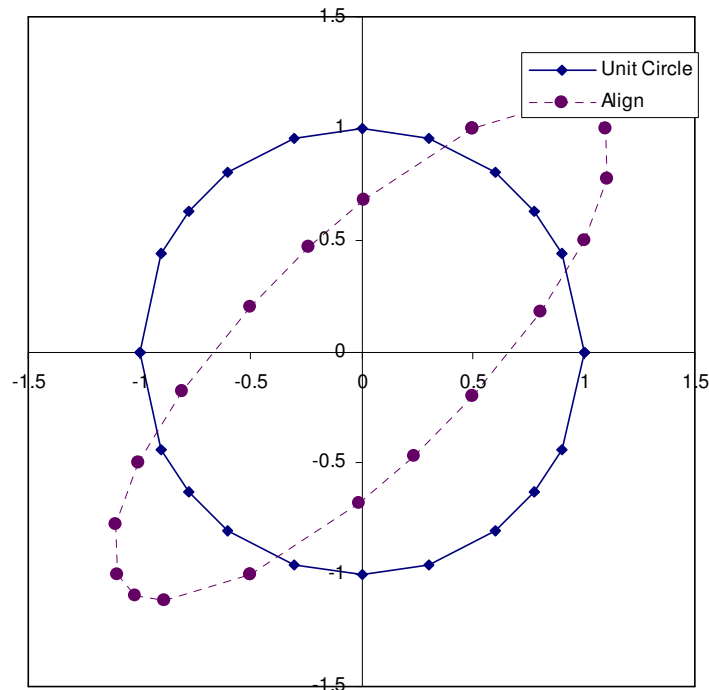


Figure D - 6: Action of V (“Align”) Matrix on Stretched Circle

This physical representation of the SVD process is critical to understanding the EIV RAIM method. If we extrapolate this example to the 5-dimensional matrix on which SVD is performed in the EIV method, we see that the $\sqrt{\text{USSE}}$ test statistic is effectively a measure of the “stretch” caused by inconsistencies in the observations, whilst the H/e statistic is a measure of the rotation of the coordinate frame caused by these inconsistencies. This is the basis for using the SVD method to produce two independent test statistics for RAIM.

D.3 SVD Solution of the Least-Squares (LS) Problem

As mentioned earlier, the Singular Value Decomposition can be employed as an alternative to the normal equations as a means to

solving the least squares (LS) problem. Whilst this particular method is not employed in the calculations of RAIM, this section is included to provide background understanding of the SVD.

The least-squares solution for the (N=4)-dimensional position vector, \mathbf{x} , using the normal equations is given by:

$$\mathbf{x} = (\mathbf{G}^T \cdot \mathbf{G})^{-1} \cdot \mathbf{G}^T \cdot \mathbf{y}$$

Equation D- 5

in the un-weighted form ($\mathbf{x} = (\mathbf{G}^T \cdot \mathbf{W} \cdot \mathbf{G})^{-1} \cdot \mathbf{G}^T \cdot \mathbf{W} \cdot \mathbf{y}$ in the weighted form), where:

\mathbf{G} is the M x N design matrix, \mathbf{y} is the M-dimensional vector of residuals, \mathbf{W} is the M x M weighting matrix and M is the number of visible satellites.

Taking the un-weighted case as example, the singular value decomposition of \mathbf{G} as:

$$\mathbf{G} = \mathbf{U} \cdot \mathbf{\Sigma} \cdot \mathbf{V}^T$$

Equation D- 6

produces the least-squares position solution:

$$\mathbf{x} = \mathbf{V} \cdot \mathbf{\Sigma}^{-1} \cdot \mathbf{U}^T \cdot \mathbf{y}$$

Equation D- 7

Extra robustness is given to this method by the added substitution of any elements of the inverse matrix, $\mathbf{\Sigma}^{-1}$ with zero where the corresponding elements of the matrix, $\mathbf{\Sigma}$ are zero (or very small in comparison with the machine error). Whilst this may seem counter-intuitive, it actually means that one of the simultaneous equations which is dominated by round-off error is being disregarded and hence improving the position solution. This method is very robust and theoretically can not fail to find a solution.

It is an interesting point to note that in the SVD solution of the least-squares problem, non-zero elements of matrix, $\mathbf{\Sigma}$, $\sigma_1, \dots, \sigma_P$ are inversely proportional to the lengths of the principal axes of the error ellipsoid of the least-squares position fit.

D.4 SVD Solution of the Total Least-Squares (EIV) Problem

The standard least-squares solution to the RAIM problem assumes that all errors are confined to the vector of residuals, \mathbf{y} . To perform a more

accurate analysis one has to consider that the errors are instead distributed between the \mathbf{y} vector and the design matrix, \mathbf{G} .

Let us consider a general problem, characterised by the set of simultaneous, linear equations:

$$\mathbf{G}.\mathbf{X} = \mathbf{Y}$$

Equation D- 8

where \mathbf{G} is an $M \times N$ matrix, \mathbf{X} is an $M \times d$ matrix (or an M -dimensional vector, \mathbf{x} in the “one-dimensional” case where $d = 1$, as in the EIV RAIM method) and \mathbf{Y} is an $M \times d$ matrix, \mathbf{y} (or an M -dimensional vector in the “one-dimensional” case). The total least-squares method aims not at reducing the sum of the squares of the errors on \mathbf{Y} ; rather it aims to reduce the sum of the squares of the errors on both \mathbf{Y} and \mathbf{G} at the same time. If we term the matrix of the errors on \mathbf{G} as the $M \times N$ matrix, \mathbf{H} and the matrix of the errors on \mathbf{Y} as the $M \times d$ matrix, \mathbf{E} then the aim of the total least-squares solution is to minimise the Frobenius norm of the weighted augmented matrix, $\mathbf{C}.[\mathbf{H} \ \mathbf{E}].\mathbf{D}$, i.e.:

$$\min_{\text{range}(\mathbf{Y}+\mathbf{E}) \subseteq \text{range}(\mathbf{G}+\mathbf{H})} \|\mathbf{C}.[\mathbf{H} \ \mathbf{E}].\mathbf{D}\|_F$$

Equation D- 9

where:

\mathbf{C} and \mathbf{D} are suitably defined weighting matrices such that $\mathbf{C} = \text{diag}(c_1, \dots, c_M)$ and $\mathbf{D} = \text{diag}(d_1, \dots, d_{N+d})$

If we call the weighted, augmented matrix, $\mathbf{C}.[\mathbf{G} \ \mathbf{Y}].\mathbf{D}$, \mathbf{A} and then perform Singular Value Decomposition upon this matrix, we have:

$$\mathbf{C}.[\mathbf{G} \ \mathbf{Y}].\mathbf{D} = \mathbf{A} = \mathbf{U}.\mathbf{\Sigma}.\mathbf{V}^T$$

Equation D- 10

where the following partitions apply:

$$\mathbf{A} = \begin{array}{c|c} \mathbf{A}_1 & \mathbf{A}_2 \\ \hline N & d \end{array}$$

$$\mathbf{U} = \begin{array}{c|c} \mathbf{U}_1 & \mathbf{U}_2 \\ \hline N & d \end{array}$$

$$\mathbf{V} = \left| \begin{array}{cc|c} \mathbf{V}_{11} & \mathbf{V}_{12} & N \\ \mathbf{V}_{21} & \mathbf{V}_{22} & d \\ N & d & \end{array} \right|$$

$$\mathbf{\Sigma} = \left| \begin{array}{cc|c} \mathbf{\Sigma}_1 & \mathbf{0} & N \\ \mathbf{0} & \mathbf{\Sigma}_2 & d \\ N & d & \end{array} \right|$$

If $\sigma_n(\mathbf{A}_1) > \sigma_{n+1}(\mathbf{A})$, then the matrix, $[\mathbf{H}_{\text{tls}} \ \mathbf{E}_{\text{tls}}]$ defined by:

$$\mathbf{C} \cdot [\mathbf{H}_{\text{tls}} \ \mathbf{E}_{\text{tls}}] \cdot \mathbf{D} = -\mathbf{U}_2 \cdot \mathbf{\Sigma}_2 \cdot [\mathbf{V}_{12}^T \ \mathbf{V}_{22}^T]$$

Equation D- 11

Which solves Equation D- 9. If $\mathbf{D}_1 = \text{diag}(d_1, \dots, d_N)$ and $\mathbf{D}_2 = \text{diag}(d_{N+1}, \dots, d_{N+d})$ then the position solution matrix, \mathbf{X}_{TLS} :

$$\mathbf{X}_{\text{TLS}} = -\mathbf{D}_1 \cdot \mathbf{V}_{12} \cdot \mathbf{V}_{22}^{-1} \cdot \mathbf{D}_2^{-1}$$

Equation D- 12

exists and is a unique solution to $(\mathbf{G} + \mathbf{H}) \cdot \mathbf{X} = \mathbf{Y} + \mathbf{E}$.

As stated earlier, the EIV RAIM total least-squares problem is termed “one-dimensional” in that the value of d is 1 (we do not have multiple right-hand sides). Thus in this case,

$$\mathbf{x}_{\text{TLS}} = -\mathbf{D}_1 \cdot \mathbf{V}_{15} \cdot \mathbf{V}_{55}^{-1} \cdot \mathbf{D}_5^{-1}$$

Equation D- 13

where the following partitioning scheme has been employed:

$$\mathbf{A} = \left| \begin{array}{cc|c} \mathbf{A}_1 & \mathbf{A}_5 & \\ 4 & 1 & \end{array} \right|$$

$$\mathbf{U} = \left| \begin{array}{cc|c} \mathbf{U}_1 & \mathbf{U}_5 & \\ 4 & 1 & \end{array} \right|$$

$$\mathbf{V} = \left| \begin{array}{cc|c} \mathbf{V}_{11} & \mathbf{V}_{15} & 4 \\ \mathbf{V}_{51} & \mathbf{V}_{55} & 1 \\ 4 & 1 & \end{array} \right|$$

$$\Sigma = \begin{array}{c|cc|c} & \Sigma_1 & \mathbf{0} & 4 \\ & \mathbf{0} & \Sigma_5 & 1 \\ \hline & 4 & 1 & \end{array}$$

Similarly, the $M \times 5$ matrix, containing the errors, $[\mathbf{H}_{t|s} \mathbf{e}_{t|s}]$ is defined by:

$$\mathbf{C} \cdot [\mathbf{H}_{t|s} \mathbf{e}_{t|s}] \cdot \mathbf{D} = -\mathbf{U}_5 \cdot \Sigma_5 \cdot [\mathbf{V}_{15}^T \mathbf{V}_{55}^T]$$

Equation D- 14

Or, more usefully,

$$[\mathbf{H}_{t|s} \mathbf{e}_{t|s}] = -\sigma_5 \cdot \mathbf{C}^{-1} \cdot \mathbf{U}_5 \cdot [\mathbf{V}_{15}^T \mathbf{V}_{55}^T] \cdot \mathbf{D}^{-1}$$

Equation D- 15

Back-substituting this value for $[\mathbf{H}_{t|s} \mathbf{e}_{t|s}]$ gives:

$$\min_{\text{range}(Y+E) \subseteq \text{range}(G+H)} \|\mathbf{C} \cdot [\mathbf{H} \mathbf{e}] \cdot \mathbf{D}\|_F = \sigma_5$$

Equation D- 16

Thus providing the basic equations from which the EIV RAIM test statistics are derived in Section 10.4.